Graph Spectra and Modal Dynamics
of Oscillatory Networks

by

Babak Ayazifar

B.S., California Institute of Technology (1989)

S.M., Massachusetts Institute of Technology (1992)

Submitted to the Department of Electrical Engineering and Computer Science
in partial fulfillment of the requirements for the degree of

Doctor of Philosophy

at the

MASSACHUSETTS INSTITUTE OF TECHNOLOGY

September 2002

Author⎯⎯⎯⎯⎯⎯⎯⎯⎯⎯⎯⎯⎯⎯⎯⎯⎯⎯⎯⎯⎯⎯⎯⎯⎯⎯⎯⎯⎯⎯⎯⎯⎯
Department of Electrical Engineering and Computer Science
September 19, 2002

Certified by⎯⎯⎯⎯⎯⎯⎯⎯⎯⎯⎯⎯⎯⎯⎯⎯⎯⎯⎯⎯⎯⎯⎯⎯⎯⎯⎯⎯⎯⎯⎯
George C. Verghese
Professor of Electrical Engineering and Computer Science
Thesis Supervisor

Accepted by⎯⎯⎯⎯⎯⎯⎯⎯⎯⎯⎯⎯⎯⎯⎯⎯⎯⎯⎯⎯⎯⎯⎯⎯⎯⎯⎯⎯⎯⎯⎯
Arthur C. Smith
Chairman, Departmental Committee on Graduate Students

**Graph Spectra and Modal Dynamics
of Oscillatory Networks**
by
Babak Ayazifar

Submitted to the Department of Electrical Engineering and Computer Science
on September 19, 2002, in partial fulfillment of the
requirements for the degree of
Doctor of Philosophy

Abstract

Our research focuses on developing design-oriented analytical tools that enable us to better understand how a network comprising dynamic and static elements behaves when it is set in oscillatory motion, and how the interconnection topology relates to the spectral properties of the system. Such oscillatory networks are ubiquitous, extending from miniature electronic circuits to large-scale power networks.

We tap into the rich mathematical literature on graph spectra, and develop theoretical extensions applicable to networks containing nodes that have finite nonnegative weights—including nodes of zero weight, which occur naturally in the context of power networks. We develop new spectral graph-theoretic results spawned by our engineering interests, including generalizations (to node-weighted graphs) of various structure-based eigenvalue bounds.

The central results of this thesis concern the phenomenon of dynamic coherency, in which clusters of vertices move in unison relative to each other. Our research exposes the relation between coherency and network structure and parameters. We study both approximate and exact dynamic coherency. Our new understanding of coherency leads to a number of results. We expose a conceptual link between theoretical coherency and the confinement of an oscillatory mode to a node cluster. We show how the eigenvalues of a coherent graph relate to those of its constituent clusters. We use our eigenvalue expressions to devise a novel graph design algorithm; given a set of vertices (of finite positive weight) and a desired set of eigenvalues, we construct a graph that meets the specifications. Our novel graph design algorithm has two interesting corollaries: the graph eigenvectors have regions of support that monotonically decrease toward faster modes, and we can construct graphs that exactly meet our generalized eigenvalue bounds.

It is our hope that the results of this thesis will contribute to a better understanding of the links between structure and dynamics in oscillatory networks.

Thesis Supervisor: George C. Verghese
Title: Professor of Electrical Engineering and Computer Science

Dedication

to my gorgeous niece Iman, the twinkle in my eyes,

my mom Mahin and dad Amir, who nurtured me since frail,

my sweetest sister Mitra, whose caring knows no bounds,

my cherub, my angel Sara, in whose tenderness I drown,

my selfless aunt Mansurah, and so, too, aunt Aminah,

whose love does never end,

my precious cousin Siddiqah, whose prayer warms my heart,

my dearest cousin Mustafa, indeed my elder bro,

whose blood was spilt in deserts vast, fending against foe,

my Grandma Tuba and Baba Ali,

whose memory soothes my soul,

alas, O companion, and indeed above all else,

to my Creator and Sustainer, my Hope and my Support,

Most Compassionate, Most Merciful, Master of the World,

to ye, O my dear ones, and especially to Thee O Lord,

I do dedicate these leaves, upon which are inscribed,

fruits of my humble toil.

Acknowledgements

Yes, it has come to this, hasn't it? Here I am, just hours ahead of the deadline for the submission of my thesis, smelling the musk at the finish line of the longest marathon of my life to date, and I have no idea what to write here. How am I to capture—in this little time, and in only a few pages—the experiences of many years, and the contributions of every wonderful soul, here at the Institute and beyond, who has colored my life?

Throughout the past year, I compiled a list of over 110 people (yes, one hundred and ten) whom I wanted to acknowledge here. But, alas, it is a monumental task to recognize all those who have touched my life and so profoundly enriched it. Those who, over the years, have had a tremendous influence in my life, cared for me, and brought me joy (and they know exactly who they are), should know that I do recognize, and am thankful for, the sweet blessing of their presence in my life, and I do try to show a token of my gratitude by praying for them to God Almighty, regularly.

In fact, with the remembrance of His name, Most High, I begin my attempt to pen this section of the thesis. God, Majestic and Exalted in His Might, is the First and the Last. It is only befitting for me to commence in His Name. My frail human gratitude, however sincere and passionate, is woefully inadequate in the face all the blessings that He has granted me throughout my life—through good times and through hardships. By blessing me with worldly comfort, He has obliged me to remain close to Him by being thankful to Him. And by the trials that He has spread along my journey, He has blessed me with the reminder that He alone is my resort, and that from Him alone I shall seek ultimate help. Exalted is the Lord, who created me, protected me, and nurtured me. To Him, indeed, belongs all praise.

Turning now to the mortals, I surmise that few people can claim to have been blessed with the company of as many extraordinary people as I have been, during my long tenure as a student. I begin with my thesis advisor, **Professor George Verghese**.

From the first day I met George in June 1995, I was impressed with the aura of warmth and encouragement with which he received me. His compassion shone through. George is a dynamite advisor! There are many things about him that amaze me. He is always available; if I need to see him, I simply have to walk over to his office and knock on his door. He goes out of his way and takes the time—or makes the time—to chat with me about anything from research, to politics, to life's many joys, as well as its occasional disappointments.

When I get together with George to discuss research, our meetings last in excess of two hours—sometimes even three. Incredibly enough, at the end of every session, I wonder

how time flew. The answer, though, is obvious. Our one-on-one meetings are delightful! George gets his hands dirty; he goes to the blackboard, and actively contributes to the technical discussions—in great detail.

Unlike many other professors, who care mainly about the results that their students obtain from one meeting to the next, George is there in the center of the ring, helping me tread my way through an otherwise perplexing web of research issues, puzzles, and mazes. He is always full of insightful and refreshing ideas about what routes to take, whom to talk to, and where to look things up. His mind comprises an impressively vast and ever-expanding encyclopedia of technical reference material, and a turbo-powered intellect with which he puts his knowledge to use and breaks new ground—helping his students do the same! You name it, George knows it; or at the very least, he knows how and where to learn more about it, rapidly and with depth! I cannot even begin to count the number of times when, during our one-on-one research meetings, he would suddenly rise from his seat, walk over to his Goliath personal library, pluck out a book from a shelf (or from under a tall stack of books and journals), and find the exact location where a particular technical issue is addressed.

Invariably, I would emerge from our meetings with my motivation rekindled, my research vision uncluttered, and my hopes of thesis progress reinvigorated. I have felt like a Major-League athlete; off the field, George has been the ideal coach who knows just how to guide me, motivate me, and hone my skills, whereas on the field he always has been there cheering on for my success, just as would an ardent fan.

George trains his students to be multi-talented like himself, getting us to think about several different topics simultaneously; so research has never been monotonous. Anytime I hit a brick wall in one front, there was always another with a burning issue—one that could use some attention—to keep me engaged and interested; in the meantime, George has helped me pierce through, and indeed tear down, the occasional walls and move on.

In my case, George's guidance most prominently affirmed its "miracle touch" as I saw myself dive into alien topics about which I knew virtually nothing at the outset, and evolve to a state where I feel I'm actually in a position to make meaningful research contributions. I can't even begin to imagine how I could have learnt so much under any other circumstances or with anyone else guiding my research. George shames me into striving to live up to my potential—not by coercion or pressure, nor through invocation of negative feelings, and never through put-downs, but rather, by the tremendous generosity that he grants me with his time, his unbounded encouragement, powerful and effective motivations, and most important, his patience!

From a rare breed of educators, indeed he is. To attest to this are his burning desire to see his students succeed, his highly refined interpersonal skills, his social tact and diplomacy, his great sense of humor, his humility, his immaculate work and professional ethics, his enthusiasm, his technical expertise, a universal and unconditional respect that he commands

among his peers (at MIT and around the world), and his unwavering and unbounded support for his students. I can only dream that one day, I may exhibit even a fraction of the style that George brings to his career. For now, I hope that this document at least partially meets his high standards, and reflects the enormous investment he made in me over the years.

Next, I want to thank my other, very patient, thesis committee members, **Professor Bernard Lesieutre** and **Professor Jacob White**. I have interacted with both of them not only as part of this thesis, but also in a teaching capacity. **Bernie** has always provided pleasant company and great insight. He even flew from Europe to Boston just to attend my thesis defense. I am incredibly indebted to him for that. From when he was on my Ph.D. Area-Exam committee to the day of the thesis defense, he always has been available whenever I've needed to discuss a technical subject with him (or any other subject for that matter).

Jacob was my teaching mentor when he was a lecturer (and I a recitation instructor) for our EECS Department's introductory signals and systems course, on two separate semesters. I very much respect his skills as a manager of a large team of instructors and teaching assistants, running a course with over 200 students. It has always been a pleasure working with him. I am still embarrassed that I dragged him to work during his summer vacation and sabbatical, just to attend my thesis defense.

Outside my thesis committee I owe a tremendous gratitude to **Professor Al Drake**. From him I learned the philosophy and ethics of teaching, the value of students, and the importance of compassion in dealing with young minds. He has been incredibly supportive of me over the years, and an outstanding advisor and mentor. When I needed a summer job on two occasions, he helped me secure teaching assignments in the Sloan School of Management. Only someone as caring, trusting, and well-connected as Al could have, or would have, done that for me. Over the years, he also has extended his support in other ways. From offering his help on occasions when I had difficulties, to writing letters of recommendation, to picking up the phone and talking to the right people to resolve the bureaucratic problems that distracted my attention, he has been an outstanding supporter throughout my long stay here. Indeed, if I were to be the protegé of any two people at MIT, I would be Al's and George's. Life here at the Institute would not have been anywhere as exciting without Al and George looking after my welfare.

Over the course of many years, I have had the privilege of working under the supervision of a distinguished company of educators here at MIT—people from whom I have learnt an enormous amount. They are: **George Verghese**, **Bob Gallager**, **Al Drake**, **Jae Lim**, **Jacob White**, **Jim Orlin** (of the Sloan School of Management), **Mitchell Trott**, and **Dr. Tom Quatieri**. I have been very fortunate, in that these folks have allowed me to work as nearly full partner with them in the running of their respective courses. They have given me ample leeway and autonomy over what to cover in recitations and guest lectures, they have routinely counted on me to devise exam problems, and they have even allowed me to influence the course structure in important ways. I very much appreciate the trust that

they have placed in my teaching instincts and judgment, over the years. When I go in front of any crowd to give a lecture or talk, a part of everything I say owes itself to what I have learnt from these folks.

Mitch Trott was also a terrific friend with whom I could discuss many non-academic issues. Only someone like Mitch would think of ordering Latin-American chocolate bullions to keep us on the necessary sugar high during our exciting months of working together.

Among the EECS Department administrators and assistants, I gratefully acknowledge the enormous support that I received from the following wonderful people.

Marilyn Pierce is a gem in the administration. Always patient and unbounded in her support, she is one who impresses me with her uncanny memory and attention to detail! I must be one of her biggest "problem students" in the Department—though, I suspect, one of her favorites as well!

Peggy Carney has been instrumental in my financial survival here at the Institute. On more than one occasion, she extended Departmental support when no other source of funding was available to me. To her I am very grateful and indebted.

Professor Arthur C. Smith—with whom I had the pleasure of co-teaching our introductory signals and systems course, when we were recitation instructors—has been very understanding of the occasional, albeit critical, administrative issues that have crept my way during my graduate career. I am very grateful to him for his generous help and support.

Our amazing administrative assistant **Vivian Mizuno** is one about whom I can not write enough. She is the glue that keeps us all together down here in the Laboratory for Electronic and Electromagnetic Systems (LEES). Always full of energy, I often find myself having to restrain her, because she always insists on doing more than what I ask of her. She is our proverbial "mama goose" down here in the otherwise dreary basement of Building 10, where we do time!

Cindy LeBlanc was our group's "den mother" during the time I was working toward my master's degree, and continues to be a source of support to this day. For all her invaluable help with academic and departmental matters, for her hospitality when she invited our entire group to her home for delicious meals, for her caring about my welfare and going the extra distance to alleviate whatever problems she could help me with, I thank her. She is a wonderful lady whom our EECS Department should be proud of.

Lisa Bella has been a most delightful administrator to know over the years. From the old days when I was working toward my master's degree to the present, she has never ceased to extend to me her help with teaching assignments, her insight into departmental matters, and even her home-cooked soup. My success has always brought joy to her. I am very fortunate to have known her over these many years.

Monica Bell, until she retired a few months ago, was another one of the folks whom I was always happy to have on my side. With her charming personality and witty teasers, she always brightened my day. I tried hard to graduate before she retired, but, alas, she beat me to it. I know she would have been very happy to see the signed cover page of my thesis on her desk. I'll try to compensate by sending her a copy.

Mibsy Brooks was always very supportive, and went out of her way to help me with many course-related administrative issues. I lost count of how many times I barged into her office, pestering her about room changes and reserving halls for exams. I appreciate all her help.

Karin Janson-Strasswimmer who is an administrator in our lab headquarters, has impressed me with her compassion for, and knowledge of, the plight of peoples around the world. It is always a pleasure discussing international affairs with her. She has enriched my view of the world—especially that of Europe—with her unique perspective.

Mary Murray, my student account representative, has been one of the most understanding folks in the MIT administration. Always eager to help resolve issues surrounding my bursar's account, she has been invaluable in my financial survival here at the Institute. To top it off, she cheered me on to the finish line every time we met. Thanks, Mary!

Dean Ike Colbert is a gem in MIT's higher echelons. Of a rare breed of administrators, he is keenly aware that Institute regulations are designed with the ultimate goal of making life more pleasant for students, not more strenuous. He exercises his authority and lends his support to students with that spirit in mind. I am very grateful for his assistance.

I now want to acknowledge the students in our lab with whom I have been fortunate enough to interact—both on a personal level and a professional one. **James Hockenberry** is one of the most memorable people. Aside from being stooped into helping me move from my old apartment several years ago—expecting that it would take only four hours, only to find himself sleeping overnight on the bare floor, in a nearly empty apartment with no amenities—he has been a true friend in every sense of the word. He is a man of many interests, he is caring of the world he lives in, and he possesses deep technical insight. He is likely to remain the only person I know who would shuttle up Massachusetts Avenue to Harvard University, to take language courses in Croatian!

Vahe Caliskan is another extraordinary friend whom I had the pleasure of sharing this lab with for many years. His insistence on explaining his jokes were—as much as I hate to admit—actually funny! He has a gentle soul and a giving heart. I cannot begin to count the many times when he went far out of his way to help me. My colleagues **Jesko Hagee**, **Chalee Asavathirtham**, **Sandip Roy**, and **Ernst Scholtz** have been instrumental in my technical development here, and I am very fortunate to have worked with all of them. Among others I would like to acknowledge **Ankur Garg**, **Tushar Parlikar**, **Tim Neugebaur**, **Joshua Phinney**, **Steve Shaw**, and **John Rodriguez** whose companionship

has greatly enhanced my experience in the Lab.

To my friends here at MIT and around the globe, you are way too many to mention. What am I to do?

I thank my friend **Ali** who lent me his notebook PC—the lifesaver that enabled me to typeset this thesis at a time when I was tormented by the thought of being holed up in my apartment behind my desktop, doing the same task. Your generosity has meant a great deal to me.

Ammar, thank you for the countless hours you invested of your time teaching me the beauties of Arabic and the nuances of the recitation of the Qur'an. Your friendship has meant a great deal to me. Thanks also to your wife Nada for all those home-cooked meals and baked sweets with which she made all our get-togethers and your Arabic lessons more enjoyable.

Ayman, you have been a friend and brother to me in the true sense of the word. Your integrity, calm demeanor, and soft speech have been inspiration for me, and a model to emulate. God bless you.

Belal, you have been a terrific friend and a spiritual inspiration for me. Your reminders of supererogatory religious acts prompted me to go beyond the minimum required. I pray that you earn a large share of whatever reward God will grant for the acts of worship that you encourage the people around you to perform. Thank you also for being my confidant for so long. I also owe a large debt of gratitude to your wife **Sarah**, for her warm hospitality at your home as well as her invaluable and selfless assistance with other, far more important, matters.

Farhan, you make me proud of being your brother, and give me hope about the future of our worldwide community. With outstanding, brilliant folks like you, we cannot expect anything but a brighter future. The breadth and depth of your knowledge has never ceased to amaze me. May God bless you, and give us more people like you.

Humera, may God bless you for all your support and prayers. You are a bona fide devotee of God, and the world would be a far better place with more folks like you. I cannot thank you enough for the countless ways you assisted me.

Ihsan, thank you for your hospitality, for being an exemplary model of youthful exertion and introspection, for being there when I needed your help, and for altering the course of my life.

Jalal, you have done so much for me that I cannot possibly list all of them. So I will simply recall the plight that you shared with Farhan and **James** when you helped me move. You have been a tremendous friend.

Kashif, you are one of the coolest guys I know. You have been an extraordinary friend, an awesome computer whiz, and outstandingly generous with your time. You and your wife **Marilene** have enriched my experience here immensely. I honed my debate skills based on my interactions with you, and I cultivated the ability to pinpoint loopholes in my own arguments and reasonings, before opening my mouth, from years of exciting companionship with you and the MBC boys.

Mohammed, your companionship, insight, and wit has meant a world to me. The hospitality and care that you and your wife **Wejdan** have extended to me (especially all the dishes that you prepared for me when I had the flu on several occasions), as well as the many legs of lamb and barbecues to which you invited me, are manifestations of your kindness that are etched in my heart and memory. May God bless you and your family.

Numan, you zany New Yorker! For all the times when you simply listened to me confide in you, making it easier for me to tread life's testier moments, for all those times when you generously loaned me your car, and for bringing a fresh perspective into every intellectual debate, I thank you.

Osamah, you are just a downright cool dude! Thanks for lending me a listening ear, for your invaluable advice, and for being there for me. For your generous use of your car, your hospitality (along with your brother **Khalid**'s delicious cooking), and your companionship over the years, I am very grateful.

Salim, you appeared in my life several years ago like a survival package parachuting from the heavens. Life has never been the same since I met you. For your selfless assistance, support, and companionship I am very grateful. Your sincerity and piety inspire me greatly.

Soosan, I have learnt a great deal from you in my life. May God bless you with His bounties and grant you a beautiful future.

Suheil, thanks for being there when I most needed your help. I have also learnt a great deal about my religion from you, and have found our discussions and debates on theological matters very enriching and challenging. May God bless you.

Mahmood, **Ali Abbas**, **Shaun**, and **Vahid**, I am ever-so-thankful to have known you, and for having learnt immeasurable amounts about my religion from you. Your dedication, attention to detail, and hospitality have etched an indelible mark on my heart and mind.

So as not to give away the entirety of my social circle of zany friends, I will acknowledge the rest of you in groups. To my close circle of friends, the **MBC Boys and Associates**, my hat goes off to you for all the loving support that you have given me over the years; I have already acknowledged most of you individually. To the **MSA-Social** and **MSA-Kewl** gangs, especially the sisters who graced me with their exquisite culinary and baking talents, I thank you; may God Almighty reward you. To the graduate and undergraduate

friends in the **MITMSA**, thank you for providing me with such a warm environment, and for putting up with my quirks, lamentations, and commentary for so long. You are in my prayers.

To my family, I refer you to the dedications page. I hope you accept my first serious attempt at a poem as a gesture from the depths of my heart—a token of my appreciation for all that you have done for me throughout my life. To **Mehrdad**, who has been a part of my family for several years now, I thank you for your companionship and for taking such great care of my sister and parents.

To **Sara**, I could not have survived this place without your prayers, care, and support. A cherub indeed you are, and a true blessing in my life. May God never remove the shadow of your presence from my life.

The humble document you see before you has been made possible only God's Grace; any errors are mine, of course. Praise belongs solely to God, the Lord of the Worlds. As He is the Last, I close with His remembrance.

Contents

List of Figures

List of Tables

Introduction and Contributions

Had John Steinbeck been commissioned to the task, he may have titled this document

Of Modes and Matrices: the Confluence of the Graph Structure,
Spectrum, and Dynamics of Oscillatory Networks.

The goal of the research culminating in this dissertation has been to understand how a network of dynamic elements behaves when it is set in oscillatory motion, and how the interconnection topology influences (or, conversely, is inferred from) the spectral properties of the underlying graph model. Along the way, we study the mutual influence of network structure and its spectrum, and develop a set of tools geared toward a design-oriented analysis of lumped-parameter oscillatory dynamic systems.

Broadly speaking, the overall contribution of our work is twofold:

- We establish a connection—previously more or less overlooked—between the mathematical theory of graphs and the dynamic analysis of oscillatory networks. Seaming the gap between algebraic graph theory [6, 14, 17, 18, 16, 38] and oscillatory networks allows us to tap into the rich corpus of results already known to mathematicians, and to apply, adapt, and extend those results to the study of network dynamics. For their share, it is expected that engineering applications stimulate new graph-theoretic problems toward the solution of which novel theory needs to be developed.

  There is a plethora of theorems about graphs and their spectra; by modeling physical dynamic networks with graphs, we allow ourselves access to a vast arsenal of tools with which to study their oscillatory behavior. This is a resource that engineers interested in power-systems or mechanical structural-dynamics (to cite just two research communities), by and large, have yet to tap into. The applications of interest to us, such as electric power networks or mechanical vibrational systems that have lumped mass-spring representations, provide a physical motivation and an intuitive backbone for the study of

graph dynamics.

- The second aspect of our overall contribution relates to the historical development of spectral graph theory to date. Undoubtedly, mathematicians have displayed tremendous intuition in developing theoretical results about graphs and their spectra; in fact, at times one is astounded as to how (or, more important, why) they even thought of certain problems that they tackled or theorems that they set out to prove. What makes their work impressive is that, by and large, graph theorists have been motivated to develop the subject matter, not by the types of physical systems of interest to applications-oriented engineers, but, rather, out of pure mathematical curiosity or by other very theoretical fields outside of mathematics. There is a large body of spectral graph-theoretic literature inspired, for example, by combinatorial problems and interests; the field of algebraic combinatorics is a case in point [37].

  That said, spectral graph theory *has* had applications in chemistry (in particular, molecular dynamics), theoretical physics and quantum mechanics, and—in recent times—communications networks and theoretical computer science. However, engineers in such research fields as systems and control, power networks, or structural dynamics have not seen their problems of interest motivate spectral graph theoretic investigations. We set out to effect a change in this regard, insofar as it is possible to do so within the confines of a Ph.D. dissertation.

  As a result of the emphasis and flavor of interests in spectral graph theory thus far, studies conducted over the past few decades usually have dealt with graphs with very strong "uniformity" features, such as unity-weighted nodes. The overwhelming majority of papers in the field also consider graph edges to be uniformly valuated at unity, although prominent exceptions do exist, such as the papers by Mohar [59, 60, 61, 63], the outstanding monograph *Spectral Graph Theory* by Chung [14], and some others. There is, however, a dearth of material in the literature about *node-weighted* graphs; the few exceptions that we have seen relate predominantly to spectral graph partitioning, e.g., Bolla and Tusnády [7] and Zien, et al. [76]. We are aware of no prior work that has tackled graphs containing nodes of *zero weight*.

  We have thus inherited not only a fertile research field to till and to cultivate, but also a prolific breeding ground in which to develop new theory and to extend many results—already known to graph theorists—and apply them to networks that contain weighted nodes and edges. Some of these extensions, albeit straightforward, are, nevertheless, intuitively illuminating, especially from an engineering viewpoint: in particular, results for weighted graphs in which the node weights are strictly positive and finite (but otherwise arbitrary) have immediate engineering applications (such as in stability analysis

and mode shape studies) that we shall expound on as the thesis unfolds. When nodes of zero weight are introduced, the theory oft becomes quite nontrivial. Dealing with graphs that contain zero-weighted nodes is an important contribution of our research.

Devising fresh nomenclature to facilitate our coverage, we distinguish between two types of nodes, and give each a name: *Gravis nodes* (equivalently, G-nodes or G-type nodes), inspired from the Latin word meaning "weighty," have strictly positive (but finite) weights, whereas *levis nodes* (equivalently, L-nodes or L-type nodes), from the Latin meaning "light," have zero weight. These two types of graph vertices are qualitatively different, and graphs that contain L-nodes have quirks that require special care in handling, as well as interesting features that we can exploit to advantage; we shall point these out along the way.

Furthermore, the physical systems that are amenable to graph models motivate theoretical problems that the mathematics and the computer-science communities have not focused on before. Our discussion of graphs with zero node weights (arising in power networks that contain *load nodes*), of dynamic coherency (arising, again, in power systems), or of modes confined to subnetworks (which is of interest to structural engineers who have studied mode localization, as well as to engineers with interests in network partitioning) are examples of phenomena that graph theorists either have not studied, or have studied without realizing the potential impact of graph dynamics on their work on such physical applications. Dynamic coherency is an example of an engineering phenomenon whose investigation (and underlying theory) is closely related to the graph-theoretic work on equitable partitions; yet, the connection between the two has not been made to date. In a sense, therefore, our contribution can be thought of as being directed at both the engineering and the mathematics communities. We hope that bridging the gap between the two fields will spawn a new and exciting genre of problems, and generate equally interesting theory to accompany the new developments.

1.1 Organization of this Thesis

This dissertation consists of seven chapters and three appendices.

Chapter 2 motivates the introduction of spectral graph theory—in particular, the Laplacian matrix paradigm—to the study of oscillatory networks. We derive the dynamic equations governing applications such as circuit theory, mass-spring systems, and power networks, showing how in each case a matrix of "admittances" emerges, whose spectral properties

(taking into account the diagonal node-weight matrix of the system) determine the dynamic behavior of the overall network.

Chapter 3 lays out the symmetric generalized eigenvalue problem (SGEP) for weighted graphs, and covers some of the matrix-theoretic background critical to understanding the remainder of the thesis; our brief survey includes a discussion on M-matrices and Laplacian matrices, and their spectral properties. We set up the problem as $\mathbf{A}\,x = \lambda\,\mathbf{B}\,x$, a form that involves a semi-definite, diagonal node-weight matrix $\mathbf{B}$ whose diagonal elements are nonnegative (including possibly zero, if the corresponding node is L-type). This SGEP has as many eigenvalues at infinity as there are L-nodes in the graph. We describe under what conditions the SGEP for a graph is well-posed, and show how avoiding those conditions imposes no unreasonable restriction on the actual physical systems of interest to us. In particular, we show that for the SGEP to be well-posed, every connected subgraph of L-nodes must have at least one connection to a G-type node; in power networks, for example, this is always case, for it makes no physical sense for a connected set of load nodes (L-nodes) to operate without being connected to at least one driving generator (a G-node).

Chapter 4 introduces the notion of the Schur contraction of graphs, which is a method to collapse a graph with respect to any subset of its L-nodes. This has been done in the power-system area for years, but the exact relationship between the contracted graph and the parent graph, or the dependence of the eigenvector components of the L-nodes on those of the G-nodes, was not well-understood until now. We show how the eigenvector component corresponding to any L-node is a convex combination of those associated with its neighboring nodes in the graph (regardless of the types of neighbors involved). Furthermore, we prove that when we contract the graph with respect to a subset of the L-nodes, all the vertices that initially neighbored the contracted L-nodes become fully connected. This result is obtained through properties of nonsingular M-matrices.

Chapter 5 takes a novel look at dynamic coherency theory. Coherency is a feature of certain oscillatory networks (such as power systems) in which groups of nodes oscillate in tandem, at a constant level with respect to each other. For over two decades, the approximate form of this phenomenon has been studied in networks that comprise q clusters of nodes that are weakly connected with each other, but that internally have strong links. It is observed in such networks that the slowest q modes of the overall network exhibit approximate, slow coherency. Power system engineers have even studied exact (theoretical) coherency [21], albeit far less extensively than the approximate, slow coherency.

From a high-level vantage point, our contributions in this chapter are twofold: (1) We provide a new, much simpler, proof for approximate slow coherency; and (2) We develop necessary and sufficient conditions for theoretical (exact) coherency. We show under what conditions a graph exhibits exact coherency. It turns out that the theory we develop in this chapter has other interesting ramifications. Suppose we are given a set of q disjoint, but internally connected, clusters (subgraphs) of nodes, and we are asked to interconnect these clusters, so that (1) the overall network will exhibit exact coherency in q of its modes (not necessarily the q slowest ones), and (2) all the oscillatory modes of the individual clusters will be confined to their respective clusters *even after* they are interconnected. We solve this problem, and make several design-oriented observations that we then illustrate through example networks.

One of the interesting side effects of our coherency theory is that we get a clue as to how to tackle mode localization problems in graph-theoretic terms. Mode localization is a phenomenon long observed and studied in the physics and structural mechanics communities. Consider a structure that has uniformity of features (e.g., it may consist of a cascade of identical subsystems). It is generally easy to show, using symmetry arguments and the like, that the mode shapes of such a system are extensive, i.e., its region of support physically spans the entire structure. However, if a parameter of the same structure is slightly perturbed in one of its subsystems (say, a mass in the chain is slightly perturbed to something different from the other masses), then the modes of the resulting system exhibit localization around the point of perturbation, especially as the mode number increases (i.e., faster mode shapes are more geographically confined than slower modes). We look at one example where our study unveils why this happens.

Chapter 6 covers other interesting consequences of our investigation into exact coherency with mode confinement. We develop a technique to design completely connected G-type graphs, with pre-specified, positive, finite node weights and a set of desired eigenvalues. In other words, given a set of n node weights, and a set of $n-1$ desired, oscillatory (strictly positive) eigenvalues, our backward-recursive algorithm constructs a fully-connected graph[1] such that the Laplacian spectrum has the desired oscillatory eigenvalues (plus the ubiquitous zero eigenvalue). In addition, our design technique results in mode shapes that progressively have more and more zero components, i.e., they are increasingly confined to smaller regions in the graph, as we index toward the fastest mode (which has a region of support of only two vertices).

---

[1]A fully-connected graph is one in which every node is adjacent to every other node.

Also in this chapter generalize (to node-weighted graphs) some eigenvalue bounds that are based on the physical features of the graph, such as node (or cluster) degrees and weights. One of our contributions here is that we show how graphs can be designed that meet some of the eigenvalue bounds exactly.

Chapter 7 draws conclusions and suggests future research.

Appendix A specifies the basic notation that we will follow throughout our presentation.

Appendix B introduces the rudiments of graph-theoretic terminology.

Appendix C gives a tutorial overview of first-order perturbation theory for the class of symmetric generalized eigenvalue problems (SGEPs) of interest to us. We cover, in particular, multiple eigenvalue perturbation theory. Our novel proof of approximate, slow coherency makes direct use of the rudimentary material in this appendix. The material in this appendix is a straightforward extension of the ordinary eigenvalue problem, as covered in the classic textbook titled, *Mathematical Physics*, by Butkov [10].

1.2   The Intended Audience

This thesis is intended for anyone with a serious interest in spectral graph theory and oscillatory networks. The intended reader spans the gamut from the applied mathematician with an eye to expand graph-theoretic results beyond the traditional combinatorial (optimization) context; to the chemist or chemical engineer who studies molecular dynamics and would like to incorporate the extended results in this dissertation into his or her arsenal of analysis tools; to the structural engineer who wants to better understand vibrational systems, such as large space structures, that lend themselves well to a lumped mass-spring network model; to the investigator who employs finite-element methods to convert continuous vibrational system models into lumped-parameter representations; to the electric power network engineer who wants to get a better feel for how network structure affects modal behavior; to the network designer and analyst who wishes to explore new ways of partitioning large-scale networks into smaller, more analytically tractable subsystems; to the circuit designer who wants to adopt new techniques for devising systems with pre-specified natural frequencies: or to any engineer who deals with oscillatory networks and wishes to deepen his or her understanding of how such systems can be analyzed or designed.

1.3 A Useful Bibliography

To assist the you, and to prevent you from having to reinvent the wheel in finding the necessary background material, we review some of the matrix-theoretic concepts that normally are not covered in traditional undergraduate linear algebra or first-year graduate matrix analysis courses (e.g., M-matrices, the Schur complement, extremal properties of eigenvalues, majorization, etc.); however, our coverage of matrix theory is anything but self-contained.

What we found helpful throughout our investigations was having the useful references at hand, and to become gradually (if not already) familiar with them. A matrix analysis text at the level of Horn and Johnson [47, 48]) is essential. So is developing maturity in understanding linear vector-space concepts (some good companion books, although by no means prerequisites, are Halmos [43], Naylor and Sell [64], and Luenberger [53]). You may find the very well-written books by Parlett [67] and Stewart [73] to be invaluable companions for understanding issues related to symmetric matrices and perturbation problems, respectively. Lancaster and Tismenetsky [52] also provide a well-written reference textbook on matrix theory, but their work contains far more than is needed for a proper understanding and appreciation of this thesis. We have found Harville [44] and Lütkepohl to be valuable handbook-style references for matrix identities and properties; the former contains many proofs not readily found in one place. Our discovery of the title by Fiedler, *Special Matrices and their Applications in Numerical Mathematics* [28], was akin to stumbling across a hidden treasure. Fiedler, whose publications have tremendously influenced the development of this research, has summarized some of the important graph-related matrix-theoretic concepts in his outstanding—but regrettably little known and expensive—book.

This being a research area that involves dynamic systems, a basic understanding of linear system theory, at the level of an intermediate undergraduate course that covers state-space representations would be very helpful, although, naturally, exposure to an introductory graduate subject in dynamic systems—at the level of Kailath [50] or Luenberger [54]— would enhance your appreciation for graph dynamics.

For a basic study of graph theory, a very readable textbook (although it does not cover spectral issues) is by Diestel [22], which can be found in electronic form on the world-wide web (in downloadable PDF format) at the following URL:

http://www.math.uni-hamburg.de/home/diestel/books/graph.theory/ .

Another readable textbook on general graph theory is by Bollobás [8].

For spectral graph theory, there are several excellent references. The classic title, *Algebraic Graph Theory,* by Biggs [6] and its modern sequel and namesake by Godsil and Royle [38] are very useful; the latter has an entire chapter devoted to the Laplacian matrix—the matrix that is our epic hero as we tell the tale in this dissertation. The classic works by Cvetkovic, et al., namely [17, 18, 16] are indispensable (even though they do not place much emphasis on the Laplacian matrix), as is the title by Chung, *Spectral Graph Theory* [14]; Chung's monograph has an extensive coverage of Laplacian matrices, and deals with extremal properties of eigenvalues that we have found useful and extensible to the cases of interest to us.

Graphs and Linear Dynamic Models of Oscillatory Networks

In this chapter, we look at a few examples of non-dissipative, linear (or linearizable) dynamic networks, and illustrate how naturally we may use graph models to study their oscillatory behavior. A survey of basic graph-theoretic definitions and terminology—setting our language for the remainder of the thesis—appears in Appendix B. Regardless of your prior experience with graph theory, this is a good time to at least skim through the appendix and get acquainted with the particular notation that we will use throughout our presentation.

For each example system that we introduce in this chapter, we set up the governing dynamic equations using basic laws of Newtonian mechanics or electric circuit theory (Kirchhoff's current and voltage laws). The equations—involving the Laplacian matrices associated with graphs—illustrate how closely spectral graph theory and the study of network dynamics are related. We conclude the chapter by illustrating how the modes of a state-space representation of an oscillatory network relate to those of its graph model; in particular, we show how the generalized eigenvalues and eigenvectors of the Laplacian and node-weight matrix pairs relate to the modes of a state-space representation of the network. By the end of this chapter, the motivation for employing a graph-theoretic paradigm to study oscillatory networks will be established. This chapter, in a sense, broadly highlights one of the main contributions of the thesis, which is the bridging of the gap between spectral graph theory (wherein much is known about the eigenvalues and eigenvectors of graphs) and the engineering study the modal dynamics of linear oscillatory networks.

2.1   Oscillatory Networks with Graph Representations

Graph models can be used to describe any linear (or linearizable) lumped-parameter system that has a direct network model (comprising nodes and edges). By way of example, we will cite a lumped-parameter LC-circuit, two vibrational mass-spring systems, and the swing-equation model for a power network. Graph also may be used to study distributed-parameter systems that have lumped-network discretized models. However, this latter category is outside the scope of the thesis.

2.1.1   Dynamic Model of an LC Circuit

Undriven, linear (or linearizable) electrical networks—containing no dissipative elements and no dependent sources—are good examples for our graph-theoretic modelling. Consider the circuit of Figure 2.1 which has neither independent nor dependent sources, contains linear dynamic elements (capacitors and inductors), but no dissipative elements (resistors); all the dynamics are due to the initial state of the capacitors and inductors. Our particular example has the topology of a ring with an additional node in the center. Every node has associated with it a shunt capacitance, except for Node 6. In graph-theoretic terms, we say that node 6 has a weight of zero. We shall deal with nodes of this type in subsequent chapters, where we call them L-nodes (or *Levis* nodes).

Let us write down the dynamic equations of the circuit by applying KCL for each node. We know that the constitutive equation governing the current for a capacitor is

$$i_C(t) = C\,\frac{dv_C(t)}{dt} \tag{2.1}$$

and that for an inductor is

$$i_L(t) = \frac{1}{L}\int_0^t v_L(\tau)d\tau \ . \tag{2.2}$$
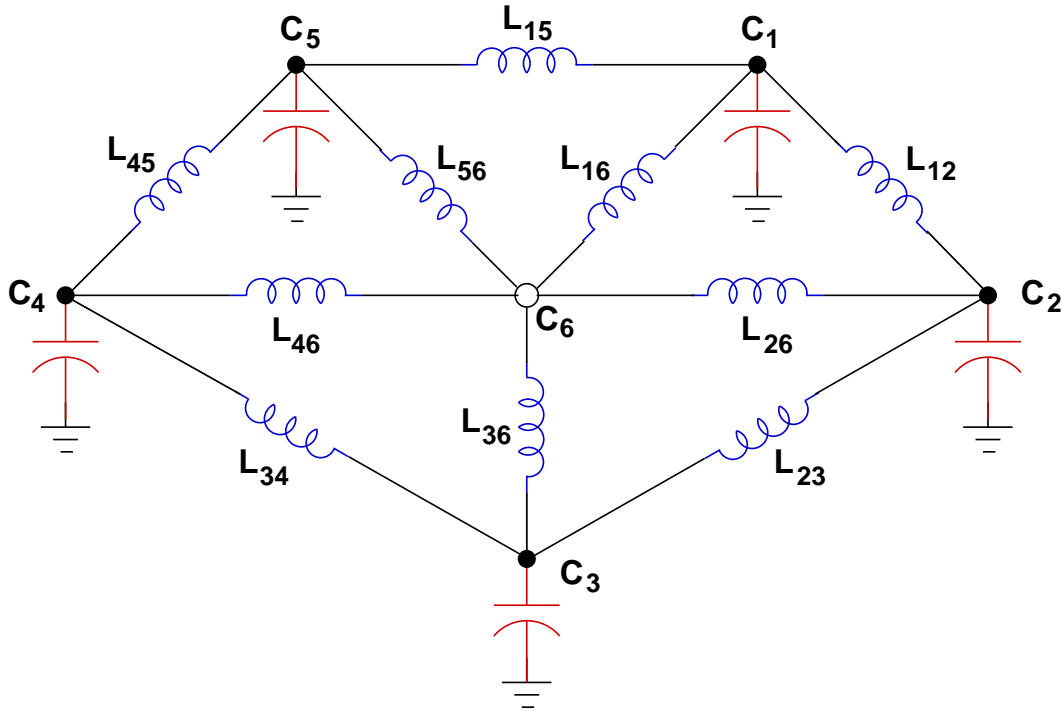
Figure 2.1: An *LC*-circuit that represents an undamped oscillatory network.

With that in mind, we can write the equations for nodes 1 through 5 as follows:

$$C_1 \frac{dv_1}{dt} + \frac{1}{L_{15}} \int (v_1 - v_5)\, d\tau + \frac{1}{L_{12}} \int (v_1 - v_2)\, d\tau + \frac{1}{L_{16}} \int (v_1 - v_6)\, d\tau = 0 \qquad (2.3\text{a})$$

$$C_2 \frac{dv_2}{dt} + \frac{1}{L_{12}} \int (v_2 - v_1)\, d\tau + \frac{1}{L_{23}} \int (v_2 - v_3)\, d\tau + \frac{1}{L_{26}} \int (v_2 - v_6)\, d\tau = 0 \qquad (2.3\text{b})$$

$$C_3 \frac{dv_3}{dt} + \frac{1}{L_{23}} \int (v_3 - v_2)\, d\tau + \frac{1}{L_{34}} \int (v_3 - v_4)\, d\tau + \frac{1}{L_{36}} \int (v_3 - v_6)\, d\tau = 0 \qquad (2.3\text{c})$$

$$C_4 \frac{dv_4}{dt} + \frac{1}{L_{34}} \int (v_4 - v_3)\, d\tau + \frac{1}{L_{45}} \int (v_4 - v_5)\, d\tau + \frac{1}{L_{46}} \int (v_4 - v_6)\, d\tau = 0 \qquad (2.3\text{d})$$

$$C_5 \frac{dv_5}{dt} + \frac{1}{L_{45}} \int (v_5 - v_4)\, d\tau + \frac{1}{L_{45}} \int (v_5 - v_4)\, d\tau + \frac{1}{L_{56}} \int (v_5 - v_6)\, d\tau = 0 \qquad (2.3\text{e})$$

and the one for the center node 6 as:

$$\frac{1}{L_{16}} \int (v_6 - v_1)\, d\tau + \frac{1}{L_{26}} \int (v_6 - v_2)\, d\tau + \frac{1}{L_{36}} \int (v_6 - v_3)\, d\tau$$
$$+ \frac{1}{L_{46}} \int (v_6 - v_4)\, d\tau + \frac{1}{L_{56}} \int (v_6 - v_5)\, d\tau = 0\,. \qquad (2.3\text{f})$$

Differentiating both sides of Equations (2.3), and rewriting the result in matrix-vector form, we arrive at the following differential-algebraic equation:

$$\mathbf{B}\,\ddot{\boldsymbol{v}}(t) + \mathbf{L}\,\boldsymbol{v}(t) = \mathbf{0}\ , \tag{2.4}$$

which, written in greater detail, is as follows:

$$
\underbrace{\begin{bmatrix}
C_1 & & & & & \\
& C_2 & & & & \\
& & C_3 & & & \\
& & & C_4 & & \\
& & & & C_5 & \\
& & & & & 0
\end{bmatrix}}_{\mathbf{B}}
\underbrace{\begin{bmatrix}
\ddot{v}_1 \\ \ddot{v}_2 \\ \ddot{v}_3 \\ \ddot{v}_4 \\ \ddot{v}_5 \\ \ddot{v}_6
\end{bmatrix}}_{\ddot{\boldsymbol{v}}(t)}
$$

$$
+\ \underbrace{\begin{bmatrix}
\frac{1}{L_{12}}+\frac{1}{L_{15}}+\frac{1}{L_{16}} & -\frac{1}{L_{12}} & 0 & 0 & -\frac{1}{L_{15}} & -\frac{1}{L_{16}} \\[4pt]
-\frac{1}{L_{12}} & \frac{1}{L_{12}}+\frac{1}{L_{23}}+\frac{1}{L_{26}} & -\frac{1}{L_{23}} & 0 & 0 & -\frac{1}{L_{26}} \\[4pt]
0 & -\frac{1}{L_{23}} & \frac{1}{L_{23}}+\frac{1}{L_{34}}+\frac{1}{L_{36}} & -\frac{1}{L_{34}} & 0 & -\frac{1}{L_{36}} \\[4pt]
0 & 0 & -\frac{1}{L_{34}} & \frac{1}{L_{34}}+\frac{1}{L_{45}}+\frac{1}{L_{46}} & -\frac{1}{L_{45}} & -\frac{1}{L_{46}} \\[4pt]
-\frac{1}{L_{15}} & 0 & 0 & -\frac{1}{L_{45}} & \frac{1}{L_{15}}+\frac{1}{L_{45}}+\frac{1}{L_{56}} & -\frac{1}{L_{56}} \\[4pt]
-\frac{1}{L_{16}} & -\frac{1}{L_{26}} & -\frac{1}{L_{36}} & -\frac{1}{L_{46}} & -\frac{1}{L_{56}} & \frac{1}{L_{16}}+\frac{1}{L_{26}}+\frac{1}{L_{36}}+\frac{1}{L_{46}}+\frac{1}{L_{56}}
\end{bmatrix}}_{\mathbf{L}}
\underbrace{\begin{bmatrix}
v_1 \\ v_2 \\ v_3 \\ v_4 \\ v_5 \\ v_6
\end{bmatrix}}_{\boldsymbol{v}(t)}
$$

$$
=\ \underbrace{\begin{bmatrix}
0 & 0 & 0 & 0 & 0 & 0
\end{bmatrix}}_{\mathbf{0}}
$$

2.1.2   Undamped, Linear Mass-Spring Chain with Rigid-Body Motion

In this and in the next section, we look at mass-spring networks—prototypical lumped-parameter mechanical vibration systems. Mass-spring networks not only are worthy of study in their own right, but also model other types of systems, such as linearized power networks, quite well. This further adds to their importance. Here, we consider a simple linear chain of masses and springs; we will make the connection to power networks later in the chapter.

Consider a set of n masses connected as in Figure 2.2. There is no damping (no friction). The masses can move only horizontally, back and forth, as shown in the figure.
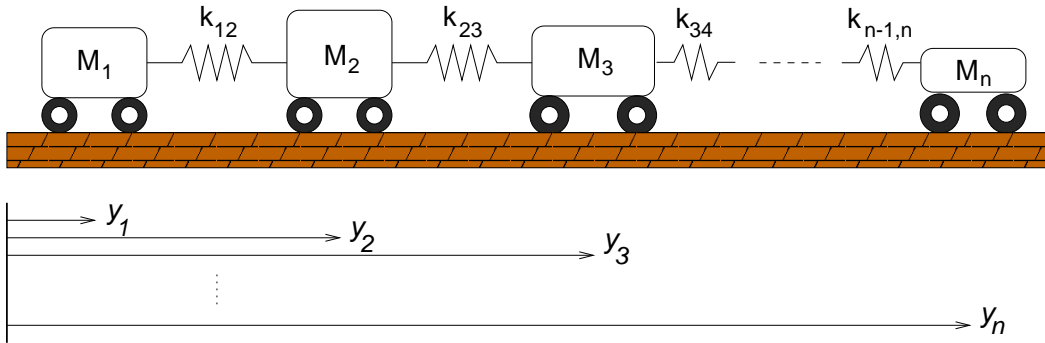
Figure 2.2: Undamped, unforced mass-spring network.

Let M_i and $y_i(t)$, $i = 1, \ldots, n$ denote the vertex weights and displacements, respectively. The springs are initially at rest. We formulate the dynamic equations through a straight-forward application of Newton's second law of motion and Hooke's law for linear springs:

$$M_1 \ddot{y}_1 = k_{12}(y_2 - y_1) \tag{2.5}$$

$$\vdots$$

$$M_i \ddot{y}_i = k_{i+1,i}(y_{i+1} - y_i) - k_{i-1,i}(y_i - y_{i-1}) \tag{2.6}$$

$$\vdots$$

$$M_n \ddot{y}_n = -k_{n-1,n}(y_n - y_{n-1}) \, . \tag{2.7}$$

Rewriting in matrix-vector form, we have:

$$\underbrace{\begin{bmatrix} M_1 & & & & \\ & \ddots & & & \\ & & M_i & & \\ & & & \ddots & \\ & & & & M_n \end{bmatrix}}_{\mathbf{B}} \underbrace{\begin{bmatrix} \ddot{y}_1(t) \\ \vdots \\ \ddot{y}_i(t) \\ \vdots \\ \ddot{y}_n(t) \end{bmatrix}}_{\ddot{\boldsymbol{y}}(t)} + \underbrace{\begin{bmatrix} k_{12} & -k_{12} & & & \\ -k_{12} & k_{12}+k_{23} & -k_{23} & & \\ & -k_{23} & \ddots & -k_{n-1,n} & \\ & & -k_{n-1,n} & k_{n-1,n} & \end{bmatrix}}_{\mathbf{L}} \underbrace{\begin{bmatrix} y_1(t) \\ \vdots \\ y_i(t) \\ \vdots \\ y_n(t) \end{bmatrix}}_{\boldsymbol{y}(t)} = \mathbf{0} \ .$$

$$(2.8)$$

In other words, the equation governing the dynamics of this linear chain of masses and springs is given by the second-order differential (or differential-algebraic) equation

$$\mathbf{B}\,\ddot{\boldsymbol{y}}(t) + \mathbf{L}\,\boldsymbol{y}(t) = \mathbf{0} \ . \tag{2.9}$$

2.1.3 Vibrational Mass-Spring Grid Capable of Rigid-Body Motion

One of the most widely-used linear models for the dynamics of electric power networks is that of a mass-spring grid, which is a topological generalization of the linear chain that we considered in the previous section. The mass-spring grid well illustrates how graphs can be used to model dynamic networks, such as power systems.

Consider an imaginary horizontal plane on which we place n point masses, serving as our graph vertices and with respective weights given by $(M_1, \ldots, M_n$. The movement of each node is restricted to be along an imaginary, thin, rigid rod, oriented perpendicularly with respect to the plane. The nodes are connected to each other through a set of ideal linear springs that serve as graph edges, with respective weights a_{ij} connecting nodes i and j. Each spring exerts zero vertical force when the two mass nodes at its terminal ends are at the same vertical position, i.e., $z_j(t) = z_i(t)$. We shall ignore the effects of gravity.

Let

$\mathbf{A} = (a_{ij}) \quad \triangleq \quad$ Adjacency matrix of spring constants.

                 We consider only networks with no self-loops, $a_{ii} = 0 \quad \forall i$,

                 and, by convention, $a_{ij} = 0$ if nodes i and j are not connected.

$$\mathbf{D} \ \triangleq \ \mathsf{diag}\,(d_1, \ldots, d_i, \ldots, d_n)$$

$$\triangleq \ \text{Diagonal matrix of node degrees} \ \left(d_i = \sum_{j=1}^{n} a_{ij}\right)$$

$$\mathbf{L} \ \triangleq \ \mathbf{D} - \mathbf{A} \triangleq \text{Laplacian matrix for the mass-spring grid}$$

$$\mathbf{B} \ \triangleq \ \mathsf{diag}\,(M_1, \ldots, M_n)$$

$$\triangleq \ \text{Diagonal matrix of node weights}$$

$$h_{ij} \ \triangleq \ \text{Constant horizontal separation between nodes } i \text{ and } j.$$

$$r_{ij}(t) \ \triangleq \ \sqrt{h_{ij}^2 + [z_j(t) - z_i(t)]^2}$$

$$\triangleq \ \text{Extended separation between nodes } i \text{ and } j,$$

$$\text{when the spring connecting them is stretched.}$$

$$\boldsymbol{z}(t) \ \triangleq \ \begin{bmatrix} z_1(t) \\ \vdots \\ z_i(t) \\ \vdots \\ z_n(t) \end{bmatrix} \triangleq \text{Vertical node displacement vector (at time } t)$$

$$\boldsymbol{f}(t) \ \triangleq \ \begin{bmatrix} f_1(t) \\ \vdots \\ f_i(t) \\ \vdots \\ f_n(t) \end{bmatrix} \triangleq \text{Vertical force vector (at time } t)$$

Consider two nodes i and j, at vertical positions z_i and z_j, respectively, which are connected by a spring of elasticity a_{ij}. We have dropped the time dependence for notational simplicity, although it should be understood that the position and force terms have a dependence on time t. Looking at Figure (2.3), we note that the force acting on node i, along the positive $z-$axis and due to node j, is given by:

$$f_i^{(j)} = a_{ij} r_{ij} \sin(\alpha_{ij}) = a_{ij} r_{ij} \frac{z_j - z_i}{r_{ij}} = a_{ij}(z_j - z_i) \,. \tag{2.10}$$

Note that $f_i^{(i)} = 0$ for obvious reasons, and $f_i^{(j)} = 0$ if nodes i and j are not adjacent, *i.e.*, if there is no edge connecting them. The total vertical force acting on node i, due to all other
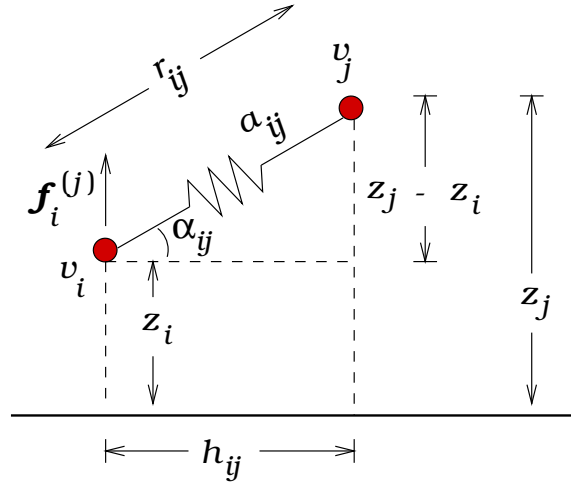
Figure 2.3: Adjacent nodes i and j, at vertical positions z_i and z_j, respectively. Force $f_i^{(j)}$ is the vertical component of the force that acts on node i, due to its connection with node j.

nodes in the graph, is therefore given by

$$f_i = \sum_{j=1}^n f_i^{(j)} = \sum_{j=1}^n a_{ij}(z_j - z_i) \, . \tag{2.11}$$

Stacking up these equations (one equation for every node), we obtain the force vector:

$$
\boldsymbol{f} \;=\; \begin{bmatrix} f_1 \\ \vdots \\ f_i \\ \vdots \\ f_n \end{bmatrix} = \begin{bmatrix} \sum_{j=1}^n a_{1j}(z_j - z_1) \\ \vdots \\ \sum_{j=1}^n a_{ij}(z_j - z_i) \\ \vdots \\ \sum_{j=1}^n a_{nj}(z_j - z_n) \end{bmatrix} = - \begin{bmatrix} \sum_{j=1}^n a_{1j}(z_1 - z_j) \\ \vdots \\ \sum_{j=1}^n a_{ij}(z_i - z_j) \\ \vdots \\ \sum_{j=1}^n a_{nj}(z_n - z_j) \end{bmatrix}
$$

$$
= \; - \begin{bmatrix} \left(\sum_{j=1}^n a_{1j}\right) z_1 - \sum_{j=1}^n a_{1j} z_j \\ \vdots \\ \left(\sum_{j=1}^n a_{ij}\right) z_i - \sum_{j=1}^n a_{ij} z_j \\ \vdots \\ \left(\sum_{j=1}^n a_{nj}\right) z_n - \sum_{j=1}^n a_{nj} z_j \end{bmatrix} = - \begin{bmatrix} d_1 z_1 - \sum_{j=1}^n a_{1j} z_j \\ \vdots \\ d_i z_i - \sum_{j=1}^n a_{ij} z_j \\ \vdots \\ d_n z_n - \sum_{j=1}^n a_{nj} z_j \end{bmatrix}
$$

We note that

$$\boldsymbol{f} = -\left(\mathbf{D}\,\boldsymbol{z} - \mathbf{A}\,\boldsymbol{z}\right) = -(\mathbf{D} - \mathbf{A})\,\boldsymbol{z} = -\mathbf{L}\,\boldsymbol{z} \, . \tag{2.12}$$

From Newton's Law, we know that $f = \mathbf{B}\,\ddot{z}$. We now can readily obtain the equation governing the dynamic behavior of the mass-spring grid. Noting that $\mathbf{B}\,\ddot{z} = -\mathbf{L}\,z$, we arrive at the dynamic equation of the undamped mass-spring grid:

$$\mathbf{B}\,\ddot{z} + \mathbf{L}\,z = \mathbf{0} \ . \tag{2.13}$$

Equations (2.13) and (2.9) are identical in general form. The distinction between them lies in the Laplacian matrix $\mathbf{L}$ that represents the topology and interconnection weights of each network. For the linear chain example the Laplacian matrix is tridiagonal, whereas in the mass-spring grid it has a more general structure that depends on the particular way in which the network vertices are interconnected. We can further generalize our mass-spring example by not insisting that the network correspond to a planar structure. Non-planar oscillatory networks can be found in applications such as power systems.

2.1.4   Electric Power Networks

Electromechanical models of large-scale multi-machine power systems constitute another important class of networks with second-order dynamics. The importance of understanding the behavior of these large-scale systems was highlighted by the repeated failures of the power grid, resulting in extensive blackouts in the western United States, in the summer of 1996. From a purely theoretical standpoint, too, power systems motivate a rich set of problems in analysis, model reduction, and control.

We are concerned with a particular type of power-system representation, namely, the undamped, linearized, swing-equation model.[1] This simple representation is one that cuts through the clutter of unnecessary details, and facilitates an understanding of the salient dynamic features of the system. In particular, we can learn much about a power network's behavior by linearizing its governing dynamic equation about an equilibrium operating position. This linearized model is a natural analogue of the mechanical vibration networks of the previous sections, and it has a straightforward graph representation. Figure 2.4 shows a simple power network comprising three machines (generators) and two loads [2].

Each bus (represented by a thick horizontal line segment) constitutes a node in the network. A graph representation of this system is shown in Figure 2.5. Generator nodes (or

---

[1]The presentation here very closely follows that given in [41].

G-nodes, as we shall call them) are shown in solid color whereas load nodes (or L-nodes) are depicted with hollow circles. This will be our convention throughout the thesis.
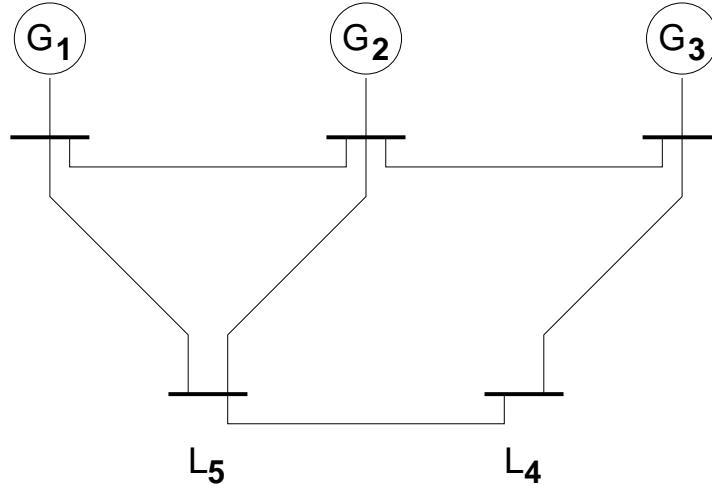
Figure 2.4: A seven-node power network with three generator and two load buses.
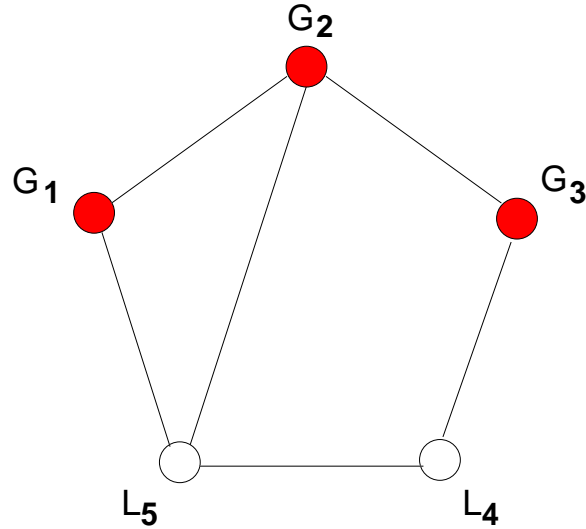
Figure 2.5: The graph representation of the three-machine, two-load power network.

We first set our notation. Let

$$\mathbf{J} = \mathsf{diag}\,(M_1, \ldots, M_{n_\mathsf{G}}) \stackrel{\triangle}{=} \text{Real diagonal}$$
$$\text{matrix of normalized generator inertias}$$
$$\mathbf{S} \stackrel{\triangle}{=} \text{Network susceptance matrix} \ (\in \mathbb{R}^{n \times n})$$

$$
v \;=\; \begin{bmatrix} v_{\mathsf{G}} \\ v_{\mathsf{L}} \end{bmatrix} \triangleq \text{Bus voltage magnitudes } (\in \mathbb{R}^n)
$$

$$
\delta \;=\; \begin{bmatrix} \delta_{\mathsf{G}} \\ \delta_{\mathsf{L}} \end{bmatrix} \triangleq \text{Bus voltage phase angles } (\in \mathbb{R}^n)
$$

$$
p_{\mathsf{G}}^{\mathsf{I}} \;\triangleq\; \text{Mechanical power injection at}
$$
$$
\text{generators}(\in \mathbb{R}^{n_{\mathsf{G}}})
$$

$$
p_{\mathsf{L}}^{\mathsf{I}}(v) \;\triangleq\; \text{Injected active power at } \textit{load}
$$
$$
\text{buses } (\in \mathbb{R}^{n_{\mathsf{L}}})
$$

$$
p^{\mathsf{I}}(v) \;=\; \begin{bmatrix} p_{\mathsf{G}}^{\mathsf{I}} \\ p_{\mathsf{L}}^{\mathsf{I}} \end{bmatrix} (\in \mathbb{R}^n)
$$

$$
p^{\mathsf{N}}(\delta, v) \;=\; \begin{bmatrix} p_{\mathsf{G}}^{\mathsf{N}}(\delta, v) \\ p_{\mathsf{L}}^{\mathsf{N}}(\delta, v) \end{bmatrix} \triangleq \text{Active power absorbed by}
$$
$$
\text{the network at buses } (\in \mathbb{R}^n)
$$

2.1.4.1   Structure-Preserving Swing Model

Representing the generators in classical undamped form, the electromechanical power balance laws lead to the following nonlinear *differential-algebraic equation (DAE)* that governs the power system:

$$
\mathbf{J}\ddot{\delta}_{\mathsf{G}} \;=\; p_{\mathsf{G}}^{\mathsf{I}} - p_{\mathsf{G}}^{\mathsf{N}}(\delta, v) \tag{2.14a}
$$

$$
0 \;=\; p_{\mathsf{L}}^{\mathsf{I}}(v) - p_{\mathsf{L}}^{\mathsf{N}}(\delta, v) \quad . \tag{2.14b}
$$

The ith component of $p^{\mathsf{N}}(\delta, v)$ is given by

$$
p_i^{\mathsf{N}}(\delta, v) = v_i \sum_{j=1}^{n} [\mathbf{S}]_{ij} \, v_j \, \sin(\delta_i - \delta_j) \quad . \tag{2.15}
$$

The factor $[\mathbf{S}]_{ij}$ denotes the transmission line susceptance between buses i and j. We have omitted writing the algebraic balance equations for the reactive power q as these are not explicitly needed for what follows, although they are important in completing the model

(2.14).

Linearizing (2.14) about an equilibrium $(\boldsymbol{\delta}_0, \boldsymbol{v}_0)$ (whose computation requires the algebraic balance equations for $\boldsymbol{q}$ along with the equations in (2.14) above) and assuming approximate $(\boldsymbol{p},\boldsymbol{\delta})$ and $(\boldsymbol{q},\boldsymbol{v})$ decoupling, we have, in matrix form,

$$
\underbrace{\begin{bmatrix} \mathbf{J} & \mathbf{0} \\ \mathbf{0} & \mathbf{0} \end{bmatrix}}_{\mathbf{B}} \begin{bmatrix} \Delta\ddot{\boldsymbol{\delta}}_{\mathsf{G}} \\ \Delta\ddot{\boldsymbol{\delta}}_{\mathsf{L}} \end{bmatrix} = - \begin{bmatrix} \frac{\partial}{\partial \boldsymbol{\delta}} \boldsymbol{p}_{\mathsf{G}}^{\mathrm{N}}(\boldsymbol{\delta}_0, \boldsymbol{v}_0) \\ \frac{\partial}{\partial \boldsymbol{\delta}} \boldsymbol{p}_{\mathsf{L}}^{\mathrm{N}}(\boldsymbol{\delta}_0, \boldsymbol{v}_0) \end{bmatrix} \begin{bmatrix} \Delta\boldsymbol{\delta}_{\mathsf{G}} \\ \Delta\boldsymbol{\delta}_{\mathsf{L}} \end{bmatrix}
$$

$$
= - \underbrace{\begin{bmatrix} \mathbf{L}_{\mathsf{G}} & \mathbf{L}_{\mathsf{GL}} \\ \mathbf{L}_{\mathsf{LG}} & \mathbf{L}_{\mathsf{L}} \end{bmatrix}}_{\mathbf{L}} \begin{bmatrix} \Delta\boldsymbol{\delta}_{\mathsf{G}} \\ \Delta\boldsymbol{\delta}_{\mathsf{L}} \end{bmatrix} \tag{2.16}
$$

or more compactly,

$$
\mathbf{B}\,\Delta\ddot{\boldsymbol{\delta}} + \mathbf{L}\,\Delta\boldsymbol{\delta} = \mathbf{0} \,. \tag{2.17}
$$

The vector $\Delta\boldsymbol{\delta} \in \mathbb{R}^n$ denotes the perturbation from the operating point $(\boldsymbol{\delta}_0, \boldsymbol{v}_0)$, and the matrices $\mathbf{B} \in \mathbb{R}^{n\times n}$ and $\mathbf{L} \in \mathbb{R}^{n\times n}$ are defined as in (2.16). Note that $[\mathbf{L}]_{ij}$, the $(ij)^{\text{th}}$ entry in $\mathbf{L}$, is

$$
[\mathbf{L}]_{ij} = \begin{cases} -v_i\, v_j\, [\mathbf{S}]_{ij} \cos(\delta_i - \delta_j) & \text{if } i \neq j \\[2mm] -\displaystyle\sum_{\ell=1, \ell\neq i}^{n} [\mathbf{L}]_{i\ell} & \text{if } i = j \end{cases} \tag{2.18}
$$

Equation (2.17) has the same general form as the dynamic equations (2.13), (2.9), and (2.4) for the previous cases that we studied. In terms of its analogy with the mass-spring mechanical vibration network, it is easily seen that the generator inertias denoted by J_i correspond to positive masses M_i, loads (having no inertia) correspond to weightless masses, and $\Delta\boldsymbol{\delta}$ corresponds to the mass displacement vector $\boldsymbol{y}(t)$ (or $\boldsymbol{z}(t)$) in the mechanical systems. The same underlying structure describes the systems that we have looked at in this chapter, by way of examples of oscillatory networks. There must, therefore, be a unifying theory that can describe all these systems simultaneously. It is a number of the various facets of that unifying theory that we have investigated in our research and that we will articulate in this thesis.

2.2   What's the Link to Graph Theory?

In all the systems that we have considered so far, there are striking resemblances beyond the mere general form of the dynamic equations (2.4), (2.9), (2.13), and (2.17), or the diagonal form of the node-weight matrix $\mathbf{B}$. Of great significance—and one that we will study in detail—is the structure of the matrix $\mathbf{L}$ and its effects on the modal behavior (natural frequencies and mode shapes) of the oscillatory network that it represents. The spectral properties of the matrix pair $(\mathbf{L}, \mathbf{B})$ will be our main object of study throughout this thesis.

So far, it is important to notice the following properties of the $\mathbf{L}$ matrix:

1. It is symmetric.

2. When there is no isolated node (i.e., when the network is "connected"), $\mathbf{L}$ has positive diagonal elements.

3. It has non-positive off-diagonal elements.

4. The sum of the entries in each row (and by symmetry, in each column) of $\mathbf{L}$ is zero. So the vector $\mathbf{1}$ and the eigenvalue $\lambda = 0$ form an eigenpair of the network. This corresponds to rigid-body motion wherein the entire network moves as a whole.

5. The structure of $\mathbf{L}$ tells us immediately how the network is interconnected. In other words, we can extract every information about the network topology (including edge weights) from $\mathbf{L}$. Together with the node-weight matrix $\mathbf{B}$, it is all that we need to find the dynamic behavior of the network.

The matrix $\mathbf{L}$—which, as noted earlier, in graph-theoretic language is called the Laplacian matrix—plays a crucial role in determining how the system behaves. We will see in the course of our discussions that if $\mathbf{L}$ has, say, acyclic structure (i.e., if the underlying network has a tree graph representation), then the eigenvectors exhibit sign-alternation properties in their entries, patterns that are dependent on the index number of the mode they correspond to; for example, the number of sign alternations in the eigenvector entries, corresponding to adjacent nodes, increases as the mode number increases.

The Laplacian matrix $\mathbf{L}$ falls under the category of M-matrices, which we will describe later in the thesis. Such matrices have properties that can be exploited in learning more about how the eigenvector components relate to each other. For example, we will show in

Chapter 4 that each eigenvector component corresponding to a weightless node (L-node) is a convex combination of the components corresponding to all its immediate neighbors, and also a convex combination of all the eigenvector entries in the G-nodes that surround it (whether or not they are its immediate neighbors).

These insights all are obtained from the properties of the $\mathbf{L}$ matrix. It is the fact that the general structure of this matrix is common among all the oscillatory networks of interest to us—including the sample networks that we have touched on in this chapter—that makes the study of the Laplacian matrix and its connection to spectral graph theory very important.

2.3 State-Space Models and Spectral Graph Theory

The undriven, conservative oscillatory networks that we consider in this thesis, some examples of which we have presented in this chapter, are governed by a dynamic equation with a second-order differential form,[2] as in the following:

$$\mathbf{B}\,\ddot{\boldsymbol{y}}(t) + \mathbf{L}\,\boldsymbol{y}(t) = \mathbf{0}\;. \tag{2.19}$$

Here, $\mathbf{B} \overset{\triangle}{=} \mathsf{diag}\,(M_1,\dots,M_n)$ is the diagonal matrix of nonnegative node weights, $\mathbf{L}$ is the Laplacian matrix of network admittances (containing topological and edge-weight information about the network), and $\boldsymbol{y}(t)$ is the node displacement vector. With a substitution of variables, we can find a generalized state-space representation for any nondissipative dynamic network that is governed by (2.19). Simply let $\boldsymbol{x}_1(t) = \boldsymbol{y}(t)$ and $\boldsymbol{x}_2(t) = \dot{\boldsymbol{y}}(t)$. The two portions of the state vector $\boldsymbol{x}(t) \overset{\triangle}{=} [\boldsymbol{x}_1(t)\;\boldsymbol{x}_2(t)]^{\mathsf{T}}$ are related according to the following:

$$\dot{\boldsymbol{x}}_1(t) = \dot{\boldsymbol{y}}(t) = \boldsymbol{x}_2(t) \tag{2.20}$$

$$\dot{\boldsymbol{x}}_2(t) = \ddot{\boldsymbol{y}}(t) \quad \Longrightarrow \quad \mathbf{B}\,\dot{\boldsymbol{x}}_2(t) = \mathbf{B}\,\ddot{\boldsymbol{y}}(t) = -\mathbf{L}\,\boldsymbol{y}(t) = -\mathbf{L}\,\boldsymbol{x}_1(t)\;. \tag{2.21}$$

As expected, the state vector for the system comprises node displacements $\boldsymbol{y}(t)$ and node velocities $\dot{\boldsymbol{y}}(t)$. A generalized state-space representation for the system is given by the

---

[2]Equation (2.19) has a differential-algebraic form if $\mathbf{B}$ has diagonal entries that are zero, corresponding to weightless nodes

evolution equation

$$\underbrace{\begin{bmatrix} \mathbf{I} & \mathbf{0} \\ \mathbf{0} & \mathbf{B} \end{bmatrix}}_{\mathbf{E}} \underbrace{\begin{bmatrix} \dot{\boldsymbol{x}}_1(t) \\ \dot{\boldsymbol{x}}_2(t) \end{bmatrix}}_{\dot{\boldsymbol{x}}(t)} = \underbrace{\begin{bmatrix} \mathbf{0} & \mathbf{I} \\ -\mathbf{L} & \mathbf{0} \end{bmatrix}}_{\mathbf{F}} \underbrace{\begin{bmatrix} \boldsymbol{x}_1(t) \\ \boldsymbol{x}_2(t) \end{bmatrix}}_{\boldsymbol{x}(t)} . \tag{2.22}$$

Naturally, for a network with n nodes, the system will have $2n$ state variables, and hence $2n$ eigenvalues (including multiplicities) and $2n$ eigenvectors.[3] We have kept (2.22) in the generalized state-space form

$$\mathbf{E}\,\dot{\boldsymbol{x}}(t) = \mathbf{F}\,\boldsymbol{x}(t)$$

to accommodate cases in which the network has weightless nodes. If each node has a strictly positive weight, then $\mathbf{B}$ is invertible (and hence so is $\mathbf{E}$), and the generalized state-space representation (2.22) may be converted to the standard form $\dot{\boldsymbol{x}}(t) = \mathbf{A}\,\boldsymbol{x}(t)$. The ordinary state-transition matrix $\mathbf{A}$ can be written as

$$\mathbf{A} = \begin{bmatrix} \mathbf{0} & \mathbf{I} \\ -\mathbf{B}^{-1}\,\mathbf{L} & \mathbf{0} \end{bmatrix} .$$

The natural frequencies and modal vectors of the oscillatory network are the generalized eigenvalues and eigenvectors of the matrix pair $(\mathbf{F}, \mathbf{E})$, and are closely related to the eigenvalues and eigenvectors of $(\mathbf{L}, \mathbf{B})$ in (2.19). One way to show this is to apply the standard technique for finding the solutions of linear, constant-coefficient differential (or differential-algebraic) equations. That is, let the displacement vector $\boldsymbol{y}(t)$ have the form

$$\boldsymbol{y}(t) = \boldsymbol{v}\,e^{j\omega t} . \tag{2.23}$$

Inserting (2.23) in (2.19) leads to

$$\left(-\omega^2 \mathbf{B}\,\boldsymbol{v} + \mathbf{L}\,\boldsymbol{v}\right)\,e^{j\omega t} = \mathbf{0} ,$$

which further simplifies to the symmetric, generalized eigenproblem

$$\mathbf{L}\,\boldsymbol{v} = \omega^2\,\mathbf{B}\,\boldsymbol{v} . \tag{2.24}$$

Clearly, $\boldsymbol{v}$ is a generalized eigenvector of the matrix pair $(\mathbf{L}, \mathbf{B})$. Moreover, if we let λ denote the generalized eigenvalue corresponding to $\boldsymbol{v}$, then ω and λ are related by $\lambda = \omega^2$.

---

[3]We are guaranteed to have $2n$ eigenvectors because of the symmetry of $(\mathbf{L}, \mathbf{B})$; in other words, the matrix pair is non-defective.

In other words, we are interested in the eigenproblem:

$$\mathbf{L}\,\boldsymbol{v} = \lambda\,\mathbf{B}\,\boldsymbol{v}\,. \tag{2.25}$$

The network's $2n$ natural frequencies ω are obtained from the n generalized eigenvalues λ of $(\mathbf{L}, \mathbf{B})$ as follows:

$$\omega = \pm\sqrt{\lambda}\,.$$

It is straightforward to verify that $j\omega_i$ and $-j\omega_i$, $i = 1, \ldots, n$, are generalized eigenvalues of the pair $(\mathbf{F}, \mathbf{E})$, with respective generalized eigenvectors

$$\begin{bmatrix} \boldsymbol{v}_i \\ j\omega_i\,\boldsymbol{v}_i \end{bmatrix} \qquad \text{and} \qquad \begin{bmatrix} \boldsymbol{v}_i \\ -j\omega_i\,\boldsymbol{v}_i \end{bmatrix}\,.$$

Clearly, the graph model of a conservative oscillatory network ties directly with the state-space representation of the system, and hence with the network's dynamic behavior. Knowing the eigenvalues and eigenvectors of the Laplacian/node-weight matrix pair $(\mathbf{L}, \mathbf{B})$ is tantamount to knowing the natural frequencies and mode shapes of the network's oscillations. It is this transparency between the graph and state-space models that motivated us to undertake the study culminating in this thesis. Our aim has been to bridge the gap between graph theory (which provides a wealth information about network spectra) and the traditional state-space analysis, which describes the dynamics of the system.

M-*Matrices, Laplacian Matrices, and a Symmetric Generalized Eigenproblem*

In Chapter 2, we saw how the Laplacian matrix arose in every one of the dynamic networks that we surveyed. It was there, too, that we outlined some of the more visible features of the matrix pair $(\mathbf{L}, \mathbf{B})$. This chapter, and the early part of the next, form the matrix-theoretic backbone of the thesis. Here, we shall focus on the details of the transparent features of the Laplacian matrix that we identified previously. We also will delve into other, less apparent, properties of Laplacian matrices, and use them to develop new results governing the modal behavior of dynamic graphs.

There are many excellent review articles and book chapters that deal with Laplacian matrices [59, 60, 61, 63, 62, 29, 57] and even a book that focuses on their properties [14]. Indeed, much is known about them. In this chapter, we will cover the essentials that we need for our study of oscillatory networks.

Laplacian matrices form a subset of a broader class of matrices known as M-matrices; to be more precise, Laplacian matrices are a subset of singular M-matrices (also termed matrices of class K_0 by Fiedler and Pták [31]). We will survey some of the important properties of M-matrices, and use them to establish certain features of Laplacian matrices that we will need in our subsequent discussion.

In this chapter, too, we describe the eigenproblem that lies at the heart of the dynamic analysis of linear oscillatory networks. To set our language and notation, we recall the eigenproblem (2.25), written below for the ith mode of a linear oscillatory network:

$$\mathbf{L}\,\boldsymbol{v}_i = \lambda_i\,\mathbf{B}\,\boldsymbol{v}_i\,, \qquad i = 1, \ldots, n\,. \tag{3.1}$$

We will consider a symmetric generalized eigenproblem (SGEP), as depicted by (3.1), where $\mathbf{B}$ is a diagonal matrix of nonnegative entries, and $\mathbf{L}$ is the Laplacian matrix of the

underlying network graph. First, we define the two types of graph vertices that appear in the oscillatory networks that we study.

Definition 3.1 (*Gravis* Node)
A gravis *node (or equivalently, a* G*-node or a* G*-type node), is one whose weight is strictly positive, but finite. The name is inspired from the Latin word, meaning "weighty."*

Definition 3.2 (*Levis* Node)
A levis node *(or equivalently, an* L*-node or an* L*-type node), is one whose weight is zero. The name is inspired from the Latin word, meaning "light-weight."*

You already have seen examples of these two types of nodes. As a mnemonic, think of G-nodes as "generators" in a power system, and L-nodes as "loads." A generator has inertia (hence a positive node weight) whereas a load does not. Node 6 in Example 2.1.1 and nodes 4–7 in Example 2.1.4 are L-nodes.

These two types of nodes are qualitatively different; the presence of even one L-node changes the dynamic equation governing the network, from a second-order differential equation to a second-order differential-algebraic (DAE) equation. As we shall see in this chapter, the presence of L-nodes also introduces eigenvalues at infinity in the SGEP (3.1), because the presence of such nodes makes the node-weight matrix $\mathbf{B}$ singular. It is our task in this chapter, and in the early part of the next, to sort out this and other matrix-theoretic issues, and set the stage for our analysis of the dynamics of linear oscillatory networks.

3.1   M-**Matrices and Some of Their Salient Features**

In many applications, matrices arise that have nonpositive off-diagonal and nonnegative diagonal entries, as in

$$
\mathbf{Q} = \begin{bmatrix}
+q_{11} & -f_{12} & -f_{13} & \cdots & -f_{1,n-1} & -f_{1n} \\
-f_{21} & +q_{22} & -f_{23} & \cdots & -f_{2,n-1} & -f_{2n} \\
\vdots & & & & & \vdots \\
-f_{n1} & -f_{n2} & -f_{n3} & \cdots & -f_{n,n-1} & +q_{nn}
\end{bmatrix},
\tag{3.2}
$$

where the f_{ij} and q_{ii} are nonnegative. These matrices can be expressed as

$$\mathbf{Q} = s\mathbf{I} - \mathbf{F}\,, \quad \text{where} \quad s > 0 \quad \text{and} \quad \mathbf{F} \succeq \mathbf{0}\,. \tag{3.3}$$

Naturally, from (3.3) we expect that there is a strong connection between nonnegative matrices and matrices with structure (3.2). Indeed, this is the case, and we shall make occasional use of one of the most celebrated results in the theory of nonnegative matrices, the Perron-Frobenius theorem.

M-matrices, which are a subset of those depicted by (3.2), arise in many different contexts, including graph-theoretic settings; see, for example, Fiedler and Pták [31], or Fiedler [28], where the terms "class K" and "class K_0" are coined, in reference to nonsingular and singular M-matrices, respectively.

Laplacian matrices, as we will show, fall under singular M-matrices (class K_0). It is also known that any principal submatrix of an irreducible Laplacian matrix is nonsingular—a property that will play an important role in our subsequent work. In fact, this property is known to hold for all irreducible singular M-matrices; we will go over the proof later in this chapter. Principal submatrices of Laplacian matrices are also called "grounded" Laplacian matrices, a term that almost certainly is inspired from applications in electronic circuit theory, where one or more nodes of the network are grounded. Grounded Laplacian matrices for connected networks are nonsingular M-matrices (class K).

There are several excellent references that discuss the properties of M-matrices in detail. For example, see the seminal paper by Fiedler and Pták [31], the indispensable book by Fiedler [28], the classic text by Berman and Plemmons [3], the ubiquitous reference volume by Horn and Johnson [48], and a readable textbook by Graham [40]. Although its coverage of M-matrices is scant, the textbook by Bapat and Raghavan [1] is a valuable resource for nonnegative matrices.

We begin with a few preliminary definitions, lemmas, and theorems, the proofs for some of which we relegate to the reference texts mentioned above.

Definition 3.3 (Cogredient Matrices)
Two $n \times n$ matrices $\mathbf{A}$ and $\mathbf{G}$ are cogredient, *if $\mathbf{G} = \mathbf{P}\mathbf{A}\mathbf{P}^{\mathsf{T}}$ for some permutation matrix $\mathbf{P}$.*

Definition 3.4 (Reducibility)

An $n \times n$ matrix $\mathbf{A}$ is reducible if it is cogredient with

$$\mathbf{G} = \begin{bmatrix} \mathbf{C} & \mathbf{0} \\ \mathbf{D} & \mathbf{E} \end{bmatrix} ,$$

where $\mathbf{C}$ and $\mathbf{E}$ are square matrices. Naturally, a symmetric matrix $\mathbf{A}$ is reducible if it is cogredient with

$$\mathbf{G} = \begin{bmatrix} \mathbf{C} & \mathbf{0} \\ \mathbf{0} & \mathbf{E} \end{bmatrix} ,$$

where $\mathbf{C}$ and $\mathbf{E}$ are symmetric. A matrix is irreducible if it is not reducible.

Theorem 3.5 (The Perron-Frobenius Theorem)

(a) (Perron) *Let $\mathbf{A} \succ \mathbf{0}$ be an $n \times n$ matrix. Then there exists $\boldsymbol{x} \succ \mathbf{0}$ such that $\mathbf{A}\,\boldsymbol{x} = \varrho(\mathbf{A})\,\boldsymbol{x}$; the spectral radius $\varrho(\mathbf{A})$ is an algebraically (and hence geometrically) simple eigenvalue of $\mathbf{A}$; and any other eigenvalue $\lambda(\mathbf{A})$ satisfies $|\lambda(\mathbf{A})| < \varrho(\mathbf{A})$.*

(b) (Frobenius) *Let $\mathbf{A} \succcurlyeq \mathbf{0}$ be an irreducible $n \times n$ matrix. Then $\mathbf{A}\,\boldsymbol{x} = \varrho(\mathbf{A})\,\boldsymbol{x}$ for some $\mathbf{x} \succ \mathbf{0}$; any eigenvalue $\lambda(\mathbf{A})$ other than $\varrho(\mathbf{A})$ satisfies $|\lambda(\mathbf{A})| \leq \varrho(\mathbf{A})$; the eigenvalue $\varrho(\mathbf{A})$ is simple (algebraically and hence geometrically); and any other eigenvalue $\lambda(\mathbf{A})$ whose modulus satisfies $|\lambda(\mathbf{A})| = \varrho(\mathbf{A})$, is also simple.*

Lemma 3.6

A nonnegative matrix $\mathbf{F}$ is irreducible if, and only if, for every (i, j), there exists a natural number q such that $f_{ij}^{(l)} > 0$. [1]

Proof: See Berman and Plemmons [3, Theorem 2.1, p. 29].

Corollary 3.7

Let $\mathbf{F}$ and $f_{ij}^{(k)}$ be as defined in Lemma 3.6. Then, for some $r \geq 1$,

$$\sum_{i=0}^{r} \mathbf{F}^i = \mathbf{F} + \mathbf{F}^2 + \cdots + \mathbf{F}^r \succ \mathbf{0} .$$

---

[1] *By $f_{ij}^{(l)}$ we mean the $(i, j)^{th}$ entry of $\mathbf{F}^l$.*

Definition 3.8 (Z-Matrices)

Matrices of class Z_n (or Z_n-matrices) are real, square matrices of size $n \geq 1$, whose off-diagonal entries are nonpositive. That is,

$$Z_n = \left\{ \mathbf{Z} = (z_{ij}) \in \mathbb{R}^{n \times n} \,|\, z_{ij} \leq 0 \,, i \neq j \right\} \,. \tag{3.4}$$

The union of all Z_n is

$$Z = \bigcup_{n=1}^{\infty} Z_n \,.$$

Where the size of a Z_n-matrix is unambiguous, or somehow not pertinent to the context, we simply refer to it as a Z-matrix, or as a matrix of class Z.

Theorem 3.9 (Equivalence Properties of Z-Matrices)

Let $\mathbf{A} \in Z$. Then the following conditions are equivalent to each other:
(a) Each real eigenvalue of $\mathbf{A}$ is positive;
(b) All principal minors of $\mathbf{A}$ are positive.

Proof: See Fiedler and Pták [31, Theorem 4.3] for the proof of this equivalence pair as well as others.

Next, we give a simple definition of an M-matrix:

Definition 3.10 (M-Matrices)

A matrix $\mathbf{Q}$ is said to be an M-matrix if it is expressible in the form $\mathbf{Q} = s\mathbf{I} - \mathbf{F}$, with $\mathbf{F} \succeq \mathbf{0}$ and $s \geq \varrho(\mathbf{F})$, the spectral radius of $\mathbf{F}$. More specifically,

1. *$s > \varrho(\mathbf{F})$ means $\mathbf{Q}$ is a nonsingular M-matrix, also referred to as a matrix of class K.*

2. *$s = \varrho(\mathbf{F})$, i.e., if $\mathbf{Q} = \varrho(\mathbf{F})\,\mathbf{I} - \mathbf{F}$ means $\mathbf{Q}$ is a singular M-matrix, also known as a matrix of class K_0. Furthermore, if $\mathbf{Q} \in K_0$, then $\widehat{\mathbf{Q}} = \mathbf{Q} + \epsilon\mathbf{I} \in K$ for any $\epsilon > 0$.*

Lemma 3.11 (Convergent Nonnegative Matrices)

The $n \times n$ nonnegative matrix $\mathbf{H}$ is convergent, i.e., $\varrho(\mathbf{H}) < 1$, if, and only if, $(\mathbf{I} - \mathbf{H})^{-1}$ exists and

$$(\mathbf{I} - \mathbf{H})^{-1} = \sum_{k=0}^{\infty} \mathbf{H}^k \succcurlyeq \mathbf{0} \,.$$

Proof: See Berman and Plemmons [3, p. 133].

We now have all the necessary ingredients to prove the following well-known theorem for nonsingular M-matrices.

Theorem 3.12 (Inverse Positivity of Irreducible, Nonsingular M-Matrices)
Let $\mathbf{A}$ be a nonsingular M-matrix. Then $\mathbf{A}^{-1} \succcurlyeq \mathbf{0}$. If, in addition, $\mathbf{A}$ is irreducible, then $\mathbf{A}^{-1} \succ \mathbf{0}$.

Proof: From the definition of a nonsingular M-matrix, we know that for $s > \varrho(\mathbf{F})$,

$$\mathbf{A} = s\mathbf{I} - \mathbf{F} = s\left(\mathbf{I} - \frac{\mathbf{F}}{s}\right) .$$

Therefore,

$$\mathbf{A}^{-1} = \frac{1}{s}\left(\mathbf{I} - \frac{\mathbf{F}}{s}\right)^{-1} .$$

We know that $\varrho(\frac{\mathbf{F}}{s}) < 1$, because $s > \varrho(\mathbf{F})$. Therefore, according to Lemma 3.11, $\mathbf{A}^{-1}$ can be rewritten as follows:

$$\mathbf{A}^{-1} = \frac{1}{s}\sum_{k=0}^{\infty}\frac{\mathbf{F}^k}{s^k} . \tag{3.5}$$

Each term in the summation is nonnegative, so $\mathbf{A}^{-1} \succcurlyeq \mathbf{0}$.

If $\mathbf{A}$ is irreducible, then so is $\frac{\mathbf{F}}{s}$. Corollary 3.7, then, states that the right-hand side of (3.5) is strictly positive, i.e., $\mathbf{A}^{-1} \succ \mathbf{0}$. The proof is complete. $\qquad\square$

Corollary 3.13
Let $\mathbf{A}$ be a symmetric, reducible, nonsingular M-matrix, with degree of reducibility $r - 1$; without loss of generality, we can assume that $\mathbf{A}$ is in block diagonal form

$$\mathbf{A} = \begin{bmatrix} \mathbf{A}_1 & & \mathbf{0} \\ & \ddots & \\ \mathbf{0} & & \mathbf{A}_r \end{bmatrix} , \tag{3.6}$$

where each $\mathbf{A}_i$, $i = 1, \ldots, r$, is irreducible. Then $\mathbf{A}^{-1} \succcurlyeq \mathbf{0}$, and is of the form

$$\mathbf{A}^{-1} = \begin{bmatrix} \mathbf{A}_1^{-1} & & \mathbf{0} \\ & \ddots & \\ \mathbf{0} & & \mathbf{A}_r^{-1} \end{bmatrix} , \tag{3.7}$$

where each $\mathbf{A}_i^{-1} \succ \mathbf{0}$. *The diagonal entries are positive, i.e.,* $\left[\mathbf{A}^{-1}\right]_{ii} > 0$, *whether or not* $\mathbf{A}$ *is irreducible.*

Before proving the next important theorem—on proper principal submatrices of irreducible singular M-matrices—we need the following two lemmas.

Lemma 3.14 (Two Properties of Non-singular M-Matrices)
Let $\mathbf{A} \in Z$. *Then each of the following two properties is equivalent to the statement:* "$\mathbf{A}$ *is a non-singular* M*-matrix.*"
(a) Every real eigenvalue of $\mathbf{A}$ *is positive;*
(b) All principal minors of $\mathbf{A}$ *are positive.*

Proof: See Fiedler [28, Theorem 5.1].

Lemma 3.15 (Rank of an Adjugate Matrix)
Let $\mathbf{A}$ *be an* $n \times n$ *matrix* ($n \geq 2$), *and denote its adjugate matrix by* $\mathsf{adj}\,(\mathbf{A})$. *Then*

$$\mathsf{rank}\,(\mathsf{adj}\,(\mathbf{A})) = \begin{cases} n & \text{if } \mathsf{rank}\,(\mathbf{A}) = n \\ 1 & \text{if } \mathsf{rank}\,(\mathbf{A}) = n - 1 \\ 0 & \text{if } \mathsf{rank}\,(\mathbf{A}) \leq n - 2 \,. \end{cases} \tag{3.8}$$

In particular, if $\mathbf{A}$ *has a simple eigenvalue at* 0, *then*

$$\mathsf{adj}\,(\mathbf{A}) = \frac{\mu(\mathbf{A})}{\boldsymbol{y}^\mathsf{T}\boldsymbol{x}}\,\boldsymbol{x}\boldsymbol{y}^\mathsf{T}\,, \tag{3.9}$$

where $\mu(\mathbf{A})$ *is the product of the* $n - 1$ *non-zero eigenvalues of* $\mathbf{A}$, *and* $\boldsymbol{x}$ *and* $\boldsymbol{y}$ *are such that* $\mathbf{A}\,\boldsymbol{x} = \mathbf{0}$, *and* $\boldsymbol{y}^\mathsf{T}\mathbf{A} = \mathbf{0}$. *If, further,* $\mathbf{A}$ *is known to be symmetric—as is the case with the Laplacian matrix of a connected graph—then*

$$\mathsf{adj}\,(\mathbf{A}) = \frac{\mu(\mathbf{A})}{\|\boldsymbol{x}\|^2}\,\boldsymbol{x}\boldsymbol{x}^\mathsf{T}\,. \tag{3.10}$$

Proof: See Magnus and Neudecker [56, p. 41].

The following theorem establishes two important properties of irreducible singular M-matrices. We will make use of this theorem when we discuss the properties of the Laplacian matrix of a connected graph, as well as in the context of Schur contraction of graphs in Chapter 4.

Theorem 3.16 (Fiedler and Pták [31, Theorems 5.6 and 5.7])

Let $\mathbf{A}$ *be an irreducible, singular* M-*matrix of order* n. *Then*

(a) rank $(\mathbf{A}) = n - 1$;

(b) there exists a vector $\boldsymbol{x} \succ \mathbf{0}$ *such that* $\mathbf{A}\boldsymbol{x} = \mathbf{0}$;

(c) each proper principal submatrix of $\mathbf{A}$ *(i.e., each principal submatrix of* $\mathbf{A}$ *other than* $\mathbf{A}$ *itself) is a non-singular* M-*matrix.*

Proof: (a) Let $\mathbf{A} = \alpha\mathbf{I} - \mathbf{F}$, with $\alpha > 0$ and $\mathbf{F} \succeq \mathbf{0}$. According to Definition 3.10, $\mathbf{A}$ is a singular M-matrix when $\alpha = \varrho(\mathbf{F})$. Also, if $\mathbf{A}$ is irreducible, then so is $\mathbf{F}$. The Perron-Frobenius theorem 3.5 establishes that $\varrho(\mathbf{F})$ is a simple eigenvalue with an associated eigenvector $\boldsymbol{x} \succ \mathbf{0}$. We know, however, that the smallest eigenvalue of $\mathbf{A}$ is given by

$$\lambda_{\mathsf{min}}(\mathbf{A}) = \alpha - \varrho(\mathbf{F}) = 0 .$$

It must, therefore, be algebraically simple, so rank $(\mathbf{A}) = n - 1$.

(b) Clearly,

$$\mathbf{A}\boldsymbol{x} = (\alpha - \varrho(\mathbf{F}))\boldsymbol{x} = 0 \cdot \boldsymbol{x} = \mathbf{0} .$$

(c) To prove that each proper principal submatrix of $\mathbf{A}$ is a nonsingular M-matrix, we recall the Cauchy-Binet identity:

$$\mathbf{A} \; \mathsf{adj}(\mathbf{A}) = \det(\mathbf{A}) \, \mathbf{I} . \tag{3.11}$$

Since $\mathbf{A}$ is singular, $\det(\mathbf{A}) = 0$, and thus (3.11) becomes:

$$\mathbf{A} \; \mathsf{adj}(\mathbf{A}) = \mathbf{0} .$$

Based on Lemma 3.15, we can write $\mathsf{adj}(\mathbf{A}) = \zeta\boldsymbol{y}\boldsymbol{x}^\mathsf{T}$, where the positive vectors $\boldsymbol{x}$ and $\boldsymbol{y}$ are such that $\mathbf{A}\boldsymbol{x} = \mathbf{0}$ and $\boldsymbol{y}^\mathsf{T}\mathbf{A} = \mathbf{0}$, respectively. We know $\zeta \neq 0$ because rank $(\mathsf{adj}(\mathbf{A})) = 1$. We need to show that $\zeta > 0$. The proof of this is by contradiction. Suppose $\zeta < 0$. Then by the continuity of the determinant, there would exist an $\epsilon > 0$ such that $\mathsf{adj}(\mathbf{A} + \epsilon\mathbf{I}) \prec \mathbf{0}$. But this cannot be, because according to Definition 3.10, we know that $\mathbf{A} + \epsilon\mathbf{I} \in \mathsf{K}$, and every one of its principal submatrices must have a positive determinant. Hence, we must have $\zeta > 0$. We have thus shown that every entry in $\mathsf{adj}(\mathbf{A})$—equivalently, every order-$(n - 1)$ principal minor of $\mathbf{A}$—is positive. Clearly, all principal minors of order less than $n - 1$, too, will be positive. This completes the proof (see Theorem 3.9 and Lemma 3.14). $\square$

Before we proceed to discuss Laplacian matrices, we present a few more preliminaries.

Theorem 3.17

Let $\mathbf{A} \in \mathsf{Z}$ *be a symmetric matrix. Then*

(a) $\mathbf{A} \in \mathsf{K}$, *i.e.,* $\mathbf{A}$ *is a nonsingular* M*-matrix, if, and only if, it is positive definite. A symmetric, nonsingular* M*-matrix is also known as a* Stieltjes *matrix.*

(b) $\mathbf{A} \in \mathsf{K}_0$, *i.e.,* $\mathbf{A}$ *is a singular* M*-matrix, if, and only if, it is positive semi-definite.*

Proof: See Fiedler [28, Theorems 5.2 and 5.5, pp. 121, 123].

Theorem 3.18

Consider an $n \times n$ *matrix* $\mathbf{A} \in \mathsf{Z}$. *If there exists a vector* $\boldsymbol{x} \succ \mathbf{0}$ *such that* $\mathbf{A}\boldsymbol{x} \succeq \mathbf{0}$, *then* $\mathbf{A} \in \mathsf{K}_0$.

Proof: See Fiedler [28, Theorem 5.11, p. 124].

3.2   Salient Features of the Laplacian Matrix

We are now in a position to enumerate some of the important properties of the Laplacian matrix. From Appendix B we know that the Laplacian matrix is defined as $\mathbf{L} = \mathbf{D} - \mathbf{A}$, where $\mathbf{D}$ is the matrix of node degrees and $\mathbf{A}$ is the adjacency matrix of the graph.

Property 1. *The Laplacian matrix* $\mathbf{L}$ *associated with an undirected graph is symmetric. Therefore, all its eigenvalues are real.*

Property 2. *Let* $\mathbf{F}$ *be the oriented node-edge incidence matrix for a graph* G *with* n *nodes and* m *edges. Let* $\mathbf{E} = \mathsf{diag}\,(e_1, \ldots, e_m)$ *denote the diagonal matrix of the* m *edge weights (each* $e_l > 0$ *by definition). Then*

$$\mathbf{L} = \mathbf{F}\mathbf{E}\mathbf{F}^{\mathsf{T}} . \tag{3.12}$$

Proof: See Mohar [61], where he uses slightly different notation.

In Property 2, $\mathbf{F}\mathbf{E}\mathbf{F}^{\mathsf{T}}$ is independent of the orientation that is chosen for each of the graph edges.

Property 3. *Let* $\mathbf{x}$ *denote an arbitrary vector in* $\mathbb{R}^n$. *Then*

$$\langle \boldsymbol{x}, \boldsymbol{x} \rangle_{\mathbf{L}} \overset{\triangle}{=} \boldsymbol{x}^{\mathsf{T}}\mathbf{L}\boldsymbol{x} = \sum_{(i,j) \in E} a_{ij}(x_i - x_j)^2 = \sum_{i=1}^{n-1} \sum_{j=i+1}^{n} a_{ij}(x_i - x_j)^2 . \tag{3.13}$$

Proof: Since $\mathbf{L} = \mathbf{FEF}^\mathsf{T}$, we have:

$$\boldsymbol{x}^\mathsf{T} \mathbf{L} \boldsymbol{x} = (\boldsymbol{x}^\mathsf{T} \mathbf{F}) \mathbf{E} (\mathbf{F}^\mathsf{T} \boldsymbol{x}) \ .$$

However, $\mathbf{F}^\mathsf{T} \boldsymbol{x}$ is a vector, each of whose entries is indexed by the edges of the graph, with its ℓth entry equal to $x_i - x_j$, where nodes i and j are the terminal nodes of the ℓth-edge.[2] The result follows directly from this observation.

Corollary 3.19
The Laplacian matrix $\mathbf{L}$ is positive semi-definite.

Proof: This follows directly from the nonnegativity of the right-hand side of (3.13) in Property 3. Another method, which we mention only in passing, uses the *Gershgorin eigenvalue disk theorem* to show that the Gershgorin disks corresponding to $\mathbf{L}$ all lie in the closed right-half complex plane. Therefore, the eigenvalues are all non-negative, and $\mathbf{L}$ is positive semi-definite.

Property 4. *The Laplacian matrix $\mathbf{L}$ is singular. The multiplicity of the eigenvalue 0 of $\mathbf{L}$ is equal to the number of connected components of the graph G. Hence, if G is a connected, then $\mathbf{L}$ is irreducible, and has rank $n - 1$.*

Proof: Singularity of $\mathbf{L}$ is proven by noting that every row (and column, for that matter) of $\mathbf{L}$ sums to zero. Hence, the matrix is singular. To prove that the zero eigenvalue has multiplicity equal to the number of components of the underlying graph $\mathcal{G}$, we simply re-number the vertices of $\mathcal{G}$, so that the vertices corresponding to each component are stacked together—we can do this without loss of generality, as this renumbering is equivalent to pre- and post-multiplying the original Laplacian matrix by a permutation matrix. Let $\mathcal{G}^{(1)}, \ldots, \mathcal{G}^{(\ell)}$ be the components of $\mathcal{G}$, with respective sizes $p_1, \ldots, p_\ell$. The adjacency matrix (and hence also the Laplacian matrix) of $\mathcal{G}$ will be block diagonal, because there are no edges connecting any of the nodes of one component to any node in another component. Furthermore, the number of blocks will be ℓ, equal to the number of components. The Laplacian matrix $\mathbf{L}$ will then have the following block-diagonal form:

$$\mathbf{L} = \begin{bmatrix} \mathbf{L}_1 & & \mathbf{0} \\ & \ddots & \\ \mathbf{0} & & \mathbf{L}_\ell \end{bmatrix} \ .$$

---

[2] If we think of the components of $\boldsymbol{x}$ as the potentials at the nodes of a graph, then each entry of the vector $\mathbf{F}^\mathsf{T} \boldsymbol{x}$ is the potential difference across the corresponding edge of the graph.

Clearly, since each row (and column) of $\mathbf{L}$ sums to zero, then so does every row (and column) of $\mathbf{L}_i$, $i = 1, \ldots, \ell$. This means that each of $\mathbf{L}_1, \ldots, \mathbf{L}_\ell$ is singular. Now, we also know that each of the subgraphs $\mathcal{G}^{(1)}, \ldots, \mathcal{G}^{(\ell)}$ is maximally connected, by definition; therefore, there is no permutation pre- and post-multiplication that can transform any of the $\mathbf{L}_i$'s into a block diagonal form. So each $\mathbf{L}_i$ has exactly one zero eigenvalue. Given that $\mathbf{L}$ is block diagonal, we know that $\lambda(\mathbf{L}) = \bigcup_{i=1}^{\ell} \lambda(\mathbf{L}_i)$, where $\lambda(\mathbf{L}_i)$ denotes the spectrum of matrix $\mathbf{L}_i$. Hence, $\mathbf{L}$ has exactly ℓ zero eigenvalues, equal to the number of its components. Also see Mohar [61, Proposition 2.3].

Corollary 3.20
The eigenvalue of $\mathbf{L}$ at 0 is simple if, and only if, $\mathbf{L}$ is irreducible.

Property 5. *The vector $\mathbf{1}$ is always an eigenvector of the Laplacian matrix $\mathbf{L}$ associated with the eigenvalue at 0. If the graph is connected, i.e., if $\mathbf{L}$ is irreducible, then $\mathbf{1}$ is the only eigenvector associated with the eigenvalue 0.*

Proof: As mentioned earlier, each diagonal entry in $\mathbf{L}$ is the negative of the sum of the diagonal entries of its corresponding row (and, by symmetry, its column). Therefore, $\mathbf{L1} = \mathbf{0}$. When $\mathbf{L}$ is irreducible, the eigenvalue at 0 is simple, and hence $\mathbf{1}$ becomes the only eigenvector associated with it.

Property 6. *The Laplacian matrix $\mathbf{L}$ belongs to the class K_0.*

Proof: From the definition of the Laplacian matrix, we know that $\mathbf{L} \in \mathsf{Z}$. From Property 5 and Theorem 3.18, it follows that $\mathbf{L} \in \mathsf{K}_0$.

3.3 Grounded Laplacian Matrices and Their Properties

A grounded Laplacian matrix is a principal submatrix of an ordinary Laplacian matrix. As such, it has a few salient features that we summarily describe below, and prove the important ones among which, in the sequel.

1. A grounded Laplacian matrix is symmetric, as is the ordinary Laplacian matrix from which it was obtained.

2. A grounded Laplacian matrix is nonsingular, *i.e.*, any principal submatrix of an ordinary Laplacian matrix is invertible (proper principal submatrix, *i.e.*, of size strictly smaller than the original). As the ordinary Laplacian matrix is positive semi-definite, it must be that any principle submatrix of it is positive definite.

3. We know that the ordinary Laplacian matrix is an M-matrix, and that any principal submatrix of an M-matrix must also be an M-matrix. Therefore, the second property implies that a grounded Laplacian matrix must be a nonsingular M-matrix; we know already that the ordinary Laplacian matrix is a singular M-matrix.

4. As a nonsingular M-matrix, the following can be said of a grounded Laplacian:

   (i) If the grounded Laplacian matrix is irreducible, then its inverse is strictly positive in all its entries.

   (ii) If the grounded Laplacian matrix is reducible, then—without loss of generality, and based on its symmetry—we can consider it to be block diagonal. Each diagonal block of the grounded Laplacian can then be considered to be irreducible. Hence, the inverse of such a grounded Laplacian would be block diagonal as well, with each diagonal block being strictly positive in all its entries.

   (iii) The Schur complement of any principal submatrix of a grounded Laplacian is a non-singular M-matrix, is positive definite, and is in fact a grounded Laplacian matrix in its own right.

3.4   A Symmetric Generalized Eigenvalue Problem (SGEP)

In the cases of interest to us, matrix $\mathbf{L}$ is real, symmetric, positive semi-definite, and, in fact, a Laplacian matrix. The matrix of node weights $\mathbf{B}$ is diagonal, positive semi-definite, and possibly singular, with rank n_G equal to the number of G-nodes in the network. Letting n_L denote the number of L-nodes, it must be that $n_\mathsf{G} + n_\mathsf{L} = n$. In the power-network context, n is the total number of nodes in the power grid and n_G the number of generators; the rank deficiency $n - n_\mathsf{G}$ is simply n_L, the number of load nodes in the network.

The symmetric generalized eigenproblem (SGEP) that we consider in this thesis can be written as follows:

$$\mathbf{L}\,\boldsymbol{v}_i = \lambda_i\,\mathbf{B}\,\boldsymbol{v}_i \qquad i = 1, \ldots, n_\mathsf{G} \qquad \text{(Finite eigenvalues)} \qquad (3.14)$$

$$\mathbf{B}\,\boldsymbol{v}_i = \mathbf{0} \qquad i = n_\mathsf{G} + 1, \ldots, n \qquad \text{(Infinite eigenvalues)} \qquad (3.15)$$

where the eigenvectors corresponding to the finite eigenvalues are $\mathbf{B}$-orthonormal, *i.e.*, $\langle \boldsymbol{v}_i, \boldsymbol{v}_j \rangle_{\mathbf{B}} = \boldsymbol{v}_i^{\mathsf{T}} \mathbf{B} \, \boldsymbol{v}_j = \delta_{ij}$ for $i, j = 1, \ldots, n_{\mathsf{G}}$, as we will show.

Since we have mentioned "finite" eigenvalues, it is worthwhile to describe why and how the SGEP of interest to us can have both finite and infinite eigenvalues. Without loss of generality, let the node-weight matrix be given by $\mathbf{B} = \mathsf{diag}\,(\mathbf{M}, \mathbf{0})$, where the number of zeros on the diagonal correspond to the L-nodes in the graph, and $\mathbf{M}$ is the diagonal matrix of G-node weights. Partitioning the Laplacian matrix and the eigenvector $\boldsymbol{v}$ accordingly, we can write our SGEP as

$$\beta \begin{bmatrix} \mathbf{L}_{\mathsf{G}} & \mathbf{L}_{\mathsf{GL}} \\ \mathbf{L}_{\mathsf{GL}}^{\mathsf{T}} & \mathbf{L}_{\mathsf{L}} \end{bmatrix} \begin{bmatrix} \boldsymbol{v}_{\mathsf{G}} \\ \boldsymbol{v}_{\mathsf{L}} \end{bmatrix} = \alpha \begin{bmatrix} \mathbf{M} & \mathbf{0} \\ \mathbf{0} & \mathbf{0} \end{bmatrix} \begin{bmatrix} \boldsymbol{v}_{\mathsf{G}} \\ \boldsymbol{v}_{\mathsf{L}} \end{bmatrix} . \tag{3.16}$$

Rewriting (3.16) by collecting terms to one side, we obtain the following equation:

$$\begin{bmatrix} \beta \mathbf{L}_{\mathsf{G}} - \alpha \mathbf{M} & \beta \mathbf{L}_{\mathsf{GL}} \\ \beta \mathbf{L}_{\mathsf{GL}}^{\mathsf{T}} & \beta \mathbf{L}_{\mathsf{L}} \end{bmatrix} \begin{bmatrix} \boldsymbol{v}_{\mathsf{G}} \\ \boldsymbol{v}_{\mathsf{L}} \end{bmatrix} = \begin{bmatrix} \mathbf{0} \\ \mathbf{0} \end{bmatrix} . \tag{3.17}$$

The characteristic polynomial for $(\mathbf{L}, \mathbf{B})$ is obtained by setting the determinant of the partitioned matrix on the left-hand side of (3.17) equal to zero. That determinant, according to Theorem 4.4 (to appear in Chapter 4), is:

$$\begin{aligned} \det \begin{bmatrix} \beta \mathbf{L}_{\mathsf{G}} - \alpha \mathbf{M} & \beta \mathbf{L}_{\mathsf{GL}} \\ \beta \mathbf{L}_{\mathsf{GL}}^{\mathsf{T}} & \beta \mathbf{L}_{\mathsf{L}} \end{bmatrix} &= \det\left(\beta \mathbf{L}_{\mathsf{L}}\right) \det\left(\beta \mathbf{L}_{\mathsf{G}} - \alpha \mathbf{M} - \beta \mathbf{L}_{\mathsf{GL}} \left(\frac{1}{\beta} \mathbf{L}_{\mathsf{L}}^{-1} \right) \beta \mathbf{L}_{\mathsf{GL}}^{\mathsf{T}} \right) \\ &= \beta^{n_{\mathsf{L}}} \det\left(\mathbf{L}_{\mathsf{L}}\right) \det\left(\beta \left(\mathbf{L}_{\mathsf{G}} - \mathbf{L}_{\mathsf{GL}} \mathbf{L}_{\mathsf{L}}^{-1} \mathbf{L}_{\mathsf{GL}}^{\mathsf{T}} \right) - \alpha \mathbf{M} \right) \\ &= \beta^{n_{\mathsf{L}}} \det\left(\mathbf{L}_{\mathsf{L}}\right) \det\left(\beta \mathbf{L}_{[\mathsf{L}]} - \alpha \mathbf{M} \right) , \end{aligned} \tag{3.18}$$

where $\mathbf{L}_{[\mathsf{L}]} \overset{\triangle}{=} \mathbf{L}_{\mathsf{G}} - \mathbf{L}_{\mathsf{GL}} \mathbf{L}_{\mathsf{L}}^{-1} \mathbf{L}_{\mathsf{GL}}^{\mathsf{T}}$ is the Schur complement of $\mathbf{L}_{\mathsf{L}}$ in $\mathbf{L}$, a matrix that we will discuss in great detail in Chapter 4.

3.4.1 Irreducibility, Regularity, and Definiteness

Definition 3.21 (Joint Reducibility of Symmetric Matrix Pairs)
A symmetric matrix pair $(\mathbf{F}, \mathbf{G})$ *is called jointly reducible—alternatively,* $\mathbf{F}$ *is said be reducible relative to* $\mathbf{G}$*—if a permutation matrix* $\mathbf{P}$ *exists such that*

$$\mathbf{PFP}^{\mathsf{T}} = \mathsf{diag}\left(\mathbf{F}_1, \mathbf{F}_2, \dots, \mathbf{F}_r\right)$$

and

$$\mathbf{PGP}^{\mathsf{T}} = \mathsf{diag}\left(\mathbf{G}_1, \mathbf{G}_2, \dots, \mathbf{G}_r\right),$$

where $r \geq 2$*, and*

$$\mathsf{size}\left(\mathbf{F}_i\right) = \mathsf{size}\left(\mathbf{G}_i\right) = n_i \geq 1, \qquad i = 1, \dots, r.$$

A symmetric matrix pair is said to be jointly irreducible *if it is not reducible. If* r *is the largest integer for which each matrix pair* $((\mathbf{F}_i, \mathbf{G}_i))$*,* $i = 1, \dots, r$*, is jointly irreducible, then we say that the degree of reducibility of* $(\mathbf{F}, \mathbf{G})$ *is* $r - 1$*; an irreducible matrix pair has degree or reducibility* 0*.*

Furthermore, if one of the two matrices, say $\mathbf{G}$*, is the identity matrix* $B I$*, then we only talk about the reducibility (or irreducibility) of* $\mathbf{F}$*, without the burden of specifying a matrix pair.*

For cases of interest to us (where $\mathbf{G} \stackrel{\triangle}{=} \mathbf{B}$ is a diagonal matrix), joint irreducibility of the matrix pair $(\mathbf{L}, \mathbf{B})$ is equivalent to the irreducibility of $\mathbf{L}$ alone. This is because for every permutation matrix $\mathbf{P}$ and diagonal matrix $\mathbf{B}$, it is always the case that $\mathbf{PBP}^{\mathsf{T}}$ is a diagonal matrix. We know, also, that $\mathbf{L}$ is irreducible if, and only if, the graph to which it corresponds is connected. In this thesis, unless otherwise specifically noted, the graphs that we consider are connected, and hence their Laplacian matrices are irreducible. In other words, by and large, we will consider jointly irreducible matrix pairs $(\mathbf{L}, \mathbf{B})$.

Definition 3.22 (Singular and Regular Matrix Pairs)
A square matrix pair $(\mathbf{F}, \mathbf{G})$ *is said to be* SINGULAR *if for all* λ*,*

$$\det\left(\mathbf{F} - \lambda\mathbf{G}\right) = 0.$$

Otherwise, it is called REGULAR.

Often, but not always, a matrix pair $(\mathbf{F}, \mathbf{G})$ is singular because the null spaces of $\mathbf{F}$ and $\mathbf{G}$ have a non-trivial intersection. In that case, $\det(\mathbf{F} - \lambda\mathbf{G}) = 0$ for all values of λ, because any vector in the joint null space of $\mathbf{F}$ and $\mathbf{G}$ will also be in the null space of $(\mathbf{F} - \lambda\mathbf{G})$. An example where two matrices $\mathbf{F}$ and $\mathbf{G}$ do not have overlapping null spaces, but for which the matrix pair $(\mathbf{F}, \mathbf{G})$ is singular, is given by Saad [70]:

Example 3.23

$$\mathbf{F} = \begin{bmatrix} 1 & 0 \\ 1 & 0 \end{bmatrix} \qquad\qquad \mathbf{G} = \begin{bmatrix} 0 & 2 \\ 0 & 2 \end{bmatrix}.$$

Clearly,

$$\det(\mathbf{F} - \lambda\mathbf{G}) = \det \begin{bmatrix} 1 & -2\lambda \\ 1 & -2\lambda \end{bmatrix} = 0,$$

for all values of λ.

Note that neither $\mathbf{F}$ nor $\mathbf{G}$ is symmetric. In this example, $\mathbf{F}$ and $\mathbf{G}$, although having disjoint *right* null spaces, do have overlapping *left* null spaces; in fact, the vector $\begin{bmatrix} 1 & -1 \end{bmatrix}^{\mathsf{T}}$ lies in the joint left null space of $\mathbf{F}$ and $\mathbf{G}$. The following example comprises a matrix pair having neither left nor right overlapping null spaces; yet, they make for a singular pair.

Example 3.24

$$\mathbf{F} = \begin{bmatrix} 1 & 0 & 0 \\ 0 & 0 & 1 \\ 0 & 0 & 0 \end{bmatrix} \qquad\qquad \mathbf{G} = \begin{bmatrix} 0 & -1 & 0 \\ 0 & 0 & 0 \\ 0 & 0 & -1 \end{bmatrix}.$$

We have

$$\det(\mathbf{F} - \lambda\mathbf{G}) = \det \begin{bmatrix} 1 & \lambda & 0 \\ 0 & 0 & 1 \\ 0 & 0 & \lambda \end{bmatrix} = 0, \quad \forall \lambda. \tag{3.19}$$

In the cases of interest to us, we need not worry about the Laplacian/node-weight matrix pair $(\mathbf{L}, \mathbf{B})$ being singular. To see this, partition the matrix pair as follows:

$$\mathbf{L} = \begin{bmatrix} \mathbf{L_G} & \mathbf{L_{GL}} \\ \mathbf{L_{GL}^T} & \mathbf{L_L} \end{bmatrix} \qquad\qquad \mathbf{B} = \begin{bmatrix} \mathbf{M} & \mathbf{0} \\ \mathbf{0} & \mathbf{0} \end{bmatrix} ,$$

where the subscripts G and L refer to G-nodes and L-nodes, respectively, and GL refers to coupling terms between the two types of nodes. The matrix of G-node weights is $\mathbf{M} = \mathsf{diag}\,(M_1, \ldots, M_r)$, where $r = n_\mathsf{G}$ is the number of G-nodes in the graph. Constructing $\det\,(\mathbf{F} - \lambda\mathbf{G})$, we have:

$$\det\,(\mathbf{F} - \lambda\mathbf{G}) = \begin{bmatrix} \mathbf{L_G} - \lambda\mathbf{M} & \mathbf{L_{GL}} \\ \mathbf{L_{GL}^T} & \mathbf{L_L} \end{bmatrix} . \tag{3.20}$$

From Theorem 4.4 (yet to come), so long as $\mathbf{L_L}$ is nonsingular (and this is the critical requirement) we can write the determinant of the partitioned matrix in (3.20) as follows:

$$\det\,(\mathbf{F} - \lambda\mathbf{G}) = \det\,(\mathbf{L_L}) \det\,(\mathbf{L_G} - \lambda\mathbf{M} - \mathbf{L_{GL}}\mathbf{L_L^{-1}}\mathbf{L_{GL}^T}) . \tag{3.21}$$

When $\mathbf{L_L}$ is nonsingular, the first factor $\det\,(\mathbf{L_L})$ is nonzero, and the second, "Schur complement" determinant is not identically zero for all λ, because $\mathbf{M}$ is nonsingular; that is, the matrix pair $(\mathbf{L_G} - \mathbf{L_{GL}}\mathbf{L_L^{-1}}\mathbf{L_{GL}^T}, \mathbf{M})$ is a regular pair because $\mathbf{M}$ is nonsingular. As we stated earlier, the critical requirement here is that $\mathbf{L_L}$ be nonsingular. In terms of graph interconnections, this means that there should be no isolated cluster of L-nodes (not even a cluster of size 1). This is the case for all the oscillatory networks of interest to us, because a cluster of isolated L-nodes has no dynamics of its own; here, we may think of a group of load nodes in a power network. By themselves, load nodes do not have dynamics. The generators in the power network are the nodes that have inertia, and hence introduce dynamics into the network.

Definition 3.25 (Definite Matrix Pairs)
The symmetric pair $(\mathbf{F}, \mathbf{G})$ is called DEFINITE *if*

$$\mu(\mathbf{F}, \mathbf{G}) \triangleq \min_{\substack{\boldsymbol{x} \in \mathbb{R}^n \\ \|\boldsymbol{x}\|_2 = 1}} \sqrt{(\boldsymbol{x}^\mathsf{T}\,\mathbf{F}\,\boldsymbol{x})^2 + (\boldsymbol{x}^\mathsf{T}\,\mathbf{G}\,\boldsymbol{x})^2} > 0 . \tag{3.22}$$

For the pair $(\mathbf{F}, \mathbf{G})$ to be definite, it is *not* necessary for either $\mathbf{F}$ or $\mathbf{G}$ to be nonsingular. Uhlig [75] showed that so long as $\mu(\mathbf{F}, \mathbf{G}) > 0$, there is a pair (γ, σ) such that $\widehat{\mathbf{G}} = \gamma\mathbf{G} - \sigma\mathbf{F}$

is positive definite, provided $n > 2$. In the cases of interest to us, the symmetry and regularity of the matrix pair guarantee that $\mu(\mathbf{L}, \mathbf{B}) > 0$, because the only way it could be zero is if $\mathbf{L}$ and $\mathbf{B}$ have null spaces (left of right) which nontrivially overlap. We know this to be not the case with the matrix pairs involving irreducible $\mathbf{L}$ and diagonal positive semi-definite $\mathbf{B}$.

Definiteness of a symmetric matrix pair is a generalization of the same concept in the ordinary symmetric eigenproblem. Among other things, Inequality 3.22 guarantees that even if neither $\mathbf{F}$ nor $\mathbf{G}$ is invertible, the pair can always be transformed into another pair $(\widehat{\mathbf{F}}, \widehat{\mathbf{G}})$, where $\widehat{\mathbf{G}}$ is positive definite. However, we will not be performing this kind of transformation, because we lose the physical meanings of the entries in the matrices (and their graph interpretations) if we were to do so.

Schur Contractions and Other Structural Metastases of Graphs

4.1   Introduction and Contributions

This chapter marks the beginning of our coverage of the modal properties of graphs. After going over some additional matrix-theoretic essentials, we start to collect on the investment we made in Chapter 3, where we learnt about M-matrices and their salient features. We will develop a few interesting results about the structural properties of graphs, and discuss how they relate to the graph's modal behavior.

In a latter part of the chapter we examine certain rank-one perturbations to graphs, develop expressions for the error introduced into the governing Laplacian matrices, and derive first-order eigenvalue sensitivity expressions that bring out, in a transparent manner, the dependence of the eigenvalue sensitivity expression on the parameter the rank-one perturbation (such as the weight of the edge that has been added to the graph).

It has long been known, at least in the power-system community, that to study the modes of oscillation of a power network (subject to the linearization and negligible damping assumptions that we mentioned in Chapter 2) the matrix pair $(\mathbf{L}, \mathbf{B})$ is best converted to a smaller-sized (but dynamically equivalent) one that includes only generators (G-nodes), and no loads (L-nodes). We call this process the "Schur contraction" of a graph with respect to its L-nodes. The smaller sized matrices that we mentioned are precisely the Schur complements of $\mathbf{L}$ and $\mathbf{B}$ with respect to their entries that correspond to the L-nodes. This is why we study Schur complements in this chapter; the transformation is at the heart of what is done to deal with the presence of L-nodes in a graph.

One main problem with Schur contraction is that physical intuition about the original network topology is all but lost when the Laplacian matrix for the graph (which contains the

topological information in a very accessible and transparent form) is converted to a Schur complement matrix. The results we discuss in this chapter—regarding the way L-nodes contract, as well as what happens to their neighboring nodes—is intended to assuage that loss of topological intuition when we Schur-contract a graph with respect to any subset of its L-nodes. We have sprinkled the chapter with examples that illustrate the main points that we make about Schur contraction, and the topological changes that such a contraction brings about to a dynamically-equivalent graph that has fewer nodes.

Our contributions in this chapter can be summarized as follows:

- We collect under the proverbial one roof, the essential matrix theory related to Schur complements and partitioned matrices. This material, with the notable exception of the outstanding survey article by Ouéllette [66] (which contains far more than what we need here) is scattered in the literature. It is hoped that our succinct coverage assists future research in this area and prevents unnecessary time spent fishing for the same results that have long been known to the applied mathematics community.

- Using properties of Laplacian matrices and the inverse-nonnegativity of nonsingular M-matrices, we show that the eigenvector components (also known as characteristic valuations) associated with the L-nodes in a graph are obtained through a convex combination of nodes that border them. These same characteristic valuations can be obtained, as we will show, from the G-nodes that "surround" any connected subgraph of L-nodes—even if those G-nodes are not adjacent to a particular set of L-nodes in that subgraph. By "surround" here we have a particular meaning in mind. Consider an L-node whose eigenvector component we want to compute (for any finite oscillatory mode). Then the G-nodes whose characteristic valuations *must* enter into a convex combination to give the valuation for the L-node, are *all* those that satisfy one of the following two conditions:

    1. every G-node that is adjacent to the L-node.

    2. every G-node between which and the L-node exists a path consisting entirely of L-nodes.

  This result—albeit proven using a very elementary property of M-matrices—is important because it enables us to understand several things about the dynamics of graphs more meaningfully. Through examples in this chapter, we illustrate some of these points. In a subsequent chapter, where we discuss properties of the mode shapes of graphs (as well as tree graphs), we will make use of the result concerning the convex combination dependence of L-node eigenvector components on their surrounding

nodes. The convex-combination result that we develop here will turn out to be critical in extending—to graphs with L-nodes—the proof of an important theorem by Fiedler [27] concerning the number of components induced on a graph by the nonnegative components of each of its eigenvectors.

- Using the inverse-positivity property of irreducible, nonsingular M-matrices, we prove that when a graph is Schur contracted with respect to any subset of its L-nodes, the nodes adjacent to *any* of the Schur-contracted L-nodes become fully connected. This feature has been empirically observed by, especially by those who study power systems. However, so far as we know, the precise mathematical formulation that we develop in this chapter—a formulation that explains the very phenomenon of fully-connectedness after Schur contraction—is new; it puts a mathematical justification over what has been observed by engineers in the past.

- In the latter part of this chapter, we discuss a class of dynamic order-preserving metastases of a graph (i.e., mutations of a graph that leave the number of G-nodes intact). In particular, we study a rank-one perturbation that results from a single edge addition. We will also look at the addition of L-nodes to a graph (which leaves the dynamic order intact, after Schur contraction). Interesting conclusions can be reached about the modal properties after, say, L-node addition, if it is done in certain specific ways. We will use the convex-combination results from the earlier part of the chapter to show (and illustrate by example) how a cluster of L-nodes connected to only one G-node will have constant eigenvector valuations equal to that of the G-node. We also show how if an L-node is added as a pendant node to any graph, it will not alter the dynamics of that graph. Corollaries of this type, to the results we prove early in the chapter, are plenty.

4.2 The Schur Complement

Definition 4.1 (Schur Complement)
Consider a square partitioned matrix

$$\mathbf{H} = \begin{bmatrix} \mathbf{Q} & \mathbf{R} \\ \mathbf{S} & \mathbf{T} \end{bmatrix}, \tag{4.1}$$

where $\mathbf{Q}$ and $\mathbf{T}$ are principal submatrices of $\mathbf{H}$. If $\mathbf{Q}$ is nonsingular, then we denote by $\mathbf{H}_{\langle \mathbf{Q} \rangle}$ (or $(\mathbf{H}/\mathbf{Q})$) the Schur complement of $\mathbf{Q}$ in $\mathbf{H}$, defined as follows:

$$\mathbf{H}_{\langle \mathbf{Q} \rangle} \triangleq (\mathbf{H}/\mathbf{Q}) \triangleq \mathbf{T} - \mathbf{S}\mathbf{Q}^{-1}\mathbf{R} \ . \tag{4.2}$$

Similarly, if $\mathbf{T}$ is nonsingular, then the Schur complement of $\mathbf{T}$ in $\mathbf{H}$ is

$$\mathbf{H}_{\langle \mathbf{T} \rangle} \triangleq (\mathbf{H}/\mathbf{T}) \triangleq \mathbf{Q} - \mathbf{R}\mathbf{T}^{-1}\mathbf{S} \ . \tag{4.3}$$

Theorem 4.2
Consider an $n \times n$ matrix $\mathbf{H} \in \mathsf{K}$, and let $\mathbf{Q}$ be a principal submatrix of $\mathbf{H}$, as in (4.1). Then $\mathbf{H}_{\langle \mathbf{Q} \rangle} \in \mathsf{K}$, i.e., the Schur complement of $\mathbf{Q}$ in $\mathbf{H}$ is of class K.

Proof: See Fiedler [28, Theorem 5.13, pp. 125–126]

The following theorem, which we need for our purposes, is one that we have not seen stated or proven anywhere, although it is very straightforward to show, and must already be known:

Theorem 4.3
Consider a singular M-matrix $\mathbf{H}$, and let $\mathbf{T}$ be a nonsingular principal submatrix of $\mathbf{H}$. Then $\mathbf{H}_{\langle \mathbf{T} \rangle}$, the Schur complement of $\mathbf{T}$ in $\mathbf{H}$, is a singular M-matrix.

Proof: Without loss of generality, let $\mathbf{H}$ be partitioned as in (4.1). From Theorem 3.16, we know that

- rank $(\mathbf{H}) = n - 1$;

- 0 is a simple eigenvalue of $\mathbf{H}$; and

- $\mathbf{A}\boldsymbol{x} = \mathbf{0}$ for some $\boldsymbol{x} \succ \mathbf{0}$.

Partitioning $\boldsymbol{x}$ conformally with $\mathbf{H}$, we have

$$\begin{bmatrix} \mathbf{Q} & \mathbf{R} \\ \mathbf{S} & \mathbf{T} \end{bmatrix} \begin{bmatrix} \boldsymbol{x}_1 \\ \boldsymbol{x}_2 \end{bmatrix} = \begin{bmatrix} \mathbf{0} \\ \mathbf{0} \end{bmatrix} \ . \tag{4.4}$$

We rewrite the bottom portion, and solve for $\boldsymbol{x}_2$:

$$\mathbf{S}\boldsymbol{x}_1 + \mathbf{T}\boldsymbol{x}_2 = \mathbf{0} \quad \Longrightarrow \quad \boldsymbol{x}_2 = -\mathbf{T}^{-1}\mathbf{S}\boldsymbol{x}_1 \ .$$

Inserting the expression for x_2 into the top portion of (4.4), we obtain:

$$\underbrace{\left(\mathbf{Q} - \mathbf{R}\mathbf{T}^{-1}\mathbf{S}\right)}_{\mathbf{H}_{\langle \mathbf{T}\rangle}} x_1 = \mathbf{0} \quad \implies \quad \mathbf{H}_{\langle \mathbf{T}\rangle} \, x_1 = \mathbf{0} \ . \tag{4.5}$$

The Schur complement matrix $\mathbf{H}_{\langle \mathbf{T}\rangle}$ is a Z-matrix, because $\mathbf{Q} \in \mathsf{Z}$, $\mathbf{R} \preceq \mathbf{0}$, $\mathbf{S} \preceq \mathbf{0}$, and $\mathbf{T}^{-1} \succcurlyeq \mathbf{0}$ (since $\mathbf{T} \in \mathsf{K}$). We have shown that $\mathbf{H}_{\langle \mathbf{T}\rangle} \in \mathsf{Z}$ and that $\mathbf{H}_{\langle \mathbf{T}\rangle} x_1 \succeq \mathbf{0}$ for some $x_1 \succ \mathbf{0}$. According to Theorem 3.18, $\mathbf{H}_{\langle \mathbf{T}\rangle} \in \mathsf{K}_0$. In fact, (4.5) shows that $\mathbf{H}_{\langle \mathbf{T}\rangle}$ is a *singular* M-matrix. The proof is complete. $\square$

Note that in Theorem 4.3, if we $\mathbf{H}$ is irreducible to begin with, then we need not impose nonsingularity on $\mathbf{T}$, because that is implied already by Theorem 3.16.

Theorem 4.4 (Determinants of Partitioned Matrices and the Schur Complement)
Consider the partitioned matrix $\mathbf{H}$ of (4.1). If $\mathbf{Q}$ is nonsingular, then

$$\det\left(\mathbf{H}\right) \triangleq \begin{vmatrix} \mathbf{Q} & \mathbf{R} \\ \mathbf{S} & \mathbf{T} \end{vmatrix} \tag{4.6}$$

$$= |\mathbf{Q}| \cdot \left|\mathbf{T} - \mathbf{S}\mathbf{Q}^{-1}\mathbf{R}\right| = |\mathbf{Q}| \cdot \left|\mathbf{H}_{\langle \mathbf{Q}\rangle}\right| \ . \tag{4.7}$$

Similarly, if $\mathbf{T}$ is nonsingular, then

$$\det\left(\mathbf{H}\right) = |\mathbf{T}| \cdot \left|\mathbf{Q} - \mathbf{R}\mathbf{T}^{-1}\mathbf{S}\right| = |\mathbf{T}| \cdot \left|\mathbf{H}_{\langle \mathbf{T}\rangle}\right| \ . \tag{4.8}$$

Corollary 4.5 (Invertibility of the Schur Complement)
If $\mathbf{H}$ is a singular matrix, but $\mathbf{Q}$ is nonsingular, then it must be that $\mathbf{H}_{\langle \mathbf{Q}\rangle} = \mathbf{T} - \mathbf{S}\mathbf{Q}^{-1}\mathbf{R}$ is singular, because its determinant is zero. An identical statement can be made about $\mathbf{H}_{\langle \mathbf{T}\rangle} = \mathbf{Q} - \mathbf{R}\mathbf{T}^{-1}\mathbf{S}$. Along the same lines, if both $\mathbf{H}$ and $\mathbf{Q}$ are nonsingular, then so is $\mathbf{H}_{\langle \mathbf{Q}\rangle}$. An identical statement can be made about $\mathbf{H}_{\langle \mathbf{T}\rangle}$, if both $\mathbf{H}$ and $\mathbf{T}$ are nonsingular.

Note that Corollary 4.5 could have been used in the proofs of Theorems 4.2 and 4.3.

Theorem 4.6 (Rank Additivity of the Schur Complement)
If the principal submatrix $\mathbf{Q}$ is nonsingular, then

$$\operatorname{rank}\left(\mathbf{H}\right) = \operatorname{rank}\begin{bmatrix} \mathbf{Q} & \mathbf{R} \\ \mathbf{S} & \mathbf{T} \end{bmatrix} \tag{4.9}$$

$$= \operatorname{rank}\left(\mathbf{Q}\right) + \operatorname{rank}\left(\mathbf{T} - \mathbf{S}\mathbf{Q}^{-1}\mathbf{R}\right) = \operatorname{rank}\left(\mathbf{Q}\right) + \operatorname{rank}\left(\mathbf{H}_{\langle \mathbf{Q}\rangle}\right) \ . \tag{4.10}$$

Similarly, if $\mathbf{T}$ *is nonsingular, then*

$$\text{rank}\,(\mathbf{H}) = \text{rank}\,(\mathbf{T}) + \text{rank}\,(\mathbf{Q} - \mathbf{R}\mathbf{T}^{-1}\mathbf{S}) = \text{rank}\,(\mathbf{T}) + \text{rank}\,(\mathbf{H}_{\langle\mathbf{T}\rangle})\,. \tag{4.11}$$

Corollary 4.7 (Invertibility of the Schur Complement Revisited)
If $\mathbf{H}$ *and* $\mathbf{Q}$ *are both nonsingular, then so is* $\mathbf{H}_{\langle\mathbf{Q}\rangle} = \mathbf{T} - \mathbf{S}\mathbf{Q}^{-1}\mathbf{R}$. *Similarly, if* $\mathbf{H}$ *and* $\mathbf{T}$ *are both nonsingular, then so is* $\mathbf{H}_{\langle\mathbf{T}\rangle} = \mathbf{Q} - \mathbf{R}\mathbf{T}^{-1}\mathbf{S}$.

This confirms the same result we obtained from the determinantal expression for the partitioned matrix $\mathbf{H}$. Corollary 4.7 can also be used for a quick proof of Theorem 4.2.

The next theorem illustrates how the Schur complement enters the various expressions for the inverse of a partitioned matrix. According to the extensive survey by Ouéllette [66], evidently Banachiewicz was the first researcher to express the inverse of a partitioned matrix in terms of Schur complements; others, such as Hotelling, rewrote some of the results a few years later.

Theorem 4.8 (Inverse of a Partitioned Matrix)
Consider the partitioned matrix $\mathbf{H}$ *as in (4.1), which we repeat here for convenience:*

$$\mathbf{H} = \begin{bmatrix} \mathbf{Q} & \mathbf{R} \\ \mathbf{S} & \mathbf{T} \end{bmatrix}\,. \tag{4.12}$$

Let $\mathbf{H}$ *be nonsingular, and recall the Schur complements*

$$\mathbf{H}_{\langle\mathbf{Q}\rangle} = \mathbf{T} - \mathbf{S}\mathbf{Q}^{-1}\mathbf{R} \qquad and \qquad \mathbf{H}_{\langle\mathbf{T}\rangle} = \mathbf{Q} - \mathbf{R}\mathbf{T}^{-1}\mathbf{S}\,,$$

each properly defined whenever $\mathbf{Q}$ *and* $\mathbf{T}$ *is nonsingular, respectively. If* $\mathbf{Q}$ *is nonsingular, then:*

$$\mathbf{H}^{-1} = \left[\begin{array}{c|c} \mathbf{Q}^{-1} + \mathbf{Q}^{-1}\mathbf{R}\mathbf{H}_{\langle\mathbf{Q}\rangle}^{-1}\mathbf{S}\mathbf{Q}^{-1} & -\mathbf{Q}^{-1}\mathbf{R}\mathbf{H}_{\langle\mathbf{Q}\rangle}^{-1} \\ \hline -\mathbf{H}_{\langle\mathbf{Q}\rangle}^{-1}\mathbf{S}\mathbf{Q}^{-1} & \mathbf{H}_{\langle\mathbf{Q}\rangle}^{-1} \end{array} \right] \tag{4.13}$$

$$= \left[\begin{array}{c|c} \mathbf{Q}^{-1} & \mathbf{0} \\ \hline \mathbf{0} & \mathbf{0} \end{array} \right] + \left[\begin{array}{c} \mathbf{Q}^{-1}\mathbf{R} \\ -\mathbf{I}_r \end{array} \right] \mathbf{H}_{\langle\mathbf{Q}\rangle}^{-1} \left[\begin{array}{c|c} \mathbf{S}\mathbf{Q}^{-1} & -\mathbf{I}_r \end{array} \right]\,. \tag{4.14}$$

If $\mathbf{T}$ *is nonsingular, then*

$$\mathbf{H}^{-1} = \left[\begin{array}{c|c} \mathbf{H}_{\langle\mathbf{T}\rangle}^{-1} & -\mathbf{H}_{\langle\mathbf{T}\rangle}^{-1}\mathbf{R}\mathbf{T}^{-1} \\ \hline -\mathbf{T}^{-1}\mathbf{S}\mathbf{H}_{\langle\mathbf{T}\rangle}^{-1} & \mathbf{T}^{-1} + \mathbf{T}^{-1}\mathbf{S}\mathbf{H}_{\langle\mathbf{T}\rangle}^{-1}\mathbf{R}\mathbf{T}^{-1} \end{array} \right] \tag{4.15}$$

$$= \left[\begin{array}{c|c} \mathbf{0} & \mathbf{0} \\ \hline \mathbf{0} & \mathbf{T}^{-1} \end{array} \right] + \left[\begin{array}{c} -\mathbf{I}_n \\ \mathbf{T}^{-1}\mathbf{S} \end{array} \right] \mathbf{H}_{\langle\mathbf{T}\rangle}^{-1} \left[\begin{array}{c|c} -\mathbf{I}_n & \mathbf{R}\mathbf{T}^{-1} \end{array} \right] . \tag{4.16}$$

If both $\mathbf{Q}$, *and* $\mathbf{T}$ *are nonsingular, then*

$$\mathbf{H}^{-1} = \left[\begin{array}{c|c} \mathbf{H}_{\langle\mathbf{T}\rangle}^{-1} & -\mathbf{Q}^{-1}\mathbf{R}\mathbf{H}_{\langle\mathbf{Q}\rangle}^{-1} \\ \hline -\mathbf{T}^{-1}\mathbf{S}\mathbf{H}_{\langle\mathbf{T}\rangle}^{-1} & \mathbf{H}_{\langle\mathbf{Q}\rangle}^{-1} \end{array} \right] . \tag{4.17}$$

Corollary 4.9 (Matrix Inversion Lemma)

Consider a nonsingular matrix $\mathbf{A} \in \mathbb{R}^{n \times n}$ *with a known inverse* $\mathbf{A}^{-1}$. *Then*

$$(\mathbf{A} + \mathbf{B}\mathbf{C}\mathbf{D})^{-1} = \mathbf{A}^{-1} - \mathbf{A}^{-1}\mathbf{B} \left(\mathbf{C}^{-1} + \mathbf{D}\mathbf{A}^{-1}\mathbf{B} \right)^{-1} \mathbf{D}\mathbf{A}^{-1} , \tag{4.18}$$

where $\mathbf{C} \in \mathbb{R}^{r \times r}$ *is nonsingular,* $\mathbf{B} \in \mathbb{R}^{n \times r}$, *and* $\mathbf{D} \in \mathbb{R}^{r \times n}$.

Proof: Consider the partitioned matrix

$$\mathbf{H} = \begin{bmatrix} \mathbf{A} & \mathbf{B} \\ \mathbf{D} & -\mathbf{C}^{-1} \end{bmatrix} . \tag{4.19}$$

Clearly, the Schur complement $\mathbf{H}_{\langle-\mathbf{C}^{-1}\rangle} \triangleq \left(\mathbf{H}/(-\mathbf{C}^{-1}) \right) = \mathbf{A} + \mathbf{B}\mathbf{C}\mathbf{D}$. Equating the top-left blocks of (4.13) and (4.15), and letting $\mathbf{Q} = \mathbf{A}$, $\mathbf{R} = \mathbf{B}$, $\mathbf{S} = \mathbf{D}$, and $\mathbf{T} = -\mathbf{C}^{-1}$, we obtain the expression on the right-hand side of (4.18). $\qquad\square$

Corollary 4.10 (Inversion After a Rank-One Perturbation)

Consider a nonsingular matrix $\mathbf{A} \in \mathbb{R}^{n \times n}$ *with a known inverse* $\mathbf{A}^{-1}$. *Then*

$$\left(\mathbf{A} + \boldsymbol{p}\boldsymbol{q}^{\mathsf{T}} \right)^{-1} = \mathbf{A}^{-1} - \frac{1}{1 + \boldsymbol{q}^{\mathsf{T}}\mathbf{A}^{-1}\boldsymbol{p}} \mathbf{A}^{-1}\boldsymbol{p}\,\boldsymbol{q}^{\mathsf{T}}\mathbf{A}^{-1} , \tag{4.20}$$

where it is assumed that $\boldsymbol{q}^{\mathsf{T}}\mathbf{A}^{-1}\boldsymbol{p} \neq -1$.

Proof: In (4.18) let $\mathbf{C} = 1$ be a scalar, $\mathbf{B} = \boldsymbol{p} \in \mathbb{R}^n$, and $\mathbf{D} = \boldsymbol{q}^{\mathsf{T}}$, where $\boldsymbol{q} \in \mathbb{R}^n$. The result then follows. $\qquad\square$

The expression on the right-hand side of (4.20) takes on a special structure if both $\mathbf{A}$ and the perturbation matrix pq^T are symmetric. For the perturbation matrix to be symmetric, we must have $p = q$. In this case, (4.20) becomes:

$$\left(\mathbf{A} + p\,p^\mathsf{T}\right)^{-1} = \mathbf{A}^{-1} - \frac{1}{1 + p^\mathsf{T}\mathbf{A}^{-1}p}\left(\mathbf{A}^{-1}p\right)\left(\mathbf{A}^{-1}p\right)^\mathsf{T}. \tag{4.21}$$

Theorem 4.11 (Inertia Additivity of the Schur Complement)
Consider the symmetric, partitioned matrix

$$\mathbf{H} = \begin{bmatrix} \mathbf{Q} & \mathbf{R} \\ \mathbf{R}^\mathsf{T} & \mathbf{T} \end{bmatrix}. \tag{4.22}$$

If $\mathbf{Q}$ is nonsingular, then

$$\mathsf{In}\ \mathbf{H} = \mathsf{In}\ \mathbf{Q} + \mathsf{In}\ \mathbf{H}_{\langle\mathbf{Q}\rangle}\,, \tag{4.23}$$

where $\mathbf{H}_{\langle\mathbf{Q}\rangle} = \mathbf{T} - \mathbf{R}^\mathsf{T}\mathbf{Q}^{-1}\mathbf{R}$.

Similarly, if $\mathbf{T}$ is nonsingular, then

$$\mathsf{In}\ \mathbf{H} = \mathsf{In}\ \mathbf{T} + \mathsf{In}\ \mathbf{H}_{\langle\mathbf{T}\rangle}\,, \tag{4.24}$$

where $\mathbf{H}_{\langle\mathbf{T}\rangle} = \mathbf{Q} - \mathbf{R}\mathbf{T}^{-1}\mathbf{R}^\mathsf{T}$.

$$\tag{4.25}$$

Theorem 4.12 (Quotient Property of the Schur Complement)
Consider the matrix

$$\mathbf{H} = \left[\begin{array}{c|c} \mathbf{Q} & \mathbf{R} \\ \hline \mathbf{S} & \mathbf{T} \end{array}\right] \tag{4.26}$$

$$= \left[\begin{array}{cc|c} \mathbf{E} & \mathbf{F} & \mathbf{R}_1 \\ \mathbf{G} & \mathbf{H} & \mathbf{R}_2 \\ \hline \mathbf{S}_1 & \mathbf{S}_2 & \mathbf{T} \end{array}\right], \tag{4.27}$$

where $\mathbf{Q}$, $\mathbf{R}$, and $\mathbf{S}$ are conformably partitioned, and $\mathbf{Q}$ and $\mathbf{E}$ are nonsingular.

1. *Then the Schur complement* $\mathbf{Q}_{\langle\mathbf{E}\rangle} = \mathbf{H} - \mathbf{GE}^{-1}\mathbf{F}$ *is a nonsingular leading principal submatrix of the Schur complement*

$$\mathbf{H}_{\langle\mathbf{E}\rangle} = \left[\begin{array}{c|c} \mathbf{H} & \mathbf{R}_2 \\ \hline \mathbf{S}_2 & \mathbf{T} \end{array}\right] - \left[\begin{array}{c} \mathbf{G} \\ \hline \mathbf{S}_1 \end{array}\right] \mathbf{E}^{-1} \left[\begin{array}{c|c} \mathbf{F} & \mathbf{R}_1 \end{array}\right] \tag{4.28}$$

$$= \left[\begin{array}{c|c} \mathbf{H} - \mathbf{GE}^{-1}\mathbf{F} & \mathbf{R}_2 - \mathbf{GE}^{-1}\mathbf{R}_1 \\ \hline \mathbf{S}_2 - \mathbf{S}_1\mathbf{E}^{-1}\mathbf{F} & \mathbf{T} - \mathbf{S}_1\mathbf{E}^{-1}\mathbf{R}_1 \end{array}\right] \tag{4.29}$$

$$= \left[\begin{array}{c|c} \mathbf{Q}_{\langle\mathbf{E}\rangle} & \mathbf{R}_2 - \mathbf{GE}^{-1}\mathbf{R}_1 \\ \hline \mathbf{S}_2 - \mathbf{S}_1\mathbf{E}^{-1}\mathbf{F} & \mathbf{T} - \mathbf{S}_1\mathbf{E}^{-1}\mathbf{R}_1 \end{array}\right]. \tag{4.30}$$

2. *Furthermore, the following "quotient property" holds:*

$$\mathbf{H}_{\langle\mathbf{Q}\rangle} = \left(\mathbf{H}_{\langle\mathbf{E}\rangle}/\mathbf{Q}_{\langle\mathbf{E}\rangle}\right). \tag{4.31}$$

Theorem 4.13 (The Schur Complement and the Laplacian Matrix)

Let $\mathcal{H} \subset \mathcal{G}$ be a proper, induced subgraph of $\mathcal{G}$, and let $\overline{\mathcal{H}}$ be the complementary induced subgraph of $\mathcal{H}$, with node set $V(\overline{\mathcal{H}}) = V(\mathcal{G})\backslash V(\mathcal{H})$. The Laplacian matrix of $\mathcal{G}$ can be partitioned as follows:

$$\mathbf{L} = \begin{bmatrix} \mathbf{L}_{\mathcal{H}} & \mathbf{L}_{\mathcal{H}\overline{\mathcal{H}}} \\ \mathbf{L}_{\overline{\mathcal{H}}\mathcal{H}} & \mathbf{L}_{\overline{\mathcal{H}}} \end{bmatrix}, \tag{4.32}$$

where $\mathbf{L}_{\mathcal{H}\overline{\mathcal{H}}} = \mathbf{L}_{\overline{\mathcal{H}}\mathcal{H}}^{\mathsf{T}} \preccurlyeq \mathbf{0}$. (Note that this means $\overline{\mathcal{H}}$ is not disjoint from $\mathcal{H}$, the rest of the graph.)

Denote by

$$\mathbf{L}_{\langle\overline{\mathcal{H}}\rangle} = \left(\mathbf{L}\backslash\mathbf{L}_{\overline{\mathcal{H}}}\right) = \mathbf{L}_{\mathcal{H}} - \mathbf{L}_{\mathcal{H}\overline{\mathcal{H}}}\mathbf{L}_{\overline{\mathcal{H}}}^{-1}\mathbf{L}_{\overline{\mathcal{H}}\mathcal{H}}, \tag{4.33}$$

the Schur complement of $\overline{\mathcal{H}}$ in $\mathcal{G}$. Then $\mathbf{L}_{\langle\overline{\mathcal{H}}\rangle}$ is a Laplacian matrix.

Proof: We know that the Laplacian matrix $\mathbf{L}$ is a singular M-matrix. As $\overline{\mathcal{H}}$ is not a disjoint subgraph of $\mathcal{G}$, it must be that $\mathbf{L}_{\overline{\mathcal{H}}}$ is nonsingular. Therefore, according to Theorem 4.3, the Schur complement matrix $\mathbf{L}_{\langle\overline{\mathcal{H}}\rangle}$ must be a singular M-matrix. It is easy to show that $\mathbf{L}_{\langle\overline{\mathcal{H}}\rangle}\mathbf{1}_{\mathcal{H}} = \mathbf{0}$, where $\mathbf{1}_{\mathcal{H}}$ is the vector of all-ones, the size of $\overline{\mathcal{H}}$. Therefore, $\mathbf{L}_{\langle\overline{\mathcal{H}}\rangle}$ is a Laplacian matrix. The proof is complete. $\square$

4.3   Convex Combination Dependence of Levis-Node Eigenvector Components on Those of Their Neighboring-Nodes

In this section, we prove an important result governing the mode shapes of L-nodes in an oscillatory network. To our best assessment, this result is novel, and has not been shown previously.

In a nutshell, we will show that in every single mode, the eigenvector component associated with an L-node (i.e., the characteristic valuation of that L-node) is a convex combination of the eigenvector components (characteristic valuations) of all its immediate neighbors. Carrying the discussion further, we will show, as well, that the characteristic valuation of any L-node is a convex combination of those belonging to the G-nodes that border the connected L-node cluster to which it belongs, *even if those G-nodes are not its immediate neighbors.*

This convex-combination dependence of L-node eigenvector components on those of their neighbors and G-node counterparts is a striking result, yet one that follows directly from the inverse-positivity property of irreducible M-matrices (Theorem 3.12).

Theorem 4.14
Consider the partitioned Laplacian matrix

$$\mathbf{L} = \begin{bmatrix} \mathbf{L}_{\mathcal{H}} & \mathbf{L}_{\mathcal{H}\overline{\mathcal{H}}} \\ \mathbf{L}_{\overline{\mathcal{H}}\mathcal{H}} & \mathbf{L}_{\overline{\mathcal{H}}} \end{bmatrix} \, , \tag{4.34}$$

where the induced subgraphs $\mathcal{H}$ and $\overline{\mathcal{H}}$ are defined as in Theorem 4.13. If $\mathbf{L}_{\overline{\mathcal{H}}}$ is nonsingular (that is, if $\overline{\mathcal{H}}$ is not disconnected from the rest of the graph), then $-\mathbf{L}_{\overline{\mathcal{H}}}^{-1}\mathbf{L}_{\overline{\mathcal{H}}\mathcal{H}}$ is a row-stochastic matrix, i.e.,

$$\mathbf{0} \preccurlyeq -\mathbf{L}_{\overline{\mathcal{H}}}^{-1}\mathbf{L}_{\overline{\mathcal{H}}\mathcal{H}} \tag{4.35}$$

and

$$\mathbf{1}_{\overline{\mathcal{H}}} = -\mathbf{L}_{\overline{\mathcal{H}}}^{-1}\mathbf{L}_{\overline{\mathcal{H}}\mathcal{H}}\,\mathbf{1}_{\mathcal{H}} \, , \tag{4.36}$$

where we have denoted by $\mathbf{1}_{\mathcal{H}}$ the all-ones vector of size equal to the cardinality of $\mathcal{H}$, and

defined $\mathbf{1}_{\overline{\mathcal{H}}}$ in a similar fashion.

Proof: We know that

$$\mathbf{1}_n = \begin{bmatrix} \mathbf{1}_{\mathcal{H}} \\ \mathbf{1}_{\overline{\mathcal{H}}} \end{bmatrix}$$

is a null vector of the Laplacian matrix $\mathbf{L}$. That is,

$$\begin{bmatrix} \mathbf{L}_{\mathcal{H}} & \mathbf{L}_{\mathcal{H}\overline{\mathcal{H}}} \\ \mathbf{L}_{\overline{\mathcal{H}}\mathcal{H}} & \mathbf{L}_{\overline{\mathcal{H}}} \end{bmatrix} \begin{bmatrix} \mathbf{1}_{\mathcal{H}} \\ \mathbf{1}_{\overline{\mathcal{H}}} \end{bmatrix} = \begin{bmatrix} \mathbf{0} \\ \mathbf{0} \end{bmatrix} . \tag{4.37}$$

Writing the lower-block row of (4.37) and solving for $\mathbf{1}_{\overline{\mathcal{H}}}$ (knowing that $\mathbf{L}_{\overline{\mathcal{H}}}$ is nonsingular), we obtain (4.36). That the matrix $-\mathbf{L}_{\overline{\mathcal{H}}}^{-1}\mathbf{L}_{\overline{\mathcal{H}}\mathcal{H}}$ is nonnegative follows from the fact that $\mathbf{L}_{\overline{\mathcal{H}}\mathcal{H}} \preccurlyeq \mathbf{0}$, and also that $\mathbf{L}_{\overline{\mathcal{H}}}$ is a nonsingular M-matrix, and hence $\mathbf{L}_{\overline{\mathcal{H}}}^{-1} \succcurlyeq \mathbf{0}$ according to Theorem 3.12. The proof is complete. $\qquad\qquad\square$

Corollary 4.15
Consider $\mathbf{y} \in \mathbb{R}^{|\overline{\mathcal{H}}|}$ and $\mathbf{x} \in \mathbb{R}^{|\mathcal{H}|}$ related by

$$\mathbf{y} = -\mathbf{L}_{\overline{\mathcal{H}}}^{-1}\mathbf{L}_{\overline{\mathcal{H}}\mathcal{H}}\mathbf{x} . \tag{4.38}$$

Each entry of $\mathbf{y}$ is a convex combination of the entries in $\mathbf{x}$, where the coefficients of the combination are the entries on the ith row of $-\mathbf{L}_{\overline{\mathcal{H}}}^{-1}\mathbf{L}_{\overline{\mathcal{H}}\mathcal{H}}$. Furthermore, for any arbitrary finite constant α,

$$\mathbf{y} + \alpha\mathbf{1}_{\overline{\mathcal{H}}} = -\mathbf{L}_{\overline{\mathcal{H}}}^{-1}\mathbf{L}_{\overline{\mathcal{H}}\mathcal{H}}\left(\mathbf{x} + \alpha\mathbf{1}_{\mathcal{H}}\right) . \tag{4.39}$$

Theorem 4.16
Consider the SGEP

$$\begin{bmatrix} \mathbf{L}_{\mathsf{G}} & \mathbf{L}_{\mathsf{GL}} \\ \mathbf{L}_{\mathsf{GL}}^{\mathsf{T}} & \mathbf{L}_{\mathsf{L}} \end{bmatrix} \begin{bmatrix} v_{\mathsf{G}} \\ v_{\mathsf{L}} \end{bmatrix} = \lambda \begin{bmatrix} \mathbf{M} & \mathbf{0} \\ \mathbf{0} & \mathbf{0} \end{bmatrix} \begin{bmatrix} v_{\mathsf{G}} \\ v_{\mathsf{L}} \end{bmatrix} . \tag{4.40}$$

Each L-node eigenvector component is a convex combination of the eigenvector components of the G-nodes in the graph.

Proof: Rewriting the lower-block equations, $\mathbf{L}_{\mathsf{GL}}^{\mathsf{T}}v_{\mathsf{G}} + \mathbf{L}_{\mathsf{L}}v_{\mathsf{L}} = \mathbf{0}$, and solving for v_{L}, we have:

$$v_{\mathsf{L}} = -\mathbf{L}_{\mathsf{L}}^{-1}\mathbf{L}_{\mathsf{GL}}^{\mathsf{T}}v_{\mathsf{G}} . \tag{4.41}$$

The rest follows immediately from Corollary 4.15, where $\mathbf{L}_{\mathcal{H}}$ is analogous to $\mathbf{L}_{\mathsf{G}}$, and $\mathbf{L}_{\overline{\mathcal{H}}}$ is akin to $\mathbf{L}_{\mathsf{L}}$. A few points are worth mentioning here:

- Only those G-nodes that border a connected L-node cluster contribute to the eigenvector components of every L-node in that cluster (whether or not the G-node is an immediate neighbor of a given L-node, so long as the G-node borders the cluster of L-nodes to which any particular L-node belongs, it will influence the eigenvector component of that L-node). If a G-node does not border the cluster of L-nodes in question, then its eigenvector component does not come into the computation of those of the L-nodes in that cluster. This is readily seen from (4.41). If a particular G-node does not border the L-node cluster, then the corresponding row of $\mathbf{L}_{GL}$ (and column of $\mathbf{L}_{GL}^{\mathsf{T}}$) is entirely zero. It is clear, then, from (4.41), that the corresponding entry in v_G does not enter into the computation of *any* of the L-nodes under study. In other words, all the G-nodes to which a given L-node has a path, that consists entirely of L-nodes, will affect the computation of the eigenvector component corresponding to that L-node; otherwise, it does not. So if there is no path from an L-node ν_L to a G-node ν_G that comprises only L-node intermediate vertices, then the characteristic valuation of ν_G does not enter into the convex combination relation governing the valuation of ν_L.

- If, on the other hand, a particular G-node is the neighbor to even one L-node in a given cluster, then the corresponding column of $\mathbf{L}_{LG}^{\mathsf{T}}$ will have at least one nonzero entry, which then will be picked up by the strictly positive $\mathbf{L}_L^{-1}$; that means, a G-node that borders *any* L-node in the connected subgraph (cluster) of L-nodes will affect the values of the eigenvector components of *every* L-node in that cluster.

- The cluster of L-nodes that we consider as $\overline{\mathcal{H}}$ need not include *every* L-node in the graph. The subgraph $\overline{\mathcal{H}}$ need only be a connected subgraph induced by a subset of the L-nodes; in other words, we are allowed to include L-nodes in $\mathcal{H}$.

Example 4.17

Consider the six-node graph shown in Figure 4.1. In this example, we verify that the eigenvector components associated with the L-nodes ν_5 and ν_6 depend on the G-nodes through a convex combination relation. We also verify that node 3 does not enter into the convex combination relation governing the valuation of node 5, and that, similarly, node 1 does not enter into the convex combination relation governing the eigenvector component of node 6. This is because there is no L-only path that joins ν_5 with ν_3, nor is there one that joins ν_6 with ν_1.
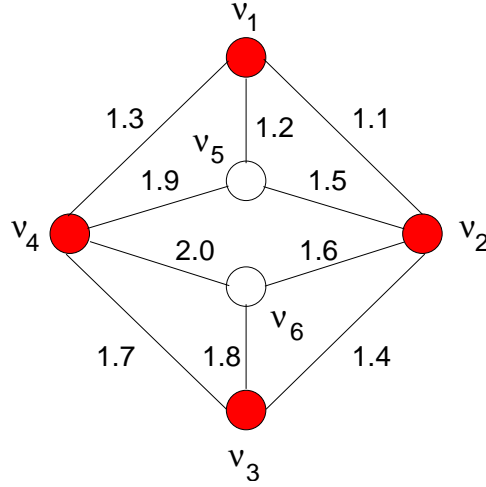
Figure 4.1: A six-node graph with two L-nodes. According to Theorem 4.16, the characteristic valuations of ν_5 and ν_6 are given by a convex combination of those corresponding to the G-nodes surrounding them.

The Laplacian matrix for the graph is given below:

$$\mathbf{L} = \begin{bmatrix} 3.6 & -1.1 & 0 & -1.3 & -1.2 & 0 \\ -1.1 & 5.6 & -1.4 & 0 & -1.5 & -1.6 \\ 0 & -1.4 & 4.9 & -1.7 & 0 & -1.8 \\ -1.3 & 0 & -1.7 & 6.9 & -1.9 & -2.0 \\ -1.2 & -1.5 & 0 & -1.9 & 4.6 & 0 \\ 0 & -1.6 & -1.8 & -2.0 & 0 & 5.4 \end{bmatrix}. \tag{4.42}$$

The diagonal matrix of node weights is $\mathbf{B} \overset{\triangle}{=} \mathsf{diag}\,(\mathbf{M}, 0, 0) = \mathsf{diag}\,(1.1, 2.2, 3.2, 4.5, 0, 0)$. An eigenanalysis of the matrix pair $(\mathbf{L}, \mathbf{M})$ reveals that the four finite eigenvalues, and corresponding eigenvectors, are as shown in Table 4.17.

Theorem 4.16, in particular Equation (4.41), specifies the convex combination dependence of the L-nodes on the G-nodes. Let $\mathbf{Q} \overset{\triangle}{=} -\mathbf{L}_{\mathsf{L}}^{-1}\mathbf{L}_{\mathsf{GL}}^{\mathsf{T}}$. For our graph, $\mathbf{Q}$ is given by:

$$\mathbf{Q} = -\underbrace{\begin{bmatrix} 4.6 & 0 \\ 0 & 5.4 \end{bmatrix}^{-1}}_{\mathbf{L}_{\mathsf{L}}^{-1}} \underbrace{\begin{bmatrix} -1.2 & -1.5 & 0 & -1.9 \\ 0 & -1.6 & -1.8 & -2.0 \end{bmatrix}}_{\mathbf{L}_{\mathsf{GL}}^{\mathsf{T}}}$$

$$= \begin{bmatrix} 0.2609 & 0.3261 & 0 & 0.4130 \\ 0 & 0.2963 & 0.3333 & 0.3704 \end{bmatrix}. \tag{4.43}$$

$\lambda_1 = 0.0000$	$\lambda_2 = 1.7034$	$\lambda_3 = 2.1304$	$\lambda_4 = 3.8001$
1.0000	*-0.6139*	*0.7944*	*1.0000*
1.0000	*0.2279*	*1.0000*	*-0.4323*
1.0000	*1.0000*	*-0.3796*	*0.1480*
1.0000	*-0.6724*	*-0.4131*	*-0.1383*
1.0000	*-0.3636*	*0.3627*	*0.0628*
1.0000	*0.1518*	*0.0167*	*-0.1300*

Table 4.1: Eigenvalues and eigenvectors of the six-node graph of Figure 4.1, containing two L-nodes. In the table, we have demarcated the eigenvector components corresponding to the L-nodes ν_5 and ν_6.

Clearly, $\mathbf{Q} \succeq \mathbf{0}$. Also, note the positions of the zero entries in $\mathbf{Q}$. The zeros appear exactly at the positions where the theory predicts they would be. In other words, looking at the 0 in the $(1,3)$ position of $\mathbf{Q}$ means that ν_5 has no dependence on ν_3. Similarly, the 0 at position $(2,1)$ in $\mathbf{Q}$ means that the characteristic valuation of ν_1 does not enter into the computation of the valuation for ν_6. Furthermore, it is straightforward to verify that $\mathbf{Q}$ is row-stochastic, i.e., that it is nonnegative each of its rows sums to 1. Last, we verify that $\mathbf{Q}$ actually maps the G-node eigenvector matrix $\mathbf{V_G}$ into its L-node counterpart $\mathbf{V_L}$:

$$\mathbf{V_L} = \mathbf{Q}\mathbf{V_G} \ . \tag{4.44}$$

$$\underbrace{\begin{bmatrix} 1.0000 & -0.3636 & 0.3627 & 0.0628 \\ 1.0000 & 0.1518 & 0.0167 & -0.1300 \end{bmatrix}}_{\mathbf{V_L}} = \mathbf{Q} \underbrace{\begin{bmatrix} 1.0000 & -0.6139 & 0.7944 & 1.0000 \\ 1.0000 & 0.2279 & 1.0000 & -0.4323 \\ 1.0000 & 1.0000 & -0.3796 & 0.1480 \\ 1.0000 & -0.6724 & -0.4131 & -0.1383 \end{bmatrix}}_{\mathbf{V_G}} \ . \tag{4.45}$$

Another direct corollary of the convex-combination dependence of L-node eigenvector components on their G-node counterparts is that if a subgraph of L-nodes has no path to the rest of the graph except through *one* G-node, then all the eigenvector components of those L-nodes will be constant, and equal to the characteristic valuation of the "gateway" G-node. The following example illustrates this point.
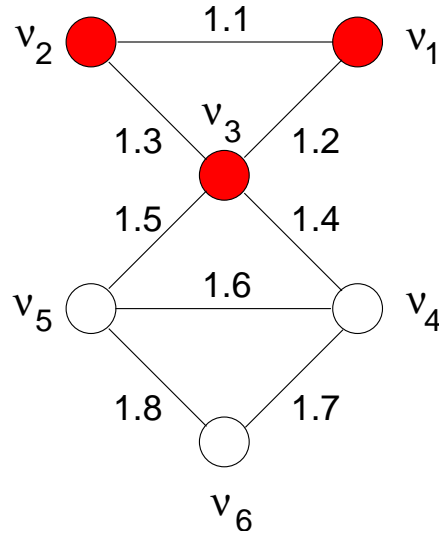
Figure 4.2: A six-node graph with three L-nodes that have only one gateway G-node. According to Theorem 4.16, the characteristic valuations of ν_4, ν_5, and ν_6 are constant, and equal to that of the G-node ν_3.

Example 4.18

Consider the graph of Figure 4.2. The three nodes do not have L-only path to any of the G-nodes in the graph, except ν_3. Given that their characteristic valuations must be a convex combination of those corresponding to their surrounding G-nodes, it must be that there is only one coefficient in that convex combination, namely 1. Clearly, then, the eigenvector components of the three L-nodes must all equal the value of ν_3. The Laplacian matrix for the graph in Figure 4.2 is given below:

$$\mathbf{L} = \begin{bmatrix} 2.3 & -1.1 & -1.2 & 0 & 0 & 0 \\ -1.1 & 2.4 & -1.3 & 0 & 0 & 0 \\ -1.2 & -1.3 & 5.4 & -1.4 & -1.5 & 0 \\ 0 & 0 & -1.4 & 4.7 & -1.6 & -1.7 \\ 0 & 0 & -1.5 & -1.6 & 4.9 & -1.8 \\ 0 & 0 & 0 & -1.7 & -1.8 & 3.5 \end{bmatrix}. \tag{4.46}$$

The node-weight matrix is given by $\mathbf{B} = \mathsf{diag}\,(1.1, 1.2, 1.3, 0, 0, 0)$. An eigenanalysis of the $(\mathbf{L}, \mathbf{B})$ confirms the theoretical assertion that the eigenvector components corresponding to the ν_4, ν_5, and ν_6 are equal to that of ν_3, the gateway G-node through which the three L-nodes connect to the remainder of the graph.

$\lambda_1 = 0.0000$	$\lambda_2 = 3.0000$	$\lambda_3 = 3.0140$
1.0000	-0.5000	-1.0000
1.0000	1.0000	0.0000
1.0000	-0.5000	0.8462
1.0000	-0.5000	0.8462
1.0000	-0.5000	0.8462
1.0000	-0.5000	0.8462

Table 4.2: Eigenvalues and eigenvectors of the six-node graph of Figure 4.2. In the table, we have demarcated the eigenvector components corresponding to the three L-nodes ν_4, ν_5, and ν_6. Clearly, the eigenvector components of the three L-nodes are identical to the only gateway G-node which they have access to.

4.4 Schur Contraction of a Graph with Respect to a Subset of Its L-Nodes

Definition 4.19

Consider a graph $\mathcal{G}$ and two complementary subgraphs $\mathcal{H}$ and $\overline{\mathcal{H}}$, where the latter consists of a subset of the graph L-nodes; the subgraph $\overline{\mathcal{H}}$ may contain as many as all of the graph L-nodes, and as few as one. We say that the Schur contraction of the graph $\mathcal{G}$, with respect to $\overline{\mathcal{H}}$, is the graph $\mathcal{G}_{\langle \overline{\mathcal{H}} \rangle}$ whose Laplacian matrix is given by

$$\mathbf{L}_{\langle \overline{\mathcal{H}} \rangle} = \mathbf{L}_{\mathcal{H}} - \mathbf{L}_{\mathcal{H}\overline{\mathcal{H}}} \mathbf{L}_{\overline{\mathcal{H}}}^{-1} \mathbf{L}_{\overline{\mathcal{H}}\mathcal{H}} \; .$$

Theorem 4.20 (Fully-Connectedness After Schur Contraction)

Consider a graph $\mathcal{G}$ comprising both G-nodes and L-nodes. Denote the partitioned Laplacian matrix for the graph by

$$\mathbf{L} = \begin{bmatrix} \mathbf{L}_{\mathsf{G}} & \mathbf{L}_{\mathsf{GL}} \\ \mathbf{L}_{\mathsf{LG}} & \mathbf{L}_{\mathsf{L}} \end{bmatrix} , \tag{4.47}$$

where $\mathbf{L}_{\mathsf{LG}} = \mathbf{L}_{\mathsf{GL}}^{\mathsf{T}}$. The subscript denotes the node-type to which a submatrix corresponds. Furthermore, assume that

(a) the subgraph induced by the L-nodes is connected.

(b) every G-node is adjacent to at least one L-node in the graph.

Denote by $\mathcal{G}_{\langle L \rangle}$ the graph obtained by Schur contracting the L-nodes. We know that the Laplacian matrix for $\mathcal{G}_{\langle L \rangle}$ is the Schur complement of $\mathbf{L}_L$ in $\mathbf{L}$, i.e.,

$$\mathbf{L}_{\langle L \rangle} = \mathbf{L}_G - \mathbf{L}_{GL}\mathbf{L}_L^{-1}\mathbf{L}_{LG} . \tag{4.48}$$

Then, $\mathcal{G}_{\langle L \rangle}$ is a complete graph, i.e., it is fully connected.

Proof: The submatrix $\mathbf{L}_L$ is irreducible because the subgraph induced by the L-nodes is connected. Moreover, as a principal submatrix of the irreducible matrix $\mathbf{L}$, we know that $\mathbf{L}_L$ is a nonsingular M-matrix. Therefore, $\mathbf{L}_L^{-1} \succ \mathbf{0}$.

The second piece of information, that every G-node is adjacent to an L-node, implies that every column of $\mathbf{L}_{LG}$ must have a nonzero entry in it.

Putting it all together, it must be that every entry of $\mathbf{L}_L^{-1}\mathbf{L}_{LG}$ is nonzero. Hence,

$$-\mathbf{L}_{GL}\mathbf{L}_L^{-1}\mathbf{L}_{LG} \succ \mathbf{0} .$$

It is now clear that the Laplacian matrix for $\mathcal{G}_{\langle L \rangle}$, which is given by (4.48), cannot have any zero off-diagonal terms. Thus, very node in $\mathcal{G}_{\langle L \rangle}$ neighbors every other node, which means $\mathcal{G}_{\langle L \rangle}$ is a fully-connected graph. The proof is complete. $\qquad\qquad\square$
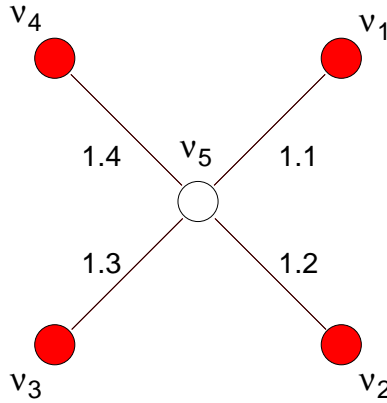
Figure 4.3: A five-node graph with one L-node.

Example 4.21

Figure 4.3 depicts a star graph with four G-nodes and one L-node. The G-nodes are not neighbors, as can be seen from the diagram. The Laplacian matrix for the star graph is

$$
\mathbf{L} = \begin{bmatrix}
1.1 & 0 & 0 & 0 & -1.1 \\
0 & 1.2 & 0 & 0 & -1.2 \\
0 & 0 & 1.3 & 0 & -1.3 \\
0 & 0 & 0 & 1.4 & -1.4 \\
-1.1 & -1.2 & -1.3 & -1.4 & 5
\end{bmatrix}.
$$

In terms of the oscillatory dynamics of the graph, however, the G-nodes behave according to the graph in which node 5, the only L-node, is Schur-contracted. The result of the Schur contraction is shown in Figure 4.4. As theoretically predicted, the Schur-contracted graph is fully connected, with the edge weights shown in the figure, and depicted by the Laplacian matrix $\mathbf{L}_{\langle L \rangle}$ below:

$$
\mathbf{L}_{\langle L \rangle} = \begin{bmatrix}
1.1 & 0 & 0 & 0 \\
0 & 1.2 & 0 & 0 \\
0 & 0 & 1.3 & 0 \\
0 & 0 & 0 & 1.4
\end{bmatrix} - \begin{bmatrix}
-1.1 \\
-1.2 \\
-1.3 \\
-1.4
\end{bmatrix} \left(\frac{1}{5} \right) \begin{bmatrix} -1.1 & -1.2 & -1.3 & -1.4 \end{bmatrix}
$$

$$
= \begin{bmatrix}
0.858 & -0.264 & -0.286 & -0.308 \\
-0.264 & 0.912 & -0.312 & -0.336 \\
-0.286 & -0.312 & 0.962 & -0.364 \\
-0.308 & -0.336 & -0.364 & 1.008
\end{bmatrix}.
$$
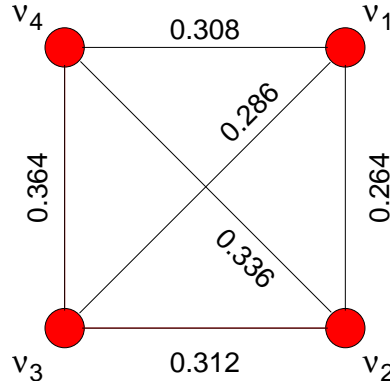
Figure 4.4: Schur contraction of the five-node graph into a four-node fully-connected dynamic equivalent.

Example 4.22 (The Star-Delta Transformation)

The Star-Delta transformation is a well-known technique among electrical engineers, especially those with interests in circuit theory or power systems. The idea is that a star-shaped four-node circuit segment can be turned into a triangular (delta) equivalent. We demonstrate this in a very straightforward manner, with graphs and with what we have learnt so far about fully connectedness of nodes that surround a Schur-contracted L-node. This example we will work out analytically, instead of numerically, because it is reasonably tractable, and the result is useful in analytical form.

The Laplacian matrix for the star graph is given by:

$$\mathbf{L} = \begin{bmatrix} a_{14} & 0 & 0 & -a_{14} \\ 0 & a_{24} & 0 & -a_{24} \\ 0 & 0 & a_{34} & -a_{34} \\ -a_{14} & -a_{24} & -a_{34} & d \end{bmatrix}, \tag{4.49}$$

where $d = a_{14} + a_{24} + a_{34}$ is the degree of the L-node that sits at the center of the star. We know that if we Schur contract the graph with respect to the L-node, the result would be a fully-connected graph with three node, i.e., a triangle (delta). Our task now is to find expressions for the edge weights of the delta graph.

The Laplacian of the Schur contracted graph is given by:

$$\mathbf{L}_{\langle \mathsf{L} \rangle} \overset{\triangle}{=} \mathbf{L}_{\mathsf{G}} - \mathbf{L}_{\mathsf{GL}} \mathbf{L}_{\mathsf{L}}^{-1} \mathbf{L}_{\mathsf{LG}} \tag{4.50}$$

$$
= \begin{bmatrix} a_{14} & 0 & 0 \\ 0 & a_{24} & 0 \\ 0 & 0 & a_{34} \end{bmatrix} - \begin{bmatrix} -a_{14} \\ -a_{24} \\ -a_{34} \end{bmatrix} \left(\frac{1}{d} \right) \begin{bmatrix} -a_{14} & -a_{24} & -a_{34} \end{bmatrix} \tag{4.51}
$$

$$
\mathbf{L}_{\langle \mathsf{L} \rangle} = \begin{bmatrix} a_{14} - \dfrac{a_{14}^2}{d} & -\dfrac{a_{14}}{d} & -\dfrac{a_{14}a_{34}}{d} \\[2mm] -\dfrac{a_{14}a_{24}}{d} & a_{24} - \dfrac{a_{24}^2}{d} & -\dfrac{a_{24}a_{34}}{d} \\[2mm] -\dfrac{a_{14}a_{34}}{d} & -\dfrac{a_{24}a_{34}}{d} & a_{34} - \dfrac{a_{34}^2}{d} \end{bmatrix}
$$

$$
\mathbf{L}_{\langle \mathsf{L} \rangle} = \frac{1}{a_{14} + a_{24} + a_{34}} \begin{bmatrix} a_{14}(a_{24} + a_{34}) & -a_{14}a_{24} & -a_{14}a_{34} \\ -a_{14}a_{24} & a_{24}(a_{14} + a_{34}) & -a_{24}a_{34} \\ -a_{14}a_{34} & -a_{24}a_{34} & a_{34}(a_{14} + a_{24}) \end{bmatrix} \tag{4.52}
$$

Denoting the Laplacian matrix of the Delta graph by

$$
\mathbf{L}_\Delta = \begin{bmatrix} b_{12} + b_{13} & -b_{12} & -b_{13} \\ -b_{12} & b_{12} + b_{23} & -b_{23} \\ -b_{13} & -b_{23} & b_{13} + b_{23} \end{bmatrix} \, ,
$$

we find that:

$$
b_{ij} = \frac{a_{i4}a_{j4}}{d} \qquad i \neq j \tag{4.53a}
$$

$$
b_{11} = \frac{a_{14}(a_{24} + a_{34})}{d} \tag{4.53b}
$$

$$
b_{22} = \frac{a_{24}(a_{14} + a_{34})}{d} \tag{4.53c}
$$

$$
b_{33} = \frac{a_{34}(a_{14} + a_{24})}{d} \tag{4.53d}
$$

$$
d = a_{14} + a_{24} + a_{34} \, . \tag{4.53e}
$$

Equations (4.53) carry precisely the expressions that have long been known about the Star-Delta transformation in circuit theory. It is worth noting here that understanding how to expand a fully-connected graph into a tree-graph structure with additional L-nodes is an issue that requires further research. In this case the expansion is from a Delta graph to a four-node star. This size turns out to be straightforward to solve; the four-node star it the small tree with just the right number of degrees of freedom, so that when arbitrary positive edges are specified on the Delta graph, we can compute the edge weights on the four-node star graph. Can we devise a K_n-Tree extension of the Star-Delta transformation? This is a subject for further research.

The converse of the problem of expanding out to a tree is the following one: "What properties must a graph with L-nodes have, so that its Schur contraction with respect to its L-nodes, is a tree?" As we will see in a subsequent chapter, much can be said about the eigenvector properties of tree graphs. Therefore, identifying the properties of graphs that Schur-contract into trees gives us the ability to use what we know about the characteristic valuations of L-nodes, along with the properties that we will show govern the eigenvectors of trees, to make statements about the graph eigenvector structures prior to Schur contraction.
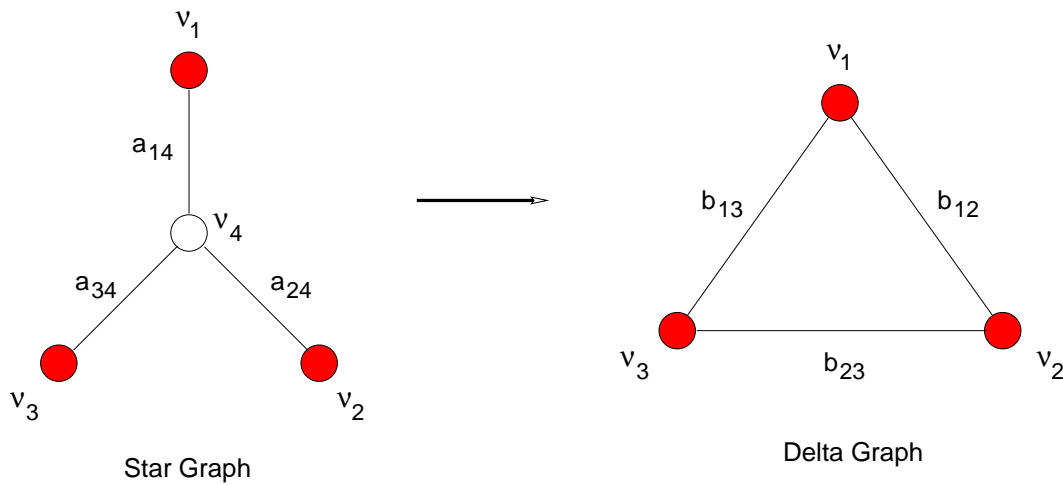
Figure 4.5: Schur contraction of a four-node graph with an L-node at its center. The result is a fully-connected three-node graph (i.e., a triangle, or a delta). The edge weights after the Schur contraction show how they are related to those in the star graph.

We can generalize Theorem 4.20 to include cases where there are nodes in the graph that do not border the Schur-contracted L-nodes. The following theorem states a more general result.

Theorem 4.23 (Fully Connectedness Of Neighboring Nodes Upon Partial Schur Contraction)

Consider a connected graph $\mathcal{G}$, and let $\overline{\mathcal{H}}$ denote a connected subgraph induced by a subset of the L-nodes in $\mathcal{G}$. Let $\mathcal{E}$ denote the subset of nodes in $\mathcal{G}$ that do not border any node in $\overline{\mathcal{H}}$; let $\mathcal{F}$ represent those that do. (There is no requirement that $\mathcal{E}$ or $\mathcal{F}$ must contain only G-nodes.) We have, $V(\mathcal{E}) = V(\mathcal{E}) \cup V(\mathcal{F}) \cup V(\mathcal{H})$. Upon Schur contracting the nodes in $\overline{\mathcal{H}}$, the subgraph induced by $\mathcal{F}$ will be fully connected. Furthermore, the edges connecting $\mathcal{E}$ and $\mathcal{F}$ will not be affected by the Schur contraction.

Proof: To prove this theorem, we write the Laplacian matrix for $\mathcal{G}$ in the appropriate partitioned form as shown below:

$$
\mathbf{L} = \begin{bmatrix} \mathbf{L}_{\mathcal{E}} & \mathbf{L}_{\mathcal{E}\mathcal{F}} & \mathbf{0} \\ \mathbf{L}_{\mathcal{F}\mathcal{E}} & \mathbf{L}_{\mathcal{F}} & \mathbf{L}_{\mathcal{F}\overline{\mathcal{H}}} \\ \mathbf{0} & \mathbf{L}_{\overline{\mathcal{H}}\mathcal{F}} & \mathbf{L}_{\overline{\mathcal{H}}} \end{bmatrix} .
\tag{4.54}
$$

The zero blocks indicate that the nodes in $\mathcal{E}$ do not border any node in $\overline{\mathcal{H}}$. Schur contracting the nodes in $\overline{\mathcal{H}}$ results in the following Laplacian matrix:

$$
\begin{aligned}
\mathbf{L}_{\langle\overline{\mathcal{H}}\rangle} &= \begin{bmatrix} \mathbf{L}_{\mathcal{E}} & \mathbf{L}_{\mathcal{E}\mathcal{F}} \\ \mathbf{L}_{\mathcal{F}\mathcal{E}} & \mathbf{L}_{\mathcal{F}} \end{bmatrix} - \begin{bmatrix} \mathbf{0} \\ \mathbf{L}_{\mathcal{F}\overline{\mathcal{H}}} \end{bmatrix} \mathbf{L}_{\overline{\mathcal{H}}}^{-1} \begin{bmatrix} \mathbf{0} & \mathbf{L}_{\overline{\mathcal{H}}\mathcal{F}} \end{bmatrix} \\
&= \begin{bmatrix} \mathbf{L}_{\mathcal{E}} & \mathbf{L}_{\mathcal{E}\mathcal{F}} \\ \mathbf{L}_{\mathcal{F}\mathcal{E}} & \mathbf{L}_{\mathcal{F}} \end{bmatrix} - \begin{bmatrix} \mathbf{0} & \mathbf{0} \\ \mathbf{0} & \mathbf{L}_{\mathcal{F}\overline{\mathcal{H}}}\mathbf{L}_{\overline{\mathcal{H}}}^{-1}\mathbf{L}_{\overline{\mathcal{H}}\mathcal{F}} \end{bmatrix} \\
&= \begin{bmatrix} \mathbf{L}_{\mathcal{E}} & \mathbf{L}_{\mathcal{E}\mathcal{F}} \\ \mathbf{L}_{\mathcal{F}\mathcal{E}} & \mathbf{L}_{\mathcal{F}} - \mathbf{L}_{\mathcal{F}\overline{\mathcal{H}}}\mathbf{L}_{\overline{\mathcal{H}}}^{-1}\mathbf{L}_{\overline{\mathcal{H}}\mathcal{F}} \end{bmatrix}
\end{aligned}
\tag{4.55}
$$

It is clear from (4.55) that neither the internal connections within $\mathcal{E}$, nor the interconnections between $\mathcal{E}$ and $\mathcal{F}$ are affected by the Schur contraction. Furthermore, after the Schur contraction, the nodes in $\mathcal{F}$ are fully connected, because the bottom-right quadrant of the Laplacian matrix $\mathbf{L}_{\langle\overline{\mathcal{H}}\rangle}$ in (4.55) has strictly negative off-diagonal entries, as stipulated by Theorem 4.20. The proof is complete. $\qquad\qquad\square$

Example 4.24

Consider a six-node graph comprising three G-*nodes and an equal number of* L-*nodes. Figure 4.6 depicts the graph and its edge weights.*

The Laplacian matrix for this graph is given by

$$
\mathbf{L} = \begin{bmatrix} 7 & -2 & 0 & 0 & -5 & 0 \\ -2 & 6 & 0 & 0 & 0 & -4 \\ 0 & 0 & 1 & 0 & 0 & -1 \\ 0 & 0 & 0 & 9 & -6 & -3 \\ -5 & 0 & 0 & -6 & 11 & 0 \\ 0 & -4 & -1 & -3 & 0 & 8 \end{bmatrix} .
$$

Suppose we want to find the Schur contraction of the graph with respect to node 6; that is, node 6 is the only one among the L-*nodes that we want to contract. The resulting graph will, as the theory*

predicts, be as shown in Figure 4.7.

The Laplacian matrix corresponding to the Schur-contracted graph of Figure 4.7 is

$$
\mathbf{L}_{\langle \nu_6 \rangle} = \begin{bmatrix} 7 & -2 & 0 & 0 & -5 \\ -2 & 6 & 0 & 0 & 0 \\ 0 & 0 & 1 & 0 & 0 \\ 0 & 0 & 0 & 9 & -6 \\ -5 & 0 & 0 & -6 & 11 \end{bmatrix} - \begin{bmatrix} 0 \\ -4 \\ -1 \\ -3 \\ 0 \end{bmatrix} \left(\frac{1}{8} \right) \begin{bmatrix} 0 & -4 & -1 & -3 & 0 \end{bmatrix}
$$

$$
= \begin{bmatrix} 7 & -2 & 0 & 0 & -5 \\ -2 & 4.000 & -0.500 & -1.500 & 0 \\ 0 & -0.500 & 0.875 & -0.375 & 0 \\ 0 & -1.500 & -0.375 & 7.875 & -6 \\ -5 & 0 & 0 & -6 & 11 \end{bmatrix} .
$$

As Theorem 4.23 predicted, nodes 2, 3, and 4 are now fully connected while the edges $(1,2),(1,5)$, and $(4,5)$ are unaffected by the Schur contraction of node 6, because node 1 nor node 5 are not neighbors of the contracted node 6 in the original graph of Figure 4.6.
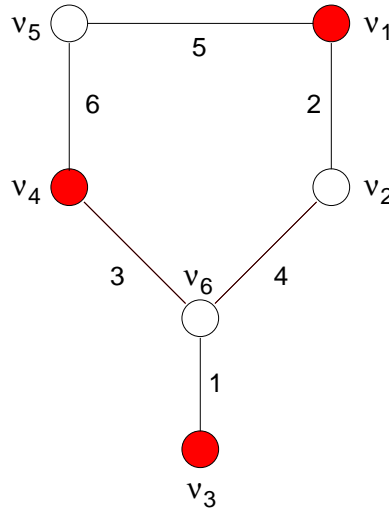
Figure 4.6: A six-node graph that is Schur-contracted with respect to a subset of its L-nodes, and that has nodes not neighboring the contracted L-node.
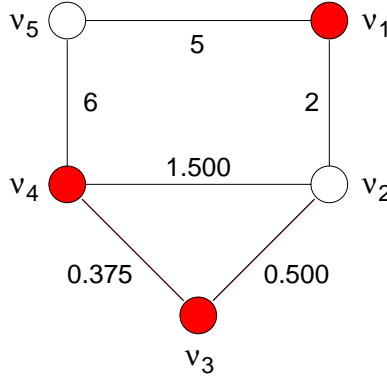
Figure 4.7: Schur contraction of the six-node graph with respect to node 6. Edges $(1, 2)$, $(1, 5)$, and $(4, 5)$ are unaffected by the Schur contraction.

4.5　A Look at Structural Perturbations to Graphs

4.5.1　Edge Addition: A Rank-One Perturbation and the Schur Complement

Proposition 4.25

Consider a partitioned matrix

$$\mathbf{H} = \begin{bmatrix} \mathbf{Q} & \mathbf{R} \\ \mathbf{S} & \mathbf{Z} \end{bmatrix}$$

and a rank-one perturbation matrix

$$\mathbf{E} = \boldsymbol{x}\boldsymbol{y}^{\mathsf{T}} = \begin{bmatrix} \boldsymbol{x}_q \\ \boldsymbol{x}_z \end{bmatrix} \begin{bmatrix} \boldsymbol{y}_q^{\mathsf{T}} & \boldsymbol{y}_z^{\mathsf{T}} \end{bmatrix} = \begin{bmatrix} \boldsymbol{x}_q \boldsymbol{y}_q^{\mathsf{T}} & \boldsymbol{x}_q \boldsymbol{y}_z^{\mathsf{T}} \\ \boldsymbol{x}_z \boldsymbol{y}_q^{\mathsf{T}} & \boldsymbol{x}_z \boldsymbol{y}_z^{\mathsf{T}} \end{bmatrix} ,$$

where $\boldsymbol{x}$ and $\boldsymbol{y}$ are partitioned conformally with $\mathbf{H}$. Denote the perturbed matrix by

$$\widetilde{\mathbf{H}} = \begin{bmatrix} \widetilde{\mathbf{Q}} & \widetilde{\mathbf{R}} \\ \widetilde{\mathbf{S}} & \widetilde{\mathbf{Z}} \end{bmatrix} = \mathbf{H} + \mathbf{E} = \begin{bmatrix} \mathbf{Q} + \boldsymbol{x}_q \boldsymbol{y}_q^{\mathsf{T}} & \mathbf{R} + \boldsymbol{x}_q \boldsymbol{y}_z^{\mathsf{T}} \\ \mathbf{S} + \boldsymbol{x}_z \boldsymbol{y}_q^{\mathsf{T}} & \mathbf{Z} + \boldsymbol{x}_z \boldsymbol{y}_z^{\mathsf{T}} \end{bmatrix} .$$

Let $\mathbf{H}_{\langle \mathbf{Z} \rangle} = \mathbf{Q} - \mathbf{R}\mathbf{Z}^{-1}\mathbf{S}$ be the Schur complement of $\mathbf{Z}$ in $\mathbf{H}$. Then

$$\widetilde{\mathbf{H}}_{\langle \widetilde{\mathbf{z}} \rangle} = \mathbf{H}_{\langle \mathbf{Z} \rangle} + \frac{1}{1 + \boldsymbol{y}_z^{\mathsf{T}} \mathbf{Z}^{-1} \boldsymbol{x}_z} \left(\boldsymbol{x}_q - \mathbf{R}\mathbf{Z}^{-1}\boldsymbol{x}_z \right) \left(\boldsymbol{y}_q - \mathbf{S}^{\mathsf{T}}\mathbf{Z}^{-1}\boldsymbol{y}_z \right)^{\mathsf{T}} . \tag{4.56}$$

That is, the Schur complement $\mathbf{H}_{\langle \mathbf{Z} \rangle}$ undergoes a rank-one perturbation $\boldsymbol{g}\boldsymbol{h}^{\mathsf{T}}$, where

$$g = \frac{1}{\sqrt{1 + \boldsymbol{y}_z^{\mathsf{T}} \mathbf{Z}^{-1} \boldsymbol{x}_z}} \left(\boldsymbol{x}_q - \mathbf{R}\mathbf{Z}^{-1}\boldsymbol{x}_z \right) \tag{4.57}$$

and

$$h = \frac{1}{\sqrt{1 + \boldsymbol{y}_z^{\mathsf{T}} \mathbf{Z}^{-1} \boldsymbol{x}_z}} \left(\boldsymbol{y}_q - \mathbf{S}^{\mathsf{T}}\mathbf{Z}^{-1}\boldsymbol{y}_z \right) . \tag{4.58}$$

Moreover, if $\mathbf{H}$ and the perturbation matrix $\mathbf{E}$ are symmetric, i.e., $\mathbf{Q} = \mathbf{Q}^{\mathsf{T}}$, $\mathbf{Z} = \mathbf{Z}^{\mathsf{T}}$, $\mathbf{S} = \mathbf{R}^{\mathsf{T}}$, $\mathbf{E} = \boldsymbol{x}\boldsymbol{y}^{\mathsf{T}}$, where $\boldsymbol{x} = \boldsymbol{y} = [\boldsymbol{x}_q^{\mathsf{T}} \ \boldsymbol{x}_z^{\mathsf{T}}]^{\mathsf{T}}$, and $\mathbf{H}_{\langle \mathbf{Z} \rangle} = \mathbf{Q} - \mathbf{R}\mathbf{Z}^{-1}\mathbf{R}^{\mathsf{T}}$ is the Schur complement of $\mathbf{Z}$ in $\mathbf{H}$, then:

$$\widetilde{\mathbf{H}}_{\langle \widetilde{\mathbf{z}} \rangle} = \mathbf{H}_{\langle \mathbf{Z} \rangle} + \frac{1}{1 + \boldsymbol{x}_z^{\mathsf{T}} \mathbf{Z}^{-1} \boldsymbol{x}_z} \left(\boldsymbol{x}_q - \mathbf{R}\mathbf{Z}^{-1}\boldsymbol{x}_z \right) \left(\boldsymbol{x}_q - \mathbf{R}\mathbf{Z}^{-1}\boldsymbol{x}_z \right)^{\mathsf{T}} . \tag{4.59}$$

That is, the Schur complement $\mathbf{H}_{\langle \mathbf{Z} \rangle}$ undergoes a symmetric, rank-one perturbation $\boldsymbol{h}\boldsymbol{h}^{\mathsf{T}}$, where

$$h = \frac{1}{\sqrt{1 + \boldsymbol{x}_z^{\mathsf{T}} \mathbf{Z}^{-1} \boldsymbol{x}_z}} \left(\boldsymbol{x}_q - \mathbf{R}\mathbf{Z}^{-1}\boldsymbol{x}_z \right) . \tag{4.60}$$

Proof: To prove (4.56) we need to invoke the rank-one perturbation expression (4.20), and carry out some algebraic manipulations, the main trick being to group the algebraic terms in just the right way. By definition, we know that

$$\widetilde{\mathbf{H}}_{\langle \widetilde{\mathbf{z}} \rangle} = \widetilde{\mathbf{Q}} - \widetilde{\mathbf{R}}\widetilde{\mathbf{Z}}^{-1}\widetilde{\mathbf{S}} \tag{4.61}$$

$$= \mathbf{Q} + \boldsymbol{x}_q\,\boldsymbol{y}_q^{\mathsf{T}} - \left(\mathbf{R} + \boldsymbol{x}_q\boldsymbol{y}_z^{\mathsf{T}} \right) \left(\mathbf{Z} + \boldsymbol{x}_z\boldsymbol{y}_z^{\mathsf{T}} \right)^{-1} \left(\mathbf{S} + \boldsymbol{x}_z\boldsymbol{y}_q^{\mathsf{T}} \right) . \tag{4.62}$$

Based on the rank-one perturbation expression (4.20) of Corollary 4.10, we can expand $\left(\mathbf{Z} + \boldsymbol{x}_z\boldsymbol{y}_z^{\mathsf{T}} \right)^{-1}$ as follows:

$$\left(\mathbf{Z} + \boldsymbol{x}_z\boldsymbol{y}_z^{\mathsf{T}} \right)^{-1} = \mathbf{Z}^{-1} - \frac{1}{1 + \boldsymbol{y}_z^{\mathsf{T}} \mathbf{Z}^{-1} \boldsymbol{x}_z} \left(\mathbf{Z}^{-1}\boldsymbol{x}_z \right) \left(\boldsymbol{y}_z^{\mathsf{T}}\mathbf{Z}^{-1} \right) . \tag{4.63}$$

Letting

$$f = \mathbf{Z}^{-1}\boldsymbol{x}_z \, ,$$
$$\boldsymbol{g}^{\mathsf{T}} = \boldsymbol{y}_z^{\mathsf{T}}\mathbf{Z}^{-1} \, ,$$
$$\frac{1}{\alpha} = \frac{1}{1 + \boldsymbol{y}_z^{\mathsf{T}}\mathbf{Z}^{-1}\boldsymbol{x}_z} \, ,$$

and

$$\boldsymbol{y}_z^{\mathsf{T}}\mathbf{Z}^{-1}\boldsymbol{x}_z = \boldsymbol{y}_z^{\mathsf{T}}f = f^{\mathsf{T}}\boldsymbol{y}_z = \boldsymbol{g}^{\mathsf{T}}\boldsymbol{x}_z = \alpha - 1 \, ,$$

we have:

$$
\begin{aligned}
\widetilde{\mathbf{H}}_{\langle\tilde{\mathbf{z}}\rangle} &= \mathbf{Q} + \boldsymbol{x}_q\boldsymbol{y}_q^{\mathsf{T}} - \left(\mathbf{R} + \boldsymbol{x}_q\boldsymbol{y}_z^{\mathsf{T}}\right)\left(\mathbf{Z}^{-1} - \frac{1}{\alpha}f\boldsymbol{g}^{\mathsf{T}}\right)\left(\mathbf{S} + \boldsymbol{x}_z\boldsymbol{y}_q^{\mathsf{T}}\right) \\
&= \mathbf{Q} + \boldsymbol{x}_q\boldsymbol{y}_q^{\mathsf{T}} - \left(\mathbf{R} + \boldsymbol{x}_q\boldsymbol{y}_z^{\mathsf{T}}\right)\mathbf{Z}^{-1}\left(\mathbf{S} + \boldsymbol{x}_z\,\boldsymbol{y}_q^{\mathsf{T}}\right) \\
&\quad + \frac{1}{\alpha}\left(\mathbf{R} + \boldsymbol{x}_q\boldsymbol{y}_z^{\mathsf{T}}\right)f\boldsymbol{g}^{\mathsf{T}}\left(\mathbf{S} + \boldsymbol{x}_z\boldsymbol{y}_q^{\mathsf{T}}\right) \\
&= \underbrace{\mathbf{Q} - \mathbf{R}\mathbf{Z}^{-1}\mathbf{S}}_{\mathbf{H}_{\langle\mathbf{Z}\rangle}} + \boldsymbol{x}_q\boldsymbol{y}_q^{\mathsf{T}} - \mathbf{R}\underbrace{\mathbf{Z}^{-1}\boldsymbol{x}_z}_{f}\boldsymbol{y}_q^{\mathsf{T}} - \boldsymbol{x}_q\underbrace{\boldsymbol{y}_z^{\mathsf{T}}\mathbf{Z}^{-1}}_{\boldsymbol{g}^{\mathsf{T}}}\mathbf{S} - \boldsymbol{x}_q\underbrace{\boldsymbol{y}_z^{\mathsf{T}}\mathbf{Z}^{-1}\boldsymbol{x}_z}_{(\alpha-1)}\boldsymbol{y}_q^{\mathsf{T}} \\
&\quad + \frac{1}{\alpha}\mathbf{R}f\boldsymbol{g}^{\mathsf{T}}\mathbf{S} + \frac{1}{\alpha}\mathbf{R}f\underbrace{\boldsymbol{g}^{\mathsf{T}}\boldsymbol{x}_z}_{(\alpha-1)}\boldsymbol{y}_q^{\mathsf{T}} + \frac{1}{\alpha}\boldsymbol{x}_q\underbrace{\boldsymbol{y}_z^{\mathsf{T}}f}_{(\alpha-1)}\boldsymbol{g}^{\mathsf{T}}\mathbf{S} + \frac{1}{\alpha}\boldsymbol{x}_q\underbrace{\boldsymbol{y}_z^{\mathsf{T}}f}_{(\alpha-1)}\underbrace{\boldsymbol{g}^{\mathsf{T}}\boldsymbol{x}_z}_{(\alpha-1)}\boldsymbol{y}_q^{\mathsf{T}} \\
&= \mathbf{H}_{\langle\mathbf{Z}\rangle} + \boldsymbol{x}_q\boldsymbol{y}_q^{\mathsf{T}} - \mathbf{R}f\boldsymbol{y}_q^{\mathsf{T}} - \boldsymbol{x}_q\boldsymbol{g}^{\mathsf{T}}\mathbf{S} - (\alpha-1)\boldsymbol{x}_q\boldsymbol{y}_q^{\mathsf{T}} \\
&\quad + \frac{1}{\alpha}\mathbf{R}f\boldsymbol{g}^{\mathsf{T}}\mathbf{S} + \frac{\alpha-1}{\alpha}\mathbf{R}f\boldsymbol{y}_q^{\mathsf{T}} + \frac{\alpha-1}{\alpha}\boldsymbol{x}_q\boldsymbol{g}^{\mathsf{T}}\mathbf{S} + \frac{(\alpha-1)^2}{\alpha}\boldsymbol{x}_q\boldsymbol{y}_q^{\mathsf{T}} \\
&= \mathbf{H}_{\langle\mathbf{Z}\rangle} + \left[1 - (\alpha-1) + \frac{(\alpha-1)^2}{\alpha}\right]\boldsymbol{x}_q\boldsymbol{y}_q^{\mathsf{T}} + \left[\frac{\alpha-1}{\alpha} - 1\right]\mathbf{R}f\boldsymbol{y}_q^{\mathsf{T}} \\
&\quad + \left[\frac{\alpha-1}{\alpha} - 1\right]\mathbf{x}_q\boldsymbol{g}^{\mathsf{T}}\mathbf{S} + \frac{1}{\alpha}\mathbf{R}f\boldsymbol{g}^{\mathsf{T}}\mathbf{S} \\
&= \mathbf{H}_{\langle\mathbf{Z}\rangle} + \frac{1}{\alpha}\boldsymbol{x}_q\boldsymbol{y}_q^{\mathsf{T}} - \frac{1}{\alpha}\mathbf{R}f\boldsymbol{y}_q^{\mathsf{T}} - \frac{1}{\alpha}\mathbf{x}_q\boldsymbol{g}^{\mathsf{T}}\mathbf{S} + \frac{1}{\alpha}\mathbf{R}f\boldsymbol{g}^{\mathsf{T}}\mathbf{S} \\
&= \mathbf{H}_{\langle\mathbf{Z}\rangle} + \frac{1}{\alpha}\left(\boldsymbol{x}_q - \mathbf{R}f\right)\boldsymbol{y}_q^{\mathsf{T}} - \frac{1}{\alpha}\left(\boldsymbol{x}_q - \mathbf{R}f\right)\boldsymbol{g}^{\mathsf{T}}\mathbf{S} \\
&= \mathbf{H}_{\langle\mathbf{Z}\rangle} + \frac{1}{\alpha}\left(\boldsymbol{x}_q - \mathbf{R}f\right)\left(\boldsymbol{y}_q - \mathbf{S}^{\mathsf{T}}\boldsymbol{g}\right)^{\mathsf{T}} \, .
\end{aligned}
$$

Re-inserting the expressions for α, f, and $\boldsymbol{g}$, we obtain:

$$\widetilde{\mathbf{H}}_{\langle\tilde{\mathbf{z}}\rangle} = \mathbf{H}_{\langle\mathbf{Z}\rangle} + \frac{1}{1 + \boldsymbol{y}_z^{\mathsf{T}}\mathbf{Z}^{-1}\boldsymbol{x}_z}\left(\boldsymbol{x}_q - \mathbf{R}\mathbf{Z}^{-1}\boldsymbol{x}_z\right)\left(\boldsymbol{y}_q - \mathbf{S}^{\mathsf{T}}\mathbf{Z}^{-1}\boldsymbol{y}_z\right)^{\mathsf{T}} . \qquad (4.64)$$

For the symmetric case, we know the following: $\boldsymbol{x} = \boldsymbol{y}$, and hence $\boldsymbol{x}_q = \boldsymbol{y}_q$ and $\boldsymbol{x}_z = \boldsymbol{y}_z$; $\mathbf{S} = \mathbf{R}^{\mathsf{T}}$; and $\mathbf{Z} = \mathbf{Z}^{\mathsf{T}}$, which means $\boldsymbol{f} = \boldsymbol{g} = \mathbf{Z}^{-1}\boldsymbol{x}_z$. Substituting all these in (4.56), we obtain Equation (4.59). The proof is now complete. $\square$

The result of Proposition 4.25 helps our understanding of how a rank-one structural perturbation to a graph—in the form of an edge addition or deletion—manifests itself in the dynamics of the graph. We now consider different types of edge addition to a graph $\mathcal{G}$, depending on whether the ends of the edge are G-nodes, L-nodes, or one of each type. We simply tailor and simplify Equation (4.59) to the case at hand.

In what follows we consider a graph $\mathcal{G}$ with n_{G} gravis nodes (G-nodes) and n_{L} levis nodes (L-nodes). We number the G-nodes $1, \ldots, n_{\mathsf{G}}$, and the L-nodes $1, \ldots, n_{\mathsf{L}}$.

4.5.2 First-Order Eigenvalue Sensitivities Due to Rank-One Graph Perturbations

We know from basic perturbation theory, that if an eigenproblem is perturbed from

$$\mathbf{L}\boldsymbol{v}_{\mathsf{G}} = \lambda \mathbf{M}\boldsymbol{v}_{\mathsf{G}}$$

to

$$(\mathbf{L} + \mathbf{E})(\boldsymbol{v} + d\boldsymbol{v}) = (\lambda + d\lambda)\mathbf{M}(\boldsymbol{v} + d\boldsymbol{v}) \,,$$

the first-order sensitivity expression for the eigenvalue λ is given by:

$$d\lambda = \frac{\boldsymbol{v}^{\mathsf{T}}\mathbf{E}\boldsymbol{v}}{\boldsymbol{v}^{\mathsf{T}}\mathbf{M}\boldsymbol{v}} \,. \tag{4.65}$$

Earlier, we showed that a rank-one perturbation to a symmetric matrix translates to a rank-one perturbation in any of its properly defined Schur complements. Adapting that result from (4.59) into the context of graphs with G- and L-nodes, the expression for the error matrix $\mathbf{E}$ is given as follows:

$$\mathbf{E} = \frac{1}{1 + \boldsymbol{x}_{\mathsf{L}}^{\mathsf{T}}\mathbf{L}_{\mathsf{L}}^{-1}\boldsymbol{x}_{\mathsf{L}}} \left(\boldsymbol{x}_{\mathsf{G}} - \mathbf{L}_{\mathsf{GL}}\mathbf{L}_{\mathsf{L}}^{-1}\boldsymbol{x}_{\mathsf{L}}\right)\left(\boldsymbol{x}_{\mathsf{G}} - \mathbf{L}_{\mathsf{GL}}\mathbf{L}_{\mathsf{L}}^{-1}\boldsymbol{x}_{\mathsf{L}}\right)^{\mathsf{T}} \,. \tag{4.66}$$

Assuming that $\boldsymbol{v}_{\mathsf{G}}$ is already $\mathbf{M}$-normalized, i.e., $\boldsymbol{v}_{\mathsf{G}}^{\mathsf{T}}\mathbf{M}\boldsymbol{v}_{\mathsf{G}} = 1$, we apply (4.65) to (4.66) to

obtain

$$d\lambda = v_\mathsf{G}^\mathsf{T}\mathbf{E}v_\mathsf{G} = \frac{1}{1 + x_\mathsf{L}^\mathsf{T}\mathbf{L}_\mathsf{L}^{-1}x_\mathsf{L}} \left(v_\mathsf{G}^\mathsf{T}x_\mathsf{G} - v_\mathsf{G}^\mathsf{T}\mathbf{L}_\mathsf{GL}\mathbf{L}_\mathsf{L}^{-1}x_\mathsf{L}\right)\left(x_\mathsf{G}^\mathsf{T}v_\mathsf{G} - x_\mathsf{L}^\mathsf{T}\mathbf{L}_\mathsf{L}^{-1}\mathbf{L}_\mathsf{LG}v_\mathsf{G}\right) . \quad (4.67)$$

From Theorem 4.16 and Equation (4.41) we know that

$$v_\mathsf{L} = -\mathbf{L}_\mathsf{L}^{-1}\mathbf{L}_\mathsf{GL}^\mathsf{T}v_\mathsf{G} \, . \, .$$

The sensitivity expression for the eigenvalue simplifies to:

$$d\lambda = \frac{1}{1 + x_\mathsf{L}^\mathsf{T}\mathbf{L}_\mathsf{L}^{-1}x_\mathsf{L}}\left(v_\mathsf{G}^\mathsf{T}x_\mathsf{G} + v_\mathsf{L}^\mathsf{T}x_\mathsf{L}\right)\left(x_\mathsf{G}^\mathsf{T}v_\mathsf{G} + x_\mathsf{L}^\mathsf{T}v_\mathsf{L}\right) = \frac{\left(v^\mathsf{T}x\right)^2}{1 + x_\mathsf{L}^\mathsf{T}\mathbf{L}_\mathsf{L}^{-1}x_\mathsf{L}} , \quad (4.68)$$

where $v = [v_\mathsf{G} \; v_\mathsf{L}]^\mathsf{T}$ and x is defined similarly.

We now consider three different types of rank-one perturbation to a graph. In each case, we will derive exact expressions for the error matrix $\mathbf{E}$, and comment on how the eigenvalue sensitivity expression specializes to each type of perturbation.

4.5.2.1 Gravis-Gravis (GG-Type) Edge Addition

Consider a graph $\mathcal{G}$ comprising G-nodes and L-nodes, whose Laplacian matrix is partitioned as follows:

$$\mathbf{L} = \begin{bmatrix} \mathbf{L}_\mathsf{G} & \mathbf{L}_\mathsf{GL} \\ \mathbf{L}_\mathsf{LG} & \mathbf{L}_\mathsf{L} \end{bmatrix} .$$

Let the Schur complement of $\mathbf{L}_\mathsf{L}$ in $\mathbf{L}$ be denoted by $\mathbf{L}_{\langle\mathsf{L}\rangle} = \mathbf{L}_\mathsf{G} - \mathbf{L}_\mathsf{GL}\mathbf{L}_\mathsf{L}^{-1}\mathbf{L}_\mathsf{LG}$. Suppose we join two non-neighboring G-nodes, say the ith and the jth, with an edge of weight γ. The perturbation matrix corresponding to such an edge addition ($x_\mathsf{L} = 0$) is given below:

$$\mathbf{E} = xx^\mathsf{T} = \begin{bmatrix} x_\mathsf{G} \\ x_\mathsf{L} \end{bmatrix}\begin{bmatrix} x_\mathsf{G}^\mathsf{T} & x_\mathsf{L}^\mathsf{T} \end{bmatrix} = \begin{bmatrix} x_\mathsf{G} \\ 0 \end{bmatrix}\begin{bmatrix} x_\mathsf{G}^\mathsf{T} & 0^\mathsf{T} \end{bmatrix} = \begin{bmatrix} x_\mathsf{G}x_\mathsf{G}^\mathsf{T} & 0 \\ 0 & 0 \end{bmatrix} . \quad (4.69)$$

We note that Equation (4.59), adapted to the notation of the Laplacian matrix, simplifies to:

$$\widetilde{\mathbf{L}}_{\langle\widetilde{\mathsf{L}}\rangle} = \mathbf{L}_{\langle\mathsf{L}\rangle} + x_\mathsf{G}x_\mathsf{G}^\mathsf{T} . \quad (4.70)$$

Furthermore, x_G has the following form:

$$
x_G = \sqrt{\gamma} \begin{pmatrix} 0 \\ +1 \\ 0 \\ -1 \\ 0 \end{pmatrix}_{n_G \times 1} \begin{matrix} \\ \leftarrow \ i^{\text{th}} \text{ row} \\ \\ \leftarrow \ j^{\text{th}} \text{ row} \\ \\ \end{matrix} = \sqrt{\gamma} \left(e_{i|(n_G)} - e_{j|(n_G)} \right) . \tag{4.71}
$$

Therefore, the perturbation matrix that modifies the original Schur complement $\mathbf{L}_{\langle L \rangle}$ is:

$$
x_G x_G^{\mathsf{T}} = \gamma \begin{matrix} & i^{\text{th}} & j^{\text{th}} \\ & \text{col} & \text{col} \\ & \downarrow & \downarrow \\ \begin{pmatrix} & & \\ +1 & -1 \\ & & \\ -1 & +1 \end{pmatrix} & \begin{matrix} \\ \leftarrow i^{\text{th}} \text{ row} \\ \\ \leftarrow j^{\text{th}} \text{ row} \end{matrix} \end{matrix} . \tag{4.72}
$$

Except for the entries shown, the matrix is zero everywhere. Note that $x_G x_G^{\mathsf{T}}$ is a Laplacian matrix in its own right. The eigenvalue sensitivity expression (4.68) for this type of edge perturbation (remember $x_L = 0$) takes the form:

$$
d\lambda = \left(v_G^{\mathsf{T}} x_G \right)^2 = \gamma \left(v_G(i) - v_G(j) \right)^2 , \tag{4.73}
$$

where the indices i and j correspond to the ith and j^{th} G-nodes, respectively.

4.5.2.2   Levis-Levis (LL-Type) Edge Addition

Now suppose we join two L-nodes, say the ith and the jth, with an edge of weight ζ. The perturbation matrix corresponding to such an edge addition ($x_G = 0$) would be:

$$
\mathbf{E} = xx^{\mathsf{T}} = \begin{bmatrix} x_G \\ x_L \end{bmatrix} \begin{bmatrix} x_G^{\mathsf{T}} & x_L^{\mathsf{T}} \end{bmatrix} = \begin{bmatrix} 0 \\ x_L \end{bmatrix} \begin{bmatrix} 0^{\mathsf{T}} & x_L^{\mathsf{T}} \end{bmatrix} = \begin{bmatrix} 0 & 0 \\ 0 & x_L x_L^{\mathsf{T}} \end{bmatrix} . \tag{4.74}
$$

The perturbation vector corresponding to the LL-edge is

$$
\boldsymbol{x}_{\mathsf{L}} = \sqrt{\zeta}\begin{pmatrix} 0 \\ +1 \\ 0 \\ -1 \\ 0 \end{pmatrix}_{n_{\mathsf{L}} \times 1} \begin{array}{l} \\ \leftarrow\ i^{\text{th}}\ \text{row} \\ \\ \leftarrow\ j^{\text{th}}\ \text{row} \\ \\ \end{array} = \sqrt{\zeta}\left(\boldsymbol{e}_{i|(n_{\mathsf{L}})} - \boldsymbol{e}_{j|(n_{\mathsf{L}})}\right)\ . \tag{4.75}
$$

For such an LL-connection, we note that Equation (4.59), adapted to the notation of the Laplacian matrix, simplifies to:

$$
\widetilde{\mathbf{L}}_{\langle\widetilde{\mathsf{L}}\rangle} = \mathbf{L}_{\langle\mathsf{L}\rangle} + \frac{1}{1 + \boldsymbol{x}_{\mathsf{L}}^{\mathsf{T}}\mathbf{L}_{\mathsf{L}}^{-1}\boldsymbol{x}_{\mathsf{L}}}\mathbf{L}_{\mathsf{GL}}\mathbf{L}_{\mathsf{L}}^{-1}\boldsymbol{x}_{\mathsf{L}}\boldsymbol{x}_{\mathsf{L}}^{\mathsf{T}}\mathbf{L}_{\mathsf{L}}^{-1}\mathbf{L}_{\mathsf{GL}}^{\mathsf{T}}\ . \tag{4.76}
$$

Letting $\mathbf{Q} = -\mathbf{L}_{\mathsf{L}}^{-1}\mathbf{L}_{\mathsf{GL}}^{\mathsf{T}}$ be the row-stochastic matrix discussed in Theorem 4.14, we express it by its rows as follows:

$$
\mathbf{Q} = -\mathbf{L}_{\mathsf{L}}^{-1}\mathbf{L}_{\mathsf{GL}}^{\mathsf{T}} = \begin{bmatrix} \boldsymbol{q}_1^{\mathsf{T}} \\ \vdots \\ \boldsymbol{q}_{n_{\mathsf{L}}}^{\mathsf{T}} \end{bmatrix}\ . \tag{4.77}
$$

Equation (4.76) then simplifies to:

$$
\widetilde{\mathbf{L}}_{\langle\widetilde{\mathsf{L}}\rangle} = \mathbf{L}_{\langle\mathsf{L}\rangle} + \frac{\zeta}{1 + \zeta\left(\left[\mathbf{L}_{\mathsf{L}}^{-1}\right]_{ii} + \left[\mathbf{L}_{\mathsf{L}}^{-1}\right]_{jj} - 2\left[\mathbf{L}_{\mathsf{L}}^{-1}\right]_{ij}\right)}\left(\boldsymbol{q}_i - \boldsymbol{q}_j\right)\left(\boldsymbol{q}_i - \boldsymbol{q}_j\right)^{\mathsf{T}}\ , \tag{4.78}
$$

where we have noted that for $\boldsymbol{x}_{\mathsf{L}}$ given in (4.75),

$$
\begin{aligned}
\boldsymbol{x}_{\mathsf{L}}^{\mathsf{T}}\mathbf{L}_{\mathsf{L}}^{-1}\boldsymbol{x}_{\mathsf{L}}^{\mathsf{T}} &= \zeta\left(\boldsymbol{e}_{i|(n_{\mathsf{L}})} - \boldsymbol{e}_{j|(n_{\mathsf{L}})}\right)^{\mathsf{T}}\mathbf{L}_{\mathsf{L}}^{-1}\left(\boldsymbol{e}_{i|(n_{\mathsf{L}})} - \boldsymbol{e}_{j|(n_{\mathsf{L}})}\right) \\
&= \zeta\left(\left[\mathbf{L}_{\mathsf{L}}^{-1}\right]_{ii} + \left[\mathbf{L}_{\mathsf{L}}^{-1}\right]_{jj} - 2\left[\mathbf{L}_{\mathsf{L}}^{-1}\right]_{ij}\right)\ .
\end{aligned}
$$

From Theorem 3.12 we know that $\left[\mathbf{L}_{\mathsf{L}}^{-1}\right]_{ii} > 0,\ i = 1, \ldots, n_{\mathsf{L}}$. Moreover, if the subgraph induced by the L-nodes on graph $\mathcal{G}$ is connected, *i.e.* if $\mathbf{L}_{\mathsf{L}}$ is irreducible, the theorem further stipulates that $\left[\mathbf{L}_{\mathsf{L}}^{-1}\right]_{ij} > 0,\ i, j = 1, \ldots, n_{\mathsf{L}}, i \neq j$. If, however, the subgraph induced by the L-nodes is not connected, *i.e.*, if $\mathbf{L}_{\mathsf{L}}$ is reducible, then $\left[\mathbf{L}_{\mathsf{L}}^{-1}\right]_{ij} \geq 0$, with equality if, and only if, the ith and j^{th} nodes belong to two disconnected induced subgraphs. Regardless, it is clear that the denominator term $\boldsymbol{x}_{\mathsf{L}}^{\mathsf{T}}\mathbf{L}_{\mathsf{L}}^{-1}\boldsymbol{x}_{\mathsf{L}}^{\mathsf{T}} > 0$.

The eigenvalue sensitivity expression for this LL-type edge addition is simply

$$d\lambda = \frac{\left(v_{\mathsf{L}}^{\mathsf{T}} x_{\mathsf{L}}\right)^2}{1 + x_{\mathsf{L}}^{\mathsf{T}} \mathbf{L}^{-1} x_{\mathsf{L}}} = \frac{\zeta \left(v_{\mathsf{L}}(i) - v_{\mathsf{L}}(j)\right)^2}{1 + \zeta \left(\left[\mathbf{L}_{\mathsf{L}}^{-1}\right]_{ii} + \left[\mathbf{L}_{\mathsf{L}}^{-1}\right]_{jj} - 2 \left[\mathbf{L}_{\mathsf{L}}^{-1}\right]_{ij}\right)} \; . \tag{4.79}$$

4.5.2.3 Gravis-Levis (GL-Type) Edge Addition

Suppose we connect the ith G-node to the jth L-node, where $i = 1, \ldots, n_{\mathsf{G}}$ and $j = 1, \ldots, n_{\mathsf{L}}$; let the weight of the connection be θ. The perturbation matrix corresponding to such an edge addition would be:

$$\mathbf{E} = xx^{\mathsf{T}} = \begin{bmatrix} x_{\mathsf{G}} \\ x_{\mathsf{L}} \end{bmatrix} \begin{bmatrix} x_{\mathsf{G}}^{\mathsf{T}} & x_{\mathsf{L}}^{\mathsf{T}} \end{bmatrix} = \begin{bmatrix} x_{\mathsf{G}} x_{\mathsf{G}}^{\mathsf{T}} & x_{\mathsf{G}} x_{\mathsf{L}}^{\mathsf{T}} \\ x_{\mathsf{L}} x_{\mathsf{G}}^{\mathsf{T}} & x_{\mathsf{L}} x_{\mathsf{L}}^{\mathsf{T}} \end{bmatrix} , \tag{4.80}$$

where x_{G} and x_{L} are given by:

$$x_{\mathsf{G}} = \sqrt{\theta} \begin{pmatrix} \mathbf{0} \\ +1 \\ \mathbf{0} \end{pmatrix}_{n_{\mathsf{G}} \times 1} \qquad \leftarrow i^{\text{th}} \text{ row} = \sqrt{\theta}\, e_{i|(n_{\mathsf{G}})} \tag{4.81}$$

$$x_{\mathsf{L}} = \sqrt{\theta} \begin{pmatrix} \mathbf{0} \\ -1 \\ \mathbf{0} \end{pmatrix}_{n_{\mathsf{L}} \times 1} \qquad \leftarrow j^{\text{th}} \text{ row} = -\sqrt{\theta}\, e_{j|(n_{\mathsf{L}})} \; . \tag{4.82}$$

For x_{G} and x_{L} as given by (4.81) and (4.82), Equation (4.59) adapts as follows:

$$\widetilde{\mathbf{L}}_{\langle \tilde{\mathsf{L}} \rangle} = \mathbf{L}_{\langle \mathsf{L} \rangle} + \frac{\theta}{1 + \theta e_{j|(n_{\mathsf{L}})}^{\mathsf{T}} \mathbf{L}_{\mathsf{L}}^{-1} e_{j|(n_{\mathsf{L}})}} \left(e_{i|(n_{\mathsf{G}})} + \mathbf{Q}^{\mathsf{T}} e_{j|(n_{\mathsf{L}})}\right) \left(e_{i|(n_{\mathsf{G}})} + \mathbf{Q}^{\mathsf{T}} e_{j|(n_{\mathsf{L}})}\right)^{\mathsf{T}} .$$

This simplifies to:

$$\widetilde{\mathbf{L}}_{\langle \tilde{\mathsf{L}} \rangle} = \mathbf{L}_{\langle \mathsf{L} \rangle} + \frac{\theta}{1 + \theta \left[\mathbf{L}_{\mathsf{L}}^{-1}\right]_{jj}} \left(e_{i|(n_{\mathsf{G}})} + q_j\right) \left(e_{i|(n_{\mathsf{G}})} + q_j\right)^{\mathsf{T}} , \tag{4.83}$$

where $\mathbf{Q}$ is as defined in (4.77), and

$$x_{\mathsf{L}}^{\mathsf{T}} \mathbf{L}_{\mathsf{L}}^{-1} x_{\mathsf{L}} = \left(\sqrt{\theta}\, e_{j|(n_{\mathsf{L}})}^{\mathsf{T}}\right) \mathbf{L}_{\mathsf{L}}^{-1} \left(\sqrt{\theta}\, e_{j|(n_{\mathsf{L}})}\right) = \theta \left[\mathbf{L}_{\mathsf{L}}^{-1}\right]_{jj} \; .$$

Theorem 3.12 implies strict positivity for $\left[\mathbf{L}_{\mathsf{L}}^{-1}\right]_{jj}$, $j = 1, \ldots, n_{\mathsf{L}}$. The first-order eigenvalue sensitivity expression for this case is given below:

$$d\lambda = \frac{\theta \left(\boldsymbol{v}_{\mathsf{G}}(i) - \boldsymbol{v}_{\mathsf{L}}(j)\right)^2}{1 + \theta \left[\mathbf{L}_{\mathsf{L}}^{-1}\right]_{jj}} \ . \tag{4.84}$$

4.5.3   L-Node Addition

Adding of an L-node is qualitatively different from adding a G-node to a graph, because the Schur contraction necessary for extracting the dynamic properties of the network are done with respect to the L-nodes. In this section, we show that when an L-node is added to a graph through only one edge (*i.e.*, the added L-node is a terminal vertex), the dynamics of the graph do not change: the finite eigenvalues do not move (there will be one additional infinite eigenvalue though), and the eigenvectors corresponding to the finite eigenvalues of the graph do not change. This is regardless of whether the added terminal L-node connects to another L-node or a G-node in the network.

4.5.3.1   Added L-node connected to G-nodes only

Suppose we connect the added the L-node only to G-nodes. In this case, the size of the Laplacian matrix of the graph increases by one, and can be written in partitioned form as follows:

$$\mathbf{L} = \left[\begin{array}{cc|cc} \mathbf{L}_{\mathsf{G}} + \mathbf{H} & & \mathbf{L}_{\mathsf{GL}} & \boldsymbol{h} \\ \hline \mathbf{L}_{\mathsf{LG}} & & \mathbf{L}_{\mathsf{L}} & \mathbf{0} \\ \boldsymbol{h}^{\mathsf{T}} & & \mathbf{0}^{\mathsf{T}} & \gamma \end{array} \right] , \tag{4.85}$$

where $\mathbf{H} = -\operatorname{diag}\left(\boldsymbol{h}\right)$, and $\gamma = -\boldsymbol{h}^{\mathsf{T}}\mathbf{1}$ is the degree of the added L-node. The Laplacian matrix of the Schur-contracted graph is:

$$\mathbf{Q} = \mathbf{L}_G + \mathbf{H} - \begin{bmatrix} \mathbf{L}_{GL} & \boldsymbol{z} \end{bmatrix} \begin{bmatrix} \mathbf{L}_L^{-1} & \mathbf{0} \\ \mathbf{0} & \gamma^{-1} \end{bmatrix} \begin{bmatrix} \mathbf{L}_{LG} \\ \boldsymbol{z}^T \end{bmatrix} \tag{4.86}$$

$$= \mathbf{L}_G - \mathbf{L}_{GL} \mathbf{L}_L^{-1} \mathbf{L}_{LG} + \mathbf{H} - \frac{1}{\gamma} \boldsymbol{h}\boldsymbol{h}^T \tag{4.87}$$

$$= \mathbf{L}_{\langle L \rangle} + \mathbf{H} - \frac{1}{\gamma} \boldsymbol{h}\boldsymbol{h}^T . \tag{4.88}$$

When the added L-node is connected to only one G-node, say the ith, $\boldsymbol{p}$ is given by:

$$\boldsymbol{h} = \gamma \begin{pmatrix} \mathbf{0} \\ +1 \\ \mathbf{0} \end{pmatrix}_{n_G \times 1} \quad \leftarrow i^{\text{th}} \text{ row} \tag{4.89}$$

Clearly, $\mathbf{H} = \frac{1}{\gamma} \boldsymbol{h}\boldsymbol{h}^T$, thus leading to the interesting result:

$$\mathbf{Q} = \mathbf{L}_{\langle L \rangle} . \tag{4.90}$$

This result is consistent with our discussion of the fully-connectedness of the Schur contracted subgraphs, and how the segments of the graph not in contact with the subgraph with respect to which the Schur contraction is performed, do not get affected.

4.5.3.2   Added L-node connected to L-nodes only

Now suppose we connect the added the L-node only to other L-nodes. In this case, the size of the Laplacian matrix of the graph increases by one, and can be written in partitioned form as follows:

$$\mathbf{L} = \begin{bmatrix} \mathbf{L}_G & \mathbf{L}_{GL} & \mathbf{0} \\ \hline \mathbf{L}_{LG} & \mathbf{L}_L + \mathbf{Z} & \boldsymbol{z} \\ \mathbf{0} & \boldsymbol{z}^T & \xi \end{bmatrix} , \tag{4.91}$$

where $\mathbf{Z} = -\,\mathsf{diag}\,(\boldsymbol{z})$, and $\xi = -\boldsymbol{z}^T \mathbf{1}$ is the degree of the added L-node. The Laplacian matrix of the Schur-contracted graph is:

$$\mathbf{R} = \mathbf{L_G} - \begin{bmatrix} \mathbf{L_{GL}} & \mathbf{0} \end{bmatrix} \begin{bmatrix} \mathbf{L_L} & z \\ z^\mathsf{T} & \xi \end{bmatrix}^{-1} \begin{bmatrix} \mathbf{L_{LG}} \\ \mathbf{0^\mathsf{T}} \end{bmatrix} \tag{4.92}$$

$$= \mathbf{L_G} - \mathbf{L_{GL}} \left(\mathbf{L_L} + \mathbf{Z} - \frac{1}{\xi} z z^\mathsf{T} \right)^{-1} \mathbf{L_{LG}} . \tag{4.93}$$

When the added L-node is connected to only one L-node, say the ith, z is given by:

$$z = \xi \begin{pmatrix} \mathbf{0} \\ +1 \\ \mathbf{0} \end{pmatrix}_{n_\mathsf{L} \times 1} \quad \leftarrow i^{\text{th}} \text{ row} \tag{4.94}$$

Clearly, $\mathbf{Z} = \frac{1}{\xi} z z^\mathsf{T}$, thus leading to a similar result as before:

$$\mathbf{R} = \mathbf{L_{\langle L \rangle}} . \tag{4.95}$$

A Graph-Theoretic Look at Dynamic Coherency

5.1 Introduction and Contributions

The dynamic behavior of large-scale vibrational networks has been the subject of active research over the past two decades. A variety of approaches has been developed to expose modal structures of large dynamic systems, each scheme having its own assumptions and conclusions, and geared toward a specific purpose—for example, partitioning and model reduction. Among these methods, the one that is of immediate interest to us is broadly termed *coherency*; it is applied predominantly to the study of modal structures of power networks.

In this chapter, we look at coherency from a graph-theoretic vantage point. We consider not only approximate slow-coherency, but also exact (theoretical) coherency over an arbitrary set of modes (chord). Our analysis demonstrates how coherency need *not* occur *only* in the slowest modes. It also suggests a design strategy by which we can construct a graph with a desired set of coherent modes. The design begins with a smaller, aggregate graph that oscillates at the frequencies in which we want to see coherency in the designed graph; furthermore, the shapes of the coherent modes in the designed graph are closely related to those of the aggregate graph from which the design originates.

The contributions of this chapter are as follows:

- We present a matrix-perturbation approach to explain slow coherency, one that is far simpler, crisper, and cleaner than the slow-fast, two-time-scale approaches used so far in the literature. Using the Laplacian matrix of a graph, we begin with a set of disconnected components, each with its own Laplacian matrix and intra-component edge weights of order $O(1)$. We then connect the components by edge weights of order $O(\epsilon)$

where $\epsilon \ll 1$, leaving the actual topology of the inter-component links (*i.e.*, the decision as to which node in V_k connects to which node in V_l) for someone else to specify, while we insist on assigning the actual nonzero weights to those inter-area edges. We then show—through a simple perturbation analysis—how the network exhibits slow coherency.

- We look at exact (theoretical) coherency, and describe a method to design—from an aggregate graph $G[\mathcal{V}_q]$ (of order q and modes $(\theta, \boldsymbol{c})$)—a larger graph G of order $n > q$, such that G has a q-partition $\mathcal{V}_q$, with respect to which it is coherent in exactly q modes of the form $(\theta, \mathbf{X}\boldsymbol{c})$, where $\mathbf{X}$ is the partition matrix that describes $\mathcal{V}_q$.

- As part of our design, we specify necessary and sufficient conditions for the designed graph G to not only have q modes exactly as specified above, but also have the remaining oscillatory modes localized to their respective q areas. This leads to a very interesting design, with the following properties: (a) $q - 1$ of the q non-oscillatory modes of the disconnected network are replaced by the q oscillatory modes of the aggregate graph from which the design originates; (b) one non-oscillatory mode of the interconnected network remains at frequency zero; (c) each of the oscillatory modes of the original components ($n_G - q$ oscillatory modes in total, where n_G is the number of G-nodes) becomes a localized mode of the larger, interconnected network, with an eigenvalue that closely relates to the corresponding one in the individual component from which it came; and (d) the intra-area connections can be specified completely independently of the requirements imposed on the coherent modes, because each coherent mode—constant over a particular component—is in the null space of the corresponding local Laplacian matrix. What (d) implies is that we can design the intra-area connections such that the intra-area eigenvalues are arbitrarily situated relative to those of the coherent modes; this is how we can design a network that exhibits exact coherency, but not necessarily in the slowest q modes; we can make the intra-area modes arbitrarily small by insisting on weak links within one or more component.

- Our design unveils the requirements that must be satisfied for L-nodes to be introduced into the larger network, while maintaining exact coherency. In particular, our analysis makes apparent why a q-partition $\mathcal{V}_q$ may not include L-nodes that border an area $G(V_k)$; that is, an L-node may not be connected to any node outside the area in which it resides. For approximate slow coherency, as we shall see, this requirement is lifted, due to the mathematics of weak link approximations.

- The theory behind designing an exactly coherent graph that also has only local oscillatory modes suggests a relation between the mode confinement that we see in exact

coherency and the phenomenon of mode localization. We briefly, via an example, show how mode localization may be explained for an network with a particularly symmetric topology. We shall return to the topic of mode localization in Chapter 6.

5.2   A New Formulation of Slow Coherency

Slow-coherency theory is premised on the assumption that a large-scale power network comprises a number, say q, of groups of generators (or areas), with inter-area link weights of order $O(\epsilon)$, where $\epsilon \ll 1$, and intra-area connections of $O(1)$ strength. The consequences of these assumptions can be summarized as follows:

1. For a large-scale network with q weakly linked areas (or groups), there are $q - 1$ "slow" modes at frequencies of order $O(\epsilon)$. There is also one non-oscillatory mode which is the trivial $\lambda = 0$, corresponding to "rigid body motion" (generator angles all equal). These slow modes—also called "inter-area" or "inter-group" modes—are "extensive" in that their eigenvectors are not confined to just one or two areas; rather, they extend over the entire network.

2. The remaining $n - q$ eigenvalues are considered "fast" modes—also known as "intra-area" or "intra-group" modes—of the system, and are of order $O(1)$. The eigenvectors of these modes generally (but not always) are confined to one of the areas. If say two of the areas, considered separately, have the same fast eigenvalue, then the fast mode in the overall network (with $O(\epsilon)$ inter-area links inserted) will extend over those two areas.

3. For small enough ϵ, the generators in an area move coherently when only the slow modes are excited. In graph-theoretic terms, this means that the eigenvector of each of the slow modes is roughly constant over the nodes of a given area (or group).

In this section we establish a graph/matrix-theoretic proof for slow coherency, explaining several of the points summarized above. Of special consequence is our proof of Item 3. In the process, conditions under which slow-coherency's insights and predictions hold true will be exposed.

Before we proceed, however, we need to establish some terminology.

Definition 5.1 (Aggregate Graph)

Consider a connected graph G with node-weight matrix $\mathbf{M} = \mathsf{diag}\,(M_1, \ldots, M_n)$ and Laplacian matrix $\mathbf{L}$, where a_{ij} is the weight of the edge that connects distinct nodes ν_i and ν_j. Let $\mathcal{V}_q = \{V_1, \ldots, V_q\}$ be a q-partition of G, where $G(V_i)$ is connected for every $i = 1, \ldots, q$. Denote the node weight matrix for each $G(V_i)$ by $\mathbf{M}_i$ (so that we can alternatively write $\mathbf{M} = \mathsf{diag}\,(\mathbf{M}_1, \ldots, \mathbf{M}_q)$). Then $G[\mathcal{V}_q]$, the aggregate graph of G with respect to partition $\mathcal{V}_q$, is defined as follows:

1. *$G[\mathcal{V}_q]$ has q vertices $\vartheta_1, \ldots, \vartheta_q$, each of weight*

$$M[i] = \sum_{l \in V_i} M_l = \boldsymbol{x}_i^\mathsf{T} \mathbf{M} \boldsymbol{x}_i \ ,$$

   where $\boldsymbol{x}_i$ is the indicator vector for cluster V_i.

2. *The edge connecting distinct nodes ϑ_k with ϑ_l in $G[\mathcal{V}_q]$ has weight*

$$\xi_{kl} = \sum_{\nu_i \in V_k, \nu_j \in V_l} a_{ij} \ .$$

In other words, to construct the aggregate graph $G[\mathcal{V}_q]$, we simply represent each V_k-induced subgraph $G(V_k)$ with an "aggregate node" ϑ_k; assign to the aggregate node an "aggregate weight" equal to the sum of all the node weights in $G(V_k)$; and define the "aggregate weight" of the edge between distinct aggregate nodes ϑ_k and ϑ_l to be the sum of all edges in G that connect a node in $G(V_k)$ with another in $G(V_l)$. We denote the Laplacian matrix of $G[\mathcal{V}_q]$ by $\mathbf{L}_{[q]}$ and its node weight matrix by $\mathbf{M}_{[q]} = \mathsf{diag}\,(M[1], \ldots, M[q])$.

Example 5.2

Figure 5.1 shows a partitioned graph along with its aggregate graph. Each node ϑ_i in the aggregate graph has weight equal to the total weight of the nodes in the corresponding subgraph $G(V_i)$, and each edge joining ϑ_i and ϑ_j has weight equal to the total weight of edges connecting V_i and V_j.

Theorem 5.3 (Slow-Coherency in Graph-Theoretic Terms)

Consider a graph G with n vertices, Laplacian matrix $\mathbf{L}$, and vertex weight matrix $\mathbf{M}$. Let the graph have a q-partition $\mathcal{V}_q = \{V_1, \ldots, V_q\}$, where each cluster $G(V_i)$ contains at least one G-node. The intra-area edge weights are of order $O(1)$, while the inter-area link strengths are of order $O(\epsilon)$. Then

1. *the fastest $n_\mathsf{G} - q$ eigenvalues of $(\mathbf{L}, \mathbf{M})$ are of order $O(1)$.*
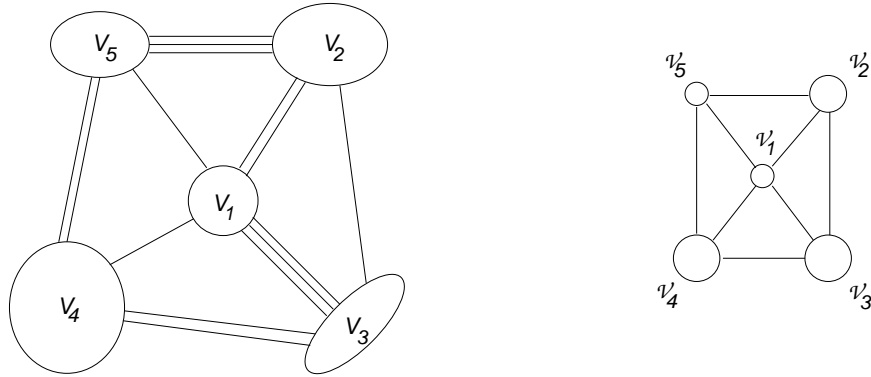
Figure 5.1: A partitioned graph and its aggregate.

2. *the slowest q eigenvalues of $(\mathbf{L}, \mathbf{M})$ are of order $O(\epsilon)$.*

3. *the slowest q eigenvectors of $(\mathbf{L}, \mathbf{M})$ exhibit approximate coherency,* i.e., *they are approximately constant over any given area $G(V_i)$, $i = 1, \ldots, q$.*

Proof: Consider the graph G with all the inter-area edges nulled; that is, consider

$$\widehat{G} = G(V_1) \oplus \cdots \oplus G(V_q) \, ,$$

which has the Laplacian matrix

$$\widehat{\mathbf{L}} = \mathsf{diag}\left(\mathbf{L}_1, \ldots, \mathbf{L}_q\right)$$

and vertex weight matrix

$$\mathbf{M} = \mathsf{diag}\left(\mathbf{M}_1, \ldots, \mathbf{M}_q\right) .$$

We shall consider $\mathbf{L}$ as an $O(\epsilon)$ perturbation of $\widehat{\mathbf{L}}$, *i.e.*, $\mathbf{L} = \widehat{\mathbf{L}} + \mathbf{E}$, where $\mathbf{E} \sim \epsilon$.

As each $G(V_i)$ is connected, the matrix pair $(\widehat{\mathbf{L}}, \mathbf{M})$ has exactly q eigenvalues at zero. The fastest $n_{\mathsf{G}} - q$ eigenvalues will be given by the Courant-Fischer theorem

Clearly, as the entries in $\widehat{\mathbf{L}}$ are $O(1)$ and an eigenvector $\boldsymbol{v}$ has unit $\mathbf{M}$-norm, the fastest $n - q$ eigenvalues must be $O(1)$. When the $O(\epsilon)$ inter-area edges are inserted into $\overline{G}$, these $n - q$ fast eigenvalues shift only slightly, thus retaining their $O(1)$ magnitudes.

The complication that arises here—related to the q slowest eigenvalues—has to do with the fact that the zero eigenvalue is of multiplicity q. Therefore, techniques outlined in

Appendix C need to be employed to study the effect of the $O(\epsilon)$ perturbations properly.

The symmetric perturbation matrix $\mathbf{E}$ that incorporates the $O(\epsilon)$ inter-area links, is a Laplacian matrix in its own right, and can be partitioned as follows:

$$
\mathbf{E} = \begin{bmatrix} \mathbf{E}_1 & \mathbf{E}_{12} & \cdots & \mathbf{E}_{1q} \\ \mathbf{E}_{21} & \mathbf{E}_2 & \cdots & \mathbf{E}_{2q} \\ \vdots & \vdots & \ddots & \vdots \\ \mathbf{E}_{q1} & \mathbf{E}_{q2} & \cdots & \mathbf{E}_q \end{bmatrix}. \tag{5.1}
$$

Below are some observations about the perturbation matrix $\mathbf{E}$:

- Each block $\mathbf{E}_i$ is a diagonal matrix because it does not represent any intra-area edge (intra-area edges of $G(V_i)$ already are accounted for in $\mathbf{L}_i$). Each diagonal entry of $\mathbf{E}_i$ is the sum of all the inter-area edges connected to the node corresponding to that diagonal entry. If a particular node in $G(V_i)$ is connected only to other nodes within the ith subgraph, then the corresponding diagonal entry in $\mathbf{E}_i$ is zero. Otherwise, it is a positive quantity denoting the inter-area degree of that node.

- The inter-area links are represented by $\mathbf{E}_{ij} \preceq \mathbf{0}$.

- Clearly, $-\boldsymbol{x}_k^\mathsf{T}\mathbf{E}\boldsymbol{x}_l = -\mathbf{1}_{n_k}^\mathsf{T}\mathbf{E}_{kl}\mathbf{1}_{n_l} = \xi_{kl}$, the sum of the edge weights connecting clusters V_k and V_l, which is also the edge weight ξ_{kl} in the aggregate graph $G[\mathcal{V}_q]$.

- $\delta_k = \boldsymbol{x}_k^\mathsf{T}\mathbf{E}\boldsymbol{x}_k = -\displaystyle\sum_{\substack{l=1 \\ l\neq k}}^{q} \boldsymbol{x}_k^\mathsf{T}\mathbf{E}\boldsymbol{x}_l = -\displaystyle\sum_{\substack{l=1 \\ l\neq k}}^{q} \mathbf{1}_{n_k}^\mathsf{T}\mathbf{E}_{kl}\mathbf{1}_{n_l} = \displaystyle\sum_{\substack{l=1 \\ l\neq k}}^{q} \xi_{kl}$, where δ_k is the degree of node ϑ_k in $G[\mathcal{V}_q]$, which is the same as the inter-area degree of cluster V_k.

We now proceed to examine how the q eigenvalues of $\overline{\mathbf{L}}$ at zero are perturbed. The multiplicity of the zero eigenvalue means that we must follow a procedure as outlined in Appendix C. We begin by specifying a set of q unit $\mathbf{M}$-norm eigenvectors for $\overline{\mathbf{L}}$. This is straightforward. If we index the nodes of G cluster-by-cluster, the partition matrix $\mathbf{X}$ corresponding to $\mathcal{V}_q$ would be:

$$\mathbf{X} = \begin{bmatrix} \mathbf{1}_{n_1} & \mathbf{0} & \cdots & \mathbf{0} \\ \mathbf{0} & \mathbf{1}_{n_2} & \cdots & \vdots \\ \vdots & \ddots & \ddots & \mathbf{0} \\ \mathbf{0} & \cdots & \mathbf{0} & \mathbf{1}_{n_q} \end{bmatrix} = \mathsf{diag}\left(\mathbf{1}_{n_1}, \ldots, \mathbf{1}_{n_q}\right), \tag{5.2}$$

where $\boldsymbol{x}_k$, the kth column of $\mathbf{X}$, is the indicator vector for cluster V_k, *i.e.*,

$$\boldsymbol{x}_k(i) = \begin{cases} 1 & \text{if } \nu_i \in V_i \\ 0 & \text{otherwise.} \end{cases}$$

It is clear, then, that the $n \times q$ matrix $\mathbf{W}$ defined below has columns that can serve as mutually M-orthonormal eigenvectors for the q zero eigenvalues of $(\overline{\mathbf{L}}, \mathbf{M})$.

$$\mathbf{W} = \mathbf{X}\mathbf{M}_{[q]}^{-1/2} = \left[\left. \frac{\boldsymbol{x}_1}{\sqrt{M[1]}} \right| \cdots \left| \frac{\boldsymbol{x}_q}{\sqrt{M[q]}} \right. \right], \tag{5.3}$$

where

$$\boldsymbol{w}_k = \frac{\boldsymbol{x}_k}{\sqrt{M[k]}}$$

denotes our choice of the kth eigenvector for the zero eigenvalue of $(\overline{\mathbf{L}}, \mathbf{M})$.

To find the actual eigenvectors $\boldsymbol{u}_i$, $i = 1, \ldots, q$ to which the perturbed ones reduce, we follow the procedure outlined in Appendix C. Namely, we create the matrix $\mathbf{G} = \mathbf{W}^{\mathsf{T}}\mathbf{E}\mathbf{W}$, and solve the eigenproblem of Equation (C.25): $\mathbf{G}\mathbf{C} = \mathbf{C}\boldsymbol{\Theta}$. Given our choice of $\mathbf{W}$, the matrix $\mathbf{G}$ is given by:

$$\mathbf{G} = \mathbf{W}^{\mathsf{T}}\mathbf{E}\mathbf{W} = \mathbf{M}_{[q]}^{-1/2}\mathbf{X}^{\mathsf{T}}\mathbf{E}\mathbf{X}\mathbf{M}_{[q]}^{-1/2}. \tag{5.4}$$

Based on the observations we made of the perturbation matrix $\mathbf{E}$ as well as the structure of the partition matrix $\mathbf{X}$, it is clear that $\mathbf{X}^{\mathsf{T}}\mathbf{E}\mathbf{X}$ is of the form of a Laplacian matrix:

$$\mathbf{X}^{\mathsf{T}}\mathbf{E}\mathbf{X} = \begin{bmatrix} \delta_1 & -\xi_{12} & \cdots & -\xi_{1q} \\ -\xi_{21} & \delta_2 & \cdots & -\xi_{2q} \\ \vdots & \vdots & \ddots & \vdots \\ -\xi_{q1} & -\xi_{q2} & \cdots & \delta_q \end{bmatrix}, \tag{5.5}$$

where we have already defined $\delta_k = \sum_{\substack{l=1 \\ l \neq k}}^{q} \xi_{kl}$. Clearly, $\mathbf{X}^{\mathsf{T}} \mathbf{E} \mathbf{X}$ is the Laplacian matrix of the aggregate graph $G[\mathcal{V}_q]$. That is,

$$\mathbf{L}_{[q]} = \mathbf{X}^{\mathsf{T}} \mathbf{E} \mathbf{X} . \tag{5.6}$$

Hence, we have: $\mathbf{G} = \mathbf{M}_{[q]}^{-1/2} \mathbf{L}_{[q]} \mathbf{M}_{[q]}^{-1/2}$.

We can now recast the eigenproblem of Equation (C.25) $\mathbf{G} \mathbf{C} = \mathbf{C} \boldsymbol{\Theta}$ into the following GEP form:

$$\mathbf{L}_{[q]} \mathbf{C}_{[q]} = \mathbf{M}_{[q]} \mathbf{C}_{[q]} \boldsymbol{\Theta} , \tag{5.7}$$

where $\mathbf{C}_{[q]} = \mathbf{M}_{[q]}^{-1/2} \mathbf{C}$.

Equation (5.7) is precisely the GEP for the aggregate graph $G[\mathcal{V}_q]$; furthermore, $\boldsymbol{\Theta} = \mathsf{diag}\,(d\lambda_1, \ldots, d\lambda_q)$ denotes the first-order eigenvalue shifts.

Assuming that the aggregate graph $G[\mathcal{V}_q]$ has no repeated eigenvalues, we simply use Equation (C.23) to find the zero eigenvectors $\mathbf{U}$ to which the perturbed ones reduce as $\mathbf{E} \longrightarrow \mathbf{0}$, *i.e.*, $\mathbf{U} = \mathbf{W} \mathbf{C}_{[q]}$. That is to say, the zero eigenvectors to which the perturbed ones reduce are given by:

$$\mathbf{U} = \mathbf{W} \mathbf{C} = \underbrace{\mathbf{X} \mathbf{M}_{[q]}^{-1/2}}_{\mathbf{W}} \underbrace{\mathbf{M}_{[q]}^{1/2} \mathbf{C}_{[q]}}_{\mathbf{C}} = \mathbf{X} \mathbf{M}_{[q]}^{-1} \mathbf{C}_{[q]} . \tag{5.8}$$

It is clear now that the zero eigenvectors to which the perturbed ones reduce are simply linear combinations of the indicator vectors for the various clusters, the coefficients in that linear combination being the columns of the matrix $\mathbf{M}_{[q]}^{-1} \mathbf{C}$. Hence, with a perturbation matrix that is vanishingly small (of order $O(\epsilon)$), and assuming that the aggregate graph—represented by the pair $(\mathbf{L}_{[q]}, \mathbf{M}_{[q]})$—has no repeated eigenvalues (we can ensure this if we are given the prerogative of specifying the inter-area edge valuations), then the q slowest eigenvectors of G will be roughly constant over each of the clusters V_i, as they reduce to the columns of $\mathbf{U}$ above.

If we are not given the prerogative of specifying the inter-area edge-weights, there is a possibility that the aggregate matrix will have repeated eigenvalues, in which case we

need to carry the first-order perturbation analysis to the next higher order.

Regarding the eigenvalues to which the q zero eigenvalues are perturbed, we have shown in Appendix C that they are of order $O(\epsilon)$. The proof is now complete. $\qquad\qquad\square$

Before we proceed to the next corollary, we need to define the notions of a "block acyclic matrix" and a "block spanning tree."

Definition 5.4 (Block Acyclic Matrix)
A symmetric $n \times n$ matrix $\mathbf{A}$ is "block acyclic of order q" (or "q-block acyclic") if (a) its graph $G(\mathbf{A})$ has nonnegative edges, and (b) there exists a q-partition $\mathcal{V}_q = \{V_1, \ldots, V_q\}$ of $G(\mathbf{A})$, with a corresponding partition matrix $\mathbf{X} = \mathsf{diag}\,(\boldsymbol{x}_1, \ldots, \boldsymbol{x}_q)$, where $\boldsymbol{x}_i$ is the indicator vector for cluster V_i, such that, for some integer $1 \leq q \leq n$, the matrix $\mathbf{X}^\mathsf{T}\mathbf{A}\mathbf{X}$ is acyclic.

Example 5.5
The following graph, said to have "block tree" structure, has a block acyclic Laplacian matrix.
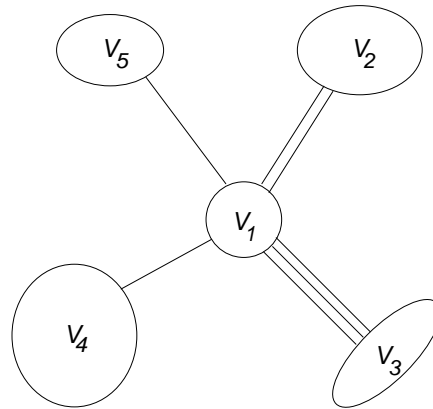
Figure 5.2: A graph with a block tree structure (and block acyclic Laplacian matrix.)

Proposition 1. *A symmetric matrix $\mathbf{A}$ is block acyclic if, and only if, its graph has a aggregate graph that is a tree.*

Definition 5.6 (Spanning Block-Tree)
Specify a q-partition $\mathcal{V}_q = \{V_1, \ldots, V_q\}$ on a connected graph G. A spanning block tree of G with respect to $\mathcal{V}_q$ is obtained by:

1. *considering the aggregate companion graph $G[\mathcal{V}_q]$.*

2. *selecting a spanning tree of $G[\mathcal{V}_q]$.*

3. *deleting all the edges between areas V_i and V_j in G if the corresponding edge between ϑ_i and ϑ_j in $G[\mathcal{V}_q]$ is not in the spanning tree of $G[\mathcal{V}_q]$ that was selected in Item 1.*

Clearly, the Laplacian matrix of a spanning block-tree of G must be block acyclic.
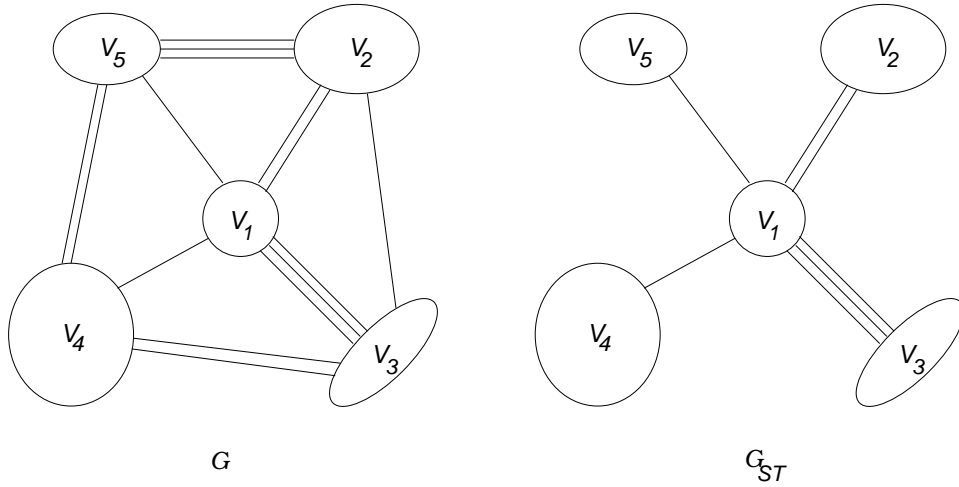
Figure 5.3: A q-partitioned graph G and a spanning block tree ($q = 5$).

Corollary 5.7

Consider a graph similar to the one described by the slow coherency theorem, except that this one has a block tree structure. Then for the kth slowest mode, $1 \leq k \leq q$, there are exactly $k - 1$ eigenvector sign alternations across cluster boundaries.

Proof: The aggregate graph $G([\mathcal{V}_q])$ corresponding to G has a tree structure. Therefore, according to Fiedler's results for acyclic matrices (and our extensions of his results in the previous chapter), the eigenvector components of $G([\mathcal{V}_q])$ show exactly $k - 1$ sign alternations for the kth slowest mode. These eigenvectors being the coefficients of the indicator vectors that form the columns of $\mathbf{X}$, in producing the eigenvectors of G, it is clear that for sufficiently small ϵ, the perturbed eigenvector of the kth slowest mode will have exactly $k - 1$ sign alternations across cluster boundaries.

The proof is now complete. $\qquad\qquad\qquad\qquad\qquad\qquad\qquad\qquad\qquad\qquad\qquad$ $\square$

Example 5.8

Consider the block-acyclic graph of Figure 5.4, which comprises four clusters (indicated by dashed circles) that have intra-area links of order $O(1)$, but are weakly connected to each other according to weights of order $O(\epsilon)$.

Table 5.2 shows the four slow, approximately coherent modes of the block-acyclic graph. Notice that the sign alternations across clusters, in the four slow modes, follow the results of Fiedler and our extensions for weighted trees graphs.
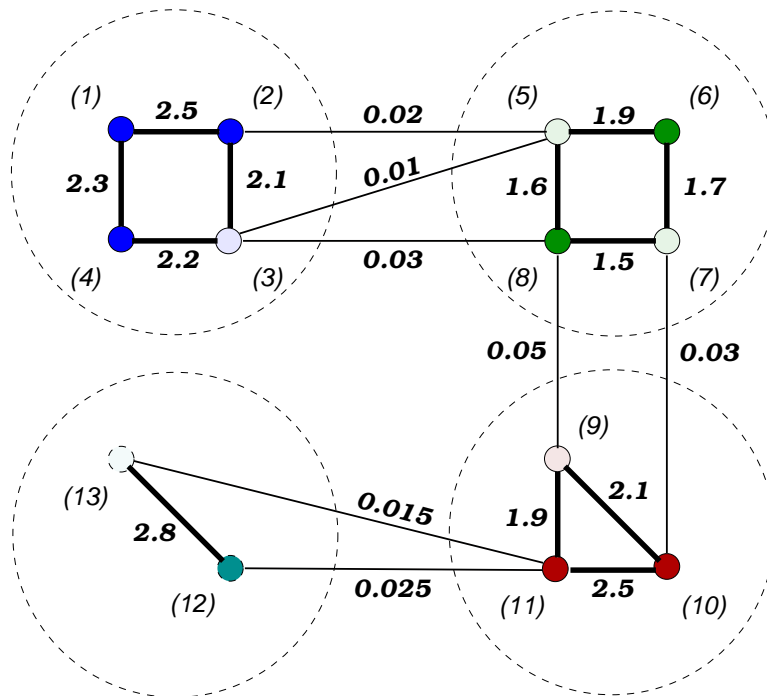
Figure 5.4: A $(q = 4)$-cluster network that is block acyclic (in this case it is a block linear array). The intra-area connections are of order $O(1)$, whereas the inter-area links are of order $O(\epsilon)$.

The following is an extension of a theorem due to Fiedler (see Theorem 3.8 in [27]), and one that is closely related to slow coherency.

Theorem 5.9

Let G be a connected graph of n vertices. Let the graph have a q-partition $\mathcal{V}_q = \{V_1, \ldots, V_q\}$ and a corresponding q-way cut $\mathcal{K}_q$ such that each component $G(V_i)$ induced by V_i is connected, and contains at least one G-node. Then there exists a positive valuation of edges of G such that the slowest q eigenvectors of the matrix pair $(\mathbf{L}, \mathbf{M})$ provide spectral node valuations (i.e., eigenvector components corresponding to each node) that have at least $k - 1$ sign alternations (for the kth

$\lambda_1 = 0.0000$	$\lambda_2 = 0.0198$	$\lambda_3 = 0.0558$	$\lambda_4 = 0.1120$	$\lambda_5 = 3.3654$	$\lambda_6 = 4.2792$	$\lambda_7 = 6.4896$	$\lambda_8 = 7.0300$
1.0000	0.6705	0.3002	0.2119	-0.0055	0.1242	-1.0000	0.0001
1.0000	0.6657	0.2942	0.2033	-0.0020	-1.0000	0.4010	0.0000
1.0000	0.6612	0.2885	0.1955	0.0055	-0.0425	0.4998	0.0000
1.0000	0.6689	0.2982	0.2091	-0.0005	0.8707	0.6033	0.0000
1.0000	0.0059	-0.5381	-0.9729	-0.1041	-0.0034	0.0019	0.0023
1.0000	0.0010	-0.5492	-1.0000	-0.9774	0.0031	0.0000	0.0021
1.0000	-0.0045	-0.5437	-0.9644	-0.0185	0.0025	-0.0021	-0.0067
1.0000	-0.0011	-0.5405	-0.9620	1.0000	0.0021	-0.0044	0.0025
1.0000	-0.4962	-0.4034	0.9017	0.0051	0.0000	0.0000	-0.0488
1.0000	-0.4999	-0.4058	0.9247	-0.0071	0.0000	0.0000	-0.9989
1.0000	-0.5050	-0.3971	0.9253	-0.0076	0.0000	0.0001	1.0000
1.0000	-1.0000	1.0000	-0.5123	0.0001	0.0000	0.0000	-0.0057
1.0000	-0.9974	0.9926	-0.5046	0.0001	0.0000	0.0000	-0.0004

Table 5.1: The finite modes of an interconnected network exhibiting approximate, slow coherency, with cluster sign-patterns designed to be those of a block-acyclic graph. The first $q = 4$ columns belong to the slow, approximately coherent modes.

slowest most) across cluster boundaries; within each $G(V_i)$ there is coherency, and therefore, a single eigenvector sign corresponding to the each slow eigenvector.

Proof: We are given the topology of the interconnections, but left to choose the edge weights. A priori, we claim that we need not concern ourselves with any intra-area edge weight. We merely need determine the inter-area edge weights. First, construct the aggregate graph $G(\mathcal{V}_{[q]})$. Then select a spanning tree of $G(\mathcal{V}_{[q]})$, and call it $T(\mathcal{V}_{[q]})$. Assign edge weights of order $O(\epsilon)$ to the interarea edges of G that correspond to the edges in $T(\mathcal{V}_q)$. If all other inter-cluster edges are nulled, then the result of the previous corollary applies. We can now assign edge valuations of order $O(\epsilon^2)$ to the remaining inter-cluster edges (those that were nulled when we formed $T(\mathcal{V}_{[q]})$). For sufficiently small ϵ the eigenvectors of the G so constructed will have the same sign alternation properties as a graph with block tree structure would.

The one issue we need to worry about is to ascribe edge valuations in a way that prevents the aggregate spanning tree $T(\mathcal{V}_{[q]})$ from having multiple eigenvalues. If $T(\mathcal{V}_{[q]})$ has a Hamilton path, *i.e.*, a path that traverses every vertex in $T(\mathcal{V}_{[q]})$, then we simply select that path as our spanning tree, ascribe edge weights of order $O(\epsilon)$ to its corresponding inter-cluster edges, and valuate all other edges on the order $O(\epsilon^2)$. The benefit of this is that a Hamilton path is essentially a connected linear array, whose Laplacian is an irreducible tridiagonal matrix, which always has distinct eigenvalues. Barring this, we can always valuate the edges of $T(\mathcal{V}_{[q]})$ such that it does not have repeated eigenvalues. The proof is now complete.   □

Example 5.10 (Special Case When $q = 2$)
When $q = 2$, the result of the previous corollary specializes to that of Theorem 3.8 of Fiedler [27]. Consider a bi-partitioned graph with connected components $G(V_1)$ and $G(V_2)$.
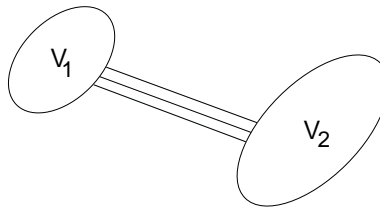
Figure 5.5: A two-cluster approximately coherent graph.

Then the matrix $\mathbf{W}$ *is given by:*

$$\mathbf{W} = \underbrace{\begin{bmatrix} \mathbf{1}_{n_1} & \mathbf{0} \\ \mathbf{0} & \mathbf{1}_{n_2} \end{bmatrix}}_{\mathbf{X}} \underbrace{\begin{bmatrix} \frac{1}{\sqrt{M[1]}} & 0 \\ 0 & \frac{1}{\sqrt{M[2]}} \end{bmatrix}}_{\mathbf{M}_{[q]}^{-1/2}}. \tag{5.9}$$

The aggregate graph for this case would be a two-node graph with edge weight $\xi = \xi_{12}$ *denoting the edge between them (i.e., the sum of the edge weights between clusters* V_1 *and* V_2*), and each with respective weight* $M[1]$ *and* $M[2]$*.*
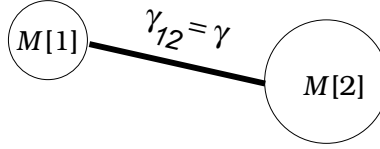
Figure 5.6: Aggregate graph for the two-cluster graph.

The Laplacian matrix $\mathbf{L}_{[q]}$ *is given by*

$$\mathbf{L}_{[q]} = \begin{bmatrix} \xi & -\xi \\ -\xi & \xi \end{bmatrix},$$

and the node weight matrix $\mathbf{M}_{[q]}$ *is:*

$$\mathbf{M}_{[q]} = \begin{bmatrix} M[1] & 0 \\ 0 & M[2] \end{bmatrix}.$$

It is easy to verify that the eigenvalues of the matrix pair $(\mathbf{L}_{[q]}, \mathbf{M}_{[q]})$ *are* $\theta_1 = d\lambda_1 = 0$ *and* $\theta_2 = d\lambda_2 = \dfrac{\xi_{12}}{(M[1]) \parallel (M[2])}$*, where* $M[1] \parallel M[2] = \dfrac{M[1]M[2]}{M[1] + M[2]}$*. The eigenvectors are given by:*

$$\mathbf{C}_{[q]} = \frac{1}{\sqrt{M[1] + M[2]}} \begin{bmatrix} 1 & +\sqrt{M[2]/M[1]} \\ 1 & -\sqrt{M[1]/M[2]} \end{bmatrix}. \tag{5.10}$$

The unperturbed eigenvectors to which the perturbed ones reduce to as $\mathbf{E} \longrightarrow \mathbf{0}$ *are:*

$$\mathbf{U} = \mathbf{X}\,\mathbf{C}_{[q]} = \mathbf{X}\,\frac{1}{\sqrt{M[1] + M[2]}} \begin{bmatrix} 1 & \sqrt{M[2]/M[1]} \\ 1 & -\sqrt{M[1]/M[2]} \end{bmatrix} \tag{5.11}$$

From this we obtain

$$\boldsymbol{u}_2 = \frac{1}{\sqrt{M[1] + M[2]}} \begin{bmatrix} \sqrt{M[2]/M[1]} \, \mathbf{1}_{n_1} \\ \sqrt{M[1]/M[2]} \, \mathbf{1}_{n_2} \end{bmatrix}, \tag{5.12}$$

which reduces precisely to Fiedler's result, if we consider the special case that he dealt with, namely: $M_1 = \cdots = M_n = 1$, $M[1] = \sum_{\nu_i \in V_i} M_i = |V_1| = n_1$, *and* $M[2] = n_2$, *where* $n_1 + n_2 = n$.

Example 5.11

Consider the block-acyclic graph of Figure 5.7, which comprises four clusters (indicated by dashed circles) that have intra-area links of order $O(1)$, but weakly connected to each other according to weights of order $O(\epsilon)$. Now add links of order $O(\epsilon^2)$ between clusters 1 and 4. Figure 5.7 depicts our example.

An eigenanalysis of the graph shows that it approximates a block-acyclic graph with the same sign patterns for coherent areas as was predicted by Theorem 5.9. Table 5.2 shows the approximately coherent slow modes, and the sign alternations between clusters.
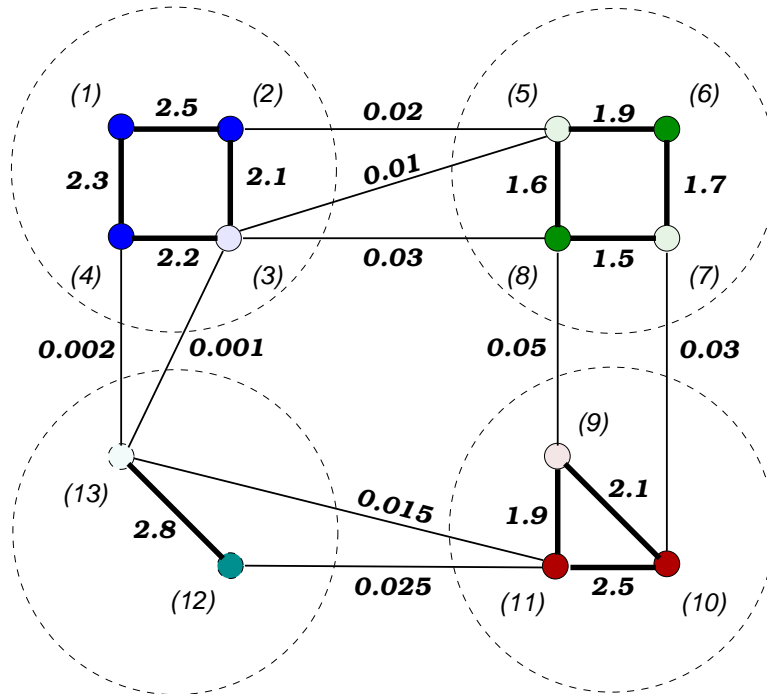
Figure 5.7: A four-cluster network that is a slightly perturbed away from being block acyclic (in this case, the block linear array has been perturbed by links of order $O(\epsilon^2)$ to form a block ring network). The intra-area connections are of order $O(1)$, whereas all except one of the inter-area links are of order $O(\epsilon)$. The one except is the set of links that shape the network in the form of a block ring.

$\lambda_1 = 0.0000$	$\lambda_2 = 0.0226$	$\lambda_3 = 0.0565$	$\lambda_4 = 0.1124$	$\lambda_5 = 3.3654$	$\lambda_6 = 4.2800$	$\lambda_7 = 6.4903$	$\lambda_8 = 7.0300$
1.0000	0.7201	0.2689	-0.2192	0.0055	-0.1247	1.0000	-0.0001
1.0000	0.7148	0.2631	-0.2105	0.0020	1.0000	-0.4009	0.0000
1.0000	0.7091	0.2581	-0.2023	-0.0055	0.0425	-0.4999	0.0000
1.0000	0.7175	0.2673	-0.2160	0.0005	-0.8706	-0.6037	0.0000
1.0000	-0.0106	-0.5282	0.9728	0.1041	0.0034	-0.0019	-0.0023
1.0000	-0.0160	-0.5391	1.0000	0.9774	-0.0031	0.0000	-0.0021
1.0000	-0.0219	-0.5333	0.9643	0.0185	-0.0025	0.0021	0.0067
1.0000	-0.0182	-0.5302	0.9619	-1.0000	-0.0021	0.0044	-0.0025
1.0000	-0.5523	-0.3673	-0.9061	-0.0051	0.0000	0.0000	0.0488
1.0000	-0.5566	-0.3693	-0.9292	0.0071	0.0000	0.0000	0.9989
1.0000	-0.5616	-0.3607	-0.9296	0.0076	0.0000	-0.0001	-1.0000
1.0000	-1.0000	1.0000	0.5426	-0.0001	0.0004	0.0003	0.0057
1.0000	-0.9958	0.9920	0.5340	-0.0001	-0.0002	-0.0003	0.0004

Table 5.2: The finite modes of an interconnected network exhibiting approximate, slow coherency, with cluster sign-patterns designed to approximate those of a block-acyclic graph. The first $q = 4$ columns belong to the slow, approximately coherent modes.

Definition 5.12 (A q-Partition Induced Splitting of the Laplacian Matrix L)

Consider $\mathcal{V}_q = \{V_1, \ldots, V_q\}$, a q-partition of a connected graph G. We say that $\mathcal{V}_q$ induces a splitting of the Laplacian matrix $\mathbf{L}$ into intra- and inter-area Laplacian matrices as follows:

$$\mathbf{L} = \underbrace{\begin{bmatrix} \widehat{\mathbf{L}}_1 & \mathbf{0} & \cdots & \mathbf{0} \\ \mathbf{0} & \widehat{\mathbf{L}}_2 & \ddots & \vdots \\ \vdots & \ddots & \ddots & \mathbf{0} \\ \mathbf{0} & \cdots & \mathbf{0} & \widehat{\mathbf{L}}_q \end{bmatrix}}_{\widehat{\mathbf{L}}} + \underbrace{\begin{bmatrix} \widetilde{\mathbf{L}}_1 & \widetilde{\mathbf{L}}_{12} & \cdots & \widetilde{\mathbf{L}}_{1q} \\ \widetilde{\mathbf{L}}_{21} & \widetilde{\mathbf{L}}_2 & \cdots & \vdots \\ \vdots & \ddots & \ddots & \widetilde{\mathbf{L}}_{q-1,q} \\ \widetilde{\mathbf{L}}_{q1} & \cdots & \widetilde{\mathbf{L}}_{q,q-1} & \widetilde{\mathbf{L}}_q \end{bmatrix}}_{\widetilde{\mathbf{L}}} , \qquad (5.13)$$

where $\widehat{\mathbf{L}}$ and $\widetilde{\mathbf{L}}$ contain the intra-area and the inter-area connection information, respectively. Note that each $\widehat{\mathbf{L}}_i$ is an irreducible Laplacian matrix in its own right. The matrix

$$\widehat{\mathbf{L}} = \widehat{\mathbf{L}}_1 \oplus \cdots \oplus \widehat{\mathbf{L}}_q$$

is the Laplacian matrix of the graph

$$\widehat{G} = \widehat{G}(V_1) \oplus \cdots \oplus \widehat{G}(V_q) ,$$

wherein all the clusters V_i of G are decoupled from each other.

The Laplacian matrix $\widetilde{\mathbf{L}}$, on the other hand, describes the inter-area couplings. Furthermore, each of its diagonal blocks $\widetilde{\mathbf{L}}_i$ is a diagonal matrix containing the inter-area degrees of each node in cluster V_i; it is diagonal because it contains no information about the intra-area links for cluster V_i. In general, $\widetilde{\mathbf{L}}_i$ could have some zero-valued diagonal entries if it has nodes that are not connected to any cluster other than V_i; we will argue later that for exact coherency, the only nodes whose corresponding diagonal entries in $\widetilde{\mathbf{L}}_i$ are allowed to be zero are L-type nodes. Moreover, it must be that $\widetilde{\mathbf{L}}_i \neq \mathbf{0}$, because cluster V_i would be disconnected from the rest of the graph otherwise—a contradiction to our supposition that G is connected.

Example 5.13 (Ramaswamy [68], Example 2.1)

Consider a vibrational network with Laplacian matrix

$$\mathbf{L} = \begin{bmatrix} +6.2 & -0.2 & -1.0 & -1.0 & -2.0 & -2.0 \\ -0.2 & +6.2 & -1.0 & -1.0 & -2.0 & -2.0 \\ -1.0 & -1.0 & +3.6 & -0.8 & -0.4 & -0.4 \\ -1.0 & -1.0 & -0.8 & +3.6 & -0.4 & -0.4 \\ -2.0 & -2.0 & -0.4 & -0.4 & +5.0 & -0.2 \\ -2.0 & -2.0 & -0.4 & -0.4 & -0.2 & +5.0 \end{bmatrix},$$

and a 3-partition $\mathcal{V}_3 = \{\{1,2\}, \{3,4\}, \{5,6\}\}$. Then the $\mathcal{V}_3$-induced splitting of the Laplacian matrix $\mathbf{L}$ is given by:

$$\mathbf{L} = \underbrace{\begin{bmatrix} +0.2 & -0.2 & 0.0 & 0.0 & 0.0 & 0.0 \\ -0.2 & +0.2 & 0.0 & 0.0 & 0.0 & 0.0 \\ 0.0 & 0.0 & +0.8 & -0.8 & 0.0 & 0.0 \\ 0.0 & 0.0 & -0.8 & +0.8 & 0.0 & 0.0 \\ 0.0 & 0.0 & 0.0 & 0.0 & +0.2 & -0.2 \\ 0.0 & 0.0 & 0.0 & 0.0 & -0.2 & +0.2 \end{bmatrix}}_{\widehat{\mathbf{L}}} + \underbrace{\begin{bmatrix} +6.0 & 0.0 & -1.0 & -1.0 & -2.0 & -2.0 \\ 0.0 & +6.0 & -1.0 & -1.0 & -2.0 & -2.0 \\ -1.0 & -1.0 & +2.8 & 0.0 & -0.4 & -0.4 \\ -1.0 & -1.0 & 0.0 & +2.8 & -0.4 & -0.4 \\ -2.0 & -2.0 & -0.4 & -0.4 & +4.8 & 0.0 \\ -2.0 & -2.0 & -0.4 & -0.4 & 0.0 & +4.8 \end{bmatrix}}_{\widetilde{\mathbf{L}}}.$$

$$(5.14)$$

Definition 5.14 (Dynamic Coherency)

Consider a connected graph G described by the $n \times n$ matrix pair $(\mathbf{L}, \mathbf{M})$, where $\mathbf{L}$ and $\mathbf{M}$ are the Laplacian and vertex weight matrices, respectively. Let the modes of the graph be given by $(\lambda_i^{\uparrow}, \boldsymbol{u}_i)$, $i = 1, \ldots, n$. Let $\mathcal{F} = \{\lambda_{k_1}, \ldots, \lambda_{k_r}\}$ be a spectral chord of $(\mathbf{L}, \mathbf{M})$, where $1 = k_1 < k_2 < \cdots < k_r \le n$, and $\mathcal{V}_q = \{V_1, \ldots, V_q\}$ be a q-partition of G. Then G is said to exhibit $(\mathcal{F}, \mathcal{V}_q)$-coherency—or be $(\mathcal{F}, \mathcal{V}_q)$-coherent—if the mode shapes (modulo normalization) corresponding to $\mathcal{F}$ are given by:

$$\underbrace{\left[\boldsymbol{u}_{k_1} \mid \cdots \mid \boldsymbol{u}_{k_r} \right]}_{\mathbf{U}_{\mathcal{F}}} = \underbrace{\begin{bmatrix} \mathbf{1}_{n_1} & \mathbf{0} & \cdots & \mathbf{0} \\ \mathbf{0} & \mathbf{1}_{n_2} & \ddots & \vdots \\ \vdots & \ddots & \ddots & \mathbf{0} \\ \mathbf{0} & \cdots & \mathbf{0} & \mathbf{1}_{n_q} \end{bmatrix}}_{\mathbf{X}} \underbrace{\begin{bmatrix} \eta_{11} & \cdots & \eta_{1r} \\ \vdots & \ddots & \vdots \\ \eta_{q1} & \cdots & \eta_{qr} \end{bmatrix}}_{\mathbf{C}} \qquad (5.15)$$

$$\mathbf{U}_{\mathcal{F}} = \mathbf{X}\,\mathbf{C}\,. \qquad (5.16)$$

On occasion, we might abuse terminology and say that a particular mode $(\lambda, \boldsymbol{u})$ of G (or equivalently, a mode of $(\mathbf{L}, \mathbf{M})$) is coherent, with respect to $\mathcal{V}_q$, if the eigenvector $\boldsymbol{u}$ is of the form:

$$\boldsymbol{u} = \begin{bmatrix} c_1 \mathbf{1}_{n_1} \\ \vdots \\ c_q \mathbf{1}_{n_q} \end{bmatrix} = \mathbf{X}\,\boldsymbol{c}\,.$$

Theorem 5.15

Let a connected graph G, described by the $n \times n$ matrix pair $(\mathbf{L}, \mathbf{M})$, be $(\lambda, \mathcal{V}_q)$-coherent, with respect to the q-partition $\mathcal{V}_q$, i.e., let the eigenvector corresponding to λ be

$$\boldsymbol{u} = \begin{bmatrix} c_1 \mathbf{1}_{n_1} \\ \vdots \\ c_q \mathbf{1}_{n_q} \end{bmatrix} = \underbrace{\begin{bmatrix} \mathbf{1}_{n_1} & \mathbf{0} & \cdots & \mathbf{0} \\ \mathbf{0} & \mathbf{1}_{n_2} & \ddots & \vdots \\ \vdots & \ddots & \ddots & \mathbf{0} \\ \mathbf{0} & \cdots & \mathbf{0} & \mathbf{1}_{n_q} \end{bmatrix}}_{\mathbf{X}} \underbrace{\begin{bmatrix} c_1 \\ \vdots \\ c_q \end{bmatrix}}_{\boldsymbol{c}}\,.$$

Then $(\lambda, \boldsymbol{c})$ is a mode of the aggregate graph $G[\mathcal{V}_q]$, described by the matrix pair $(\mathbf{L}_{[q]}, \mathbf{M}_{[q]})$.

Proof: We are given that $\mathbf{L}\,\boldsymbol{u} = \lambda\,\mathbf{M}\,\boldsymbol{u}$, and know that $\boldsymbol{u} = \mathbf{X}\,\boldsymbol{c}$. Putting these two together we have:

$$\mathbf{L}\,\mathbf{X}\,\boldsymbol{c} = \lambda\,\mathbf{M}\,\mathbf{X}\,\boldsymbol{c}\,.$$

Pre-multiplying both side with $\mathbf{X}^{\mathsf{T}}$ yields:

$$\underbrace{\mathbf{X}^{\mathsf{T}}\,\mathbf{L}\,\mathbf{X}}_{\mathbf{L}_{[q]}}\,\boldsymbol{c} = \lambda\,\underbrace{\mathbf{X}^{\mathsf{T}}\,\mathbf{M}\,\mathbf{X}}_{\mathbf{M}_{[q]}}\,\boldsymbol{c} \tag{5.17}$$

which is the eigenproblem

$$\mathbf{L}_{[q]}\,\boldsymbol{c} = \lambda\,\mathbf{M}_{[q]}\,\boldsymbol{c}\,. \tag{5.18}$$

The proof is now complete. $\square$

5.3   Necessary & Sufficient Conditions for Exact Coherency

In this section we describe necessary and sufficient conditions for a graph G to exhibit exact coherency and mode confinement. First, we state necessary and sufficient conditions for a graph to exhibit $(\mathcal{V}_q, \mathcal{F})$-coherency. This is encapsulated by Theorem 5.16 below. Next, we impose an additional constraint; not only do we want the graph G to be $(\mathcal{V}_q, \mathcal{F})$-coherent, but we also insist that when a disturbance (not to include a zero-mode disturbance) is confined to one of the areas $G(V_i)$, it will not excite other areas in the overall interconnected network. That is to say, we look for necessary and sufficient conditions for a graph to be coherent in a set of q modes, while having each of the remaining $n - q$ "modes" confined to one of the q areas; we have placed "modes" in quotes because the eigenvectors corresponding to infinite eigenvectors are included in our statement. This will be addressed by Theorem 5.21.

The results of this section suggest a design strategy for constructing, from a graph of size q and a chosen set of disconnected graphs $G(V_i)$—each of respective size n_i, $i = 1, \ldots, q$ (possibly containing even L-type nodes)—a graph $G(V)$ of size $n = \sum_{i=1}^{q} n_i$, such that G exhibits coherency, and—in the case described by Theorem 5.21—even mode confinement.

5.3.1   Exact Coherency Theorem

The theorem we are about to state and prove lays out the requirements for a graph G to be coherent with respect to a q-partitioning $\mathcal{V}_q$, over a chord $\mathcal{F}$ that consists of q eigenvalues. The backbone of this theorem was formulated by Chow [13] (in his Corollary 4.5.1, p. 81); however, he stated the theorem in a manner that does not accommodate L-nodes. We restate the theorem in a form that takes into account the presence of L-nodes in the graph. Building on that, we infer corollaries that impose structure on the inter-area links that G-nodes and L-nodes may have in a graph so that $(\mathcal{V}_q, \mathcal{F})$-coherency is feasible.

Theorem 5.16 (Exact Coherency Theorem (ECT))
Consider a graph G described by the matrix pair $(\mathbf{L}, \mathbf{M})$, having modes $(\mathbf{\Lambda}, \mathbf{U})$, where $\mathbf{\Lambda} = \mathsf{diag}\,(\lambda_1, \ldots, \lambda_n)$ and $\mathbf{U} = [\boldsymbol{u}_1, \ldots, \boldsymbol{u}_n]$. Let $\mathcal{V}_q = \{V_1, \ldots, V_q\}$ be a q-partition of G where each area V_i has size n_i, with $n_1 + \cdots + n_q = n$. Let $\mathbf{X} = \mathsf{diag}\,(\mathbf{1}_{n_1}, \ldots, \mathbf{1}_{n_q})$ be the corresponding $n \times q$ partition matrix. Let the aggregate graph $G[\mathcal{V}_q]$ be described by the matrix pair $(\mathbf{L}_{[q]}, \mathbf{M}_{[q]})$

given by

$$
\mathbf{L}_{[q]} = \mathbf{X}^\mathsf{T} \mathbf{L} \mathbf{X} = \begin{bmatrix} \delta_1 & -\xi_{12} & \cdots & -\xi_{1q} \\ -\xi_{21} & \delta_2 & \cdots & -\xi_{2q} \\ \vdots & \vdots & \ddots & \vdots \\ -\xi_{q1} & -\xi_{q2} & \cdots & \delta_q \end{bmatrix} \qquad \mathbf{M}_{[q]} = \mathbf{X}^\mathsf{T} \mathbf{M} \mathbf{X} = \begin{bmatrix} M[1] & & \\ & \ddots & \\ & & M[q] \end{bmatrix},
$$

$$(5.19)$$

having modes $(\boldsymbol{\Theta}, \mathbf{C})$*, where* $\boldsymbol{\Theta} = \mathsf{diag}\,(\theta_1, \ldots, \theta_q)$ *and* $\mathbf{C} = [\boldsymbol{c}_1, \ldots, \boldsymbol{c}_q] \in \mathbb{R}^{q \times q}$*. Let* $\mathcal{F} = \{\theta_1, \ldots, \theta_q\}$ *be the chord of frequencies of interest. And let* $\mathbf{L} = \widehat{\mathbf{L}} + \widetilde{\mathbf{L}}$ *be the* $\mathcal{V}_q$*-induced splitting of the Laplacian matrix* $\mathbf{L}$*.*

Then the graph G *is* $(\mathcal{V}_q, \mathcal{F})$*-coherent if, and only if,*

$$
\widetilde{\mathbf{L}}_i = \frac{\delta_i}{M[i]} \, \mathbf{M}_i \qquad i = 1, \ldots, q \tag{5.20}
$$

and

$$
\widetilde{\mathbf{L}}_{ij} \mathbf{1}_{n_j} = -\frac{\xi_{ij}}{M[i]} \, \underbrace{\mathbf{M}_i \mathbf{1}_{n_i}}_{\boldsymbol{m}_i} = -\frac{\xi_{ij}}{M[i]} \, \boldsymbol{m}_i \, . \tag{5.21}
$$

Proof: If G is $(\mathcal{V}_q, \mathcal{F})$-coherent, then the eigenproblem for the q coherent modes may be written as:

$$
\left(\widehat{\mathbf{L}} + \widetilde{\mathbf{L}}\right) \mathbf{X} \mathbf{C} = \widetilde{\mathbf{L}} \mathbf{X} \mathbf{C} = \mathbf{M} \mathbf{X} \mathbf{C} \boldsymbol{\Theta} \quad \Longleftrightarrow \quad \widetilde{\mathbf{L}} \mathbf{X} = \mathbf{M} \mathbf{X} \mathbf{C} \boldsymbol{\Theta} \mathbf{C}^{-1} \, . \tag{5.22}
$$

We also know from the eigenproblem associated with $(\mathbf{L}_{[q]}, \mathbf{M}_{[q]})$ that:

$$
\mathbf{L}_{[q]} \mathbf{C} = \mathbf{M}_{[q]} \mathbf{C} \boldsymbol{\Theta} \Longleftrightarrow \mathbf{C} \boldsymbol{\Theta} \mathbf{C}^{-1} = \mathbf{M}_{[q]}^{-1} \mathbf{L}_{[q]} \, . \tag{5.23}
$$

Substituting the expression for $\mathbf{C} \boldsymbol{\Theta} \mathbf{C}^{-1}$ of (5.23) in (5.22), we obtain:

$$
\widetilde{\mathbf{L}} \mathbf{X} = \mathbf{M} \mathbf{X} \mathbf{M}_{[q]}^{-1} \mathbf{L}_{[q]} \, . \tag{5.24}
$$

Rewriting (5.24) in partitioned form yields:

$$
\begin{bmatrix}
\widetilde{\mathbf{L}}_1 \mathbf{1}_{n_1} & \widetilde{\mathbf{L}}_{12} \mathbf{1}_{n_2} & \cdots & \widetilde{\mathbf{L}}_{1q} \mathbf{1}_{n_q} \\
\widetilde{\mathbf{L}}_{21} \mathbf{1}_{n_1} & \widetilde{\mathbf{L}}_2 \mathbf{1}_{n_2} & \cdots & \widetilde{\mathbf{L}}_{2q} \mathbf{1}_{n_q} \\
\vdots & \vdots & \ddots & \vdots \\
\widetilde{\mathbf{L}}_{q1} \mathbf{1}_{n_1} & \widetilde{\mathbf{L}}_{q2} \mathbf{1}_{n_2} & \cdots & \widetilde{\mathbf{L}}_q \mathbf{1}_{n_q}
\end{bmatrix}
=
\begin{bmatrix}
\dfrac{\boldsymbol{m}_1}{M[1]} & & \\
& \ddots & \\
& & \dfrac{\boldsymbol{m}_q}{M[q]}
\end{bmatrix}
\begin{bmatrix}
\delta_1 & -\xi_{12} & \cdots & -\xi_{1q} \\
-\xi_{21} & \delta_2 & \cdots & -\xi_{2q} \\
\vdots & \vdots & \ddots & \vdots \\
-\xi_{q1} & -\xi_{q2} & \cdots & \delta_q
\end{bmatrix}
$$

$$
=
\begin{bmatrix}
\dfrac{\delta_1}{M[1]} \boldsymbol{m}_1 & -\dfrac{\xi_{12}}{M[1]} \boldsymbol{m}_1 & \cdots & -\dfrac{\xi_{1q}}{M[1]} \boldsymbol{m}_1 \\[2mm]
-\dfrac{\xi_{21}}{M[2]} \boldsymbol{m}_2 & \dfrac{\delta_2}{M[2]} \boldsymbol{m}_2 & \cdots & -\dfrac{\xi_{2q}}{M[2]} \boldsymbol{m}_2 \\[2mm]
\vdots & \vdots & \ddots & \vdots \\[2mm]
-\dfrac{\xi_{q1}}{M[q]} \boldsymbol{m}_q & -\dfrac{\xi_{q2}}{M[q]} \boldsymbol{m}_q & \cdots & \dfrac{\delta_q}{M[q]} \boldsymbol{m}_q
\end{bmatrix} . \tag{5.25}
$$

Setting equal the corresponding diagonal blocks on each side, we obtain:

$$
\widetilde{\mathbf{L}}_i \mathbf{1}_{n_i} = \frac{\delta_i}{M[i]} \boldsymbol{m}_i . \tag{5.26}
$$

We recall that $\widetilde{\mathbf{L}}_i$ is a diagonal matrix of size n_i. Therefore, it must be that:

$$
\widetilde{\mathbf{L}}_i = \frac{\delta_i}{M[i]} \mathbf{M}_i . \tag{5.27}
$$

Analogously, setting equal the off-diagonal blocks, say the $(i, j)^{\text{th}}$, we have:

$$
\widetilde{\mathbf{L}}_{ij} \mathbf{1}_{n_j} = -\frac{\xi_{ij}}{M[i]} \boldsymbol{m}_i . \tag{5.28}
$$

All the steps we took in the proof have involved necessity and sufficiency. Therefore, the proof is complete. Nevertheless, we may easily verify sufficiency by taking the necessity properties (5.27) and (5.28) as the starting point, and then showing that the graph G exhibits coherency in the set of modes corresponding to those of $(\mathbf{L}_{[q]}, \mathbf{M}_{[q]})$. $\qquad\square$

5.3.2 A Few Design-Oriented Observations and Implications

Clearly, the Exact Coherency Theorem 5.16 does accommodate the presence of L-nodes in each of the individual areas $G(V_i)$. We can therefore make the following observation, in the form of a corollary to Theorem 5.16:

Corollary 5.17

If G exhibits exact coherency, as in Theorem 5.16, then every L-node must be internal to each area; it cannot have any inter-area connections.

Proof: We arrive at this simply by noting that the corresponding element on the diagonal matrix $\widetilde{\mathbf{L}}_i$ in (5.27), which is the inter-area degree of each node in the ith area $G(V_i)$, is zero when the corresponding node is L-type. To prove this, we note that the row of $\widetilde{\mathbf{L}}_{ij}$ corresponding to an L-node in $G(V_i)$ must be zero for all $j \neq i$, as the row-sum must be proportional to the weight of the node corresponding to that row (which, in the case of an L-node is zero). This is because $\widetilde{\mathbf{L}}_{ij} \preceq \mathbf{0}$; hence, when a particular row-sum is zero, it must be that all elements on that row are zero. By the symmetry of $\widetilde{\mathbf{L}}$, coherency must be exhibited also by the left eigenvectors (which are the same as the right eigenvectors). Therefore, the properties that we have arrived at must hold for corresponding columns of each $\widetilde{\mathbf{L}}_{ij}$ block as well. To summarize, for every $\widetilde{\mathbf{L}}_{ij}$, which is of size $n_i \times n_j$, every row corresponding to an L-node in $G(V_i)$ is zero, and every column corresponding to an L-node in $G(V_j)$ is zero. □

It is convenient for us to index the nodes of the graph such that within each area the L-nodes are listed last. This way, $\widetilde{\mathbf{L}}_i$ and $\widetilde{\mathbf{L}}_{ij}$ take the forms:

$$\widetilde{\mathbf{L}}_i = \begin{bmatrix} \bigstar_{n_{\mathsf{G}}^{(i)} \times n_{\mathsf{G}}^{(i)}} & \mathbf{0}_{n_{\mathsf{G}}^{(i)} \times n_{\mathsf{L}}^{(i)}} \\ \mathbf{0}_{n_{\mathsf{L}}^{(i)} \times n_{\mathsf{G}}^{(i)}} & \mathbf{0}_{n_{\mathsf{L}}^{(i)} \times n_{\mathsf{L}}^{(i)}} \end{bmatrix} \qquad \widetilde{\mathbf{L}}_{ij} = \begin{bmatrix} \bigstar_{n_{\mathsf{G}}^{(i)} \times n_{\mathsf{G}}^{(j)}} & \mathbf{0}_{n_{\mathsf{G}}^{(i)} \times n_{\mathsf{L}}^{(j)}} \\ \mathbf{0}_{n_{\mathsf{L}}^{(i)} \times n_{\mathsf{G}}^{(j)}} & \mathbf{0}_{n_{\mathsf{L}}^{(i)} \times n_{\mathsf{L}}^{(j)}} \end{bmatrix} \tag{5.29}$$

The next observation is the dual of Corollary 5.17, and it is a necessary restriction imposed on the G-nodes.

Corollary 5.18

If a connected graph G exhibits exact coherency, as described in Theorem 5.16, then every G-node of G must have at least one inter-area connection to at least one node (of G-type, according to Corollary 5.17) in a different cluster.

Proof: Suppose a G-node in area $G(V_i)$ is not linked to any other cluster $G(V_j)$, $j \neq i$. Then, the entire row in $\widetilde{\mathbf{L}}$, corresponding to that G-node, is nulled. This implies that cluster $G(V_i)$ is not connected to any other cluster, because the only way for a row of $\widetilde{\mathbf{L}}_{ij}$ to be zero is for the corresponding ξ_{ij} to be zero in the aggregate graph, or, for the node in question to be L-type. If $G(V_i)$ is not connected to any other cluster, then the graph G is not connected: a contradiction. The proof is complete. □

Another observation is that

$$\mathbf{1}_{n_i}^{\mathsf{T}}\, \widetilde{\mathbf{L}}_{ij}\, \mathbf{1}_{n_j} = -\frac{\xi_{ij}}{M[i]}\, \underbrace{\mathbf{1}_{n_i}^{\mathsf{T}}\, \boldsymbol{m}_i}_{M[i]} = -\xi_{ij}\ . \tag{5.30}$$

In terms of designing a coherent graph G from the various areas $G(V_i)$, this means that whenever in the aggregate graph, from which we start the design, a particular edge is non-existent ($\xi_{ij} = 0$), the corresponding areas $G(V_i)$ and $G(V_j)$ are not connected to each other, *i.e.*, $\widetilde{\mathbf{L}}_{ij} = \mathbf{0}$. Rewriting $\widetilde{\mathbf{L}}_{ij} = -\xi_{ij}\, \overline{\mathbf{L}}_{ij}$ for areas that are connected to each other, (5.30) becomes $\mathbf{1}_{n_i}^{\mathsf{T}}\, \overline{\mathbf{L}}_{ij}\, \mathbf{1}_{n_j} = 1$.

Another observation is that because $\widetilde{\mathbf{L}}$ is symmetric, we must have $\widetilde{\mathbf{L}}_{ij}^{\mathsf{T}} = \widetilde{\mathbf{L}}_{ji}$. Taking the transpose of both sides of (5.28) we get:

$$\mathbf{1}_{n_j}^{\mathsf{T}}\, \widetilde{\mathbf{L}}_{ij}^{\mathsf{T}} = \mathbf{1}_{n_j}^{\mathsf{T}}\, \widetilde{\mathbf{L}}_{ji} = -\frac{\xi_{ij}}{M[i]}\, \boldsymbol{m}_i^{\mathsf{T}}\ . \tag{5.31}$$

Since i and j are merely generic indexing variables, we can rewrite (5.31) for $\widetilde{\mathbf{L}}_{ij}$ as follows:

$$\mathbf{1}_{n_i}^{\mathsf{T}}\, \widetilde{\mathbf{L}}_{ij} = -\frac{\xi_{ij}}{M[j]}\, \boldsymbol{m}_j^{\mathsf{T}}\ . \tag{5.32}$$

So not only do we have a constraint on the row-sums of $\widetilde{\mathbf{L}}_{ij}$, but also—due to the symmetry of $\widetilde{\mathbf{L}}$—on the column-sums.

Example 5.19

Suppose we are given three graphs $G(V_i)$, $i = 1, 2, 3$, whose matrix pairs are given below (we also show their modes, as we will make reference to them later in this chapter):

$$\widehat{\mathbf{L}}_1 = \begin{bmatrix} 0.30 & -0.20 & 0 & -0.10 & 0 \\ -0.20 & 0.31 & -0.11 & 0 & 0 \\ 0 & -0.11 & 0.39 & -0.15 & -0.13 \\ -0.10 & 0 & -0.15 & 0.37 & -0.12 \\ 0 & 0 & -0.13 & -0.12 & 0.25 \end{bmatrix} \quad \mathbf{M}_1 = \begin{bmatrix} 1 & & & & \\ & 2 & & & \\ & & 0 & & \\ & & & 0 & \\ & & & & 0 \end{bmatrix} \tag{5.33}$$
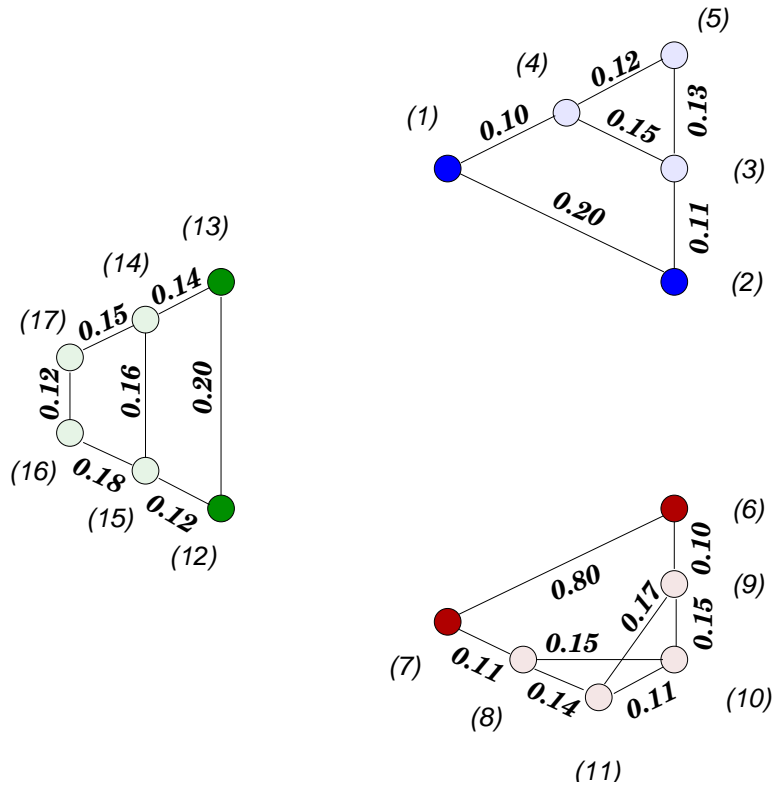
Figure 5.8: Three disjoint clusters $G(V_1)$, $G(V_2)$, and $G(V_3)$ that we want to interconnect to create a coherent network.

$$
\widehat{\mathbf{L}}_2 =
\begin{bmatrix}
0.90 & -0.80 & 0 & -0.10 & 0 & 0 \\
-0.80 & 0.91 & -0.11 & 0 & 0 & 0 \\
0 & -0.11 & 0.40 & 0 & -0.15 & -0.14 \\
-0.10 & 0 & 0 & 0.42 & -0.15 & -0.17 \\
0 & 0 & -0.15 & -0.15 & 0.41 & -0.11 \\
0 & 0 & -0.14 & -0.17 & -0.11 & 0.42
\end{bmatrix}
\qquad
\mathbf{M}_2 =
\begin{bmatrix}
5 & & & & & \\
& 7 & & & & \\
& & 0 & & & \\
& & & 0 & & \\
& & & & 0 & \\
& & & & & 0
\end{bmatrix}
$$

$$(5.34)$$

$\widehat{\lambda}_1^{(1)} = 0.0000$	$\widehat{\lambda}_2^{(1)} = 0.3630$	$\widehat{\lambda}_3^{(1)} = \infty$	$\widehat{\lambda}_4^{(1)} = \infty$	$\widehat{\lambda}_5^{(1)} = \infty$
1.0000	1.0000	0.0000	0.0000	0.0000
1.0000	-0.5000	0.0000	0.0000	0.0000
1.0000	0.0730	1.0000	0.0000	0.0000
1.0000	0.3697	0.0000	1.0000	0.0000
1.0000	0.2154	0.0000	0.0000	1.0000

Table 5.3: Eigenvalues and eigenvectors of $(\widehat{\mathbf{L}}_1, \mathbf{M}_1)$.

$\widehat{\lambda}_1^{(2)} = 0.0000$	$\widehat{\lambda}_2^{(2)} = 0.2876$	$\widehat{\lambda}_3^{(2)} = \infty$	$\widehat{\lambda}_4^{(2)} = \infty$	$\widehat{\lambda}_5^{(2)} = \infty$	$\widehat{\lambda}_6^{(2)} = \infty$
1.0000	1.0000	0.0000	0.0000	0.0000	0.0000
1.0000	-0.7143	0.0000	0.0000	0.0000	0.0000
1.0000	-0.1073	1.0000	0.0000	0.0000	0.0000
1.0000	0.3323	0.0000	1.0000	0.0000	0.0000
1.0000	0.1170	0.0000	0.0000	1.0000	0.0000
1.0000	0.1294	0.0000	0.0000	0.0000	1.0000

Table 5.4: Eigenvalues and eigenvectors of $(\widehat{\mathbf{L}}_2, \mathbf{M}_2)$.

$$
\widehat{\mathbf{L}}_3 = \begin{bmatrix} 0.32 & -0.20 & 0.00 & -0.12 & 0.00 & 0.00 \\ -0.20 & 0.34 & -0.14 & 0.00 & 0.00 & 0.00 \\ 0.00 & -0.14 & 0.45 & -0.16 & 0.00 & -0.15 \\ -0.12 & 0.00 & -0.16 & 0.46 & -0.18 & 0.00 \\ 0.00 & 0.00 & 0.00 & -0.18 & 0.30 & -0.12 \\ 0.00 & 0.00 & -0.15 & 0.00 & -0.12 & 0.27 \end{bmatrix} \quad \mathbf{M}_3 = \begin{bmatrix} 6 & & & & & \\ & 12 & & & & \\ & & 0 & & & \\ & & & 0 & & \\ & & & & 0 & \\ & & & & & 0 \end{bmatrix}.
$$

$$\tag{5.35}$$

Our design problem is to interconnect these three graphs in such a way as to make the overall graph $G(V)$, where $V = V_1 \cup V_2 \cup V_3$, coherent according to the modes of the following 3-node aggregate graph:

$$
\mathbf{L}_{[q]} = \begin{bmatrix} 13.50 & -9.00 & -4.50 \\ -9.00 & 21.00 & -12.00 \\ -4.50 & -12.00 & 16.50 \end{bmatrix} \quad \mathbf{M}_{[q]} = \begin{bmatrix} 3 & & \\ & 12 & \\ & & 18 \end{bmatrix}. \tag{5.36}
$$

$\widehat{\lambda}_1^{(3)} = 0.0000$	$\widehat{\lambda}_2^{(3)} = 0.0623$	$\widehat{\lambda}_3^{(3)} = \infty$	$\widehat{\lambda}_4^{(3)} = \infty$	$\widehat{\lambda}_5^{(3)} = \infty$	$\widehat{\lambda}_6^{(3)} = \infty$
1.0000	1.0000	0.0000	0.0000	0.0000	0.0000
1.0000	-0.5000	0.0000	0.0000	0.0000	0.0000
1.0000	0.0286	1.0000	0.0000	0.0000	0.0000
1.0000	0.3833	0.0000	1.0000	0.0000	0.0000
1.0000	0.2874	0.0000	0.0000	1.0000	0.0000
1.0000	0.1436	0.0000	0.0000	0.0000	1.0000

Table 5.5: Eigenvalues and eigenvectors of $(\widehat{\mathbf{L}}_3, \mathbf{M}_3)$.

From (5.27) it is easy to specify $\widetilde{\mathbf{L}}_i$ for $i = 1, 2, 3$. We have:

$$\widetilde{\mathbf{L}}_1 = \frac{\delta_1}{M[1]}\,\mathbf{M}_1 = \frac{13.5}{3}\begin{bmatrix} 1 & & & & \\ & 2 & & & \\ & & 0 & & \\ & & & 0 & \\ & & & & 0 \end{bmatrix} = \begin{bmatrix} 4.5 & & & & \\ & 9 & & & \\ & & 0 & & \\ & & & 0 & \\ & & & & 0 \end{bmatrix}, \tag{5.37}$$

and similarly for the others

$$\widetilde{\mathbf{L}}_2 = \frac{\delta_2}{M[2]}\,\mathbf{M}_2 = \frac{21}{12}\begin{bmatrix} 5 & & & & & \\ & 7 & & & & \\ & & 0 & & & \\ & & & 0 & & \\ & & & & 0 & \\ & & & & & 0 \end{bmatrix} = \begin{bmatrix} 8.75 & & & & & \\ & 12.25 & & & & \\ & & 0 & & & \\ & & & 0 & & \\ & & & & 0 & \\ & & & & & 0 \end{bmatrix} \tag{5.38}$$

$$\widetilde{\mathbf{L}}_3 = \frac{\delta_3}{M[3]}\,\mathbf{M}_3 = \frac{16.5}{18}\begin{bmatrix} 6 & & & & & \\ & 12 & & & & \\ & & 0 & & & \\ & & & 0 & & \\ & & & & 0 & \\ & & & & & 0 \end{bmatrix} = \begin{bmatrix} 5.5 & & & & & \\ & 11 & & & & \\ & & 0 & & & \\ & & & 0 & & \\ & & & & 0 & \\ & & & & & 0 \end{bmatrix}. \tag{5.39}$$

To complete our solution, we have to appropriately design the $\widetilde{\mathbf{L}}_{12}$, $\widetilde{\mathbf{L}}_{13}$, and $\widetilde{\mathbf{L}}_{23}$ blocks of $\widetilde{\mathbf{L}}$. We know from (5.28) and (5.32) that those rows and columns of $\widetilde{\mathbf{L}}_{ij}$ corresponding to L-nodes must be

zero. In the case of $\widetilde{\mathbf{L}}_{12}$ this leads to

$$\widetilde{\mathbf{L}}_{12} = -\xi_{12}\,\overline{\mathbf{L}}_{12} = -\xi_{12} \begin{bmatrix} \bigstar & \bigstar & 0 & 0 & 0 & 0 \\ \bigstar & \bigstar & 0 & 0 & 0 & 0 \\ 0 & 0 & 0 & 0 & 0 & 0 \\ 0 & 0 & 0 & 0 & 0 & 0 \\ 0 & 0 & 0 & 0 & 0 & 0 \end{bmatrix}, \tag{5.40}$$

where our task is to find appropriate values for the four entries marked as $\bigstar$. Furthermore, we know from (5.28) and (5.32) what the row and column sums ought to be; we also know that $\xi_{12} = 9$. Therefore, it is easy to verify that the following values substituted for $\bigstar$ would satisfy the design requirements for $\widetilde{\mathbf{L}}_{12}$:

$$\widetilde{\mathbf{L}}_{12} = -9 \begin{bmatrix} \frac{4}{36} & \frac{8}{36} & 0 & 0 & 0 & 0 \\ \frac{11}{36} & \frac{13}{36} & 0 & 0 & 0 & 0 \\ 0 & 0 & 0 & 0 & 0 & 0 \\ 0 & 0 & 0 & 0 & 0 & 0 \\ 0 & 0 & 0 & 0 & 0 & 0 \end{bmatrix} = \begin{bmatrix} -1.00 & -2.00 & 0 & 0 & 0 & 0 \\ -2.75 & -3.25 & 0 & 0 & 0 & 0 \\ 0 & 0 & 0 & 0 & 0 & 0 \\ 0 & 0 & 0 & 0 & 0 & 0 \\ 0 & 0 & 0 & 0 & 0 & 0 \end{bmatrix}. \tag{5.41}$$

These choices for the four entries marked by $\bigstar$ are by no means unique. Any other set of four non-negative values that satisfy the row- and column-sum requirements would work just as well.

Proceeding as we have, we choose an admissible set of values for the relevant entries in $\widetilde{\mathbf{L}}_{13}$ and $\widetilde{\mathbf{L}}_{23}$. The reader may verify that the following choices work

$$\widetilde{\mathbf{L}}_{13} = -4.5 \begin{bmatrix} 0 & \frac{3}{9} & 0 & 0 & 0 & 0 \\ \frac{3}{9} & \frac{3}{9} & 0 & 0 & 0 & 0 \\ 0 & 0 & 0 & 0 & 0 & 0 \\ 0 & 0 & 0 & 0 & 0 & 0 \\ 0 & 0 & 0 & 0 & 0 & 0 \end{bmatrix} = \begin{bmatrix} 0 & -1.5 & 0 & 0 & 0 & 0 \\ -1.5 & -1.5 & 0 & 0 & 0 & 0 \\ 0 & 0 & 0 & 0 & 0 & 0 \\ 0 & 0 & 0 & 0 & 0 & 0 \\ 0 & 0 & 0 & 0 & 0 & 0 \end{bmatrix}, \tag{5.42}$$

and

$$
\widetilde{\mathbf{L}}_{23} = -12 \begin{bmatrix} \frac{12}{16} & \frac{3}{16} & 0 & 0 & 0 & 0 \\ 0 & \frac{21}{36} & 0 & 0 & 0 & 0 \\ 0 & 0 & 0 & 0 & 0 & 0 \\ 0 & 0 & 0 & 0 & 0 & 0 \\ 0 & 0 & 0 & 0 & 0 & 0 \\ 0 & 0 & 0 & 0 & 0 & 0 \end{bmatrix} = \begin{bmatrix} -4 & -1 & 0 & 0 & 0 & 0 \\ 0 & -7 & 0 & 0 & 0 & 0 \\ 0 & 0 & 0 & 0 & 0 & 0 \\ 0 & 0 & 0 & 0 & 0 & 0 \\ 0 & 0 & 0 & 0 & 0 & 0 \\ 0 & 0 & 0 & 0 & 0 & 0 \end{bmatrix} \tag{5.43}
$$

Noting that $\widetilde{\mathbf{L}}_{ji} = \widetilde{\mathbf{L}}_{ij}^{\mathsf{T}}$, *we consider the design problem completed. Figure 5.9 shows the graph that we just designed.*
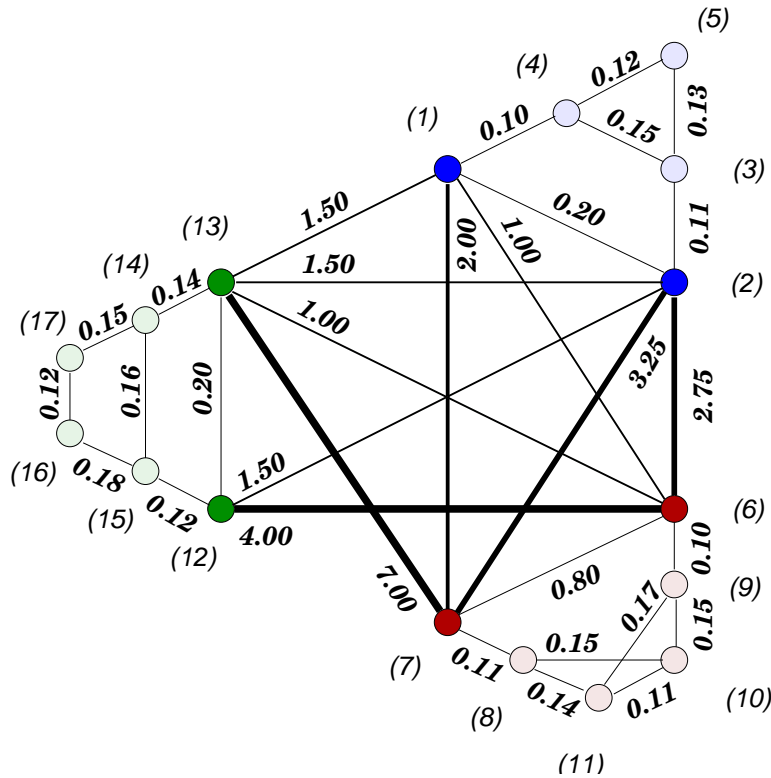

Figure 5.9: Interconnected network that is coherent in three modes.

To verify that our design meets the requirements, we first compute the eigenpairs of $(\mathbf{L}_{[q]}, \mathbf{M}_{[q]})$ *(for convenience of comparison with the larger coherent graph G, we have scaled each eigenvector so its first entry is unity).*

$\theta_1 = 0.0000$	$\theta_2 = 1.9934$	$\theta_3 = 5.1732$
1.0000	1.0000	1.0000
1.0000	1.3783	-0.2116
1.0000	-1.0855	-0.0256

It is easy to verify that θ_1, θ_2, and θ_3 are also eigenvalues of $(\mathbf{L}, \mathbf{M})$—albeit not the slowest ones. Specifically, the finite eigenvalues of $(\mathbf{L}, \mathbf{M})$ along with their eigenvectors are:

$\lambda_1 = 0.0000$	$\lambda_2 = 0.6146$	$\lambda_3 = 1.9934$	$\lambda_4 = 2.3723$	$\lambda_5 = 4.8928$	$\lambda_6 = 5.1732$
1.0000	-0.1609	1.0000	0.0192	-0.8333	1.0000
1.0000	0.0804	1.0000	-0.0096	0.4166	1.0000
1.0000	-0.0117	1.0000	0.0014	-0.0608	1.0000
1.0000	-0.0595	1.0000	0.0071	-0.3081	1.0000
1.0000	-0.0347	1.0000	0.0041	-0.1795	1.0000
1.0000	0.3565	1.3783	-0.7052	-0.0160	-0.2116
1.0000	-0.2547	1.3783	0.5037	0.0115	-0.2116
1.0000	-0.0382	1.3783	0.0756	0.0017	-0.2116
1.0000	0.1185	1.3783	-0.2343	-0.0053	-0.2116
1.0000	0.0417	1.3783	-0.0825	-0.0019	-0.2116
1.0000	0.0461	1.3783	-0.0912	-0.0021	-0.2116
1.0000	0.7075	-1.0855	0.3392	-0.0239	-0.0256
1.0000	-0.3538	-1.0855	-0.1696	0.0119	-0.0256
1.0000	0.0202	-1.0855	0.0097	-0.0007	-0.0256
1.0000	0.2712	-1.0855	0.1300	-0.0092	-0.0256
1.0000	0.2034	-1.0855	0.0975	-0.0069	-0.0256
1.0000	0.1016	-1.0855	0.0487	-0.0034	-0.0256

Table 5.6: The finite modes of an interconnected network, designed according to Theorem 5.16 to be perfectly coherent in three modes.

Our design example has involved a 3-way coherency-based partition of a seventeen-node graph, six of whose nodes are G-type and the rest L-type. None of the L-nodes has any inter-area connections, whereas every G-node has at least one neighbor in a different area—both these in consonance with our design requirements.

5.4 Exact Coherency and Mode Confinement

5.4.1 When is a Mode Confined to an Area?

The issue of a mode shape being confined to a proper subgraph of a graph G will occasionally arise in our subsequent discussion. Therefore, we take a pause to describe a simple necessary and sufficient condition for mode confinement.

Consider the matrix pair $(\mathbf{L}, \mathbf{M})$ associated with a graph G. Let a mode $(\lambda, \boldsymbol{u})$ be confined to a proper subgraph G_A of G; that is, if we consider the entries of $\boldsymbol{u}$ to be valuations of the nodes of G, then all vertices not in G_A are zero-valuated. In other words, we can write the eigenproblem corresponding to the mode as follows:

$$
\begin{bmatrix} \mathbf{L}_A & \mathbf{L}_{A\overline{A}} \\ \mathbf{L}_{\overline{A}A} & \mathbf{L}_{\overline{A}} \end{bmatrix} \begin{bmatrix} \boldsymbol{u}_A \\ \mathbf{0} \end{bmatrix} = \lambda \begin{bmatrix} \mathbf{M}_A & \mathbf{0} \\ \mathbf{0} & \mathbf{M}_{\overline{A}} \end{bmatrix} \begin{bmatrix} \boldsymbol{u}_A \\ \mathbf{0} \end{bmatrix} . \tag{5.44}
$$

Clearly, then for a mode to be confined to a proper subgraph G_A of G, it must satisfy two conditions:

1. The non-null portion $\boldsymbol{u}_A$ of the eigenvector $\boldsymbol{u}$ must be an eigenvector, corresponding to the same eigenvalue, for the subgraph G_A. That is, we must have

$$
\mathbf{L}_A = \lambda \, \mathbf{M}_A \, \boldsymbol{u}_A .
$$

2. The eigenvector $\boldsymbol{u}_A$ of G_A must be in the null space of $\mathbf{L}_{\overline{A}A}$; that is, we must have

$$
\mathbf{L}_{\overline{A}A} \, \boldsymbol{u}_A = \mathbf{0} .
$$

Example 5.20 (Ramaswamy [68], Example 2.1)
Consider a vibrational network with node-weight matrix $\mathbf{M} = \mathbf{I}$, and Laplacian matrix:

$$
\mathbf{L} = \begin{bmatrix}
+6.2 & -0.2 & -1.0 & -1.0 & -2.0 & -2.0 \\
-0.2 & +6.2 & -1.0 & -1.0 & -2.0 & -2.0 \\
-1.0 & -1.0 & +3.6 & -0.8 & -0.4 & -0.4 \\
-1.0 & -1.0 & -0.8 & +3.6 & -0.4 & -0.4 \\
-2.0 & -2.0 & -0.4 & -0.4 & +5.0 & -0.2 \\
-2.0 & -2.0 & -0.4 & -0.4 & -0.2 & +5.0
\end{bmatrix} .
$$

If we consider the partitions as $\{\nu_1, \nu_2\}$, $\{\nu_3, \nu_4\}$, and $\{\nu_5, \nu_6\}$, it is a fairly straightforward exercise to note that all $\widetilde{\mathbf{L}_{ij}}$ blocks have rows that are multiples of $\mathbf{1}^\mathsf{T} \mathbf{M}_j = \mathbf{1}^\mathsf{T}$, which is orthogonal to every oscillatory eigenvector of each of the components. This is why the network has modes local to each area.

Theorem 5.21 (Exact Coherency and Mode Confinement Theorem)

Consider a graph G described by the matrix pair $(\mathbf{L}, \mathbf{M})$. Let $\mathcal{V}_q = \{V_1, \ldots, V_q\}$ be a q-partitioning of G such that each area $G(V_i)$ has size n_i, with $n_1 + \cdots + n_q = n$. Let $\widehat{\mathbf{L}} = \mathsf{diag}\,(\widehat{\mathbf{L}}_1, \ldots, \widehat{\mathbf{L}}_q)$ be the intra-area portion of the $\mathcal{V}_q$-induced splitting of $\mathbf{L}$, and let $\mathbf{M} = \mathsf{diag}\,(\mathbf{M}_1, \ldots, \mathbf{M}_q)$ be the corresponding grouping of the node-weight matrix; each area $G(V_i)$ contains $0 < n_\mathsf{G}^{(i)} \leq n_i$ nodes of type G, and may also contain a number $0 \leq n_\mathsf{L}^{(i)} = n_i - n_\mathsf{G}^{(i)}$ of L-type nodes. Assume that distinct subgraphs $G(V_i)$ and $G(V_j)$—described by $(\mathbf{L}_i, \mathbf{M}_i)$ and $(\mathbf{L}_j, \mathbf{M}_j)$, respectively—have no finite, non-zero (oscillatory) eigenvalues in common.

Furthermore, consider the $n_j - 1$ linearly independent vectors $\boldsymbol{w}_2^{(j)}, \ldots, \boldsymbol{w}_{n_j}^{(j)}$, where

$$\boldsymbol{w}_l^{(j)} = \begin{bmatrix} \mathbf{0} \\ \boldsymbol{v}_l^{(j)} \\ \mathbf{0} \end{bmatrix}_{n \times 1} , \tag{5.45}$$

with $\{\boldsymbol{v}_2^{(j)}, \ldots, \boldsymbol{v}_{n_j}^{(j)}\}$ being the set of $n_\mathsf{G}^{(j)} - 1$ oscillatory finite, as well as the $n_\mathsf{L}^{(j)}$ infinite, eigenvectors of $(\mathbf{L}_j, \mathbf{M}_j)$

Then $\boldsymbol{w}_l^{(j)}$ is an eigenvector of $(\mathbf{L}, \mathbf{M})$ if, and only if,

$$\widetilde{\mathbf{L}}_{ij} = -\frac{\xi_{ij}}{M[i]\,M[j]}\,(\mathbf{M}_i \mathbf{1}_{n_i})\,(\mathbf{M}_j \mathbf{1}_{n_j})^\mathsf{T} = -\frac{\xi_{ij}}{M[i]\,M[j]}\,\boldsymbol{m}_i\,\boldsymbol{m}_j^\mathsf{T} \qquad i \neq j \tag{5.46}$$

and

$$\widetilde{\mathbf{L}}_i = \frac{\delta_i}{M[i]}\,\mathbf{M}_i , \tag{5.47}$$

for some constants $\xi_{ij} \geq 0$, and $\delta_i = \displaystyle\sum_{\substack{j=1 \\ j \neq i}}^{q} \xi_{ij} > 0$.

Proof: Consider the Laplacian splitting induced by $\mathcal{V}_q$, as described in Definition 5.12: $\mathbf{L} = \widehat{\mathbf{L}} + \widetilde{\mathbf{L}}$. It is clear that

$$\widehat{\mathbf{L}}\,\boldsymbol{w}_l^{(j)} = \begin{bmatrix} \mathbf{0} \\ \widehat{\mathbf{L}}_j\,\boldsymbol{v}_l^{(j)} \\ \mathbf{0} \end{bmatrix} = \begin{bmatrix} \mathbf{0} \\ \widehat{\lambda}_l^{(j)}\,\mathbf{M}_j\,\boldsymbol{v}_l^{(j)} \\ \mathbf{0} \end{bmatrix} = \widehat{\lambda}_l^{(j)}\,\mathbf{M}\begin{bmatrix} \mathbf{0} \\ \boldsymbol{v}_l^{(j)} \\ \mathbf{0} \end{bmatrix} = \widehat{\lambda}_l^{(j)}\,\mathbf{M}\,\boldsymbol{w}_l^{(j)}, \tag{5.48}$$

for $l = 2, \ldots, n_j$. Hence, we need concern ourselves only with

$$\widetilde{\mathbf{L}}\,\boldsymbol{w}_l^{(j)} = \begin{bmatrix} \widetilde{\mathbf{L}}_1 & \widetilde{\mathbf{L}}_{12} & \cdots & & \widetilde{\mathbf{L}}_{1q} \\ \widetilde{\mathbf{L}}_{21} & \widetilde{\mathbf{L}}_2 & \cdots & & \vdots \\ \vdots & \ddots & \ddots & & \widetilde{\mathbf{L}}_{q-1,q} \\ \widetilde{\mathbf{L}}_{q1} & \cdots & \widetilde{\mathbf{L}}_{q,q-1} & & \widetilde{\mathbf{L}}_q \end{bmatrix} \begin{bmatrix} \mathbf{0} \\ \boldsymbol{v}_l^{(j)} \\ \mathbf{0} \end{bmatrix} = \begin{bmatrix} \widetilde{\mathbf{L}}_{1j} \\ \vdots \\ \widetilde{\mathbf{L}}_j \\ \vdots \\ \widetilde{\mathbf{L}}_{qj} \end{bmatrix} \boldsymbol{v}_l^{(j)}. \tag{5.49}$$

To have the resulting vector be zero everywhere except in the entries corresponding to the jth group $G(V_j)$, we must have:

$$\widetilde{\mathbf{L}}_{ij}\,\boldsymbol{v}_l^{(j)} = \mathbf{0}, \tag{5.50}$$

for all $i \in \{1, \ldots, q\}$, $i \neq j$ and $l = 2, \ldots, n_j$. The only way this can happen is if each row of $\widetilde{\mathbf{L}}_{ij}$ is of the form $f_r^{(i)}\,\mathbf{1}_{n_j}^{\mathsf{T}}\mathbf{M}_j = f_r^{(i)}\,\boldsymbol{m}_j^{\mathsf{T}}$, for $r = 1, \ldots, n_i$. That is to say, letting $\boldsymbol{f}^{(i)} = [f_1^{(j)} \cdots f_{n_i}^{(j)}]^{\mathsf{T}}$, we see that $\widetilde{\mathbf{L}}_{ij} = \boldsymbol{f}^{(i)}\,\boldsymbol{m}_j^{\mathsf{T}}$ is a rank-one matrix. The symmetry of $\widetilde{\mathbf{L}}$ necessitates that we also have $\widetilde{\mathbf{L}}_{ij} = \boldsymbol{m}_i\,\boldsymbol{g}^{(j)\mathsf{T}}$ for an n_j-vector $\boldsymbol{g}^{(j)}$. Combining these two requirements, we conclude that:

$$\widetilde{\mathbf{L}}_{ij} = -\frac{\xi_{ij}}{M[i]\,M[j]}\,\boldsymbol{m}_i\,\boldsymbol{m}_j^{\mathsf{T}}, \tag{5.51}$$

for some nonnegative constant ξ_{ij}.

Furthermore, we must have

$$\widetilde{\mathbf{L}}_j\,\boldsymbol{v}_l^{(j)} = \alpha_l^{(j)}\,\mathbf{M}_j\,\boldsymbol{v}_l^{(j)}. \tag{5.52}$$

We know that $\widetilde{\mathbf{L}}_j$ is a diagonal matrix. Therefore, Equation (5.52) is satisfied if, and only if,

$$\widetilde{\mathbf{L}}_j = \alpha_l^{(j)}\,\mathbf{M}_j. \tag{5.53}$$

The Laplacian-matrix structure of $\widetilde{\mathbf{L}}$ necessitates that we have:

$$\alpha_l^{(j)} = \frac{\delta_j}{M[j]} \; . \tag{5.54}$$

The proof is now complete. $\square$

Corollary 5.22

The graph designed according to Theorem 5.21 is coherent in the q modes of its aggregate graph described by $(\mathbf{L}_{[q]}, \mathbf{M}_{[q]})$.

Proof: The diagonal blocks $\widetilde{L}_j$ in the graph of Theorem 5.21 are of the same form as those of Theorem 5.16. Therefore, all we need to show is that the off-diagonal blocks $\widetilde{\mathbf{L}}_{ij}$ satisfy the conditions imposed on them by Theorem 5.16. That $\widetilde{\mathbf{L}}_{ji} = \widetilde{\mathbf{L}}_{ij}^{\mathsf{T}}$ is obvious. Hence, we only need to confirm that the row-sum condition of Equation 5.28 is satisfied. This is straightforward:

$$\widetilde{\mathbf{L}}_{ij} \, \mathbf{1}_{n_j} = -\frac{\xi_{ij}}{M[i] \, M[j]} \; \underbrace{\boldsymbol{m}_j^{\mathsf{T}} \, \mathbf{1}_{n_j}}_{M[j]} = -\frac{\xi_{ij}}{M[i]} \; , \tag{5.55}$$

which is precisely the row-sum condition imposed on $\widetilde{\mathbf{L}}_{ij}$ by Equation 5.28 of Theorem 5.16.

Corollary 5.23

The eigenvectors $\boldsymbol{w}_l^{(j)}$ *defined in Theorem 5.21 for* $l = 2, \ldots, n_{\mathsf{G}}^{(j)}$ *and* $j = 1, \ldots, q$ *correspond to the following eigenvalues in the interconnected graph G:*

$$\lambda_l^{(j)} = \widehat{\lambda}_l^{(j)} + \frac{\delta_j}{M[j]} \; . \tag{5.56}$$

Proof: We know that:

$$\mathbf{L}\,w_l^{(j)} = \begin{bmatrix} \mathbf{0} \\ \widehat{\mathbf{L}}_j\,v_l^{(j)} \\ \mathbf{0} \end{bmatrix} + \begin{bmatrix} \widetilde{\mathbf{L}}_{1j}\,v_l^{(j)} \\ \vdots \\ \widetilde{\mathbf{L}}_j\,v_l^{(j)} \\ \vdots \\ \widetilde{\mathbf{L}}_{qj}\,v_l^{(j)} \end{bmatrix} \tag{5.57}$$

$$= \begin{bmatrix} \mathbf{0} \\ \widehat{\lambda}_l^{(j)}\,\mathbf{M}_j\,v_l^{(j)} \\ \mathbf{0} \end{bmatrix} + \begin{bmatrix} \mathbf{0} \\ \frac{\delta_j}{M[j]}\,\mathbf{M}_j\,v_l^{(j)} \\ \mathbf{0} \end{bmatrix} \tag{5.58}$$

$$= \left(\widehat{\lambda}_l^{(j)} + \frac{\delta_j}{M[j]}\right)\,\mathbf{M}\,w_l^{(j)}\,. \tag{5.59}$$

The proof is complete. □

Corollary 5.23 shows that for a graph designed according to Theorem 5.21, the oscillatory modes of any given cluster $G(V_j)$ shift by the same amount, where that amount is simply the ratio of δ_j, the aggregate inter-area degree of cluster $G(V_j)$, over the aggregate node-weight of that cluster $M[j]$.

Corollary 5.24

In the graph designed according to Theorem 5.21, every G*-node of cluster $G(V_i)$ is connected to every* G*-node of cluster $G(V_j)$, $j \neq i$, if $\xi_{ij} > 0$ in the aggregate graph $G[\mathcal{V}_q]$.*

Proof: The proof is obvious from the expression for $\widetilde{\mathbf{L}}_{ij}$.

5.5   Designing a q-Mode Coherent Graph with Otherwise Confined Modes

Theorem 5.21 suggests an obvious procedure for designing coherent graphs with confined modes. Consider a connected graph $G[\mathcal{V}_q]$ of size q, described by the matrix pair $(\mathbf{L}_{[q]}, \mathbf{M}_{[q]})$. Further, assume that the graph comprises only G-type vertices; the weights of these vertices serve as the aggregate node weights for our target graph G, and we already have stipulated that each cluster within G must have at least one G-type node. This is why we insist that $G[\mathcal{V}_q]$ contain only G-type nodes.

Theorem 5.21 then suggests one way of designing G so that it will be coherent in the q eigenvalues of $G[\mathcal{V}_q]$; Theorem 5.16 suggests alternative designs. However, Theorem 5.21 offers the unique design that not only yields a graph G that is coherent in the eigenvalues of $G[\mathcal{V}_q]$, but one that has the additional property that its finite, oscillatory modes are simply shifted versions of the corresponding oscillatory eigenvalues in the clusters $G(V_i)$.

The following example illustrates the procedure.

Example 5.25

We begin our design problem with the same three graphs $G(V_1)$, $G(V_2)$, and $G(V_3)$ from Example 5.19. This time, however, we wish to interconnect them in just the right way so that the constructed graph is exactly coherent in the three modes of the aggregate graph $G[\mathcal{V}_q]$—described by the matrix pair $(\mathbf{L}_{[q]}, \mathbf{M}_{[q]})$ of 5.36—and also has every non-coherent modes confined to one of the clusters.

The design is identical to the previous one insofar as the diagonal blocks $\widetilde{\mathbf{L}}_i$ are concerned. They are as they were designed in Example 5.19. However, the off-diagonal blocks $\widetilde{\mathbf{L}}_{ij}$ are now restricted to the form:

$$\widetilde{\mathbf{L}}_{ij} = -\frac{\xi_{ij}}{M[i]\,M[j]}\,\boldsymbol{m}_i\,\boldsymbol{m}_j^{\mathsf{T}}\,. \tag{5.60}$$

This leads to:

$$\widetilde{\mathbf{L}}_{12} = \widetilde{\mathbf{L}}_{21}^{\mathsf{T}} = -\frac{9}{3\times 12}\begin{bmatrix}1\\2\\0\\0\\0\end{bmatrix}\begin{bmatrix}5&7&0&0&0&0\end{bmatrix} = \begin{bmatrix}-\frac{5}{4}&-\frac{7}{4}&0&0&0\\-\frac{10}{4}&-\frac{14}{4}&0&0&0\\0&0&0&0&0\\0&0&0&0&0\\0&0&0&0&0\end{bmatrix}, \tag{5.61}$$

$$\widetilde{\mathbf{L}}_{13} = \widetilde{\mathbf{L}}_{31}^{\mathsf{T}} = -\frac{4.5}{3\times 18}\begin{bmatrix}1\\2\\0\\0\\0\end{bmatrix}\begin{bmatrix}6&12&0&0&0&0\end{bmatrix} = \begin{bmatrix}-\frac{1}{2}&-1&0&0&0&0\\-1&-2&0&0&0&0\\0&0&0&0&0&0\\0&0&0&0&0&0\\0&0&0&0&0&0\end{bmatrix}, \tag{5.62}$$

and

$$\widetilde{\mathbf{L}}_{23} = \widetilde{\mathbf{L}}_{32}^{\mathsf{T}} = -\frac{12}{12 \times 18} \begin{bmatrix} 5 \\ 7 \\ 0 \\ 0 \\ 0 \\ 0 \end{bmatrix} \begin{bmatrix} 6 & 12 & 0 & 0 & 0 & 0 \end{bmatrix} = \begin{bmatrix} -\frac{5}{3} & -\frac{10}{3} & 0 & 0 & 0 & 0 \\ -\frac{7}{3} & -\frac{14}{3} & 0 & 0 & 0 & 0 \\ 0 & 0 & 0 & 0 & 0 & 0 \\ 0 & 0 & 0 & 0 & 0 & 0 \\ 0 & 0 & 0 & 0 & 0 & 0 \\ 0 & 0 & 0 & 0 & 0 & 0 \end{bmatrix} \tag{5.63}$$
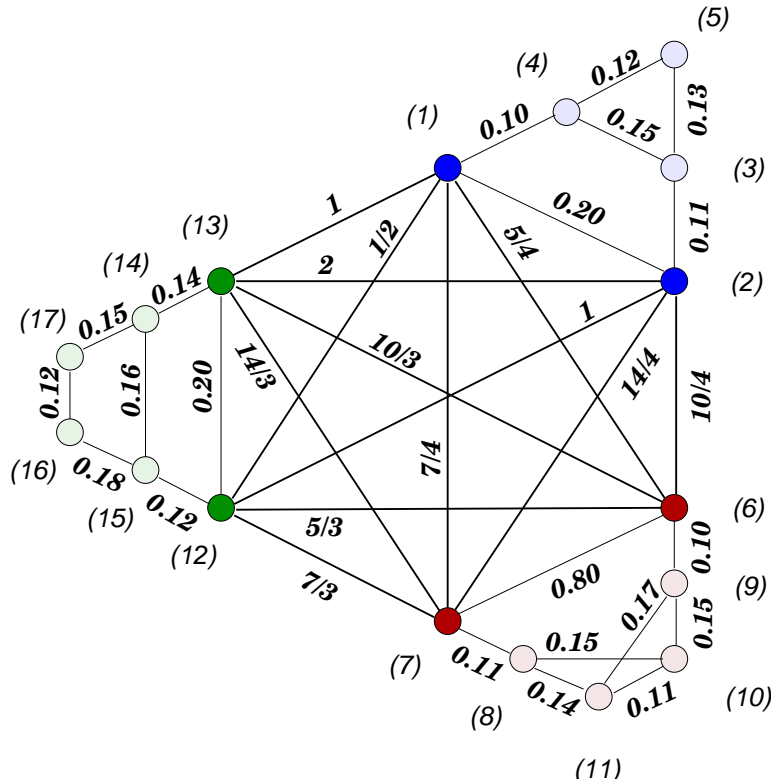
Figure 5.10: Interconnected network three of whose modes exhibit coherency, and the remaining ones are confined to one of the clusters.

Having designed the inter-area connections, we expect the following:

1. The interconnected graph G must have three coherent modes with eigenvalues equal to those of $(\mathbf{L}_{[q]}, \mathbf{M}_{[q]})$: 0.0000, 1.9934, and 5.1732.

2. The area-wise constant values in the coherent eigenvectors are proportional to the corresponding eigenvector component in the aggregate graph.

3. The non-coherent, finite, and area-confined oscillatory modes are at eigenvalues given by (5.56):

$$\widehat{\lambda}_l^{(i)} + \frac{\delta_i}{M[i]}, i = 1, \ldots, q; \, l = 2, \ldots, n_{\mathsf{G}}^{(i)}, \tag{5.64}$$

where $n_{\mathsf{G}}^{(i)}$ is the number of G-nodes of $G(V_i)$, which is, in turn, the number of finite eigenvalues of $G(V_i)$.

4. The eigenvectors corresponding to the infinite eigenvalues of the individual areas $G(V_i)$ are also the infinite eigenvectors of the interconnected network G.

A complete eigenanalysis of $(\mathbf{L}, \mathbf{M})$ confirms everything that we expect from the modes of the interconnected system. For example, Table 5.7 shows that the design requirements on the coherent modes are met. As for the non-coherent modes, that each is confined to only one area is easily observed from the table as well. Clearly, G has three coherent modes at the same eigenvalues as the aggregate graph $G[\mathcal{V}_q]$. Also, the coherent eigenvector components are consistent with those of $G[\mathcal{V}_q]$.

λ_1 = 0.0000	λ_2 = 0.9790	λ_3 = 1.9934	λ_4 = 2.0376	λ_5 = 4.8630	λ_6 = 5.1732
1.0000	0.0000	1.0000	0.0000	1.0000	1.0000
1.0000	0.0000	1.0000	0.0000	-0.5000	1.0000
1.0000	0.0000	1.0000	0.0000	0.0730	1.0000
1.0000	0.0000	1.0000	0.0000	0.3697	1.0000
1.0000	0.0000	1.0000	0.0000	0.2154	1.0000
1.0000	0.0000	1.3783	1.0000	0.0000	-0.2116
1.0000	0.0000	1.3783	-0.7143	0.0000	-0.2116
1.0000	0.0000	1.3783	-0.1073	0.0000	-0.2116
1.0000	0.0000	1.3783	0.3323	0.0000	-0.2116
1.0000	0.0000	1.3783	0.1170	0.0000	-0.2116
1.0000	0.0000	1.3783	0.1294	0.0000	-0.2116
1.0000	1.0000	-1.0855	0.0000	0.0000	-0.0256
1.0000	-0.5000	-1.0855	0.0000	0.0000	-0.0256
1.0000	0.0286	-1.0855	0.0000	0.0000	-0.0256
1.0000	0.3833	-1.0855	0.0000	0.0000	-0.0256
1.0000	0.2874	-1.0855	0.0000	0.0000	-0.0256
1.0000	0.1436	-1.0855	0.0000	0.0000	-0.0256

Table 5.7: The finite modes of a graph designed according to Theorem 5.21 to exhibit perfect coherency and mode confinement properties.

For ease of comparison, we repeat the eigenvalue-eigenvector table of the aggregate graph:

$\theta_1 = 0.0000$	$\theta_2 = 1.9934$	$\theta_3 = 5.1732$
1.0000	1.0000	1.0000
1.0000	1.3783	-0.2116
1.0000	-1.0855	-0.0256

Equally easily we can verify that the confined, non-coherent modes are at eigenvalues that are simply shifted versions of the individual cluster eigenvalues. We have three such modes:

$$\widehat{\lambda}_2^{(1)} + \frac{\delta_1}{M[1]} = 0.3630 + \frac{13.5}{3} = 4.8630 = \lambda_5 \tag{5.65}$$

$$\widehat{\lambda}_2^{(2)} + \frac{\delta_2}{M[2]} = 0.2876 + \frac{21}{12} = 2.0376 = \lambda_4 \tag{5.66}$$

$$\widehat{\lambda}_2^{(3)} + \frac{\delta_3}{M[3]} = 0.0623 + \frac{16.5}{18} = 0.9790 = \lambda_2 \ . \tag{5.67}$$

5.5.1   Relaxation of the Ban on L-Node Inter-Area Connections

We stated earlier that for exact coherency, no L-Node of any area $G(V_i)$ may be a neighbor to any node (L- or G-type) in another area $G(V_j)$, $j \neq i$. In approximate slow coherency this restriction may be lifted because of the $O(\epsilon)$ weights of the inter-area links. We now show more concretely, why this relaxation is permissible.

Suppose the eigenproblem for a graph G is written in the following partitioned form:

$$\underbrace{\left[\begin{array}{cc|c} \mathbf{L}_S & \mathbf{L}_{SW} & \mathbf{L}_{SL} \\ \mathbf{L}_{WS} & \mathbf{L}_W & \mathbf{L}_{WL} \\ \hline \mathbf{L}_{LS} & \mathbf{L}_{LW} & \mathbf{L}_L \end{array} \right]}_{\mathbf{L}} \underbrace{\left[\begin{array}{c} u_S \\ u_W \\ \hline u_L \end{array} \right]}_{u} = \lambda \underbrace{\left[\begin{array}{cc|c} \mathbf{M}_S & & \\ & \mathbf{M}_W & \\ \hline & & 0 \end{array} \right]}_{\mathbf{B}} \left[\begin{array}{c} u_S \\ u_W \\ \hline u_L \end{array} \right] , \tag{5.68}$$

where S and W denote two categories of nodes which neighbor the L-nodes—the distinction being made on account of the strength of their connections to the L-nodes. The nodes denoted by S are strongly connected to the L-nodes (with edge weights of order $O(1)$) ,

whereas those denoted by W are weakly connected with the L-nodes (with edge weights of order $O(\epsilon)$). Further, we assume that

$$\mathbf{L}_{\bar{\mathsf{L}}} = \begin{bmatrix} \mathbf{L}_\mathsf{S} & \mathbf{L}_\mathsf{SW} \\ \mathbf{L}_\mathsf{WS} & \mathbf{L}_\mathsf{W} \end{bmatrix} \sim O(1) \qquad\qquad \mathbf{L}_{\bar{\mathsf{L}}\mathsf{L}} = \begin{bmatrix} \mathbf{L}_\mathsf{SL} \\ \mathbf{L}_\mathsf{WL} \end{bmatrix} \sim O(\epsilon) \qquad (5.69)$$

$$\mathbf{L}_{\mathsf{L}\bar{\mathsf{L}}} = \begin{bmatrix} \mathbf{L}_\mathsf{LS} & \mathbf{L}_\mathsf{LW} \end{bmatrix} \sim O(\epsilon) \qquad\qquad \mathbf{L}_\mathbf{L} \sim O(1) \; . \qquad (5.70)$$

$$(5.71)$$

We showed in Chapter 4 that the eigenvector portion u_L is given by:

$$u_\mathsf{L} = -\mathbf{L}_\mathsf{L}^{-1} \mathbf{L}_\mathsf{LS}\, u_\mathsf{S} - \mathbf{L}_\mathsf{L}^{-1} \mathbf{L}_\mathsf{LW}\, u_\mathsf{W} \; . \qquad (5.72)$$

We also know from Chapter 4 that

$$\mathbf{L}_\mathsf{LS}\, \mathbf{1}_\mathsf{S} + \mathbf{L}_\mathsf{LW}\, \mathbf{1}_\mathsf{W} + \mathbf{L}_\mathsf{L}\, \mathbf{1}_\mathsf{L} = \mathbf{0} \; , \qquad (5.73)$$

which leads to

$$\mathbf{1}_\mathsf{L} = -\mathbf{L}_\mathsf{L}^{-1} \mathbf{L}_\mathsf{LS}\, \mathbf{1}_\mathsf{S} - \mathbf{L}_\mathsf{L}^{-1} \mathbf{L}_\mathsf{LW}\, \mathbf{1}_\mathsf{W} \; . \qquad (5.74)$$

As $\mathbf{L}_\mathsf{L}^{-1} \sim O(1)$, then it must be that

$$\mathbf{L}_\mathsf{L}^{-1} \mathbf{L}_\mathsf{LS} \sim O(1) \qquad \mathbf{L}_\mathsf{L}^{-1} \mathbf{L}_\mathsf{LW} \sim O(\epsilon) \quad \text{and} \quad \mathbf{1}_\mathsf{L} \approx \mathbf{L}_\mathsf{L}^{-1} \mathbf{L}_\mathsf{LS} \mathbf{1}_\mathsf{S} \; . \qquad (5.75)$$

Thus, Equation (5.72) is written in approximate form as:

$$u_\mathsf{L} \approx -\mathbf{L}_\mathsf{L}^{-1} \mathbf{L}_\mathsf{LS}\, u_\mathsf{S} \; . \qquad (5.76)$$

When $u_\mathsf{S} \approx c\, \mathbf{1}_\mathsf{S}$ (for some constant c) is an approximately coherent eigenvector component, practically constant over the subgraph represented by S, it is clear that

$$u_\mathsf{L} \approx c - \mathbf{L}_\mathsf{L}^{-1} \mathbf{L}_\mathsf{LS}\, \mathbf{1}_\mathsf{S} = c\, \mathbf{1}_\mathsf{S} \; . \qquad (5.77)$$

In other words, even though the L-nodes are externally linked, they maintain approximate

coherency with the rest of the nodes of their own cluster, because they are weakly connected with those outside nodes and strongly connected internally within their own area.

5.6   Exact Coherency, Mode Confinement, and Mode Localization

There is a connection to be made between exact coherency and a phenomenon that has been studied for over four decades now, mode localization. Broadly speaking, mode localization is what occurs when a vibrational network comprising identical subsystems and interconnected in a symmetric fashion, is perturbed. It has been observed by many researchers that faster modes of such systems tend to contract to within a short range around the point where the perturbation occurred, with this phenomenon, on the whole, becoming more acute as we look at higher and higher frequencies.

We can design and understand mode localization using our exact coherency and mode confinement analysis. Consider the following network of ten identically-weighted nodes, connected to each other in the manner shown, with each edge weight being unity. It is a trivial exercise to verify that the interconnections of clusters $\{\nu_1, \nu_2\}, \{\nu_3, \nu_4\}, \ldots \{\nu_9, \nu_{10}$ are made according to the requirements of Equations 5.52 and 5.46.
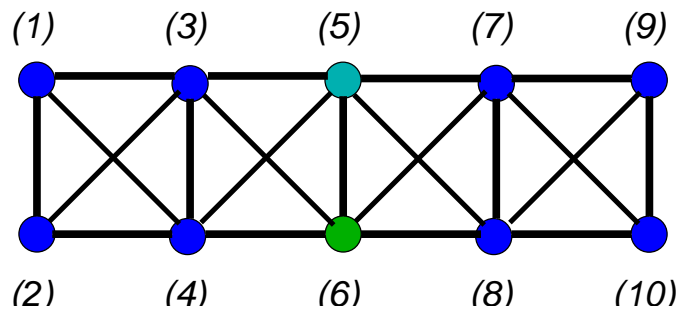

Figure 5.11: A five-cluster network comprising G-nodes only.

Suppose, however, that we perturb the weights of nodes ν_5 and ν_6 so that they are now: $M_5 = 1.05$ and $M_6 = 0.98$. What happens to the oscillatory mode of cluster $\{\nu_5, \nu_6\}$ is clear. The subsystem has been perturbed away from the others, and so it no longer shares its oscillatory eigenvalue with the other two-node clusters. The oscillatory eigenvector of this subsystem, however, does not get perturbed by much. So it is still very close to being orthogonal to all the rows of the $\widetilde{\mathbf{L}}_{ij}$ blocks. Because of the approximate (and not exact) orthogonality, this mode will spread beyond the boundaries of its home cluster (the

$\{\nu_5, \nu_6)$ cluster), but not beyond its neighboring one; even in the neighboring ones, the spreading is mild, because of the near-orthogonality of of the local oscillatory eigenvector of the $\{\nu_5, \nu_6\}$ cluster and the rows of the $\widetilde{\mathbf{L}}_{ij}$ blocks belonging to neighboring clusters. We have, in essence, produced a localized mode. The oscillatory eigenvector of the $\{\nu_5, \nu_6\}$ cluster is fair approximation to an actual eigenvector of the network; and it is localized!

Below is the eigenvector corresponding to the localized mode:

$\lambda_7 = 5.9054$
0.0238
0.0238
-0.0465
-0.0465
0.7234
-0.6824
-0.0465
-0.0465
0.0238
0.0238

Eigenvalues and Graph Design

6.1   Introduction and Contributions

So far, we have focused mostly—albeit not entirely—on mode-shape properties of graphs. In this chapter, we shift our attention to a few salient features of graph eigenvalues. It turns out that our discovery of the eigenvalue shifting property (5.56), implied by the Exact Coherency and Mode Confinement Theorem 5.21, is worth a much closer look.

Also in this chapter we examine some extremal properties of graph eigenvalues. Our eigenvalue bounds are extensions (to weighted G-node graphs) of results already known for graphs with uniform node weights. The bounds will be expressed in terms of the physical features of the graph, that is, node and edge weights.

The contributions of this chapter are:

- As an important corollary to the Exact Coherency and Mode Confinement Theorem, we devise a novel graph design algorithm that solves the following inverse eigenvalue problem:

  > Construct a connected graph comprising a set of G-nodes with weights $0 < M_1, \ldots, M_n$, and eigenvalues $0 = \lambda_1 < \lambda_2 \leq \cdots \leq \lambda_n$.

  Inclusion of L-nodes is possible but trivial—given the results of Chapter 4. So long as L-nodes are inserted according to the results of Section 4.5.3, they can be sequentially introduced into our designed graph without altering the essential modal characteristics.

  Our solution to the inverse eigenvalue problem is a complete graph K_n whose parameters are computed through a backward recursive procedure. With a design-oriented view, we will discuss several important features of our graph, including coherent dynamics and mode confinement, even though neither of these appear in the inverse eigenvalue problem.

- Although the bulk of the discussion in this chapter revolves around eigenvalues, the graph design algorithm that we devise has important ramifications for the eigenvector shapes. In particular, we will see two features in the graphs that we design:

  – We will show that with a decreasing mode index number (i.e., as we go toward slower modes) the region over which the mode exhibits coherency expands. Whereas the fastest mode exhibits coherency over one node, the Fiedler mode is coherent over $n - 1$ nodes. For the modes in between, the trend is monotonic, with a coherent region expansion by one vertex for every one unit decrease in the mode index number toward the eigenvalue at 0.

  – We also will show that as we *increase* the mode index number, the eigenvector region of support decreases by one vertex. The trend of increasing confinement (i.e., decreasing region of support) is monotonic as we go from the Fiedler mode to the fastest one, the latter having a region of support of only two vertices.

- We look at some important eigenvalue bounds, already known for non-weighted graphs, and extend them to weighted graphs. Ordinarily, the Fiedler eigenvalue and the fastest one are the two of interest. Here we describe the bound for the Fiedler eigenvalue and relate it to the physical features of the graph, including node-weight and edge-weight properties.

- We will show—using the graph design algorithm that we describe in this chapter—that some of the eigenvalue bounds are tight. We do this by constructing graphs that meet those bounds.

Our results in this chapter shed more light on the dynamic behavior of oscillatory networks, with emphasis on eigenvalues (or network natural frequencies).

6.2   A Novel Graph Design Algorithm

The mode confinement and coherency theory can be used to solve an inverse eigenvalue problem that will enable us to design graphs with desired node weights and eigenvalues. This problem, of course, is worth studying in its own right. However, we shall see later that it has additional benefits. It turns out that we can establish the tightness of certain eigenvalue bounds by constructing graphs that satisfy them exactly. In other words, tightness is proved by construction, using the design algorithm that we develop in this chapter. This is an important corollary of our novel graph design technique.

A concise statement of the inverse eigenvalue problem is the one below.

Graph Design with Specified Node Weights and Eigenvalues: Construct a graph with

- node weights $0 < M_1, \ldots, M_n$

  and

- eigenvalues $0 = \mu_1 < \mu_2 \leq \cdots \leq \mu_n$.

As expected, the design is not unique. In fact, when the desired eigenvalues and the specified G-node weights are respectively distinct, there are $n!$ ways of constructing a graph that meets the design requirements. Moreover, this multiplicity of solutions accounts only for the number of ways that we can solve the design problem using *our* technique; it does *not* include other ways that a graph can be constructed to meet the design constraints.

This non-uniqueness turns out to be an advantage, because it gives us some flexibility and design leverage over the regions of support of the eigenvectors. For example, as we will show, the graph design algorithm starts with two of the vertices, and then inserts additional G-nodes, one at a time, according to a set procedure, until the final graph of size n comprising all the G-nodes is constructed. It turns out that the faster modes (corresponding to larger eigenvalues) have increasingly confined regions of support. In fact, the increase in confinement (i.e., shrinkage in the region of support) is monotonic with the mode number; namely, as we index through the modes from slow to fast, the first non-oscillatory mode ($\mu_1 = 0$) and the Fiedler mode ($\mu_2 > 0$) each has a region of support that extends over all the nodes. Thereafter, with each unit increment in the mode index number, the region of support of the associated eigenvector shrinks by one node (while the region over which the eigenvector entries are zero expands by one vertex). This continues until the fastest mode, which has a region of support of only two nodes; these two are the first pair of nodes inserted in the design algorithm (the ones we label M_1 and M_2). All this suggests that the order in which we insert the G-nodes can be chosen according to our desire to see a subset of the modes extend over a desired group of the vertices in the graph. We do not have *complete* freedom over how to allocate the vertices to each particular mode's region of support, but we do have considerable flexibility. We shall clarify this by example.

Although the distinction is not substantial, we will differentiate between the design problem wherein each eigenvalue is simple, and another in which an eigenvalue is allowed to have algebraic multiplicity greater than one. We will, however, adhere to our overall insistence that the graph be connected; that is, we consider the non-oscillatory eigenvalue ($\mu_1 = 0$) to be simple throughout our discussion.

6.2.1   Graph Design Involving Distinct Eigenvalues

Our design algorithm, in essence, is an application of reverse engineering, one in which we invoke a backward recursion approach to solve the design problem. Our strategy is a natural consequence of Equation (5.56) in Corollary 5.23, which showed how the oscillatory eigenvalues of different graphs would shift as they are interconnected according to the Exact Coherency and Mode Confinement Theorem 5.21 (ECMCT).

We shall explain the design algorithm by outlining a step-by-step procedure to construct a graph comprising n G-nodes, without initially concerning ourselves with the eigenvalues of the resulting graph. The emphasis at this point is on the way we put together the graph. The procedure itself will suggest how to apply the algorithm, in reverse, to attain the desired spectrum for the desired graph.

Step 1: Label and index the nodes in whatever manner desired. We label the sequence of corresponding weights $M_1, \ldots, M_n$, and without ambiguity identify a node i by its weight M_i.

Step 2: Begin with node M_1. Alone, this node has only one eigenvalue $\lambda_1^{[1]} = 0$, where the superscript denotes the recursion step in the algorithm we are at, which also equals the current number of nodes in the partial graph constructed so far. Using a similar notation, we use the symbol $M_1^{[1]}$ to denote the total mass of the partial graph (at this stage, $M_1^{[1]} = M_1$).

Step 3: Bring in node M_2, and attach it to $M_1^{[1]}$. Denote the inserted weight by $M_2^{[2]} = M_2$, and the edge weight that connects the two by a_{12}. We now have a two-node graph as shown in Figure 6.1. The symbol $\delta^{[2]}$ denotes the total weight of edges that connect the
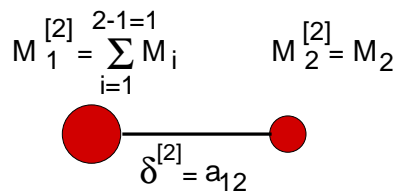
$$M_1^{[2]} = \sum_{i=1}^{2-1=1} M_i \qquad\qquad M_2^{[2]} = M_2$$

$$\delta^{[2]} = a_{12}$$

Figure 6.1: The second stage of the graph design algorithm for simple eigenvalues.

new node M_k with all the previous nodes $M_1, \ldots, M_{k-1}$. At this stage there is only one such edge—which is why $\delta^{[2]} = a_{12}$.

The eigenvalues of the new two-node graph are given by the following expressions, which are based on the results of Example 5.10:

$$\lambda_1^{[2]} = 0 \qquad\qquad \lambda_2^{[2]} = \frac{\delta^{[2]}}{M_1^{[2]} \parallel M_2^{[2]}} = \frac{a_{12}}{M_1 \parallel M_2} \; . \qquad\qquad (6.1)$$

Figure 6.2 depicts the evolution of the system eigenvalues as we go from a one-node to a two-node graph. The arrow mapping the eigenvalue $\lambda_1^{[1]} = 0$ to $\lambda_2^{[2]}$ is dotted to indicate that, strictly speaking, there is no "motion" from one to the other; rather, it is merely to give a visual sense of how the eigenvalue at zero is situated with respect to the Fiedler eigenvalue of the next stage in the recursion. In the subsequent stages, we will use solid arrows to indicate a mapping from one eigenvalue to the other. Those will represent actual shifts in the oscillatory eigenvalues.
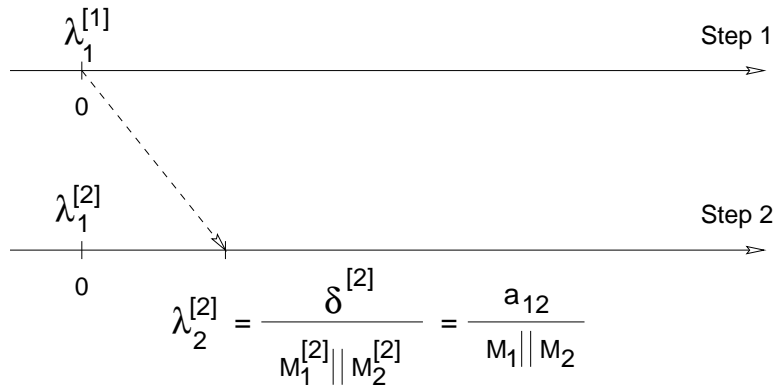

Figure 6.2: Graphical representation of the eigenvalue placements for the second stage.

Step 4: Now that we have a two-node graph, we add node M_3 by connecting it to each of the first two nodes according to the rules of Theorem 5.21. In other words, we consider as one component, the two-node graph that we have constructed so far, while treating M_3 as a separate component on its own. Figure 6.3 is a pictorial representation of this stage. Equation (5.46) of Theorem 5.21 specifies the way in which two separate graphs must be connected. Translating that constraint to our current setup, the interconnections are given by

$$\begin{bmatrix} a_{13} & a_{23} \end{bmatrix} = \frac{\delta^{[3]}}{M_1^{[3]} M_2^{[3]}} M_2^{[3]} \begin{bmatrix} M_1 & M_2 \end{bmatrix}$$

$$= \delta^{[3]} \begin{bmatrix} \dfrac{M_1}{M_1^{[3]}} & \dfrac{M_2}{M_1^{[3]}} \end{bmatrix} \; ,$$
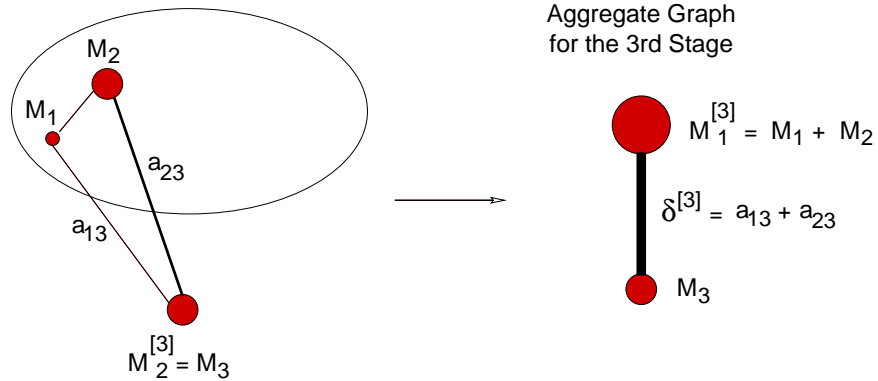
Figure 6.3: The third stage of the graph design algorithm for simple eigenvalues.

or equivalently,

$$\begin{bmatrix} a_{13} & a_{23} \end{bmatrix} = \begin{bmatrix} \dfrac{M_1}{M_1 + M_2}\delta^{[3]} & \dfrac{M_2}{M_1 + M_2}\delta^{[3]} \end{bmatrix} . \tag{6.2}$$

Equation 6.2 begs scrutiny. First, it states that the connection between the newly-added node M_3 and each previous node M_i, $i = 1, 2$, is proportional to the relative weight of node M_i over the total weight of the two-node graph to which it belongs (and to which M_3 is being connected). Second, if we sum the entries on each side of (6.2), we see that

$$\delta^{[3]} = a_{13} + a_{23} = \sum_{i=1}^{3-1=2} a_{i3} .$$

Having connected M_3 to the previous two nodes according to the ECMCT, we now know the three eigenvalues of the new three-node graph comprising M_1, M_2 and M_3. One eigenvalue, of course, is

$$\lambda_1^{[3]} = 0 .$$

Another is at

$$\lambda_2^{[3]} = \frac{\delta^{[3]}}{M_1^{[3]} \parallel M_2^{[3]}} = \frac{a_{13} + a_{23}}{(M_1 + M_2) \parallel M_3} .$$

And the third eigenvalue is obtained by shifting the oscillatory eigenvalue $\lambda_2^{[2]}$ (of the two-node graph) by an amount specified according to Equation (5.56), namely:

$$\lambda_3^{[3]} = \lambda_2^{[2]} + \frac{\delta^{[3]}}{M_1^{[3]}} = \lambda_2^{[2]} + \frac{a_{13} + a_{23}}{M_1 + M_2} .$$

Figure 6.4 is a qualitative pictorial view of the eigenvalue placements for the third stage. The third eigenvalue $\lambda_3^{[3]}$ is obtained by a direct shift of the oscillatory eigenvalue $\lambda_2^{[2]}$ from the previous stage; that is why we have used a solid arrow to show their association. In contrast, the Fiedler eigenvalue $\lambda_2^{[3]}$ has a virtual—not an actual—association with the non-oscillatory eigenvalue of the previous stage. That is why we only use a dotted arrow to link them. At this point the following question may arise: "How do

$$\lambda_1^{[1]}$$

Step 1

$$\lambda_1^{[2]} \qquad \lambda_2^{[2]} = \frac{\delta^{[2]}}{M_1^{[2]} \| M_2^{[2]}} = \frac{a_{12}}{M_1 \| M_2}$$

Step 2

$$\lambda_1^{[3]} \qquad \lambda_3^{[3]} = \lambda_2^{[2]} + \frac{\delta^{[3]}}{M_1^{[3]}} = \frac{a_{13} + a_{23}}{M_1 + M_2}$$

Step 3

$$\lambda_2^{[3]} = \frac{\delta^{[3]}}{M_1^{[3]} \| M_2^{[3]}} = \frac{a_{13} + a_{23}}{(M_1 + M_2) \| M_3}$$
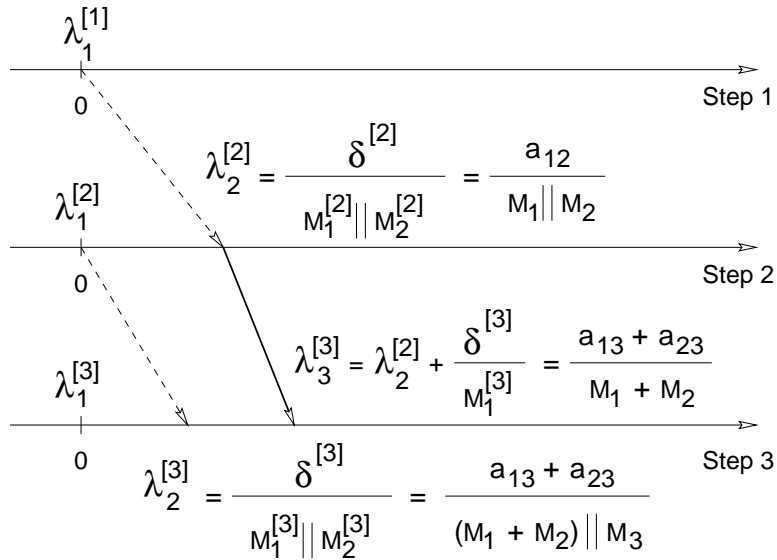
Figure 6.4: Graphical representation of the eigenvalue placements for the third stage of the construction.

we know that the eigenvalue labelled as $\lambda_2^{[2]}$ is actually smaller in value than the one we have marked as $\lambda_3^{[3]}$?" After all, the quantity $\frac{\delta^{[3]}}{M_1^{[3]} \| M_3}$ is larger than $\frac{\delta^{[3]}}{M_1^{[3]}}$, because the denominator of the first is smaller than that of the second for all finite node weights. So for a sufficiently large $\delta^{[3]}$, it is possible for the first quantity to exceed the other. This is a valid concern, but one that, as we will show when we explain the backward recursion design procedure, does not cause us trouble; by design we never let this happen. We shall return to this issue later, when we will discuss for what range of values of $\delta^{[k]}$, the eigenvalue $\frac{\delta^{[k]}}{M_1^{[k]} \| M_2^{[k]}}$ is guaranteed to be the Fiedler value.

Step 5: The remaining stages are analogous to what we have described so far. For clarity, we show the pictorial views of the generic k^{th} stage of the construction process, as well as the corresponding equations that govern the eigenvalues and edge weights. At the kth stage, we add M_k to the previous nodes $M_1, \ldots, M_{k-1}$, as shown in Figure 6.5. The Fiedler eigenvalue of the new graph, as well as the total weight of the edges that connect M_k to all the previous nodes, are reflected in the aggregate graph shown in Figure 6.5.
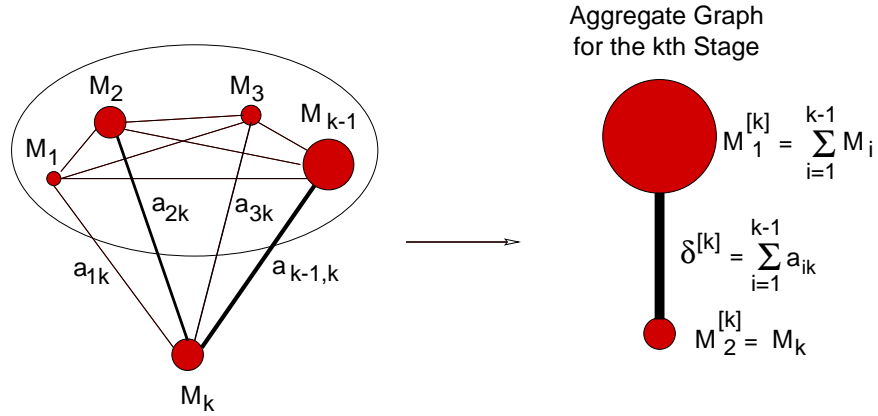
Figure 6.5: This is the kth stage of the design process. The partial graph that has been constructed so far is shown, comprising $k-1$ nodes. This partial graph has the aggregate weight $M_1^{[k]}$ shown in the diagram. The additional node $M_2^{[k]} = M_k$ is shown attached to each of the nodes in the partial subgraph, with respective weights $a_{1k}, \ldots, a_{k-1,k}$ chosen according to the ECMT.

For convenience, we rewrite the equations for the aggregate graph below.

The Laplacian and node-weight matrices for the aggregate graph are:

$$\mathbf{L}^{[k]} = \begin{bmatrix} +\delta^{[k]} & -\delta^{[k]} \\ -\delta^{[k]} & +\delta^{[k]} \end{bmatrix} \qquad \mathbf{M}^{[k]} = \begin{bmatrix} M_1^{[k]} & 0 \\ 0 & M_k \end{bmatrix}.$$

The eigenpairs for $(\mathbf{L}^{[k]}, \mathbf{M}^{[k]})$ are given below.

Non-Oscillatory Mode:

$$\lambda_1^{[k]} = 0 \qquad\qquad \boldsymbol{v}_1^{[k]} = \frac{1}{\sqrt{M_1^{[k]} + M_k}} \begin{bmatrix} 1 \\ 1 \end{bmatrix}$$

Fiedler Mode:

$$\lambda_2^{[k]} = \frac{\delta^{[k]}}{M_1^{[k]} \parallel M_k} \qquad \boldsymbol{v}_2^{[k]} = \frac{1}{\sqrt{M_1^{[k]} + M_k}} \begin{bmatrix} +\sqrt{M_k/M_1^{[k]}} \\ -\sqrt{M_1^{[k]}/M_k} \end{bmatrix}.$$

The non-oscillatory and Fiedler modes for the graph of size k, then, are given by the Exact Coherency and Mode Confinement Theorem 5.21. They are:

Non-Oscillatory Mode:

$$\lambda_1^{[k]} = 0 \qquad\qquad \boldsymbol{v}_1^{[k]} = \frac{1}{\sqrt{M_1^{[k]} + M_k}} \boldsymbol{1}_k$$

Fiedler Mode:

$$\lambda_2^{[k]} = \frac{\delta^{[k]}}{M_1^{[k]} \parallel M_k} \qquad \boldsymbol{v}_2^{[k]} = \frac{1}{\sqrt{M_1^{[k]} + M_k}} \begin{bmatrix} \boldsymbol{1}_{k-1} \\ & 1 \end{bmatrix} \begin{bmatrix} +\sqrt{M_k/M_1^{[k]}} \\ -\sqrt{M_1^{[k]}/M_k} \end{bmatrix} .$$

The remainder of the unknowns are are straightforward to express.

Edge Weights: These are the edges that connect the kth node to each of the previous ones.

$$a_{ik} = \frac{M_i}{M_1^{[k]}} \delta^{[k]} = \frac{M_i}{M_1 + \cdots + M_{k-1}} \delta^{[k]} \qquad i = 1, \ldots, k-1 , \tag{6.3}$$

where the total weight is

$$\delta^{[k]} = \sum_{i=1}^{k-1} a_{ik} . \tag{6.4}$$

Faster Eigenvalues: The ECMCT allows us to compute these recursively from the oscillatory eigenvalues of the previous stage. The recursion is given below.

$$\lambda_i^{[k]} = \lambda_{i-1}^{[k-1]} + \frac{\delta^{[k]}}{M_1^{[k]}} = \lambda_{i-1}^{[k-1]} + \frac{\delta^{[k]}}{M_1 + \cdots + M_{k-1}} \qquad (i = 3, \ldots, k-1) . \tag{6.5}$$

Step 6: We continue in this manner until all n nodes have been inserted to form a complete (K_n)-graph.

The construction of the K_n-graph according to the recursive procedure that we just described, suggests a natural way to solve the inverse eigenvalue problem that is the main object of our study. The process simply is the backward recursion of the one we just described.

Suppose we are given a set of node weights $0 < M_1, \ldots, M_n$, and a set of n eigenvalues that the graph must have: $0 = \mu_1 < \mu_2 < \cdots < \mu_n$. The design presumes that a K_n-graph exists that is built according to the procedure just described, and meets these specifications. The proof of this is by construction. Here is how it works.

STEP 1 INITIALIZATION

We know that if the K_n-graph is constructed according to the procedure we outlined above, the eigenvalues of the desired graph will be in the following correspondence with those of the K_n-graph:

$$\lambda_1^{[n]} = 0 = \mu_1 \quad < \quad \lambda_2^{[n]} = \mu_2 \quad < \quad \cdots \quad < \quad \lambda_n^{[n]} = \mu_n \; .$$

STEP 2 BACKWARD RECURSION

for $k = n : 3$

Compute the Partial Aggregate Weight

$$M_1^{[k]} = \sum_{j=1}^{k-1} M_j$$

Initialize the Marginal Weight

$$M_2^{[k]} = M_k \; .$$

Compute the Aggregate Edge Weight $\delta^{[k]}$

We know that the Fiedler eigenvalue $\lambda_2^{[k]}$ is given by

$$\lambda_2^{[k]} = \frac{\delta^{[k]}}{M_1^{[k]} \parallel M_2^{[k]}} \; .$$

Solve for the only unknown, the aggregate edge weight $\delta^{[k]}$:

$$\delta^{[k]} = \left(M_1^{[k]} \parallel M_k \right) \lambda_2^{[k]} \; .$$

Compute the Oscillatory Eigenvalues $\lambda_i^{[k-1]}$

    for $i = 2 : k - 1$

$$\lambda_i^{[k-1]} = \lambda_{i+1}^{[k]} - \frac{\delta^{[k]}}{M_1^{[k]}}$$

    end

end

$$\delta^{[2]} = \left(M_1^{[2]} \parallel M_2^{[2]} \right) \lambda_2^{[2]} = (M_1 \parallel M_2) \, \lambda_2^{[2]} \; .$$

STEP 3: COMPUTATION OF THE INDIVIDUAL EDGE WEIGHTS

From the aggregate edge weights we can find the appropriate values for each of the individual edge weights.

    for $k = 2 : n$

        for $i = 1 : k - 1$

$$a_{ik} = \frac{M_i}{M_1^{[k]}} \delta^{[k]} = \frac{M_i}{M_1 + \cdots + M_{k-1}} \delta^{[k]}$$

        end

    end

The expression for a_{ik} indicates that each node i, where $i < k$, connects to the kth node with an edge weight that is proportional to the relative weight of the ith node in the aggregate partial graph to which the first $k - 1$ nodes belong (See Figure 6.5).

6.2.2 Eigenvectors of the Designed K_n Graph

We have focused so far on the eigenvalues of the K_n graph—for the most part because the eigenvalues were the primary objects of the design problem. However, since we invoke the ECMCT in designing our graph, it is worth taking a look at the mode confinement implications of Theorem 5.21 in our design. It turns out that the eigenvectors of the designed graph have interesting mode confinement properties, as we will show below.

To understand what the mode shapes look like, we return to the stage-by-stage construction of the K_n graph, from each of the smaller graphs K_k, $k \leq n$.

Two-Node Stage (K_2) We already have shown the eigenvalues and eigenvectors of the two-node graph. Here we merely recall the eigenvectors, without regard to normalization of the magnitudes:

$$v_1^{[2]} = \mathbf{1}_2 \qquad v_2^{[2]} = \begin{bmatrix} M_2 \\ -M_1 \end{bmatrix} .$$

Three-Node Stage K_3 At this stage, we have two extensive modes, and one mode confined to the first two vertices M_1 and M_2 (in accordance with the ECMCT). The two extensive modes are the non-oscillatory mode and the Fiedler mode, given by the following expressions (again, without regard to normalization):

$$v_1^{[3]} = \mathbf{1}_3 \qquad v_2^{[3]} = \begin{bmatrix} \mathbf{1}_2 & \\ & 1 \end{bmatrix} \begin{bmatrix} +M_3 \\ -M_1^{[3]} \end{bmatrix} = \begin{bmatrix} \mathbf{1}_2 & \\ & 1 \end{bmatrix} \begin{bmatrix} +M_3 \\ -(M_1 + M_2) \end{bmatrix} .$$

The fastest mode at this 3rd stage is the one corresponding to the eigenvalue

$$\lambda_3^{[3]} = \lambda_2^{[2]} + \frac{\delta^{[3]}}{M_1^{[3]}} .$$

The ECMCT tells us that this mode will be confined to the first two vertices M_1 and M_2. In fact, the mode shape, again without regard for normalization scaling, is

$$v_3^{[3]} = \begin{bmatrix} v_2^{[2]} \\ 0 \end{bmatrix} .$$

Final Stage (K_n) Continuing in the manner described above, we have the following eigen-

vectors for the final graph K_n:

Non-Oscillatory Eigenvector:

$$\boldsymbol{v}_1^{[n]} = \mathbf{1}_n$$

Fiedler Vector:

$$\boldsymbol{v}_2^{[n]} = \begin{bmatrix} \mathbf{1}_{n-1} & \\ & 1 \end{bmatrix} \begin{bmatrix} +M_2^{[n]} \\ \\ -M_1^{[n]} \end{bmatrix}$$

Faster Eigenvectors:

$$\boldsymbol{v}_2^{[n]} = \begin{bmatrix} \boldsymbol{v}_2^{[n-1]} \\ \\ 0 \end{bmatrix}, \qquad \boldsymbol{v}_3^{[n]} = \begin{bmatrix} \boldsymbol{v}_2^{[n-2]} \\ \\ \mathbf{0}_2 \end{bmatrix}, \qquad \cdots \qquad \boldsymbol{v}_n^{[n]} = \begin{bmatrix} \boldsymbol{v}_2^{[2]} \\ \\ \mathbf{0}_{n-2} \end{bmatrix}$$

The expressions for these oscillatory eigenvectors (beyond Fiedler's) show a monotonic trend in confinement; namely, as the mode index number increases the eigenvector is more localized. More specifically, with each increase in the mode index number beyond Fiedler's, the region of support of the corresponding eigenvector decreases by one node in the graph. The trend continues through to the fastest mode, which has a region of support of only two nodes (M_1 and M_2). This confinement (or localization) of the modes is quite striking, for two reasons:

- The designed K_n-graph does not have "regularity" or symmetry features; even if all the node weights are equal, the edge weights will not be all equal.

- The monotonic trend in confinement, with increasing mode numbers, is something that is not at all customary for vibrational systems that exhibit mode localization. Ordinarily, mode-localized systems exhibit merely a general trend—not a monotonic one—toward increasing confinement of the eigenvector region of support, as the mode number increases.

The expressions for the faster eigenvectors also show that the sequence in which we insert the nodes into the design algorithm determines which one of them falls within the region of support of what mode or modes. For example, the first two vertices M_1 and M_2 fall within the region of support of all the modes, whereas M_n and M_{n-1} are stationary under all modes except the non-oscillatory and the Fiedler modes.

Earlier, we remarked on the combinatorial diversity of the graph designs that meet the eigenvalue specifications. Now that we have laid out the design algorithm, it should be

clear that for n distinct node weights M_i, there are $n!$ ways of constructing a graph with the desired eigenvalues; this is the number of distinguishable orderings in which we can insert the n vertices in the design algorithm. This is an additional luxury us; depending on the order in which we insert the nodes in the design algorithm, we can have partial control over what vertices fall within the region of support of which modes. For example, if we want the region of support of the fastest mode to be limited to two specific vertices ν and ζ, then we symbolically represent the weights of these two nodes M_1 and M_2, and insert them first into the design algorithm.

Example 6.1 (Four-Node Graph Design with Distinct Eigenvalues)
Construct a graph with node weights

$$M_1 = 1, \qquad M_2 = 4, \qquad M_3 = 3, \qquad and \qquad M_4 = 2\ ,$$

such that the graph eigenvalues are at:

$$\mu_1 = 0, \quad \mu_2 = 2, \quad \mu_3 = 3, \quad and \quad \mu_4 = 4\ .$$

STEP 1 INITIALIZATION

$$\lambda_1^{[4]} = 0 \qquad \lambda_2^{[4]} = 2 \qquad \lambda_3^{[4]} = 3 \qquad \lambda_4^{[4]} = 4$$

STEP 2 BACKWARD RECURSION

$$M_1^{[4]} = M_1 + M_2 + M_3 = 8$$
$$M_2^{[4]} = M_4 = 2$$

$$\delta^{[4]} = \left(M_1^{[4]} \parallel M_2^{[4]} \right) \lambda_2^{[4]} = (8 \parallel 2) \cdot 2 = 3.2$$

$$\lambda_2^{[3]} = \lambda_3^{[4]} - \frac{\delta^{[4]}}{M_1^{[4]}} = 3 - \frac{3.2}{8} = 3 - 0.4 = 2.6$$

$$\lambda_3^{[3]} = \lambda_4^{[4]} - \frac{\delta^{[4]}}{M_1^{[4]}} = 4 - 0.4 = 3.6$$

$$M_1^{[3]} = M_1 + M_2 = 5$$
$$M_2^{[3]} = M_3 = 3$$

$$\delta^{[3]} = \left(M_1^{[3]} \parallel M_2^{[3]} \right) \lambda_2^{[3]} = (5 \parallel 3) \cdot 2.6 = \frac{39}{8}$$

$$\lambda_2^{[2]} = \lambda_3^{[3]} - \frac{\delta^{[3]}}{M_1^{[3]}} = 3.6 - \frac{39}{40} = \frac{21}{8}$$

$$\delta^{[2]} = \left(M_1^{[2]} \parallel M_2^{[2]} \right) \lambda_2^{[2]} = (M_1 \parallel M_2) \lambda_2^{[2]} = (1 \parallel 4) \cdot \frac{21}{8} = 2.1 \ .$$

STEP 3 COMPUTATION OF THE INDIVIDUAL EDGE WEIGHTS

$$a_{12} = \delta^{[2]} = 2.1$$

$$a_{13} = \frac{M_1}{M_1^{[3]}} \delta^{[3]} = \frac{M_1}{M_1 + M_2} \delta^{[3]} = \frac{1}{5} \frac{39}{8} = \frac{39}{40} = 0.975$$

$$a_{23} = \frac{M_2}{M_1^{[3]}} \delta^{[3]} = \frac{M_2}{M_1 + M_2} \delta^{[3]} = 3.9$$

$$a_{14} = \frac{M_1}{M_1^{[4]}} \delta^{[4]} = \frac{M_1}{M_1 + M_2 + M_3} \delta^{[4]} = \frac{1}{8} \frac{32}{10} = 0.4$$

$$a_{24} = \frac{M_2}{M_1^{[4]}} \delta^{[4]} = \frac{M_2}{M_1 + M_2 + M_3} \delta^{[4]} = \frac{4}{8} \frac{32}{10} = 1.6$$

$$a_{34} = \frac{M_3}{M_1^{[4]}} \delta^{[4]} = \frac{M_3}{M_1 + M_2 + M_3} \delta^{[4]} = \frac{3}{8} \frac{32}{10} = 1.2 \ .$$

Having computed all the edge weights, we can compute the Laplacian matrix for the graph:

$$\mathbf{L} = \begin{bmatrix} 3.475 & -2.100 & -0.975 & -0.400 \\ -2.100 & 7.600 & -3.900 & -1.600 \\ -0.975 & -3.900 & 6.075 & -1.200 \\ -0.400 & -1.600 & -1.200 & 3.200 \end{bmatrix}$$

With the node-weights shown in Figure 6.6 forming the diagonal elements of the matrix $\mathbf{M}$, it is straightforward to verify that the modes of the matrix pair $(\mathbf{L}, \mathbf{M})$ are those given in Table 6.1.

Notice how the features that we had predicted for the eigenvectors manifest themselves in this numerical example. The Fiedler mode is coherent over three vertices (M_1, M_2, and M_3), the third mode is coherent over two vertices (M_1 and M_2), and the fastest mode is coherent over one vertex,
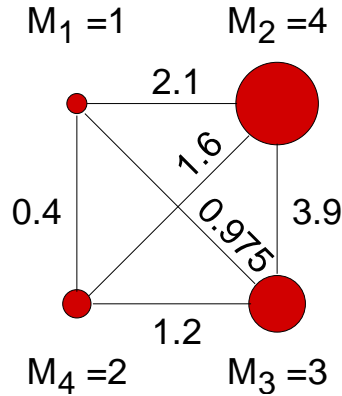
Figure 6.6: Visual representation of the four-node graph designed according to the ECMT.

$\mu_1 = 0.0000$	$\mu_2 = 2.0000$	$\mu_3 = 3.0000$	$\mu_4 = 4.0000$
-0.3162	-0.1581	0.2739	-0.8944
-0.3162	-0.1581	0.2739	0.2236
-0.3162	-0.1581	-0.4564	0.0000
-0.3162	0.6325	0.0000	0.0000

Table 6.1: Eigenvalues and eigenvectors of the four-node graph designed according to the principles of the ECMCT. The eigenvalues clearly match the desired values, and the eigenvector exhibit the coherency and mode confinement features that had been theoretically predicted.

which is a trivial case of coherency). Furthermore, we note that the fastest mode extends over only nodes M_1 and M_2, which are the two nodes we inserted into the algorithm first. The third mode extends over three nodes, and the Fiedler mode extends over all the vertices of the graph, just as we had theoretically predicted.

Design-Oriented Observations We recap now the salient features of our graph design algorithm:

- LUXURY OF ARBITRARILY LABELLED NODES, for sequential insertion into the design algorithm.

- MODE-SHAPE LOCALIZATION monotonically increases with mode index number.
    - Fiedler mode (μ_2, v_2) has a full-network region of support.
    - Fastest mode (μ_n, v_n) has a two-node region of support.

- COHERENCY observed over larger and larger subgraphs as the mode number decreases.
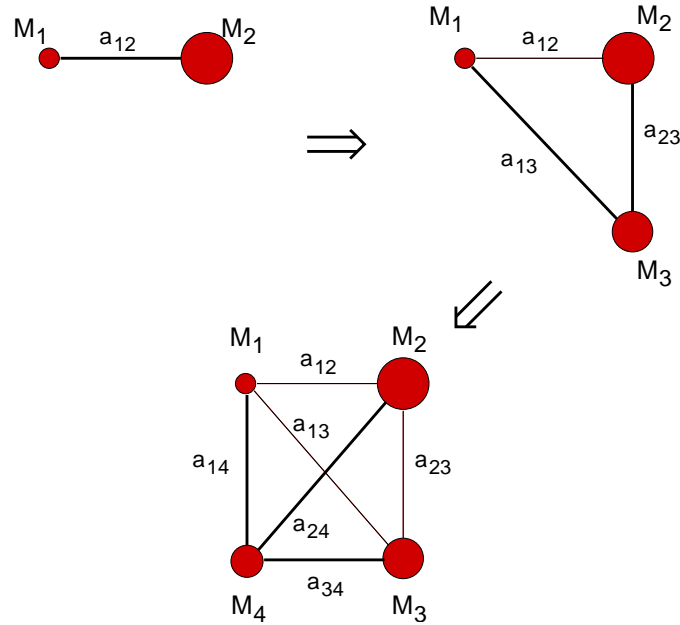
Figure 6.7: Visual representation of the step-by-step construction of the four-node example.

6.2.3 Multiple Eigenvalue Case

Designing a graph with given G-node weights and prescribed eigenvalues (some of which may have algebraic multiplicity greater than 1) is very similar to designing a graph involving only distinct eigenvalues. We can very simply incorporate the multiplicity of a particular eigenvalue by choosing an appropriate value for $\delta^{[k]}$ (at a carefully chosen stage k) such that the following equality holds:

$$\frac{\delta^{[k]}}{M_1^{[k]} \parallel M_2^{[k]}} \triangleq \lambda_2^{[k]} = \lambda_3^{[k]} \triangleq \lambda_2^{[k-1]} + \frac{\delta^{[k]}}{M_1^{[k]}} \ . \tag{6.6}$$

In other words, as we are inserting the node at stage k, we choose the total edge weight $\delta^{[k]}$ so that the Fiedler eigenvalue and the third eigenvalue coincide.

Let us illustrate this graphically. Figure 6.9 shows the kth stage of the construction. If $\delta^{[k]}$ is chosen large enough, then the Fiedler eigenvalue $\lambda_2^{[k]}$ will land on the third eigenvalue $\lambda_3^{[k]}$ as shown in the diagram. This is possible because for finite node weights, it is always the case that

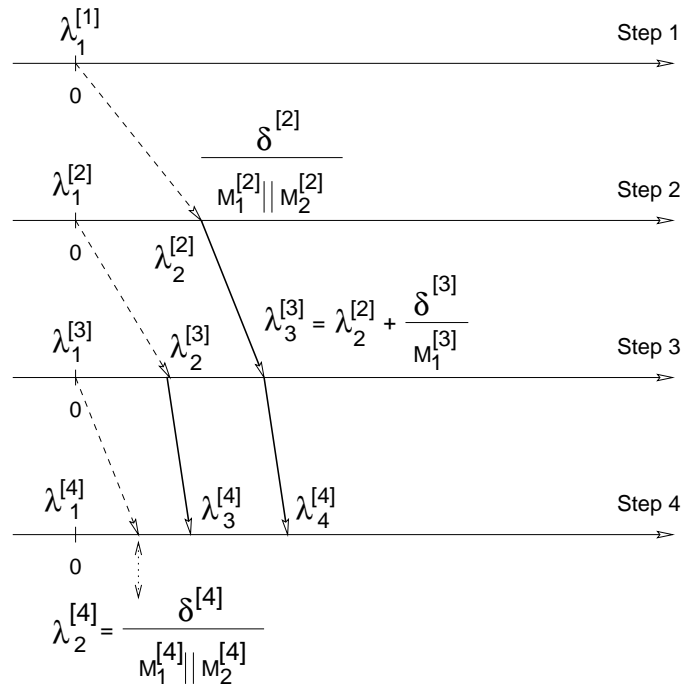$$\left(M_1^{[k]} \parallel M_2^{[k]} \right) < M_1^{[k]} \ .$$

Figure 6.8: Tracking the eigenvalues in the step-by-step construction of the four-node example.

If the desired multiplicity for a particular eigenvalue exceeds two, then at the next stage $k + 1$ we would have to choose $\delta^{[k+1]}$ large enough so that the Fiedler eigenvalue $\lambda_2^{[k+1]}$ would equal the double eigenvalue $\lambda_3^{[k+1]} = \lambda_4^{[k+1]}$. The process continues in this manner until the desired multiplicity is reached.

As for the actual design, we proceed again in the reverse direction of what we just described. The process is best described by a numerical example.

Example 6.2 (Four-Node Graph Design with Multiple Eigenvalues)
Construct a graph with node weights

$$M_1 = 1 \qquad M_2 = 2, \qquad M_3 = 3, \qquad and \qquad M_4 = 4 \ ,$$

such that the graph eigenvalues are at:

$$\mu_1 = 0, \quad \mu_2 = \mu_3 = \mu_4 = 1 \ .$$

Figure 6.10 depicts a qualitative tracking of the eigenvalues at each stage of the construction from
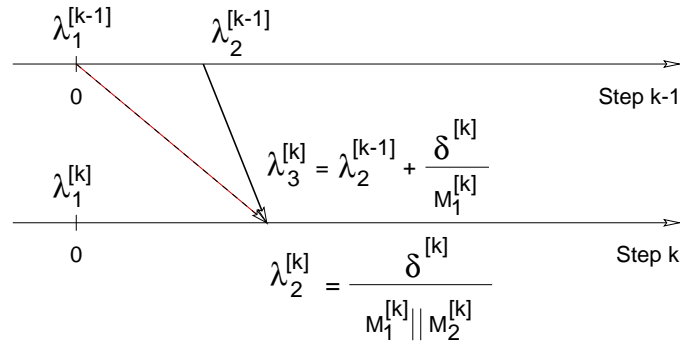
Figure 6.9: Creation of a multiple eigenvalue at Stage k.

one to four nodes. We solve for the unknown edge weights using a procedure nearly identical to the

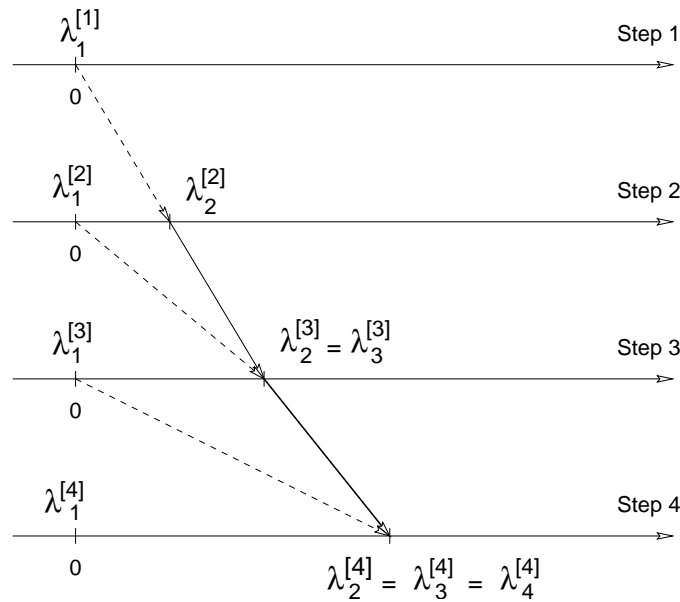Figure 6.10: Tracking of the eigenvalues for the four-node graph with triple eigenvalue at 1.

one we used for the distinct eigenvalue example. This time, we "peel" one of the multiple Fiedler eigenvalues in each backward-recursion step, and assign it to the eigenvalue at zero in the previous step.

STEP 1 INITIALIZATION

$$\lambda_1^{[4]} = 0 \qquad \lambda_2^{[4]} = \lambda_3^{[4]} = \lambda_4^{[4]} = 1$$

STEP 2 BACKWARD RECURSION

$$M_1^{[4]} = M_1 + M_2 + M_3 = 6$$
$$M_2^{[4]} = M_4 = 4$$

$$\delta^{[4]} = \left(M_1^{[4]} \parallel M_2^{[4]} \right) \lambda_2^{[4]} = (6 \parallel 4) \cdot 1 = 2.4$$

$$\lambda_2^{[3]} = \lambda_3^{[3]} = \lambda_3^{[4]} - \frac{\delta^{[4]}}{M_1^{[4]}} = 1 - \frac{2.4}{6} = 1 - 0.4 = 0.6$$

$$M_1^{[3]} = M_1 + M_2 = 3$$
$$M_2^{[3]} = M_3 = 3$$

$$\delta^{[3]} = \left(M_1^{[3]} \parallel M_2^{[3]} \right) \lambda_2^{[3]} = (3 \parallel 3) \cdot 0.6 = 0.9$$

$$\lambda_2^{[2]} = \lambda_3^{[3]} - \frac{\delta^{[3]}}{M_1^{[3]}} = 0.6 - \frac{0.9}{3} = 0.3$$

$$\delta^{[2]} = \left(M_1^{[2]} \parallel M_2^{[2]} \right) \lambda_2^{[2]} = (M_1 \parallel M_2) \lambda_2^{[2]} = (1 \parallel 2) \cdot (0.3) = 0.2 \ .$$

STEP 3 COMPUTATION OF THE INDIVIDUAL EDGE WEIGHTS

$$a_{12} = \delta^{[2]} = 0.2$$

$$a_{13} = \frac{M_1}{M_1^{[3]}} \delta^{[3]} = \frac{M_1}{M_1 + M_2} \delta^{[3]} = \frac{1}{3}(0.9) = 0.3$$
$$a_{23} = \frac{M_2}{M_1^{[3]}} \delta^{[3]} = \frac{M_2}{M_1 + M_2} \delta^{[3]} = 0.6$$

$$a_{14} = \frac{M_1}{M_1^{[4]}} \delta^{[4]} = \frac{M_1}{M_1 + M_2 + M_3} \delta^{[4]} = \frac{1}{6}(2.4) = 0.4$$
$$a_{24} = \frac{M_2}{M_1^{[4]}} \delta^{[4]} = \frac{M_2}{M_1 + M_2 + M_3} \delta^{[4]} = \frac{2}{6}(2.4) = 0.8$$
$$a_{34} = \frac{M_3}{M_1^{[4]}} \delta^{[4]} = \frac{M_3}{M_1 + M_2 + M_3} \delta^{[4]} = \frac{3}{6}(2.4) = 1.2 \ .$$

Having computed all the edge weights, we can compute the Laplacian matrix for the graph:

$$\mathbf{L} = \begin{bmatrix} 0.9 & -0.2 & -0.3 & -0.4 \\ -0.2 & 1.6 & -0.6 & -0.8 \\ -0.3 & -0.6 & 2.1 & -1.2 \\ -0.4 & -0.8 & -1.2 & 2.4 \end{bmatrix}$$

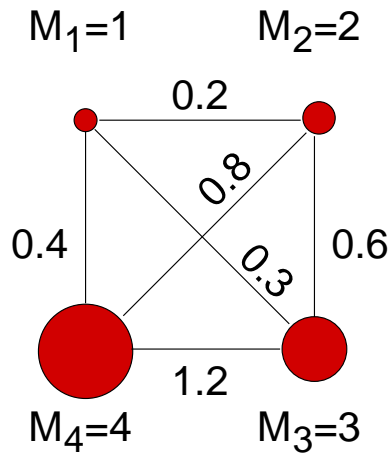*The designed graph is shown in Figure 6.11.*

Figure 6.11: Four-node graph with triple eigenvalue at 1.

It is easy to verify that the eigenvalues of this graph, i.e., the eigenvalues of the matrix pair $(\mathbf{L}, \mathbf{M})$ *satisfy the design requirements.*

6.3   Graph Eigenvalue Bounds

We devote the remainder of this chapter to a different type of eigenvalue analysis: development of eigenvalue bounds in terms of physical features of a graph, such as vertex degrees and weights.

We restrict ourselves to studying just a few of the eigenvalue bounds that are known in spectral graph theory. We extend these bounds to include *weighted* G-node graphs. We then apply our graph design technique to show how some of the bounds are tight. This is one of our main contribution in this section. We will also discuss the implications of some of the results on the stability of graphs with negative edge weights.

We begin with an eigenvalue bound that was proven by Mohar in [61, Lemma 2.6, p. 232]. He proved that if s and t are two *non-adjacent* vertices in a graph, then the Fiedler eigenvalue for the graph satisfies the following inequality:

$$\lambda_2^\uparrow \leq \frac{d_s + d_t}{2} \ . \tag{6.7}$$

We extend (6.7) in two aspects:

- We develop the bound to include G-node graphs with otherwise arbitrary (but finite) node weights.

- We modify the result to include the case where the two nodes a and b may be adjacent.

Theorem 6.3

Consider two nodes s and t in a graph defined by the matrix pair $(\mathbf{L}, \mathbf{M})$; denote the weights of the two nodes by M_s and M_t. Let a_{st} be the weight of the edge that links them ($a_{st} = 0$ if s and t are non-adjacent). Furthermore, let d_s and d_t denote the degrees of nodes s and t, respectively. Then the Fiedler eigenvalue satisfies the following inequality:

$$\lambda_2^\uparrow \leq \frac{M_t\left(\dfrac{d_s}{M_s}\right) + M_s\left(\dfrac{d_t}{M_t}\right) + 2a_{st}}{M_s + M_t} \ . \tag{6.8}$$

Proof: Define a vector $\boldsymbol{x}$ as follows:

$$x_i = \begin{cases} +M_t & i = s \\ -M_s & i = t \\ 0 & \text{otherwise.} \end{cases}$$

It is easy to verify that $\boldsymbol{x}^\mathsf{T}\mathbf{M}\boldsymbol{x} = M_s M_t(M_s + M_t)$, and that $\boldsymbol{x}$ is $\mathbf{M}$-orthogonal to $\mathbf{1}$; that is, $\boldsymbol{x}^\mathsf{T}\mathbf{M}\mathbf{1} = 0$. According to the Courant-Fischer theorem,

$$\lambda_2^\uparrow = \min_{\langle \mathbf{x}, \mathbf{1}\rangle_{\mathbf{M}} = 0} \frac{\boldsymbol{x}^\mathsf{T}\mathbf{L}\boldsymbol{x}}{\boldsymbol{x}^\mathsf{T}\mathbf{M}\boldsymbol{x}} \ . \tag{6.9}$$

Therefore, we see that for our choice of $\boldsymbol{x}$,

$$\lambda_2^\uparrow \leq \frac{\boldsymbol{x}^\mathsf{T}\mathbf{L}\boldsymbol{x}}{\boldsymbol{x}^\mathsf{T}\mathbf{M}\boldsymbol{x}} \ . \tag{6.10}$$

It only remains for us to find the expression in the numerator of (6.10). From Property 3 of the Laplacian matrix (Equation (3.13), p. 52), we know that:

$$\boldsymbol{x}^\mathsf{T}\mathbf{L}\boldsymbol{x} = \sum_{j\neq t} a_{sj}(x_s - x_j)^2 + \sum_{j\neq s} a_{sj}(x_t - x_j)^2 + a_{st}(x_s - x_t)^2 + \sum_{i,j\notin\{s,t\}} a_{ij}(x_i - x_j)^2 \ .$$

The last term in on the right-hand side is zero, because $x_i = x_j = 0$ when $i, j \neq s, t$. Through a similar argument,

$$
\begin{aligned}
\sum_{j\neq t} a_{sj}(x_s - x_j)^2 &= M_t^2(d_s - a_{st}) \\
\sum_{j\neq s} a_{tj}(x_t - x_j)^2 &= M_s^2(d_t - a_{st}) \\
a_{st}(x_s - x_t)^2 &= a_{st}(M_s + M_t)^2 \ .
\end{aligned}
$$

The result then follows immediately, and the proof is complete.   □

Our result in Theorem 6.3 readily simplifies to Inequality (6.7) by Mohar, if s and t are non-adjacent ($a_{st} = 0$) and if all the graph vertices have unity weights.

Theorem 6.4

Consider a connected graph G, and a pair of its adjacent vertices s and t, whose connecting edge is a bridge of weight a_{st}. Then the Fiedler eigenvalue satisfies the following inequality:

$$\lambda_2^\uparrow \leq \frac{a_{st}}{M_s \parallel M_t} \ . \tag{6.11}$$

Proof: As the edge (s, t) is a bridge, we can divide the graph vertices into two clusters S and T, as shown in Figure 6.12. Subgraphs S and T are formed when the bridge (s, t) is removed; S is the connected cluster that contains node s and T the one that contains t. Let M_S be the total weight of cluster S and M_T the total weight of T.

Next, define a vector $\boldsymbol{x}$ as follows:

$$
x_i = \begin{cases} +M_\mathsf{T} & i \in S \\ -M_\mathsf{S} & i \in T \ . \end{cases}
$$

It is easy to verify that $\boldsymbol{x}^\mathsf{T}\mathbf{M}\boldsymbol{x} = M_\mathsf{S}M_\mathsf{T}(M_\mathsf{S} + M_\mathsf{T})$, and that $\boldsymbol{x}$ is **M**-orthogonal to **1**; that
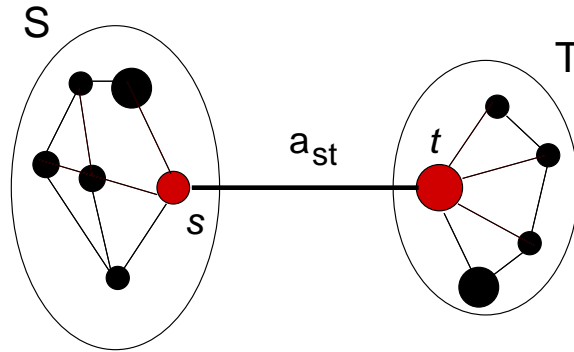
Figure 6.12: A graph with a bridge.

is, $x^\mathsf{T}\mathbf{M1} = 0$. Invoking the Courant-Fischer theorem for our choice of x, we have

$$\lambda_2^\uparrow \leq \frac{x^\mathsf{T}\mathbf{L}x}{x^\mathsf{T}\mathbf{M}x} \ .$$

Using the quadratic property of the Laplacian matrix (Property 3, p. 52), we can rewrite the numerator as follows:

$$x^\mathsf{T}\mathbf{L}x = \sum_{j \in S} a_{sj}(x_s - x_j)^2 + \sum_{j \in T} a_{sj}(x_t - x_j)^2 + a_{st}(x_s - x_t)^2 \ .$$

Each of the two summations is zero, because within the subgraphs S and T the entries of x are at constants M_S and M_T, respectively (this is how we defined x). The last term is simply

$$a_{st}(x_s - x_t)^2 = a_{st}(M_\mathsf{T} + M_\mathsf{S})^2 \ .$$

The Fiedler eigenvalue upper bound may now be written as follows:

$$\lambda_2^\uparrow \leq \frac{a_{st}(M_\mathsf{T} + M_\mathsf{S})^2}{M_\mathsf{S}M_\mathsf{T}(M_\mathsf{S} + M_\mathsf{T})} = \frac{a_{st}}{M_\mathsf{S} \parallel M_\mathsf{T}} \ .$$

The proof is complete.   □

We can extend the results of Theorems 6.3 and 6.4 even further, to include clusters of nodes S and T, instead of vertices s and t. This merely requires a redefinition of vector x in our proofs for each of these two theorems. We will state both extensions, but prove only the one corresponding to Theorem 6.3. The other proof follows in exactly the same way.

Theorem 6.5

Consider two vertex clusters S and T in a connected graph. The two clusters do not share any nodes. Denote the total weight of S by M_S and that of T by M_T. Let

$$a_{ST} = \sum_{\substack{i \in S \\ j \in T}} a_{ij}$$

be the total weight of the edges that link clusters S and T together ($a_{ST} = 0$ if S and T are non-adjacent). Furthermore, let

$$d_S = \sum_{\substack{i \in S \\ j \notin S}} a_{ij}$$

be the total degree of cluster S, and let d_T be similarly defined. Then, the Fiedler eigenvalue of the graph satisfies the following inequality:

$$\lambda_2^{\uparrow} \leq \frac{M_T \left(\dfrac{d_S}{M_S} \right) + M_S \left(\dfrac{d_T}{M_T} \right) + 2a_{ST}}{M_S + M_T} . \tag{6.12}$$

Proof: Define a vector x as follows:

$$x_i = \begin{cases} +M_T & i = S \\ -M_S & i = T \\ 0 & \text{otherwise.} \end{cases}$$

It is easy to verify that $x^{\mathsf{T}} M x = M_S M_T (M_S + M_T)$, and that $\langle x, \mathbf{1} \rangle_M = 0$. Invoking the quadratic property of the Laplacian matrix, we have:

$$x^{\mathsf{T}} L x = \sum_{\substack{i \in S \\ j \notin S \cup T}} a_{ij}(x_i - x_j)^2 + \sum_{\substack{i \in T \\ j \notin S \cup T}} a_{ij}(x_i - x_j)^2 + \sum_{\substack{i \in S \\ j \in T}} a_{ij}(x_i - x_j)^2$$

$$+ \sum_{i,j \notin S \cup T} a_{ij}(x_i - x_j)^2 + \sum_{\substack{i \in S \\ j \in S}} a_{ij}(x_i - x_j)^2 + \sum_{\substack{i \in T \\ j \in T}} a_{ij}(x_i - x_j)^2 . \tag{6.13}$$

Figure 6.13 shows two possible configurations for the multiple-cluster problem that we are considering. In the left figure the clusters S and T are adjacent, whereas in the one on the right they are not.[1]

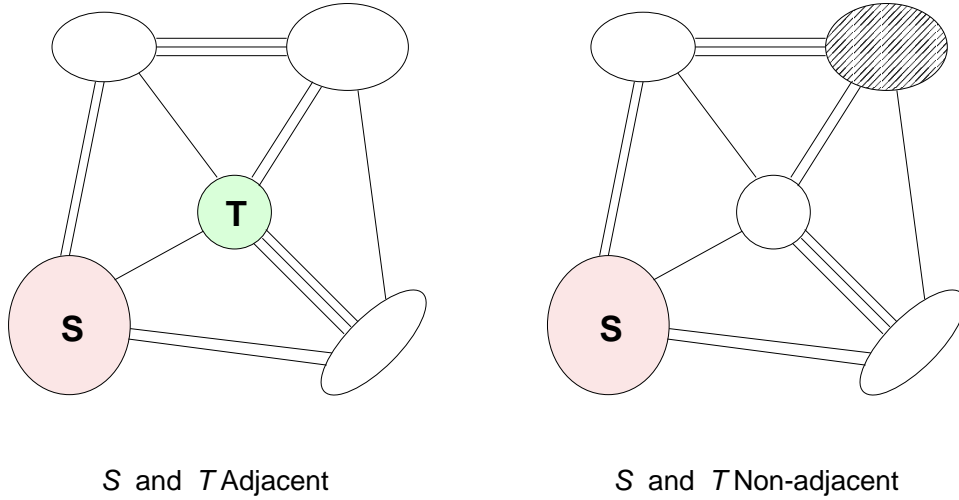S and T Adjacent S and T Non-adjacent

Figure 6.13: Two configurations for subgraphs S and T.

Each of the last three summations in the right-hand side of (6.13) is zero, because the value of the vector $\boldsymbol{x}$ is constant in the region where each summation is defined. As for the first three summations, their respective values are:

$$\sum_{\substack{i \in S \\ j \notin S \cup T}} a_{ij}(x_i - x_j)^2 = M_\mathsf{T}^2 \left(d_\mathsf{S} - a_{\mathsf{ST}}\right),$$

$$\sum_{\substack{i \in T \\ j \notin S \cup T}} a_{ij}(x_i - x_j)^2 = M_\mathsf{S}^2 \left(d_\mathsf{T} - a_{\mathsf{ST}}\right),$$

$$\sum_{\substack{i \in S \\ j \in T}} a_{ij}(x_i - x_j)^2 = (M_\mathsf{S} + M_\mathsf{T})^2 \, a_{\mathsf{ST}}.$$

Inserting these values into the Courant-Fischer inequality for the Fiedler eigenvalue, we have:

$$\lambda_2^\uparrow \leq \frac{\boldsymbol{x}^\mathsf{T}\mathbf{L}\boldsymbol{x}}{\boldsymbol{x}^\mathsf{T}\mathbf{M}\boldsymbol{x}} = \frac{M_\mathsf{T}^2 \left(d_\mathsf{S} - a_{\mathsf{ST}}\right) + M_\mathsf{S}^2 \left(d_\mathsf{T} - a_{\mathsf{ST}}\right) + (M_\mathsf{S} + M_\mathsf{T})^2 \, a_{\mathsf{ST}}}{M_\mathsf{S} \, M_\mathsf{T}(M_\mathsf{S} + M_\mathsf{T})} \ . \tag{6.14}$$

After simplifying the terms, we arrive at (6.12). This completes the proof. $\square$

---

[1]Two subgraphs S and T are *adjacent* if there is at least one edge (i, j) where $i \in S$ and $j \in T$. If no such edge exists, then the two subgraphs are non-adjacent.

The next theorem is an analogous extension of Theorem 6.4 to the case where there is more than one edge between two mutually exclusive, collectively exhaustive node clusters S and T of a connected graph.

Theorem 6.6

Consider a connected graph G and a bi-partitioning of the nodes into clusters S and T, as shown in Figure 6.14. Let M_S and M_T denote the total node weights of S and T, respectively, and denote by a_{ST}, the total edge weight between the two clusters. Then, the Fiedler eigenvalue satisfies the following inequality:

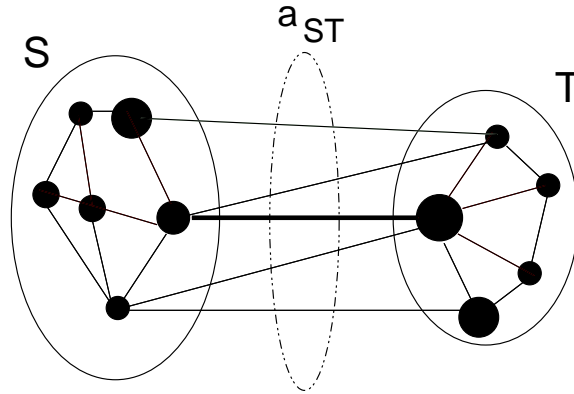$$\lambda_2^\uparrow \leq \frac{a_{ST}}{M_S \parallel M_T} \ . \tag{6.15}$$

Figure 6.14: A bi-partitioned graph with total inter-cluster edge weight given be a_{ST}. The edges that are enclosed by the dotted ellipse are the ones that contribute to a_{ST}.

Proof: Choose vector x as we did in Theorem 6.5, and the rest of the proof is very similar to what did previously. $\qquad\square$

Corollary 6.7

Consider a connected graph G, and let

$$\widehat{\delta}(G) = \min_{s \in V(G)} \frac{d_s}{M_s \parallel (M - M_s)}$$

denote the minimum single-node cut-ratio of G, where $M \stackrel{\triangle}{=} \sum_i M_i$ is the total node weight of G. Then, the Fiedler eigenvalue satisfies the following inequality:

$$\lambda_2^\uparrow \leq \widehat{\delta}(G) \ . \tag{6.16}$$

Proof: In Theorem 6.6, let $S = \{s\}$ be a single-node cluster and $T = G - s$ the remainder of the graph. This is shown in Figure 6.15. Clearly, then, $M_T = M - M_s$ is the total node weight of cluster T, and $a_{ST} = d_s = d_T$ is the degree of node s. The result then follows immediately. $\square$
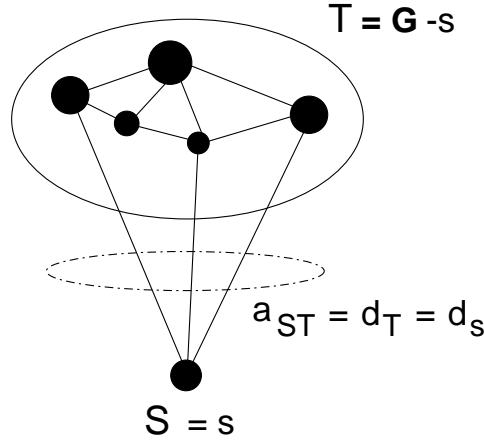

Figure 6.15: A bi-partitioned graph wherein one cluster comprises only a single node s.

Inequality 6.16 in Corollary 6.7 is the node-weighted extension of the one given by Mohar [61, Proposition 2.8, Inequality (17)]. Inequality 6.15 is the extension of the one given in Mohar [61, Lemma 3.1].

Before proceeding further, an observation is in order. Rewriting the bound of Inequality (6.15) leads to the following equivalent expression:

$$\lambda_2^\uparrow \le \left(\frac{d_{\overline{S}}}{M_S^2} + \frac{d_{\overline{T}}}{M_T^2} \right) (M_S \parallel M_T) + \frac{a_{ST}}{M_S \parallel M_T} \, , \tag{6.17}$$

where

$$d_{\overline{S}} \overset{\triangle}{=} \sum_{\substack{i \in S \\ j \notin S \cup T}} a_{ij}$$

is the total inter-cluster degree of S, minus the portion that is due to the interconnections between S and T; that is, $d_{\overline{S}} = d_S - a_{ST}$. The variable $d_{\overline{T}}$ is similarly defined for cluster T.

Inequality (6.17) highlights the relationship between the two-cluster problem and the multi-cluster one. When the nodes of a graph are divided between two mutually exclusive and collectively exhaustive sets of nodes S and T, it is clear that both $d_{\overline{S}}$ and $d_{\overline{T}}$ are zero, and the bound for Theorem 6.5 reduces to that of Theorem 6.6. So, in a sense, the first term

on the right-hand side of Inequality (6.17) is a "correction" factor that accounts for the presence of other clusters in the graph, beside S and T.

Earlier, we stated that one of our contributions is that we can use our graph design algorithm to show that some of the eigenvalue bounds that have we have extended are indeed tight. We now show how we can construct a graph of any size $n \geq 2$ that meets the Fiedler bound (6.16) exactly. So we show the tightness of the bound by construction.

Let T of Figure 6.15 be a connected graph of size $n-1$. We wish to construct a graph of size n, by adding a G-node s of finite, but otherwise arbitrary, weight M_s, such that the graph G of size n has a Fiedler eigenvalue that meets the bound (6.16) exactly.

Here, we are not concerned about how T is constructed. In fact, we even allow T to contain L-nodes. What we need to know about T are its eigenvalues, which we denote by

$$\mu_1 = 0 \quad < \quad \mu_2 \quad \leq \quad \cdots \quad \leq \quad \mu_{n-1} \; .$$

We connect the nth node s according to the principles of the exact coherency and mode confinement theorem 5.21. That is, the edges connecting the nth node with each of the $n-1$ nodes of T are given by:

$$\begin{bmatrix} a_{1s} & \cdots & a_{n-1,s} \end{bmatrix} = \begin{bmatrix} \dfrac{M_1}{M_\mathsf{T}} & \cdots & \dfrac{M_{n-1}}{M_\mathsf{T}} \end{bmatrix} d_s \; , \tag{6.18}$$

where $d_s = d_\mathsf{T}$ is the degree of node s (the nth node). We know that by interconnecting node s with T in this manner, one of the eigenvalues of the overall graph G will be

$$\frac{d_s}{M_s \parallel M_\mathsf{T}} \; .$$

Furthermore, after connecting node s according to the ECMCT, we know that the oscillatory eigenvalues of T all shift by a constant amount $\frac{d_s}{M_\mathsf{T}}$. The smallest of these will be

$$\mu_2 + \frac{d_s}{M_\mathsf{T}} \; .$$

We need to control the value of d_s so that this eigenvalue *equals or exceeds*

$$\frac{d_s}{M_s \parallel M_\mathsf{T}} \; .$$

Therefore, we must have

$$\frac{d_s}{M_s \parallel M_{\mathsf{T}}} \leq \mu_2 + \frac{d_s}{M_{\mathsf{T}}} .$$

Solving for d_s, we obtain the following inequality that it must satisfy so the Fiedler eigenvalue meets the bound $\widehat{\delta}(G)$ exactly:

$$d_s \leq M_s \, \mu_2 . \tag{6.19}$$

When we ensure that d_s satisfies (6.19), and design the edge weights a_{is} according to the ECMCT, we, in effect, guarantee two things:

- The minimum cut-ratio $\widehat{\delta}(G)$ is given by

$$\widehat{\delta}(G) = \frac{d_s}{M_s \parallel M_{\mathsf{T}}} .$$

- The Fiedler eigenvalue is

$$\lambda_2^{\uparrow} = \widehat{\delta}(G) = \frac{d_s}{M_s \parallel M_{\mathsf{T}}} .$$

Example 6.8

Consider the graph of Figure 6.16, where $M_1 = 1$, $M_2 = 2$, $M_3 = 3$, and $a_{12} = 5$. Initially, we
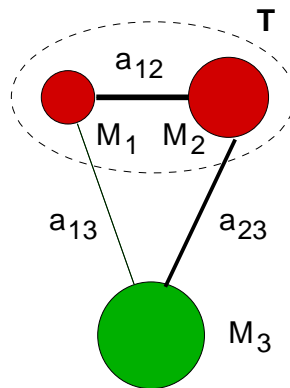
Figure 6.16: A three-node graph designed to meet the Fiedler eigenvalue upper bound 6.16 exactly.

have the two-node graph T comprising nodes M_1 and M_2. We are given the node weight M_3 and are asked to connect M_3 to the other two nodes so that the overall graph has a Fiedler eigenvalue that meets (6.16) exactly.

Our strategy, as we already have indicated, is to ensure that the edge weights a_{13} and a_{23} are

selected according to the ECMCT. Thus, we must have:

$$\begin{bmatrix} a_{13} & a_{23} \end{bmatrix} = \begin{bmatrix} \dfrac{M_1}{M_1 + M_2} & \dfrac{M_2}{M_1 + M_2} \end{bmatrix} d_3 = \begin{bmatrix} \dfrac{1}{3} & \dfrac{2}{3} \end{bmatrix} d_3 \; .$$

The ECMCT determines the relative proportionality of the edge weights a_{13} and a_{23} with respect to one another. To select a d_3 that meets the design requirements, we must choose it so that it satisfies Inequality (6.19). To do that, we need the eigenvalues of the subgraph T. These are easily seen to be

$$\mu_1 = 0 \qquad \mu_2 = \frac{a_{12}}{M_1 \parallel M_2} = \frac{5}{1 \parallel 2} = \frac{15}{2} \; .$$

Therefore, the acceptable range for d_3 is given by

$$d_3 \leq M_3 \, \mu_2 = \frac{45}{2} \; .$$

When $d_3 = \frac{45}{2}$, the maximum allowable, we expect the graph to have a Fiedler eigenvalue of multiplicity 2, given by

$$\frac{d_3}{M_3 \parallel (M_1 + M_2)} = \frac{\frac{45}{2}}{3 \parallel 3} = 15 \; .$$

In fact, when $d_3 = \frac{45}{2}$, the graph will have the following Laplacian matrix:

$$\mathbf{L} = \begin{bmatrix} 12.5 & \text{-}5.0 & \text{-}7.5 \\ \text{-}5.0 & 20.0 & \text{-}15.0 \\ \text{-}7.5 & \text{-}15.0 & 22.5 \end{bmatrix} ,$$

and it is easy to verify that the matrix pair $(\mathbf{L}, \mathbf{M})$, where the node-weight matrix $\mathbf{M} = \mathsf{diag}\,(1, 2, 3)$ has a double eigenvalue at 15. Any value of d_3 that exceeds $\frac{45}{2}$ will result in an eigenvalue at $\frac{d_3}{M_3 \parallel (M_1 + M_2)}$ that will exceed $\mu_2 + \frac{d_3}{M_1 + M_2}$, and hence will not meet the design requirements.

For example, choosing $d_3 = \frac{54}{2} = 27$, we expect one of the eigenvalues to be at

$$\frac{d_3}{M_3 \parallel (M_1 + M_2)} = \frac{27}{3 \parallel 3} = 18 \; .$$

This value exceeds the shifted eigenvalue $\mu_2 + \frac{d_3}{M_1 + M_2} = 7.5 + \frac{27}{3} = 16.5$, which is the other oscillatory eigenvalue of the graph. For this value of d_3 (that is beyond the acceptable range) the

graph will have the following Laplacian matrix:

$$\mathbf{L} = \begin{bmatrix} 14 & -5 & -9 \\ -5 & 23 & -18 \\ -9 & -18 & 27 \end{bmatrix} ,$$

and it is easy to verify that the eigenvalues of the matrix pair $(\mathbf{L}, \mathbf{M})$ *are* $\lambda_1 = 0, \lambda_2 = 16.5$, *and* $\lambda_3 = 18$, *as theoretically predicted.*

For the sake of completeness, we now choose a value of d_3 *that is strictly below the allowable limit, and show that we meet the design requirement exactly, and that the Fiedler eigenvalue has multiplicity one. Let* $d_3 = \frac{42}{2} = 21 < M_3\, \mu_2 = 22.5$. *Then we expect the Fiedler eigenvalue to be at*

$$\lambda_2 = \frac{d_3}{M_3 \parallel (M_1 + M_2)} = \frac{21}{3 \parallel 3} = 14 ,$$

and the fastest eigenvalue to be at

$$\lambda_3 = \mu_2 + \frac{d_3}{M_1 + M_2} = 7.5 + \frac{21}{3} = 14.5 .$$

Indeed, this is the case. When $d_3 = 21$, *the Laplacian matrix is given by*

$$\mathbf{L} = \begin{bmatrix} 12 & -5 & -7 \\ -5 & 19 & -14 \\ -7 & -14 & 21 \end{bmatrix} ,$$

and it is easy to verify that the eigenvalues of the matrix pair $(\mathbf{L}, \mathbf{M})$ *are* $\lambda_1 = 0, \lambda_2 = 14$, *and* $\lambda_3 = 14.5$, *as theoretically predicted. The smaller* d_3 *gets, the greater the separation between the Fiedler eigenvalue* λ_2 *and the fastest one* λ_3.

We can easily extend this design technique to prove the following:

Theorem 6.9

Consider two graphs S *and* T, *each of which is connected, with respective eigenvalues*

$$0 = \mu_1 < \mu_2 \leq \mu_3 \leq \cdots \leq \mu_q \tag{6.20}$$

$$0 = \tau_1 < \tau_2 \leq \tau_3 \leq \cdots \leq \tau_r \tag{6.21}$$

where q *and* r *denote the sizes of* S *and* T, *respectively. Then there is a way to interconnect* S *and*

T, such that the resulting graph $G = S \cup T$ has a Fiedler eigenvalue that satisfies Inequality (6.15) exactly, i.e.,

$$\lambda_2^\uparrow = \frac{a_{ST}}{M_S \parallel M_T} \ .$$

Proof: The approach to proving this theorem is nearly identical to what we have done so far. The only additional bookkeeping is that a_{ST}, the total weight of edges connecting S and T, must now satisfy the following inequality

$$a_{ST} \leq \min(M_S \tau_2, M_T \mu_2) \ .$$

The proof of this is based on a reasoning identical to the one that led to Inequality (6.19). In this case, after interconnecting S and T according to the ECMCT, the Fiedler eigenvalues of these two graphs shift to the following positions, respectively:

$$\mu_2 + \frac{a_{ST}}{M_S} \qquad \tau_2 + \frac{a_{ST}}{M_T}$$

We want the Fiedler eigenvalue, after interconnecting S and T, to be

$$\lambda_2 = \frac{a_{ST}}{M_S} \parallel M_T \ .$$

Ensuring that this value does not exceed the values to which μ_2 and τ_2 move to, we get the constraint that we specified above.

Conclusions and Future Research

In this thesis, we have tried to gain a better understanding of how linear (or linearizable) non-dissipative oscillatory networks behave. We have made the connection between a very rich area of applied mathematics—spectral graph theory—and physical networks that "vibrate." This connection is as deep as spectral graph theory on the one hand, and as rich as the engineering and physical-science applications on the other. We merely have scratched the surface here!

Throughout the thesis, we focused mainly on issues of a fundamental, theoretical, and conceptual nature. We did not venture into exploring actual engineering systems (such as power networks or vibrating space structures) or physical-science applications (such as molecular dynamics).

This omission was not intended to derogate from the importance of physical applications. After all, the ultimate goal of this research—as was stated very clearly at the outset— has been to bridge the gap between what applied mathematicians (in particular, graph theorists) know about graphs, and what engineers and scientists know about actual engineering systems, biological networks, or chemical structures, and the potential for mutual cross-disciplinary learning and research influence.

Real-world systems almost never possess the exact theoretical properties that we have modelled in our research. Therefore, focusing on actual, physical networks has the nearly-certain potential to obfuscate the underlying structure or salient features that a real network may *approximately* possess. By concentrating on exact, theoretical properties of synthetic networks, we cut through the clutter to get at the crux of the important conceptual issues. Our focus has been to gain intuition, at a basic level, about how oscillatory networks behave dynamically.

There is yet a second—perhaps more important—motivation behind our focus on theoretical properties and synthetic networks. Our research has been as much, if not more,

motivated by design of oscillatory networks as it has been by analysis. In fact, we used the phrase "design-oriented analysis" on various occasions. Although there are many actual systems that beg to be understood and analyzed (for example, power networks), we should be concerned as well with designing new systems more intelligently. It is in the design process that our theoretical emphasis should prove to be most useful. The synthetic examples throughout the thesis have been specifically designed to point out the salient theoretical issues of concern to us, and to illustrate more vividly the fundamental properties of graphs that our research has discovered.

The last reason for our deferral of the engineering and physical-science applications to another time and place has been pragmatism. We had to keep the scope of the research bounded.

With the hope that our work is useful to future researchers and developing significant applications, we enumerate here a few potential avenues for extending the results developed in this dissertation.

Modular design of networks, according to the principles of Chapter 5.

7.1 Potential Avenues of Future Research

Extension to Distributed-Parameter Networks Throughout the thesis, we have focused mainly on lumped-parameter systems. This has the benefit of keeping the network's node-weight matrix diagonal. However, distributed-parameter oscillatory systems (such as a vibrating drum) form an equally interesting genre of applications that deserve study in their own right. To make use of graph theory for such systems, they first need to be discretized to lumped-parameter networks (via finite-element approximations, for example). Often the node-weight matrix for such discretized systems will no longer be diagonal. It is of interest, therefore, to study the generalized eigenproblem under such circumstances. In fact, the eigenproblem may no longer have symmetry properties either. Sorting out the issues involved in discretizing distributed-parameter systems is one avenue of future work.

K_n**-Star Transformation** In Chapter 4, when we discussed the fully-connectedness of the nodes surrounding Schur-contracted L-nodes, we showed a graph-theoretic proof of the well-known star-delta transformation. There is a potential for extending the star-delta transformation to more complex tree-graph structures; we call these transformation K_n-

tree transformations. The problem can be stated as follows. Given a fully-connected graph (K_n) with specified edge and node weights, find a tree graph with additional L-nodes, such that when the tree-graph is Schur-contracted with respect to those L-nodes, it will result in the K-graph with precisely the specified edge weights. Our preliminary investigations indicate that to solve this problem would involve a thorough understanding of inverses of acyclic non-singular M-matrices, Groebner bases, varieties, ideals, and other similar notions in algebraic geometry.

Approximate Coherency in Arbitrary Modes Our study of theoretical coherency in arbitrary modes begs a simple question that is certain not to have an equally simple answer. Namely, how may we detect approximate coherency in systems that only approximately meet the inter-area link structure and values of the exact coherency theorem (ECT) or the exact coherency and mode confinement theorem (ECMCT) in Chapter 5. Studying how perturbations away from the constraints of those two theorems affect the network dynamics is another avenue of further study.

Spectral Partitioning of Graphs The coherency theorems for oscillatory networks suggest particular ways of interconnecting small or moderate-sized networks to create large-scale ones. How can large-scale systems be designed to meet certain desired tractability requirements? How may we exploit the theoretical principles developed in Chapters 5 and 6 to design large-scale networks more intelligently, so that they are more tractable and amenable to less complex analysis?

Extensions to the Graph Design Algorithm Our graph design algorithm has involved an incremental, one-node-at-a-time, design methodology to construct a full graph of size n with desired properties. Extensions involving conjoining clusters of nodes may prove helpful in cases where those clusters already are designed, operating graphs. Such interconnected networks would exhibit mode confinement features that are more pronounced than the current single-node design procedure.

Connections with Mode Localization For about four decades now, an important area in the study of vibrational networks has been mode localization. Typically, mode localization has been observed in systems that have strong symmetry properties, but which are perturbed away from regularity at some location in the network. We have shown in our graphs that uniformity of node weights is *not* necessary for a network to exhibit mode localization. We have also shown that we can build networks that exhibit a type of localization that monotonically increases with increasing mode number (that is, as we go to faster and faster modes). We are aware of no paper in the mode localization community where such a network is shown. Ordinarily, the systems that the researchers in

that field have studied exhibit generally, but not monotonically, increasing mode localization with increasing mode number.

Graphs with Negative Edge Weights Our focus through most of the thesis has been on graphs that have nonnegative edges. Graphs with negative edges are also important, as they can arise in certain applications (such as power networks). Issues such as continued stability are important when an edge is perturbed to have a negative sign. What features of the theory we have developed in this thesis carry over to graphs with negative edges? When does a graph turn unstable when an edge changes sign? These are sample issues to be addressed.

Estimation Theory and Statistics The covariance matrix of a random vector Y comprising a set of linearly dependent random variables is quasi-Laplacian; we say quasi because it can have off-diagonal entries that are positive (corresponding to negative edge weights in a graph). Negative edge weights are possible because the covariance of two random variables can have either positive or negative sign. This is an observation that further motivates a thorough study of graphs with negative edge weights. We know that a covariance matrix is symmetric and positive semi-definite. What properties does the graph of the covariance matrix have that guarantee its stability? Can this connection between graph theory and covariance matrices be exploited in estimation problems? We know that the eigenvectors of the covariance matrix decorrelate the random variables corresponding to that covariance matrix. So spectral graph theory has a potential application here.

Summary of Notation

Below is a list of the symbols and notation that we use in our presentation.

Symbol	Description
$\mathbb{R}$	the set of real numbers
$\mathbb{R}^n$	the set of real n-vectors
$\mathbb{R}^{m \times n}$	the set of real $m \times n$ matrices
$|\mathcal{H}|$	cardinality of $\mathcal{H}$
$\mathbf{A} = (a_{ij})$	a matrix and its $(i, j)^{\text{th}}$ entry
$[\mathbf{A}]_{ij}$	a_{ij}, the $(i, j)^{\text{th}}$ entry of $\mathbf{A}$
$a_{ij}^{(r)}$	$(i, j)^{\text{th}}$ entry of $\mathbf{A}^r$
$\boldsymbol{x}$	a vector
$\mathbf{1}_n$	the n-vector of all ones
$\mathbf{I}_n$	the identity matrix of size n; subscript is omitted if it is clear from the context or if it is irrelevant
$\mathbf{0}_n\ (\mathbf{0}_{m \times n})$	n-vector (or $m \times n$ matrix) of zeroes; subscript is omitted if it is clear from the context or if it is irrelevant
$\mathbf{P}$	permutation matrix
$\mathbf{A}^\mathsf{T}$	transpose of $\mathbf{A}$
$\mathbf{A}^{-1}$	inverse of $\mathbf{A}$
$\det \mathbf{A}, |\mathbf{A}|$	determinant of $\mathbf{A}$
$\ln (\mathbf{A})$	inertia of $\mathbf{A}$
rank $\mathbf{A}$	rank of $\mathbf{A}$
size $\mathbf{A}$	n if $\mathbf{A}$ is $n \times n$, (m, n) if $\mathbf{A}$ is $m \times n$
tr $\mathbf{A}$	trace of $\mathbf{A}$
diag $(d_1, \ldots, d_n)$	diagonal matrix with diagonal entries $d_1, \ldots, d_n$
diag $(\mathbf{A})$	diag $(a_{11}, \ldots, a_{nn})$
diag $(\mathbf{D}_1, \ldots, \mathbf{D}_n)$	block-diagonal matrix with diagonal blocks $\mathbf{D}_1, \ldots, \mathbf{D}_n$

$\mathbf{A} \rhd \mathbf{0}$	$\mathbf{A}$ is positive definite.
$\mathbf{A} \unrhd \mathbf{0}$	$\mathbf{A}$ is positive semi-definite.
$\mathbf{A} \lhd \mathbf{0}$	$\mathbf{A}$ is negative definite.
$\mathbf{A} \unlhd \mathbf{0}$	$\mathbf{A}$ is negative semi-definite matrix.
$\langle \mathbf{x}, \mathbf{y} \rangle_{\mathbf{B}}$	$\mathbf{x}^{\mathsf{T}} \mathbf{B} \mathbf{y}$, $\mathbf{B}$-innerproduct of $\mathbf{x}$ and $\mathbf{y}$ ($\mathbf{B}$ positive definite)
$\|x\|_{\mathbf{B}}$	$\sqrt{\langle \mathbf{x}, \mathbf{y} \rangle_{\mathbf{B}}}$, $\mathbf{B}$-norm of x ($\mathbf{B}$ positive definite)
$\mathbf{A} \vDash \mathbf{0}$	$a_{ij} \neq 0$ for $i = 1, \dots, m$ and $j = 1, \dots, n$)
$\mathbf{A} \succ \mathbf{0}$	$a_{ij} > 0 \quad \forall i, j$.
$\mathbf{A} \succcurlyeq \mathbf{0}$	$a_{ij} \geq 0$ and $\mathbf{A} \neq \mathbf{0}$.
$\mathbf{A} \succeq \mathbf{0}$	$a_{ij} \geq 0$ (and possibly $\mathbf{A} = \mathbf{0}$).
$\lambda_i^{\uparrow}(\mathbf{A})$	i^{th} smallest eigenvalue of $\mathbf{A}$
$\boldsymbol{\lambda}^{\uparrow}(\mathbf{A})$	$\begin{bmatrix} \lambda_1^{\uparrow}(\mathbf{A}) \\ \vdots \\ \lambda_n^{\uparrow}(\mathbf{A}) \end{bmatrix}$
$\lambda_j^{\downarrow}(\mathbf{A})$	j^{th} largest eigenvalue of $\mathbf{A}$
$\lambda_{\max}(\mathbf{A})$	$\lambda_n^{\uparrow}(\mathbf{A}) = \lambda_1^{\downarrow}(\mathbf{A})$
$\lambda_{\min}(\mathbf{A})$	$\lambda_1^{\uparrow}(\mathbf{A}) = \lambda_n^{\downarrow}(\mathbf{A})$
$\varrho(\mathbf{A})$	spectral radius of $\mathbf{A}$, i.e., $\lambda_{\max}(\mathbf{A})$
Class K	set of nonsingular M-matrices
Class K_0	set of singular M-matrices (closure of K)

Graph-Theoretic Definitions and Terminology

A *(weighted) graph* $G(V, E, \mathbf{B}, \mathbf{E})$ consists of

- a non-empty *vertex (node) set* $V = V(G) = \{v_1, v_2, \ldots, v_n\}$;

- an *edge set* $E = E(G) = \{e_{ij}\} \subseteq V \times V$, where e_{ij} denotes an edge connecting the node pair $\{v_i, v_j\}$. If $\{v_i, v_j\} = (v_i, v_j)$ is an *ordered* pair, *i.e.*, if there is a "direction of flow" associated with each edge, then G is called a *directed graph*, or, more simply, a *digraph*;

- a set of *positive* vertex (node) weights $W_v = W_v(G) = \{w_v(1), w_v(2), \ldots, w_v(n)\}$; and

- a set of *non-negative* edge weights $W_e = W_e(G) = \{w_{ij} = w_e(e_{ij}) \mid e_{ij} \in E\}$, where w_{ij} is short-hand notation denoting the weight of edge e_{ij} which connects nodes v_i and v_j.

Sometimes it might be that the graph is unweighted (*i.e.*, all vertex and edge weights are unity), or that the vertex and node weights do not concern us. In such cases, we shall use the simplified notation $G(V, E)$ to denote the graph.

B.0.1 A Glossary of Some Important Concepts

Loop: An edge of the form $e_{ii} = \{v_i, v_i\}$, $\exists v_i \in V$ is called a *loop*.

Path: A *path* is a non-empty graph P with a vertex set $V_P = \{\nu_1, \ldots, \nu_\ell\}$ and edge set $E_P = \{\{\nu_1, \nu_2\}, \{\nu_2, \nu_3\}, \ldots, \{\nu_{\ell-2}, \nu_\ell - 1\}, \{\nu_{\ell-1}, \nu_\ell\}\}$. For our purposes, the corresponding

node and edge weights are unimportant. Nodes ν_1 and ν_ℓ are said to be *linked* by P. Figure (B.1) shows a path P comprising five nodes; the edges in the path are illustrated with thicker lines.
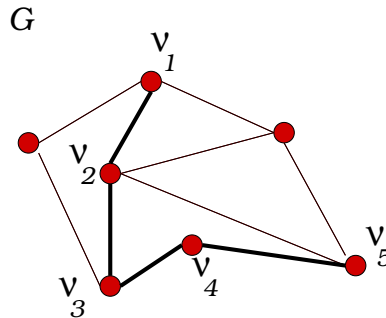

Figure B.1: A Path P

Connected Graph: A graph G is said to be (maximally) *connected* if any two of its vertices are linked by a path in G.

Subgraph: We say $G' = (V', E')$ is a subgraph of $G(V, E)$, if $V' \subseteq V$ and $E' \subseteq E$, with corresponding vertex and edge weights unchanged.

Induced Subgraph: We shall omit the reference to whether a subgraph is vertex- or edge-induced, as it would normally be clear from the context.

Component: A *maximally connected subgraph* of G is called a *component* of G. A subgraph G' is called *maximally connected* if the addition of even one more vertex to G' will cause it to be no longer connected. In other words, there is no edge between the vertices in $V - V'$ and V'.

Spanning Tree:

Chord: It is clear that a connected graph has only one component.

Multi-graph or Multi-Digraph: If graph G contains *multiple* undirected or directed edges between at least one node pair $\{v_i, v_j\}$, it is called a *multi-graph* or *multi-digraph*, respectively.
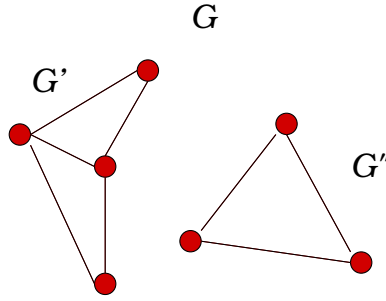
G

Figure B.2: A Graph G which cosists of two components, G' and G''.

Adjacency Matrix: Two vertices v_i and v_j are *adjacent* if there exists an edge $e_{ij} \in E$ that connects them. The (weighted) *adjacency matrix* $\mathbf{A} = \mathbf{A}(G)$ of a graph G is defined as $\mathbf{A} = (a_{ij}) \in \mathbb{R}^{n \times n}$, where

$$a_{ij} = \begin{cases} w_{ij} & \text{if } e_{ij} \in E \text{ and } i \neq j, \\ 0 & \text{otherwise.} \end{cases}$$

Note that for undirected graphs, the adjacency matrix is symmetric, *i.e.*, $\mathbf{A}^\mathsf{T} = \mathbf{A}$.

Vertex Degree (or Valency) Matrix: The *degree* (or *valency*) of a vertex v_i is defined to be the total weight of all the edges incident on v_i. Let d_i denote the degree of vertex v_i. It is clear that $d_i = \sum_{j=1}^{n} a_{ij} = \sum_{j=1}^{n} w_{ij}$, where the second equality is based on the premise that graph G is loopless—otherwise, $w_{ii} \neq 0 \quad \exists i \in \{1, \dots, n\}$, whereas $a_{ii} = 0 \quad i = 1, \dots, n$. The *vertex degree matrix* $\mathbf{D} = \mathbf{D}(G) \in \mathbb{R}^{n \times n}$ of a graph G is defined as

$$\mathbf{D} = \mathsf{diag}\,(d_1, \dots, d_n)\,.$$

q-**Partition:** We denote the $q-$partition of a graph G by $\mathcal{V}_q = \{V_1, V_2, \dots, V_q\}$, where each V_i is connected, $V_i \bigcap V_j = \phi$ for $i \neq j$, and $\bigcup_{i=1}^{q} V_i = V$.

Multi-way Edge Cut: Consider a q-partition $\mathcal{V}_q$ of $V(G)$, as defined above. The set of edges

$$\mathcal{K}_q = \bigcup_{i,j=1 i \neq j}^{q} E(V_i, V_j) \tag{B.1}$$

Assignment Matrix: Associated with every q-partition $\mathcal{V}_q$ is an assignment matrix $\mathbf{X} =$

$(x_{ik}) \in \mathbb{R}^{n \times q}$, whose entries are defined as

$$x_{ik} = \begin{cases} 1 & \text{if } v_i \in V_k \\ 0 & \text{if } v_i \notin V_k \ , \end{cases}$$

is called the *assignment matrix* for the partitioning $\mathcal{V}_q$. Its kth column $\boldsymbol{x}_k$ is an *indicator vector* for cluster V_k, *i.e.*, it is a $(0,1)$-vector which indicates the assignment of each of the n vertices to cluster V_k. We can write $\mathbf{X}$ in terms of its columns: $\mathbf{X} = [\boldsymbol{x}_1 \,|\, \boldsymbol{x}_2 \,|\, \cdots \,|\, \boldsymbol{x}_q]$. Note that the assignment matrix satisfies the *transportation constraint* $\mathbf{X}\mathbf{1}_q = \mathbf{1}_n$, where $\mathbf{1}_n \triangleq [1, \ldots, 1]^{\mathsf{T}}$ is the n-vector of all ones, and $\mathbf{1}_q$ is similarly defined.

The *partition matrix* $\mathbf{T}$, defined below, is another, equivalent way of specifying how a graph is partitioned:

Partition Matrix: The matrix $\mathbf{T} = (t_{ij}) \in \mathbb{R}^{n \times n}$, whose entries are defined as

$$t_{ij} = \begin{cases} 1 & \text{if } v_i \text{ and } v_j \text{ belong to the same group} \\ 0 & \text{otherwise} \ , \end{cases}$$

is called the *partition matrix* for the partitioning $\mathcal{V}_q$. With a proper numbering of the nodes (i.e., with an appropriate pre- and post-multiplication with a permutation matrix $\mathbf{P}$) the partition matrix can be made to look block diagonal in form, with each block containing the nodes that belong to one of the groups.

Node-Edge Incidence Matrix: The *oriented node-edge incidence matrix* $\mathbf{F} \in \mathbb{R}^{n \times m}$, for a graph with n nodes and m edges, is defined as follows. Assign an arbitrary orientation to each edge in the graph. The rows of $\mathbf{F}$ are indexed by the vertex set $V(G)$ and the columns by the edge set $E(G)$. The entry $[\mathbf{F}]_{ie} = +1$ if node i is the initial vertex of the oriented edge e, $[\mathbf{F}]_{ie} = -1$ if node i is the terminal vertex of the edge e, and $[\mathbf{F}]_{ie} = 0$ if node i is not incident on edge e.

Laplacian Matrix: The *Laplacian matrix* $\mathbf{L} = \mathbf{L}(G) \in \mathbb{R}^{n \times n}$ of a graph G is defined as $\mathbf{L} = \mathbf{D} - \mathbf{A}$. Therefore,

$$[\mathbf{L}]_{i\ell} = \begin{cases} -a_{i\ell} & \text{if } i \neq \ell \\ \displaystyle\sum_{j=1}^{n} a_{ij} & \text{if } i = \ell \end{cases} \tag{B.2}$$

This matrix will feature prominently throughout our discussion. It has such important and well-established properties that we shall devote an entire section of this thesis summarizing and discussing them. In particular, the eigenvalues and eigenvectors of the Laplacian matrix turn out to be very significant in—and in fact form the backbone of—any discussion of dynamic behavior of the networks represented by our graphs. The Laplacian matrix **L** is referred to by other names as well, such as the *admittance matrix*, the *stiffness matrix*, or the *Kirchhoff matrix*, a terminology that clearly owes itself to electrical network theory and the pioneering work of Kirchhoff in that area.

> **NOTE:** In this thesis, unless otherwise noted, whenever we use the term *graph*, we refer only to a connected (*i.e.*, single-component) graph that has a finite number of vertices (each with a *nonnegative* weight), is undirected, has no loops or multiple edges, and has *non-negative* edge weights.

Perturbation Theory for a Class of Generalized Eigenvalue Problems

We outline the salient results of the *first-order* perturbation theory for the generalized eigen-problem (GEP)

$$\mathbf{A}\,u = \lambda\,\mathbf{M}\,u\,, \tag{C.1}$$

where $\mathbf{A} \in \mathbb{R}^{n \times n}$ is symmetric, and $\mathbf{M} = \mathsf{diag}\,(M_1, \ldots, M_n)$ is a diagonal matrix with $M_i > 0$, $\forall\, i$. The perturbation results associated with (C.1) can be obtained quite simply if all the eigenvalues are distinct; the analysis is more complicated if at least one of the eigenvalues has an algebraic multiplicity greater than one.[1]. We consider each case separately.

C.1   First-Order Perturbation Theory for Multiple Eigenvalues

Consider the GEP

$$(\mathbf{A} + \mathbf{E})\,\widetilde{u} = \widetilde{\lambda}\,\mathbf{M}\,\widetilde{u}\,, \tag{C.2}$$

where $\mathbf{A}$ and $\mathbf{E}$ are symmetric, positive semi-definite $n \times n$ matrices, $\mathbf{E}$ is a perturbation matrix with entries of order ϵ, and $\mathbf{M} = \mathsf{diag}\,(M_1, \ldots, M_n)$ has positive diagonal entries $\mathbf{M}_i$. Suppose we know the solution to the unperturbed problem

$$\mathbf{A}\,u = \lambda\,\mathbf{M}\,u\,. \tag{C.3}$$

Furthermore, let the unperturbed eigenproblem (C.3) have an eigenvalue, say λ_1, with algebraic multiplicity $q > 1$ (we know that due to the symmetry of $\mathbf{A}$ and $\mathbf{E}$, and the structure of $\mathbf{M}$, the geometric multiplicity of every eigenvalue is the same as its algebraic multiplicity, *i.e.*, the matrix pairs $(\mathbf{A}, \mathbf{M})$ and $(\mathbf{A} + \mathbf{E}, \mathbf{M})$ are non-defective). Then, associated with the multiple eigenvalue λ_1 there is a q-dimensional subspace $\mathcal{V}_1$ of eigenvectors.

---

[1]Our coverage in this appendix very closely follows the treatment in Butkov [10].

Studying perturbations of such an eigenproblem is complicated by the fact that we do not know to which vector in $\mathcal{V}_1$ each perturbed eigenvector reduces as $\mathbf{E} \longrightarrow \mathbf{0}$; any set of q linearly independent vectors in $\mathcal{V}_1$ can serve as eigenvectors of λ_1 in the unperturbed problem, whereas it is *not* to any arbitrary set of q linearly independent vectors in $\mathcal{V}_1$ that the perturbed eigenvectors converge if $\mathbf{E} \longrightarrow \mathbf{0}$.

The standard approach to the problem is to first construct an $\mathbf{M}$-orthonormal basis set for $\mathcal{V}_1$. To simplify notation, however, we drop the subscript "1" from the eigenvalue and its associated eigenspace; that is, we consider λ a generic eigenvalue of algebraic multiplicity q, $\mathcal{V}$ its corresponding q-dimensional eigenspace, and so on. Using a Gram-Schmidt process, we construct a set of q vectors $\boldsymbol{w}_1, \ldots, \boldsymbol{w}_q \in \mathcal{V}$ such that $\langle \boldsymbol{w}_i, \boldsymbol{w}_j \rangle_{\mathbf{M}} = \delta_{ij}$. Thus, we have:

$$\mathbf{A}\,\boldsymbol{w}_k = \lambda\,\mathbf{M}\,\boldsymbol{w}_k \qquad k = 1, \ldots, q \tag{C.4}$$

or in a more compact matrix form,

$$\mathbf{AW} = \lambda\mathbf{MW} \, , \tag{C.5}$$

where the $n \times q$ matrix $\mathbf{W}$ is

$$\mathbf{W} = \left[\boldsymbol{w}_1 \Big| \cdots \Big| \boldsymbol{w}_q \right] \, . \tag{C.6}$$

If the perturbed eigenvalue $\widetilde{\lambda}$ converges to λ (as $\mathbf{E} \longrightarrow \mathbf{0}$), then its corresponding eigenvector $\widetilde{\boldsymbol{u}}$ must reduce to some vector in the eigenspace $\mathcal{V}$. Writing the expansion of $\widetilde{\lambda}$ and $\widetilde{\boldsymbol{u}}$ (up to first order) we have:

$$\widetilde{\lambda} \simeq \lambda + d\lambda \, , \tag{C.7}$$

$$\widetilde{\boldsymbol{u}} \simeq \boldsymbol{u} + d\boldsymbol{u} \, . \tag{C.8}$$

We note that each unperturbed eigenvector $\boldsymbol{u}$ (to which the a perturbed one reduces) must be a linear combination of $\boldsymbol{w}_1, \ldots, \boldsymbol{w}_q$; namely,

$$\boldsymbol{u}_i = \sum_{k=1}^{q} c_{ki}\boldsymbol{w}_k = \mathbf{W}\,\boldsymbol{c}_i \qquad i = 1, \ldots, q \, , \tag{C.9}$$

where

$$\boldsymbol{c}_i = \left[c_{1i} \quad \cdots \quad c_{qi} \right]^{\mathsf{T}} \tag{C.10}$$

is the ith column of the $q \times q$ matrix

$$\mathbf{C} = \left[\boldsymbol{c}_1 \middle| \cdots \middle| \boldsymbol{c}_q \right] . \tag{C.11}$$

We are therefore in search of q vectors $\boldsymbol{c}_1, \ldots, \boldsymbol{c}_q \in \mathbb{R}^q$ each of which defines, through (C.9), one of the q unperturbed eigenvectors $\boldsymbol{u}_i$. We note that the basis vectors $\boldsymbol{w}_1, \ldots, \boldsymbol{w}_q$ are $\mathbf{M}$-orthonormal, *i.e.*, $\langle \boldsymbol{w}_i, \boldsymbol{w}_j \rangle_{\mathbf{M}} = \delta_{ij}$; therefore, we have $\mathbf{W}^{\mathsf{T}} \mathbf{M} \mathbf{W} = \mathbf{I}_q$. The same holds for $\mathbf{U} \in \mathbb{R}^{n \times q}$; that is, $\mathbf{U}^{\mathsf{T}} \mathbf{M} \mathbf{U} = \mathbf{I}_q$, where

$$\mathbf{U} = \left[\boldsymbol{u}_1 \middle| \cdots \middle| \boldsymbol{u}_q \right] . \tag{C.12}$$

We can now summarize—in compact matrix form—the unperturbed and perturbed problems as follows.

C.1.1   The Unperturbed Multiple Eigenvalue Problem

$$\mathbf{A} \mathbf{U} = \lambda \mathbf{M} \mathbf{U} , \tag{C.13}$$

but because we do not know, a priori, the unperturbed eigenvectors to which the perturbed ones reduce, we construct the $\mathbf{M}$-orthonormal vectors $\boldsymbol{w}_1, \ldots, \mathbf{w}_q \in \mathcal{V}$, so that:

$$\mathbf{A} \mathbf{W} = \lambda \mathbf{M} \mathbf{W} , \tag{C.14}$$

and our task is to find the coefficient matrix $\mathbf{C} \in \mathbb{R}^{q \times q}$ that relates $\mathbf{U}$ and $\mathbf{W}$:

$$\mathbf{U} = \mathbf{W} \mathbf{C} . \tag{C.15}$$

C.1.2   The Perturbed Multiple Eigenvalue Problem

$$(\mathbf{A} + \mathbf{E}) \, \widetilde{\mathbf{U}} = \mathbf{M} \, \widetilde{\mathbf{U}} \, \widetilde{\boldsymbol{\Lambda}} , \tag{C.16}$$

where

$$\widetilde{\mathbf{\Lambda}} = \mathbf{\Lambda} + d\mathbf{\Lambda} \tag{C.17}$$

$$\widetilde{\mathbf{U}} = \mathbf{U} + d\mathbf{U} . \tag{C.18}$$

Expanding (C.16) we have:

$$(\mathbf{A} + \mathbf{E})(\mathbf{U} + d\mathbf{U}) = \mathbf{M}(\mathbf{U} + d\mathbf{U})(\lambda\mathbf{I} + d\mathbf{\Lambda}) . \tag{C.19}$$

Equating first-order terms on both sides we obtain:

$$\mathbf{A}\, d\mathbf{U} + \mathbf{E}\, \mathbf{U} = \lambda\, \mathbf{M}\, d\mathbf{U} + \mathbf{M}\, \mathbf{U}\, d\mathbf{\Lambda} . \tag{C.20}$$

Pre-multiplying each side of (C.20) by $\mathbf{W}^{\mathsf{T}}$ we get:

$$\mathbf{W}^{\mathsf{T}}\mathbf{A}\, d\mathbf{U} + \mathbf{W}^{\mathsf{T}}\mathbf{E}\, \mathbf{U} = \lambda\, \mathbf{W}^{\mathsf{T}}\mathbf{M}\, d\mathbf{U} + \mathbf{W}^{\mathsf{T}}\mathbf{M}\, \mathbf{U}\, d\mathbf{\Lambda} . \tag{C.21}$$

Recalling that

$$\mathbf{W}^{\mathsf{T}}\mathbf{A} = \lambda\, \mathbf{W}^{\mathsf{T}}\mathbf{M} \tag{C.22}$$

and

$$\mathbf{U} = \mathbf{W}\, \mathbf{C} \tag{C.23}$$

we are led to

$$\underbrace{\mathbf{W}^{\mathsf{T}}\mathbf{E}\,\mathbf{W}}_{\mathbf{G}}\, \mathbf{C} = \underbrace{\mathbf{W}^{\mathsf{T}}\mathbf{M}\,\mathbf{W}}_{\mathbf{I}_q}\, \mathbf{C}\, \underbrace{d\mathbf{\Lambda}}_{\mathbf{\Theta}} . \tag{C.24}$$

Thus, the first-order perturbation study of the original multiple eigenvalue problem has led to the ordinary $q \times q$ eigenproblem

$$\mathbf{G}\,\mathbf{C} = \mathbf{C}\,\mathbf{\Theta} , \tag{C.25}$$

where $\mathbf{G} = \mathbf{W}^{\mathsf{T}}\mathbf{E}\,\mathbf{W}$ is the new matrix, whose entries are of order ϵ, whose eigenvectors

give us the desired $\mathbf{C}$ matrix, and whose eigenvalues

$$\mathbf{\Theta} = d\mathbf{\Lambda} = \mathsf{diag}\,\big(\underbrace{d\lambda_1}_{\theta_1}, \ldots, \underbrace{d\lambda_q}_{\theta_q}\big) \tag{C.26}$$

are the admissible first-order shifts that the unperturbed multiple eigenvalue λ undergoes.

The eigenvalues $\theta_i = d\lambda_i$ of (C.25, C.26) being distinct means that the unperturbed multiple eigenvalue λ moves to a set of q distinct perturbed eigenvalue positions $\widetilde{\lambda}_{(1)}, \ldots, \widetilde{\lambda}_{(q)}$; hence, we need go no further, as we have broken the multiplicity using a first-order analysis. However, if any eigenvalue of (C.25,C.26) has multiplicity greater than unity, then we need to carry out the perturbation analysis further—to second and possibly higher order. This contingency will not be necessary in the cases that we consider in this thesis, so we shall not concern ourselves with it here.

We note that as $\mathbf{G} = \mathbf{W}^\mathsf{T}\mathbf{E}\mathbf{W}$ it must be symmetric; therefore, the system (C.25) has a full set of q linearly independent eigenvectors (columns of $\mathbf{C}$), and that the eigenvector matrix $\mathbf{C}$ is an orthogonal matrix, *i.e.*, $\mathbf{C}^\mathsf{T}\mathbf{C} = \mathbf{C}\mathbf{C}^\mathsf{T} = \mathbf{I}_q$. We also note that

$$\mathbf{\Theta} = \mathbf{C}^\mathsf{T}\mathbf{G}\mathbf{C} = (\mathbf{W}\mathbf{C})^\mathsf{T}\mathbf{E}\,(\mathbf{W}\mathbf{C})\ . \tag{C.27}$$

Referring to (C.23), we rewrite the above as:

$$\mathbf{\Theta} = \mathbf{U}^\mathsf{T}\mathbf{E}\mathbf{U}\ . \tag{C.28}$$

Clearly, the entries in $\mathbf{\Theta}$ are of order ϵ, as expected. That is, the unperturbed multiple eigenvalue λ undergoes q order-ϵ shifts as a result of the order-ϵ perturbation matrix $\mathbf{E}$ applied to $\mathbf{A}$.

All these insights have a direct bearing on our understanding of slow-coherency dynamics of certain vibrational networks. See Section 5.2 to see how we apply the principles we have covered here to a certain class of vibrational networks.

Bibliography

[1] R. B. Bapat and T. E. S. Raghavan. *Nonnegative Matrices and Applications*, volume 64 of *Encyclopedia of Mathematics and Its Applications*. Cambridge University Press, Cambridge, United Kingdom, 1997.

[2] Arthur R. Bergen and Vijay Vittal. *Power Systems Analysis*. Prentice-Hall, Upper Saddle River, New Jersey, 2nd edition, 2000.

[3] Abraham Berman and Robert J. Plemmons. *Nonnegative Matrices in the Mathematical Sciences*. Classics in Applied Mathematics. Society for Industrial and Applied Mathematics (SIAM), Philadelphia, PA, 1994.

[4] Dimitris Bertsimas and John N. Tsitsiklis. *Introduction to Linear Optimization*. Athena Scientific, Belmont, MA, 1997.

[5] Rajendra Bhatia. *Matrix Analysis*. Graduate Texts in Mathematics. Springer Verlag, New York, NY, 1997.

[6] Norman Biggs. *Algebraic Graph Theory*. Cambridge University Press, Cambridge, United Kingdom, 2nd edition, 1993.

[7] Marianna Bolla and Gábor Tusnády. Spectra and optimal partitions of weighted graphs. *Discrete Mathematics*, 128(1–3):1–20, 1994.

[8] Béla Bollobás. *Graph Theory: An Introductory Course*, volume 63 of *Graduate Texts in Mathematics*. Springer-Verlag, New York, NY, 1979.

[9] Claude Brezinski. Other manifestations of the schur complement. In *Linear Algebra and Its Applications*, volume 111, pages 231–247, 1988.

[10] Eugene Butkov. *Mathematical Physics*. Addison-Wesley Publishing Company, Reading, MA, 1968.

[11] David Carlson. What are schur complements anyway? In *Linear Algebra and Its Applications*, volume 74, pages 257–275, 1986.

[12] Pak K. Chan, Martine D. F. Schlag, and Jason Y. Zien. Spectral k-way ratio-cut partitioning and clustering. In *IEEE Transactions on Computer-Aided Design of Integrated Circuits and Systems*, volume 13, No. 9, pages 1088–1096, 1994.

[13] Joe H. Chow, editor. *Time-Scale Modeling of Dynamic Networks with Applications to Power Systems*. Number 46 in Lecture Notes in Control and Information Sciences. Springer-Verlag, New York, NY, 1982.

[14] Fan R. K. Chung, editor. *Spectral Graph Theory*. Number 92 in Regional Conference Series in Mathematics. American Mathematical Society, Providence, RI, 1997.

[15] Richard W. Cottle. Manifestations of the schur complement. In *Linear Algebra and Its Applications*, volume 8, pages 189–211, 1974.

[16] Dragos M. Cvetkovic and Michael Doob. *Recent Results in the Theory of Graph Spectra*, volume 36 of *Annals of Discrete Mathematics*. North-Holland/Elsevier Science, Ltd., New York, NY, 1988.

[17] Dragos M. Cvetkovic, Michael Doob, and Horst Sachs. *Spectra of Graphs: Theory and Applications*. Johann Ambrosius Barth Verlag, Heidelberg, Leipzig, 3rd revised and enlarged edition, 1995.

[18] Dragos M. Cvetkovic, P. Rowlinson, and S. Simić. *Eigenspaces of Graphs*, volume 66 of *Encyclopedia of Mathematics and Its Applications*. Cambridge University Press, Cambridge, United Kingdom, 1997.

[19] Susan S. D'Amato. Eigenvalues of graphs with twofold symmetry. In *Molecular Physics*, volume 37, pages 1363–1369, 1979.

[20] Ranjit A. Date and Joe H. Chow. Aggregation properties of linearized two-time-scale power networks. *IEEE Transactions on Circuits and Systems*, 38(7):720–730, 1991.

[21] U. Di Caprio. Conditions for theoretical coherency in multimachine power systems. *Automatica*, 17(5):687–701, September 1981.

[22] Reinhard Diestel. *Graph Theory*. Springer-Verlag, New York, NY, 1997.

[23] W. E. Donath and A. J. Hoffman. Lower bounds for the partitioning of graphs. In *IBM Journal of Research and Development*, volume 17, pages 420–425, 1973.

[24] Julie Falkner, Franz Rendl, and Henry Wolkowicz. A computational study of graph partitioning. In *Mathematical Programming*, volume 66, No. 2 of *Series A*, pages 211–239, 1994.

[25] Miroslav Fiedler. Algebraic connectivity of graphs. *Czechoslovak Mathematical Journal*, 23(98):298–305, 1973.

[26] Miroslav Fiedler. Eigenvectors of acyclic matrices. *Czechoslovak Mathematical Journal*, 25(100):607–618, 1975.

[27] Miroslav Fiedler. A property of eigenvectors of nonnegative symmetric matrices and its applications to graph theory. *Czechoslovak Mathematical Journal*, 25(100):619–633, 1975.

[28] Miroslav Fiedler. *Special Matrices and their applications in numerical mathematics*. Martinus Nijhoff Publishers—a member of Kluwer Academic Publishers Group, Boston, 1986.

[29] Miroslav Fiedler. Laplacians of graphs and algebraic connectivity. In *Banach Center Publications*, volume 25 of *Combinatorics and Graph Theory*, pages 57–70. PWN-Polish Scientific Publishers, Warsaw, Poland, 1989.

[30] Miroslav Fiedler. A geometric approach to the laplacian matrix of a graph. In Richard A. Brualdi, Shmuel Friedland, and Victor Klee, editors, *Combinatorial and Graph-Theoretical Problems in Linear Algebra*, volume 50 of *The IMA Volumes in Mathematics and Its Applications*, pages 73–98. Springer-Verlag, New York, NY, 1993.

[31] Miroslav Fiedler and Vlastimil Pták. On matrices with non-positive off-diagonal elements and positive principal minors. *Czechoslovak Mathematical Journal*, 12(87):382–400, 1962.

[32] M. E. Fischer. On hearing the shape of a drum. In *Journal of Combinatorial Theory*, volume 1, pages 105–125, 1966.

[33] A. P. French. *Vibrations and Waves*. The MIT Introductory Physics Series. W. W. Norton & Company, New York, NY, 1971.

[34] F. R. Gantmacher. *The Theory of Matrices*, volume 2. Chelsea Publishing Company, New York, NY, 1960.

[35] F. R. Gantmacher and M. G. Krein. *Oscillation Matrices and Kernels and Small Vibrations of Dynamical Systems*. Gostekhizdat, Moscow, 2nd edition, 1950. Russian (German translation should be available).

[36] M. Garey, D. Johnson, and L. Stockmeyer. Some simplified np-complete graph problems. In *Theoretical Computer Science*, volume 1, pages 237–267, 1976.

[37] Christopher David Godsil. *Algebraic Combinatorics*. Chapman & Hall, Inc., New York, NY, 1993.

[38] Christopher David Godsil and Gordon Royle. *Algebraic Graph Theory*. Springer-Verlag, New York, NY, 2001.

[39] Carolyn Gordon, David L. Webb, and Scott Wolpert. One cannot hear the shape of a drum. *Bull. Amer. Math. Soc. (N.S.)*, 27(1):134–138, 1992.

[40] Alexander Graham. *Nonnegative Matrices and Applicable Topics in Linear Algebra*. Mathematics and Its Applications. Ellis Horwood Limited, Chichester, United Kingdom, 1987.

[41] Jesko M. Hagee, Babak Ayazifar, George C. Verghese, and Bernard C. Lesieutre. Load bus partitioning for synchronic modal equivalencing (sme). In *28th North American Power Symposium*, pages 57–61, November 1996.

[42] K. M. Hall. An r-dimensional quadratic placement algorithm. In *Management Science*, volume 17, pages 219–229, Nov. 1970.

[43] Paul R. Halmos. *Introduction to Hilbert Space and the Theory of Spectral Multiplicity*. AMS Chelsea Publishing, Providence, 2nd edition, 1998.

[44] David A. Harville. *Matrix Algebra from a Statistician's Perspective*. Springer-Verlag, New York, NY, 1997.

[45] Bruce Hendrickson and Robert Leland. Multi-dimensional spectral load balancing. In *Sandia National Laboratory Technical Report SAND93-0074*, 1993. (Abbreviated versions appeared in Proc. 6th SIAM Conf. Parallel Proc. Sci. Comput.).

[46] Bruce Hendrickson and Robert Leland. An improved spectral graph partitioning algorithm for mapping parallel computations. In *SIAM Journal on Scientific Computing*, volume 16(2), pages 452–469, 1995.

[47] Roger A. Horn and Charles R. Johnson. *Matrix Analysis*. Cambridge University Press, Cambridge, United Kingdom, 1985.

[48] Roger A. Horn and Charles R. Johnson. *Topics in Matrix Analysis*. Cambridge University Press, Cambridge, United Kingdom, 1991.

[49] M. Kac. Can one hear the shape of a drum? In *American Mathematical Monthly*, volume 73, pages 1–23, April 1966.

[50] Thomas Kailath. *Linear Systems*. Prentice-Hall Information and System Sciences Series. Prentice-Hall, Inc., Englewood Cliffs, NJ, 1980.

[51] D. J. Klein. Treediagonal matrices and their inverses. *Linear Algebra and Its Applications*, 42:109–117, 1982.

[52] Peter Lancaster and Miron Tismenetsky. *The Theory of Matrices*. Computer Science and Applied Mathematics. Academic Press, New York, NY, second edition, 1985.

[53] David G. Luenberger. *Optimization by Vector Space Methods*. John Wiley and Sons, New York, NY, 1969.

[54] David G. Luenberger. *Introduction to Dynamic Systems: Theory, Models, and Applications*. John Wiley and Sons, Inc., New York, NY, 1979.

[55] Helmut L′utkepohl. *Handbook of Matrices*. John Wiley and Sons, New York, NY, 1996.

[56] Jan R. Magnus and Heinz Neudecker. *Matrix Differential Calculus with Applications in Statistics and Econometrics*. Wiley Series in Probability and Mathematical Statistics. John Wiley & Sons, New York, NY, 1988.

[57] Russell Merris. Laplacian matrices of graphs: A survey. In *Linear Algebra and Its Applications*, volume 197,198, pages 143–176, 1994.

[58] Nestor F. Michelena and Panos Y. Papalambros. A hypergraph framework for optimal model-based decomposition of design problems. In *Computational Optimization and Applications*, volume 8, pages 173–196, 1997.

[59] Bojan Mohar. The laplacian spectrum of graphs. In Y. Alavi, G. Chartrand, O. R. Oellermann, and A. J. Schwenk, editors, *Graph Theory, Combinatorics, and Applications: Proceedings of the Sixth Quadrennial International Conference on the Theory and Applications of Graphs*, volume 2, pages 871–898, 1988.

[60] Bojan Mohar. Laplace eigenvalues of graphs—a survey. *Discrete Mathematics*, 109(1–3):171–183, 1992.

[61] Bojan Mohar. Some applications of laplace eigenvalues of graphs. In G. Hahn and G. Sabidussi, editors, *Graph Symmetry*, pages 225–275, 1997.

[62] Bojan Mohar. Some applications of laplace eigenvalues of graphs. In Gena Hahn and Gert Sabidussi, editors, *Graph Symmetry: Algebraic Methods and Applications*, volume 497 of *NATO ASI Series. Series C: Mathematical and Physical Sciences*, pages 225–275. Kluwer Academic Publishers, Boston, MA, and Dordrecht, The Netherlands, 1997.

[63] Bojan Mohar and S. Poljak. Eigenvalues in combinatorial optimization. In Richard A. Brualdi, Schmuel Friedland, and Victor Klee, editors, *Combinatorial and Graph-Theoretical Problems in Linear Algebra*, volume 50 of *The IMA Volumes in Mathematics and Its Applications*, pages 107–151. Springer-Verlag, New York, NY, 1993.

[64] Arch W. Naylor and George R. Sell. *Linear Operator Theory in Engineering and Science*, volume 40 of *Applied Mathematical Sciences*. Springer-Verlag, New York, NY, 1982.

[65] B. T. Ooi and M. Nishimoto. Analytical structures for eigensystem study of power flow oscillations in large power systems. *IEEE Transactions Power Systems*, 3(4):1609–1615, 1988.

[66] Diane Valérie Ouellete. Schur complements and statistics. In *Linear Algebra and Its Applications*, volume 36, pages 187–295, 1981.

[67] Beresford N. Parlett. *The Symmetric Eigenvalue Problem*. Classics in Applied Mathematics. Society for Industrial and Applied Mathematics (SIAM), Philadelphia, corrected reissue edition, 1998.

[68] Ganesh N. Ramaswamy. *Modal Structures and Model Reduction with Application to Power System Equivalencing*. Ph.D. Thesis. Massachusetts Institute of Technology, 1995.

[69] Franz Rendl and Henry Wolkowicz. A projection technique for partitioning the nodes of a graph. In *Annals of Operations Research*, volume 58, pages 155–179, 1993.

[70] Youcef (Yousef) Saad. *Numerical Methods for Large Eigenvalue Problems*. Manchester University Press, Manchester, UK, and Halstead Press, New York, NY, 1992.

[71] Yousef Saad. *Iterative Methods for Sparse Linear Systems*. PWS Publishing Company, Boston, MA, 1996.

[72] Hans Sagan. *Boundary and Eigenvalue Problems in Mathematical Physics*. Dover, New York, NY, 1961.

[73] G. W. Stewart and Ji-guang Sun. *Matrix Perturbation Theory*. Academic Press, San Diego, CA, 1990.

[74] James S. Thorp, Charles E. Seyler, and Arun G. Phadke. Electromechanical wave propagation in large electric power systems. *IEEE Transactions on Circuits and Systems—I: Fundamental Theory and Applications*, 45(6):614–622, 1998.

[75] F. Uhlig. A recurring theorem about pairs of quadratic forms and extensions: A survery. *Linear Algebra Appl.*, 25:219–238, 1979.

[76] J. Y. Zien, Schlag D. F., and P. K. Chan. Multilevel spectral hypergraph partitioning with arbitrary vertex sizes. *IEEE Transactions on Computer-Aided Design of Integrated Circuits and Systems*, 18(9):1389–1399, 1999.

[77] Alphose Zingoni. A new approach for the vibration analysis of symmetric mechanical systems—part 1: Theoretical preliminaries. In *International Journal of Engineering Education*, volume 12(1), pages 59–64, 1996.

[78] Alphose Zingoni. A new approach for the vibration analysis of symmetric mechanical systems—part 2: One-dimensional systems. In *International Journal of Engineering Education*, volume 12(2), pages 152–157, 1996.

[79] Alphose Zingoni. A new approach for the vibration analysis of symmetric mechanical systems—part 3: Two-dimensional systems. In *International Journal of Engineering Education*, volume 12(3), pages 187–198, 1996.

[80] G. M. Zlokovic. *Group Theory and G-Vector Spaces in Structural Analysis*. Ellis Horwood, Chichester, United Kingdom, 1989.

[81] G. M. Zlokovic. *Group Supermatrices in Finite Element Analysis*. Ellis Horwood, Chichester, United Kingdom, 1992.